DEVELOPMENT OF BIOCATALYTIC APPROACH USING FUNGAL LACCASE TO PRODUCE NOVEL FUNCTIONAL INGREDIENTS VIA PROTEIN CROSS-LINKING AND PROTEIN/POLYSACCHARIDE CONJUGATION

by

Mingqin Li

Department of Food Science and Agricultural Chemistry
MacDonald Campus, McGill University
Quebec, Canada

May, 2020

A thesis submitted to McGill University in partial fulfillment of the requirements of the degree of Doctor of Philosophy in Food Science

SUGGESTED SHORT TITLE

PROTEIN MODIFICATION CATALYZED BY LACCASE

ABSTRACT

Laccase (E.C 1.3.10.2) is a versatile biocatalyst, which can be used for protein modification. Kinetics of biocatalytic conversions of protein-related substrate models by laccases were studied in order to contribute to the understanding of mechanistic actions of laccase in protein cross-linking. Fungal laccases exhibited higher substrate specificity towards the peptide models (K_m=0.17-0.67 mM, k_{cat}/K_m=0.56-0.81 $s^{-1}mM^{-1}$) ST-10 (SYMTDYYLST), derived from potato patatin, and AG-10 (AKKIVSDGNG), derived from egg white lysozyme (LZM), than tyrosine (Y) ($K_{m=}$ 1.10-1.12 mM, k_{cat}/K_m=0.01-0.31 $s^{-1}mM^{-1}$). This was confirmed by the molecular docking study, in which substrate/enzyme binding modes with better affinity were observed for laccase/peptides than for laccase/tyrosine. Laccase-catalyzed reaction resulted in the cross-linking of tyrosine-containing peptide ST-10 via the formation of di- and oligo-tyrosine linkages; while the cross-linking of peptide AG-10, which does not contain tyrosine residues, was achieved only in the presence of ferulic acid (FA) as reaction mediator.

Grafting of FA reactive sites on proteins via amidation followed by *Trametes versicolor* laccase -catalyzed cross-linking was performed on compact globular proteins, LZM and ovalbumin (OVA). The substrate reactivity and cross-linking efficiency of FA-modified LZM and OVA was improved as compared to their native forms. Polymerization was achieved by FA-modified LZM, whereas oligomers were the main cross-linked products of FA-OVA. The grafted FA-associated cross-links of the products were characterized using mass spectrometry, which were predominated by the form of 8-5' dehydrodiferulic acid. FA grafting/laccase-cross-linking treatment enhanced the emulsification performance of LZM and the foaming capacity of OVA. Furthermore, the cross-linked proteins (particularly LZM) exhibited lower immunoglobulin E binding capacity (up to 50% reduction) than the native forms, indicating current cross-linking treatment is able to decrease their allergenicity.

In light of our findings on the crosslinking of ST-10 peptides derived from potato patatin, a study on the cross-linking of potato proteins was carried out using laccases from *T. versicolor* and *Coriolus hirsutus* with or without the presence of FA. Higher catalytic efficiency of laccases was shown towards potato protein fraction (PAT) containing patatin, whereas smaller-sized potato protease inhibitor fraction (PIs) were faster in forming oxidative cross-linked products. The cross-linking extent was impacted by the type of laccase and the use of FA. The increase in reaction time up to 24h resulted in the shifting of the cross-linked products towards higher molecular weight, while the extended treatments (48h) led to precipitation or oxidative fragmentation.

The conjugation of PAT with selected pectic polysaccharides via laccase-catalyzed reaction was further investigated and modulated using response surface methodology (RSM) to achieve product with defined conjugation extent and emulsification performance. The highest hetero-conjugation efficiency was shown by *C. hirsutus* laccase-PAT/sugar beet pectin (SBP) reaction system. The developed predictive models revealed that PAT ratio in PAT/SBP mixture was correlated negatively with the conjugation extent but positively with the emulsification performance, and these correlations were affected by the interaction between PAT ratio and enzyme concentration or reaction time

The effect of laccase-catalyzed modification on functionality profile of potato proteins was assessed by correlating the interfacial properties with cross-linking/conjugation extent, product profile, protein unfolding, secondary structure composition and incorporation of ferulic acid. The oxidative cross-linking improved the emulsifying property of both PAT and PIs, while short time treatment and product profile with enriched 60-80 kDa fraction was associated with enhanced foaming property in PAT. The PATs conjugated with SBP had relatively low surface tension as compared to the native and cross-linked PATs at neutral pH; however, the resulted interfaces were characterized by low elasticity. The highest surface dilatational elasticity of the protein samples at neutral pH was observed with cross-linked PAT obtained from 24h reaction without FA. Extended treatments for 48h led to both cross-linking and fragmentation of PAT; the resulted products showed a higher structural stability and contributed to the low susceptibility of the interfacial behaviour of PAT to acidic pH and to relatively high surface dilatational elasticity.

RESUME

La laccase (E.C 1.3.10.2) est un biocatalyseur polyvalent, qui peut être utilisé pour la modification des protéines. Les cinétiques des bioconversions des substrats-modèles dérivés des protéines par les laccases ont été étudiées, afin de contribuer à la compréhension du mécanisme d'action de la laccase pendant la réticulation des protéines. Les laccases fongiques ont été caractérisées par une spécificité plus élevée vis-à-vis des substrats modèles peptidiques (K_m=0,17-0,67mM, k_{cat}/K_m=0,56-0,81$s^{-1}mM^{-1}$) ST-10 (SYMTDYYLST), dérivé de la patatine de pomme de terre, et AG-10 (AKKIVSDGNG), dérivé du lysozyme de blanc d'oeuf (LZM), en comparaison avec la tyrosine (Y) (K_m =1,10-1,12 mM, k_{cat}/K_m=0,01-0,31 $s^{-1}mM^{-1}$). Ces résultats ont été confirmés par l'étude moléculaire « Docking », dans laquelle des modes de liaison substrat/enzyme ayant une meilleure affinité ont été observés pour laccase/peptides que pour laccase/tyrosine. La réaction catalysée par la laccase a conduit à une réticulation du peptide ST-10 contenant de la tyrosine via la formation des liaisons de di- et oligo-tyrosine ; tandis que la réticulation du peptide AG-10, qui ne contient pas de résidu tyrosine, n'a pas pu être accomplis qu'en présence d'acide férulique (AF) comme médiateur de réaction.

Le greffage des sites réactifs du AF sur les protéines via amidation suivi d'une réticulation catalysée par la laccase de *Trametes versicolor* ont été réalisés sur des protéines globulaires compactes, LZM et ovalbumine (OVA). La réactivité du substrat et l'efficacité de la réticulation des LZM et OVA modifiées par AF étaient plus élevées en comparaison avec leurs formes natives. LZM modifiée par AF a été polymérisée, tandis que des oligomères étaient les principaux produits réticulés de AF-OVA. Les réticulations formées au niveau des greffés AF ont été caractérisées par la spectrométrie de masse, par laquelle la forme d'acide 8-5' déhydrodiférulique était identifiée comme étant la plus prédominante. Le traitement de greffage avec AF suivi de la réticulation avec laccase a amélioré la performance émulsifiante du LZM et la capacité moussante de l'OVA. De plus, les protéines réticulées présentaient une capacité de liaison aux immunoglobulines E plus faible (jusqu'à 50% de réduction pour LZM) que les formes natives, ce qui indique que le traitement de réticulation des protéines modifiés est capable de diminuer l'allergénicité.

À la lumière de nos résultats sur la réticulation des peptides ST-10 dérivés de la patatine de pomme de terre, une étude sur la réticulation des protéines de pomme de terre a été réalisée en utilisant des laccases de *T. versicolor* et *Coriolus hirsutus* avec ou sans présence d'AF. Les laccases ont montré une efficacité catalytique plus élevée vis-à-vis de la fraction de protéine de pomme de terre (PAT) contenant de la patatine, alors que l'utilisation de la fraction

contenant des inhibiteurs de protéase de pomme de terre (IP) a conduit à une formation rapide des produits de la réticulation oxydative. Le dégrée de réticulation a été affectée par le type de laccase et la présence de AF. L'augmentation du temps de réaction jusqu'à 24h a entraîné le déplacement des produits réticulés vers un poids moléculaire plus élevé, tandis qu'un traitement prolongé (48h) a entraîné une précipitation ou une fragmentation oxydative.

La conjugaison de PAT avec des polysaccharides pectiques sélectionnés à travers une réaction catalysée par la laccase a été étudiée et modulée en utilisant une méthodologie de surface de réponse (RSM) pour obtenir un produit avec un dégrée de conjugaison et de performance émulsifiante bien définie. L'hétéro-conjugaison la plus élevée a été obtenue lors de l'utilisation du système réactionnel composé de *C. hirsutus* laccase-PAT/pectine de betterave sucrière (SBP). Les modèles prédictifs développés ont révélé que la proportion de PAT dans le mélange PAT/SBP était corrélée négativement avec l'étendue de la conjugaison mais positivement avec la performance émulsifiante, et ces corrélations étaient affectées par l'interaction entre la proportion de PAT et la concentration enzymatique ou le temps de réaction

L'effet de la modification catalysée par la laccase sur le profil de fonctionnalité des protéines de pomme de terre a été évalué en corrélant les propriétés interfaciales avec l'étendue de la réticulation/conjugaison, le profil du produit, le déploiement des protéines, la composition de la structure secondaire et l'incorporation d'acide férulique. La réticulation oxydative a amélioré la propriété émulsifiante du PAT et d'IP. Un traitement de courte durée et l'enrichissement avec des produits ayant 60 - 80 kDa ont été associés avec l'amélioration de la propriété moussante de PAT. À pH neutre, PAT conjugué avec SBP a montré une tension superficielle relativement faible par rapport aux autres PAT natif et réticulés. Cependant, les interfaces résultantes ont été caractérisés par une faible élasticité. L'élasticité de dilatation de surface protéique la plus élevée à pH neutre a été observée pour le PAT réticulé obtenu à partir d'une réaction de 24h sans AF. Les traitements prolongés pendant 48 h ont entraîné à la fois la réticulation et la fragmentation du PAT. Les produits de PAT résultants de ces modifications ont démontré une stabilité structurelle plus élevée, et ont contribué à réduire la sensibilité des propriétés interraciales du PAT au pH acide et à l'élasticité relativement élevée du dilatation de surface.

STATEMENT FROM THE THESIS OFFICE

According to the regulation of the Faculty of Graduate Studies and Research of McGill University, Guidelines for Thesis Preparation include:

Candidates have the option of including, as part of the thesis, the text of one or more papers submitted, or to be submitted for publication, or the clearly-duplicated text of one or more published papers. These texts must conform to the "Guidelines for Thesis Preparation" and must be bound together as an integral part of the thesis.

The thesis must be more than a collection of manuscripts. All components must be integrated into a cohesive unit with a logical progression from one chapter to the next. In order to ensure that the thesis has continuity, connecting texts that provide logical bridges between the different papers are mandatory.

The thesis must conform to all other requirements of the "Guideline for Thesis Preparation" in addition to the manuscripts.

As manuscripts for publication are frequently very concise documents, where appropriate additional material must be provided in sufficient detail to allow a clear and precise judgement to be made of the importance and originality of the research reports in the thesis.

In general when co-authored papers are included in a thesis, the candidate must have made a substantial contribution to all papers included in the thesis. In addition, the candidate is required to make an explicit statement in the thesis as to who contributed to such work and to what extent. This statement should appear in a single section entitled "Contribution of Authors" as a preface of the thesis.

When previously published copyright material is presented in a thesis, the candidate must obtain, if necessary, signed waivers from the co-authors and publishers and submit these to the Thesis Office with the final deposition.

CONTRIBUTION OF AUTHORS

This thesis is composed of nine chapters.

Chapter I introduces general background, research rational and the objectives of current research.

Chapter II presents a comprehensive literature review on the importance of protein modification in food processing, the molecular structure/biocatalytic efficiency/mechanism of laccase, the versatile roles of laccase in protein modification, and the analytical techniques for modified proteins (cross-linked/conjugated protein) characterization.

Chapter III to VII are presented in the form of manuscripts and have been either submitted or prepared for publication. The connecting statements provide rational associations between each chapter. Chapter III provides mechanistic insights of laccase-catalyzed cross-linking of protein-related substrate models through enzyme kinetic study, molecular docking analysis, reaction time course and product profile characterization. Chapter IV, with the aim of understanding effects of the structure of protein substrates to the catalytic efficiency of laccase, reports the cross-linking of egg white lysozyme and ovalbumin via phenolic grafting followed by laccase-catalyzed reaction and the assessment of the emulsifying, foaming property and allergenicity of the cross-linked proteins. Chapter V demonstrates the modification of potato protein via laccase-catalyzed cross-linking reactions and the effects on the secondary structure and functionality profiles (solubility, foaming, emulsifying and antioxidant property). Chapter VI continues the discussion in the modification of potato protein via the conjugation with polysaccharides catalyzed by laccase and the modulation of the reaction to obtain conjugates with enhanced emulsification performance. Finally, the impacts of different laccase-catalyzed modification approaches on the structural and interfacial property of potato protein are summarized in Chapter VII.

Chapter VIII provides a general conclusion for this work.

Chapter VIIII describes the contribution and novelty of this work and recommendation for future works in protein modification using laccase-biocatalytic approaches.

Mingqin Li, the author of the thesis, was responsible for the experimental work and the preparation of the thesis and of the manuscripts for publication.

Dr. Salwa Karboune, the supervisor of the author's PhD study, guided all the research work and critically revised all manuscripts prior to their submission.

Dr. Lan Liu, the second author of manuscript #1 (Chapter III) and #2 (Chapter IV), performed mass spectrometry analysis and protein chemical modification and revised the manuscripts for publication.

Dr. Selim Kermasha, the co-supervisor of the author's PhD study and the third author of manuscript #1 (Chapter III), revised the manuscript for publication.

Dr. Lamia L'hocine, Dr. Allaoua Achouri and Ms. Melanie Pitre, co-authors of manuscript #2 (Chapter IV), contributed to assessment of foaming property and allergenicity.

Kelly Light, co-author of the manuscript #2 (Chapter IV), performed protein chemical modification and chemical characterization of the phenolic grafted proteins.

Dr. Cesar Mateo, co-author of manuscript #2 (Chapter IV), provided training and technical support in protein chemical modification.

Dr. Christophe Blecker, second author of manuscript #5 (Chapter VII), performed the assessment of interfacial property and revised the manuscript for publication.

PUBLICATIONS

1. Li, M., Liu, L., Kermasha, S., & Karboune, S. (2020). Laccase-catalyzed oxidative cross-linking of tyrosine and potato patatin- and lysozyme-derived peptides: molecular and kinetic study. *Enzyme and Microbial Technology*. (Under review)

2. Li, M., Liu, L., L'Hocine, L., Achouri, A., Pitre, M., Light, K., Mateo, C., & Karboune, S. (2020). Combining protein surface modification and laccase-catalyzed cross-linking of egg white proteins: structural, functional properties and allergenicity. *Journal of Agricultural and Food Chemistry*. (Submitted to the Journal)

3. Li, M., & Karboune, S. (2020). Oxidative cross-linking of potato proteins by fungal laccases: modification efficiency, structural and functional properties of modified proteins. (To be submitted)

4. Li, M., & Karboune, S. (2020). Laccase-catalyzed conjugation of potato protein with selected pectic polysaccharides: conjugation efficiency and emulsification properties. *Food Chemistry*. (Under review)

5. Li, M., Blecker, C., & Karboune, S. (2020). Molecular and air-water interfacial properties of potato protein upon modification via laccase-catalyzed cross-linking and conjugation with sugar beet pectin. *Food Hydrocolloids.* (Under review)

ACKNOWLEDGEMENT

First of all, I would like to express my sincere gratitude to my supervisor, Dr. Salwa Karboune. Her dedication, patience and careful guidance supported me towards the accomplishment of my PhD study.

I would like to extend my appreciation to my co-supervisor, Dr. Selim Kermasha, for his enlightened suggestions during my study.

I am grateful to Dr. Christophe Blecker and his team, Dr. Lamia L'hocine, Dr. Allaoua Achouri and Ms. Melanie Pitre for their contribution and technical supports in valuable contents in my dissertation, and to Dr. Catherine Humeau, Dr. Latifa Chebil and Dr. Mohamad Ghoul (Université de Lorraine, Nancy, France) and Dr. Cesar Mateo (Instituto de Catálisis-CSIC, Madrid, Spain) for hosting me and providing me with valuable internship/research experience in their institutes.

I would like to thank the faculty of food science for offering a great platform for me to learn and progress.

I would like to thank all my friends and colleagues, Dr. Nastaran Khodaei, Dr. Amanda Waglay, Dr. Jin Li, Afshan Malick, Neeyal Appanah, Erin Davis, Lily Chen, Dr. Juan Pablo Carrillo, Dr. Nausheen Said, Marina Nguyen, Amal Sahyoun, Mehdi Sirouspour and Elham Chidar for their constant friendship and endless supports during the six years of life in our lab. Particularly, I would like to acknowledge Dr. Sooyoun Seo, Dr. Andrea Hill and Dr. Juan Tamayo for tutoring and working with me at the beginning of my study; Dr. Lan Liu for her involvement and professional supports in my research project; Marika Houde for her contribution to improve my written English; Kelly Light and Rami Bahlawan for their delightful teamwork in many experiments.

I wish a deep thank you to my colleague/best friend/husband, Eugenio Spadoni Andreani, for his encouragement, care and love. It is treasurable experience of working hard towards our common professional and life goals together.

Last but not least, I cannot thank enough my beloved parents for their unconditional love and supports.

TABLE OF CONTENTS

LIST OF FIGURES

CHAPTER II

CHAPTER III

LIST OF TABLES

NOMENCLATURE/LIST OF ABBREVIATIONS

AG-10	Peptide model of lysozyme, AKKIVSDGNG
ST-10	Peptide model of potato patatin, SYMTDYYLST
LacTv	Laccases from *Trametes versicolor*
LacCh	Laccases from *Coriolus hirsutus*
FA	Ferulic acid
ABTS	2,2'azino-bis(3-ethylbenzothiazoline-6-sulfonic acid
HIS	Histidine
ASP	Aspartic acid
ASN	Asparagine
TYR/Y	Tyrosine
SE-HPLC	Size exclusion- high performance liquid chromatography
RP-HPLC	Reverse phase-high performance liquid chromatography
MW	Molecular weight
LC-MS	liquid chromatography -mass spectrometry
ESI	Electrospray ionization
QTOF	Quadruple-Time-of-Flight
LZM	Lysozyme
OVA	Ovalbumin
NHS	N-hydroxysuccinimide
EDCI	1-ethyl-3-(3-dimethylaminopropyl) carbodiimide hydrochloride
TNBS	2,4,6-Trinitrobenzene Sulfonic Acid
EA	Emulsifying activity
ES	Emulsion stability
IgE	Immunoglobulin E
ELISA	Enzyme linked immunosorbent assay
HCl	Hydrochloric acid
NaCl	Sodium chloride
TMB	3,3′,5,5′-tetramethylbenzidine
SDS-PAGE	Sodium dodecyl sulfate - polyacrylamide gel electrophoresis
FE	Foam expansion

G_i	Percentage of gas entrapped in the foam
R_5	Percentage of liquid retained in the foam after 5 min
PAT	Patatin-containing potato protein fraction
PIs	Potato protease inhibitors fraction
FTIR	Fourier transform infrared spectroscopy
FPLC	Fast protein liquid chromatography
PPT	Potato protein
PPS	Pectic polysaccharides
HG	Homogalacturonan
RG	Rhamnogalactorunan
SBP	Sugar beet pectin
CV	Column volume
RI	Refractive index
EAI	Emulsifying activity index
RSM	Response surface methodology
CCRD	Central composite rotatable design
PDI	Polydispersity index
MPPT	Modified potato protein
DSC	Differential scanning calorimetry
NaOH	Sodium hydroxide

CHAPTER I. GENERAL INTRODUCTION

With growing awareness of healthy diet, consumers and food industry have turned towards natural, “clean”, low sugar/fat and nutritious food products with good texture and taste. In addition to their nutritional attributes, proteins exhibit selected techno-functional properties that make them attractive alternatives to low quality food additives in various food formulations. Indeed, a wide range of techno-functional properties can be simultaneously offered by protein ingredients, as results of their water binding, structuring (aggregation, gelation) and interfacial (foaming, emulsifying) properties (Foegeding & Davis, 2011; Sun-Waterhouse et al., 2014). All these techno-functional properties of proteins are dictated by their molecular (amino acid sequence, secondary/ternary structure, molecular weight, shape, flexibility and etc.) and physicochemical properties (solubility, hydrophobicity, isoelectric points, net charge and etc.) (Mirmoghtadaie et al., 2016; Sun-Waterhouse et al., 2014; Zeeb et al., 2017). In order to promote the use of protein ingredients in the design of healthy innovative food products, the modulation of their molecular and physicochemical properties through protein modification has attracted a high interest in food science field.

Potato protein is particularly attractive as a plant-based protein as it is nutritionally comparable to eggs in terms of amino acid profile and has higher essential amino acid content than other proteins from plant sources (Glusac et al., 2017; Gorissen et al., 2018). The potential nutraceutical properties of potato protein (e.g. antioxidant and anti-carcinogenic activity) have also been proven (Kowalczewski et al., 2019; Waglay & Karboune, 2016b). The use of the dry matter of potato juice, which is a major by-product from starch industry as a source of potato protein, can contribute to the sustainable aspect of this food ingredient (Kowalczewski et al., 2019; Løkra & Strætkvern, 2009). However, the relatively low denaturation temperature (59-66 °C) of potato protein limits its application in food processing (Creusot et al., 2011; Van Koningsveld et al., 2001). To enhance the properties of potato protein, the enzymatic hydrolysis and the glycation via Maillard reaction have been investigated as protein modification approaches. Enzymatic hydrolysis enhanced the solubility of potato protein at low pH range and its foaming/emulsification capacity, while the improvement in emulsion stability was achieved by the hydrolysis at low extent (Akbari et al., 2020). The glycation of potato protein with galactoligosaccharide or galactan via Maillard reaction improved its thermal stability, while the glycation with galactose increased its ability to stabilize emulsion at acidic pH (Seo et al., 2014). As far as we are aware, only very limited studies have investigated protein cross-linking to enhance the network formation in emulsion/gel systems (Glusac et al., 2017; Gui et al., 2020).

The crosslinking and the conjugation of proteins through laccase-catalyzed oxidative reactions have the advantages of mild reaction conditions and versatility. Laccase (EC 1.10.3.2), an oxidoreductase, is able to oxidize a variety of substrates (e.g. phenolic compounds and diamines) into reactive radicals, which can undergo polymerization and/or depolymerization (Minussi et al., 2002; Rivera-Hoyos et al., 2013). Due to the broad substrate specificity, laccase is capable in catalyzing homo-cross-linking of proteins and hetero-conjugation of protein with other biopolymers (e.g. polysaccharides, polyphenols) via their inherent reactive moieties (Buchert et al., 2010; Isaschar-Ovdat & Fishman, 2018). As the oxidative action of laccase can be limited by the bulky and compact structure of proteins, their cross-linking/conjugation catalyzed by laccases can be promoted by small phenolic compounds acting as mediators (Selinheimo et al., 2008; Steffensen et al., 2009). Furthermore, the enrichment of protein surface with phenolic moieties via bioconjugation was also found to enhance effectively the substrate reactivity, the cross-linking efficiency and the reaction selectivity (Ma et al., 2011). Although laccase-catalyzed oxidative crosslinking or conjugation has been identified as a potential approach for protein modification, the mechanistic action of laccase, and the structure-function relationships of the modified proteins are still not fully understood. In addition, protein fragmentation can happen as a side reaction of laccase-catalyzed modification, which may be undesirable for certain food applications (Lantto et al., 2005; Mokoonlall, Sykora, et al., 2016). To better exploit the laccase-based biocatalytic approaches in modifying new sources of proteins, efforts need to be devoted to the understanding of the enzyme kinetics and the mechanistic action of laccases on different proteins (globular, compact vs flexible, with exposed reactive sites) as well as to the modulation of the reaction selectivity towards the targeted end-products. The understanding of the relationship between protein reactivity and the efficiency of laccase-catalyzed cross-linking is expected to lay the ground for tailoring protein techno-functionalities for specific applications.

The overall objective of the present research is to develop novel biocatalytic approaches based on laccase-catalyzed reactions to produce cross-linked proteins and protein/polysaccharide conjugates with improved functionalities. The enzymatic modification was performed on different proteins and protein-related substrates including potato proteins, lysozyme, ovalbumin, peptide substrate models and tyrosine. Prior to investigating the protein modification, laccase-catalyzed oxidative cross-linking of peptide models was carried out to gain insight into the mechanistic action of laccase-catalyzed reaction at molecular level. The effects of selected reaction parameters on the efficiency of laccase-catalyzed reactions were

studied, and the produced modified proteins were characterized in terms of structural and techno-functional properties.

The specific objectives of this study were as follows:

1) Mechanistic study of laccase-catalyzed oxidative cross-linking of substrate models (peptide models and tyrosine) via computational analysis, kinetic study and characterization of the bioconversion yield and the end-product profiles;
2) Improvement of laccase efficiency in the cross-linking of egg white lysozyme and ovalbumin via substrate engineering, and evaluation of the effect of the modification extent (incorporation of phenolic moiety) on the protein cross-linking catalyzed by laccase, and the effect of cross-linking on the functionality of the proteins;
3) Study of laccase-catalyzed cross-linking of potato protein and characterization of structural and functional properties of the product;
4) Investigation of laccase-catalyzed conjugation of potato protein with selected polysaccharides and optimization of the conjugation and emulsification performance of the conjugates;
5) Elucidation of the relationship between the structural properties and the air-water interfacial behaviors of selected modified potato proteins.

CHAPTER II. LITERATURE REVIEW

2.1. Introduction

Protein modification is an essential tool in food processing to tailor the functionality of protein ingredients and to enhance food quality. Among numerous protein modification techniques, enzymatic modification using laccase is attractive due to the versatility and specificity of this "green" biocatalytic process. This literature review covers common protein modification approaches, the biocatalysis of laccase and protein modification catalyzed by laccase. In addition, analytical techniques for the structural analysis of proteins are summarized.

2.2. Protein modification to improve its value as functional ingredients

The increasing demand for food products of healthy choice triggers the development of novel protein-based food ingredients with improved nutritional value and techno-functional properties (Liu et al., 2017; Liu et al., 2019). However, due to the susceptibility of proteins, the changes in microenvironment (pH, temperature, ionic strength, medium/solvent type, pressure) and processing and storage history can result in changes in protein functionalities and ultimately affect quality of the protein-containing foods (Zayas, 1997). In addition, protein allergenicity and the anti-nutritional factors of proteins should be addressed prior to application. Protein modification, which is an intervention strategy to cause molecular and physicochemical changes on proteins to adjust their structures and functionalities, is necessary for the thorough exploitation of the functionalities and values of protein ingredients (Feeney, 1977). Common examples of protein modification in the food industry are physical treatments (e.g. high hydrostatic pressure treatment and extrusion) (Elahi & Mu, 2017; Mirmoghtadaie et al., 2016), chemical treatments (e.g. Maillard type-glycation and free-radical grafting/cross-linking) (Jia et al., 2019; Liu, Sun, et al., 2015; Seo et al., 2014) and enzymatic treatments (hydrolysis by proteolytic enzymes and transglutaminase/oxidoreductase-catalyzed cross-linking) (Gao et al., 2019; Heck et al., 2013; Wouters et al., 2017). Physical/chemical treatments are straightforward and convenient, while enzymatic approaches are carried out under mild conditions and exhibit high specificity and low toxicity. Shown in Table 2.1 are some emerging protein functional ingredients and the modification approaches that have been applied to address their functional limitations. In addition, protein modification via hydrolysis, cross-linking and conjugation was discussed further below.

Table 2.1. A summary of functional protein ingredients from conventional and innovative sources and their modification strategies

Proteins	properties and functionalities	Limitation in application	Modification strategies	References
Fish gelatin	High digestibility as compared to those from mammal sources; good solubility and gelling property; formation of edible, biodegradable film & hydrogel	low mechanical property and water resistance; gel is sensitive to heat	Forming electrostatic composite with polysaccharide; cross-linking by glutaraldehyde; transglutaminase-catalyzed cross-linking	Fan et al. (2018); Gómez-Estaca et al. (2011); Zhang et al. (2017)
Casein	Source of bioactive peptide (antioxidant, hypertensive and anti-inflammatory properties); ingredients for hydrogel /film /nanoparticles as carriers for bioactive compounds	potential in cow milk (***β***-casein)	Hydrolysis by serine protease; laccase/tyrosinase catalyzed cross-linking with the presence of caffeic acid	Dabrowska et al. (2020); Ranadheera et al. (2016); Stanic et al. (2010)
Whey protein (***α***-lactalbumin, ***β***-lactoglobulin)	Source of bioactive peptide (Anti-cancer property); emulsifier in food	Contains allergen (***β***-lactoglobulin); limited emulsifying ability at pH <5 and emulsion stability; low elastic gel	Laccase-catalyzed cross-linking in combination with plant phenolic extracts or ferulic acid, and/or high pressure homogenization pre-treatment; laccase-catalyzed conjugation with sugar beet pectin; protease-hydrolysis prior to gelation	Jiang et al. (2017); Ma et al. (2011); Spotti et al. (2017); Tantoush et al. (2011); Gazme et al. (2014)
Potato protein	Balanced amino acid profile, source of bioactive peptides; hypoallergenic, protein supplement in infant formula; diverse functionality profile including gelling, emulsification and foaming property	Low solubility; low denaturing temperature; functional property varied by extraction process	Glycation via Maillard reaction; acetylation; high hydrostatic pressure treatment; transglutaminase/oxidoreductases-catalyzed cross-linking	Elahi and Mu (2017); Glusac et al. (2017); Gui et al. (2020); Seo et al. (2014)
lysozyme from egg white	Antimicrobial activity against Gram positive bacteria, natural food preservative; source of bioactive peptides; highly water-soluble;	Inhibiting only gram-positive bacteria; poor emulsifying property; low surface hydrophobicity	Conjugation with polysaccharides (chitosan, mannose, gums) via Maillard reaction; short time heat treatment (80-90 °C) at neutral pH; Pepsin-trypsin-catalyzed hydrolysis	Ibrahim et al. (1996); Mine et al. (2004); Song et al. (2002); You et al. (2010)

Soy protein	Rich source of lysine; biological activity includes alleviating the symptoms of menopause, preventing breast cancer; important protein ingredients for meat analog, gluten free product; can be used as emulsifier and stabilizer of colloidal system	Allergen; limited functional property due to large molecular size and low solubility	Ultrasound treatment under alkaline condition; tyrosine-catalyzed cross-linking with or without the presence of caffeic acid	Isaschar-Ovdat et al. (2016); Isaschar-Ovdat et al. (2015); Lee et al. (2016)
Wheat protein	Satiating property, rich source of sulfur containing and branched-chain amino acids; protein supplement for muscle building; forming networks with unique viscoelasticity; excellent water holding capacity; used as texturizing protein for meat/fish composite product	can trigger immunological reactions for celiac patients; low digestibility; low solubility; limited emulsifying/foaming property	Pepsin, trypsin, fungal protease or corolase-catalyzed hydrolysis; deamidation, conjugation with maltodextrin or citrus pectin via Maillard reaction	Bouferkas et al. (2019); DragoGonzález (2000); Flambeau et al. (2017); Wang, Gan, et al. (2019); Wang, Gan, et al. (2017)
Rice protein	High level of lysine and threonine; hypoallergenic ingredient, protein supplement in infant formula; anti-cancer activity; stabilizer for meat batter	Low solubility and emulsifying stability	Alcalase, flavourzyme-catalyzed hydrolysis; phosphorylation	Gomes and Kurozawa (2020); Hu et al. (2019)
Oat protein	Balanced amino acid profile, low allergenicity, high digestibility; promising gelling ability, structure building ingredient for gluten-free products	Relatively low emulsifying stability; insufficient gel viscoelasticity as compared to gluten	Amidation; flavourzyme, alcalase, pepsin and trypsin-catalyzed hydrolysis; tyrosinase, laccase-catalyzed cross-linking	Flander et al. (2011); Makinen et al. (2011); Nieto-Nieto et al. (2014)
Pea protein	High content of lysine and tryptophan; Egg replacer, texturalizer and emulsifier	Weak and low elastic gel; very hydrophobic, low heat stability	Combined endopeptidase-hydrolysis with transglutaminase-cross-linking; phosphorylation	Liu et al. (2019); Ribotta et al. (2012)

2.2.1. Protein hydrolysis

Protein hydrolysis is able to reduce the size of protein to modify its functionality and enhance its bioavailability and bioactivity (Daliri et al., 2017; Jung et al., 2005). Proteolytic reactions using proteases or peptidases are common approaches in protein hydrolysis, and has advantages such as low adverse effects, a high degree of specificity and predictability over hydrolysis with microbial fermentation or chemical approaches (Daliri et al., 2017; Lamsal et al., 2006). The properties of the protein hydrolysate are greatly dependent on the degree of hydrolysis (DH), which can be modulated via the reaction parameters such as pH, temperature, enzyme/substrate ratio (Nwachukwu & Aluko, 2019). The protein hydrolysate at low DH, from 1 to 10 %, were generally proposed for techno-functional usage, which were shown to have improved solubility, emulsification capacity, foaming and emulsion stability and viscosity as compared to the intact proteins (Jung et al., 2005; Lamsal et al., 2006; Rodriguez Patino et al., 2007; Wang & Wang, 2009). Furthermore, when the DH was more than 10%, the short-chain peptides in the protein hydrolysates are potential bioactive compounds, which have been chosen over other natural or synthetic compounds as antioxidant, antimicrobial reagent or nutraceuticals in functional food products. (Rodriguez Patino et al., 2007; Xia et al., 2012).

2.2.2. Protein cross-linking

Protein crosslinking refers to the process of forming intermolecular covalent bonds between protein molecules or constructing protein biopolymer networks in food matrices (Heck et al., 2013). It is a useful tool to generate new macro-molecules or biopolymers with modified physicochemical properties and techno-functional properties and adjust food texture and structure without changing the nutritional composition (Buchert et al., 2010; Dube et al., 2006). Heating, alkaline, photooxidative treatment and enzymatic treatments can result in protein cross-linking (Heck et al., 2013). Different chemical cross-linkers, varying in reactivity, functionality and size, can be used to induce protein cross-linking. Glyceraldehyde, glutaraldehyde and carbodiimides are common crosslinking reagents for chemical modification in food processing (Caillard et al., 2008; Daliri et al., 2017; Kuijpers et al., 1999). Cross-linking enzymes that are commonly seen in food applications include transglutaminase, peroxidase, laccase and tyrosinase. The crosslinking reaction catalyzed by transglutaminase (EC 2.3.2.13) is initiated when the carboxyl group of protein forms a thioester intermediate with the enzyme, which is subsequently replaced by amine in another protein via nucleophilic attack forming iso-peptide cross-links (Heck et al., 2013). Transglutaminase, known as “natural glue”, is

commercially applied for the texturization and structuring of innovative proteinaceous matrix as per in high quality vegan fish/meat analog, gluten-free and low-fat products and biodegradable films for food packaging (Kieliszek & Misiewicz, 2014; Zhang et al., 2018). Transglutaminase was also involved in the exploitation of proteins from innovative sources (such as rice, pea, sunflower and by-products etc.), to enhance the stability, water binding capacity and nutritional quality to the proteins (Dube et al., 2006; Kieliszek & Misiewicz, 2014). In addition, the protein cross-linking catalyzed by transglutaminase was associated with high satiation and low postprandial glucose response, which may have potential application in products for weight-management or metabolic regulation (Cassie et al., 2017; Juvonen et al., 2015). Peroxidase, laccase and tyrosinase belong to the oxidoreductase family. Protein cross-linking by oxidoreductases generally involves two sequential steps: 1) the catalysis of primary substrates by the enzyme, generating reactive intermediates such as phenoxy radicals, quinones, semiquinones and aldehydes; 2) non-enzymatic coupling of the resulting reactive species (Heck et al., 2013). Oxidoreductases act on phenolic moieties of proteins, polysaccharides and polyphenols as well as other reactive sites such as indoles, amines and thiols, and the oxidation resulted in a mixture of cross-linked products due to the radical nature of the process (Buchert et al., 2010). The broad substrate specificity of oxidoreductases endorses their wide application (Isaschar-Ovdat & Fishman, 2018). As compared to transglutaminase, the cross-linking catalyzed by oxidoreductases is not limited by the primary or three-dimensional structure of proteins (Jus et al., 2012). In addition, the oxidoreductase-treated proteins showed enhanced antioxidative capacity, higher *in-vitro* digestibility and improved interfacial properties (Hiller & Lorenzen, 2009; Tantoush et al., 2011).

2.2.3 Protein-carbohydrate conjugation

The formation of covalent bonds between protein and carbohydrate molecules was often carried out by chemical or enzymatic treatments. Maillard reaction is an established chemical approach to achieve food protein glycation. It can happen under controlled water activity, and the glycation extent is determined by temperature and reaction time (Liu et al., 2012). Protein glycation via Maillard reaction was reported to contribute to the techno-functional properties, such as solubility, emulsifying property, foaming stability, antioxidant property and has the potential to increase prebiotic activity (Liu et al., 2012; Seo et al., 2012; Sheng et al., 2020; Ter Haar et al., 2011). The protein/polysaccharide conjugation can also be achieved with the use of transglutaminase and oxidoreductases (Flanagan & Singh, 2006; Selinheimo et al., 2008). Transglutaminase has been used for the formation of covalent linkages between proteins and

chitosan and other carbohydrate biopolymers with glucosamine residues, whereas oxidoreductases have catalyzed the conjugation between proteins and feruloylated oligosaccharide/polysaccharides (Isaschar-Ovdat & Fishman, 2018). Enzymatic conjugation can limit the production of undesired by-products such as unpredictable Amadori products from Maillard reaction (Liu et al., 2017). Enzymatic treatments can form protein/oligosaccharide or polysaccharide conjugates with enhanced emulsifying stability against extreme micro-environmental conditions such as low pH, heat, and freeze-thaw cycles (Chen et al., 2018; Liu, Qiu, et al., 2015). As well, the enzymatic conjugations are promising in the development of stable food/nutraceutical delivery systems.

2.2.4. Bioconjugation

Bioconjugation is the attachment of selected bioactive molecules or functional groups to protein (Hermanson, 2013). Protein molecules are rich in reactive functional groups available for bioconjugation, including reactive carboxylic acid, amines, amides, alcohols and thiols. Numerous pathways of protein bioconjugation have been developed for drug design, enzyme engineering and stabilization and for the synthesis of novel biopolymer based materials (Díaz-Rodríguez & Davis, 2011; Gunnoo & Madder, 2016; Hermanson, 2013; Spicer & Davis, 2014). N-hydroxysuccinimide (NHS) and/or carbodiimides (EDC), are two common acylating reagents. The carboxyl groups of a grafting compounds can be activated by NHS/EDC, followed by conjugation with the reactive primary amine on protein surface, without introducing the acylating reagents into the bioconjugation product. Previous studies have reported the NHS/EDC-mediated bioconjugation of fatty acids or phenolic acids and proteins to enhance biopolymer network formation (Aewsiri et al., 2011; Ma et al., 2011; Ye et al., 2019).

2.3. Laccase

Laccases (EC1.10.3.2), a type of multicopper oxidase, were first described in 1883 by Yoshida as a component of the resin duct from the lacquer tree *Rhus vernicifera* (Yoshida, 1883). Laccases from *Basidiomycetes* white rot fungi are widely studied and they can also be found in *Ascomycetes* fungi, bacteria, insect and other plants (Guimarães et al., 2017; Rivera-Hoyos et al., 2013). Naturally, laccases participate in plants' lignin biosynthesis and in the formation of UV-resistant spores in *bacillus* species (Giardina et al., 2010), whereas in fungi, laccases are the main enzymes involved in delignification as well as in the degradation of toxins of plant origin and tannins as part of the defense mechanism of the fungi (Riva, 2006). Laccases from

various white rot fungi have been widely study, as they have relatively high redox potential and stability, and their recovery and purification is relatively simple (Giardina et al., 2010; Guimarães et al., 2017; Rivera-Hoyos et al., 2013). In general, fungal laccases show optimal activity at acidic environments ranging from pH 3-7, whereas the optimal pH for plant laccases is slightly alkaline (Rivera-Hoyos et al., 2013). Ideal temperature conditions for fungal laccases range from 50 to 70°C (Guimarães et al., 2017). Laccases can oxidize phenolic compounds (ortho- or para-diphenols, polyphenols, aminophenols), aliphatic amines (aryl-diamines, polyamines) as well as some inorganic ions (Giardina et al., 2010; Riva, 2006; Rivera-Hoyos et al., 2013). Moreover, laccases can oxidize proteins and feruloylated carbohydrates and result in the cross-linking/conjugation of the biopolymers (Figueroa-Espinoza & Rouau, 1998; Mattinen et al., 2005; Steffensen et al., 2008). Due to the broad substrate specificity, laccase was involved in many biotechnological processes in food, pulp and paper, cosmetic, textile, pharmaceutical industries and in organic synthesis and bioremediation (Bilal et al., 2019; Guimarães et al., 2017; Kudanga et al., 2017; Kunamneni et al., 2008; Osma et al., 2010).

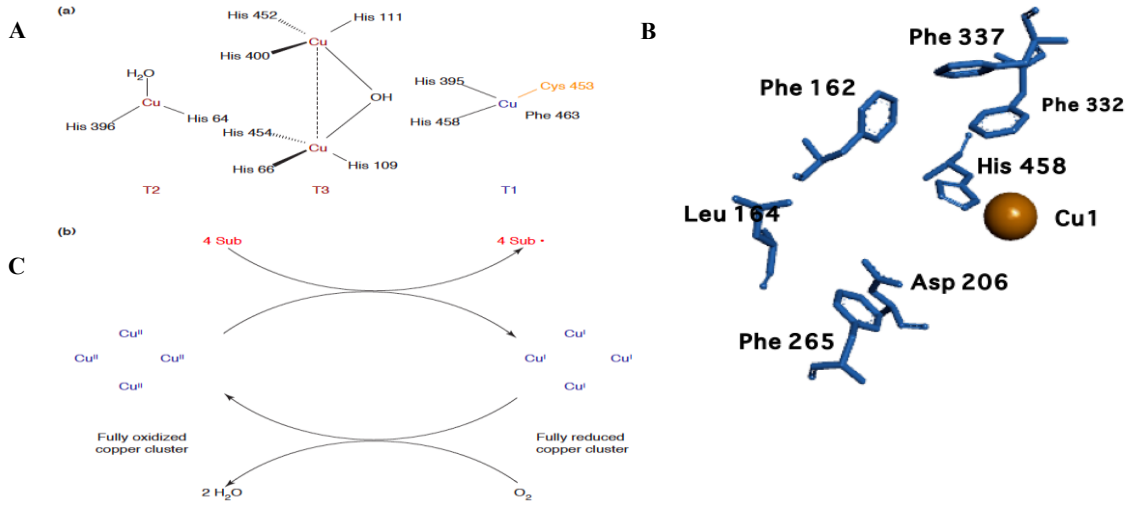

Scheme 2.1. Laccase active site (copper centers) (A) and catalytic cycle (B) (Riva, 2006), and important residues of the active site of *Trametes versicolor* laccase (PDB code: 1GYC)

2.3.1. Fungal laccase active site and redox potential

The active site of laccase is a cluster of four copper atoms (Scheme 2.1A): Type 1 (T1) copper center located at the surface center of laccase's catalytic cavity (Cu in blue); Type 2 (T2)/Type 3 (T3) copper center, a triangular shape trinuclear cluster (TNC) with one T2 copper and two

T3 coppers (Cu in red), were found behind the catalytic cavity of laccase (Riva, 2006). T1 copper is the primary electron acceptor and is coordinated to two histidine and one cysteine residues. The histidine residue (HIS458 of *Trametes versicolor* laccase), in front of the T1 copper atom, is the electron entry point, which interacts with substrate molecules via hydrogen bonding to initiate oxidation (Scheme 2.1B). The aspartic residue at the bottom of the active site (ASP206) can also form hydrogen bond with substrate, while phenylalanine and leucine residues surrounding the catalytic cavity interact with substrates via hydrophobic interactions; these are important residues stabilizing the enzyme-substrate binding and affecting the catalytic efficiency of laccase (Bertrand et al., 2002). After binding, the electrons from the substrates are transmitted via a histidine-cysteine-histidine tripeptide located behind the T1 copper to the TNC, where the reduction of oxygen molecules and release of water take place (Bertrand et al., 2002; Kunamneni et al., 2008) (Scheme 2.1C).

The redox potential E^0 of T1 copper center is a key indicator of laccase's catalytic efficiency. Despite laccases have similar distribution of copper redox centers, they possess very different E^0. Generally, fungal laccases exhibit a relatively high E^0 (700-800 mV), while a low redox potential is seen with plant laccases, for example, the E^0 of *Rhus vernicifera* laccase is approximately +400 mV (Rivera-Hoyos et al., 2013). Apart from the conformation of the copper center, the redox potential of laccases was shown to be affected by the interaction between neighboring amino acid residues of the T1 copper center (Matera et al., 2008; Piontek et al., 2002). The hydrogen bonding between GLU460 and SER113 in *T. versicolor* laccase resulted in the elongation of the distance between T1 copper and HIS458, which contributed to its high E^0 (+800 mV). Laccase from *Coprinus cinereus* showed 250 mV lower in E^0 than *T. versicolor* laccase, as it was absent with such hydrogen bonding interaction (Piontek et al., 2002). Moreover, Matera, et al. (2008) suggested that the hydrophobic interaction between PHE460 and ILE452, as well as the peripheral hydrophobic amino acid residues of the active site in laccase from *Trametes trogii* contribute to its high redox potential (+760mV) via enhancing the solvent accessibility and enzyme/substrate hydrogen bonding interaction.

2.3.2. Reaction mechanisms of laccase

During one catalytic cycle, each molecule of laccase is able to take up to four electrons in T1 center, resulting in the oxidation of four substrate molecules into substrate radicals, and the reduction of one molecule of oxygen to two molecules of water happens in T2/T3 center, which

is the sole by-products of the reaction (Giardina et al., 2010; Rivera-Hoyos et al., 2013). Due to the low redox potential of phenolic compounds/phenolic moieties, they can be easily oxidized by laccase and become phenoxy radicals. Depending on the reaction conditions, a mixture of diverse reaction pathways may happen to the phenoxy radicals including delocalization/rearrangement, coupling, C_α oxidation or degradation (Giardina et al., 2010). The low-degree oligomerized product were shown to be continuously oxidized by laccase thus undergo polymerization (Steffensen et al., 2008; Ward et al., 2001). The oxidation can be further extended to non-phenolic compounds, large complex molecules and/or compounds with a high redox potential with the use of mediators. Many compounds can be mediators for laccase-catalyzed reactions, including ABTS (2,2'-azino-bis(3-ethylbenzothiazoline-6-sulfonic acid), HBT (1-hydroxylbenzotriazole), anilines, 4-hydorxylbenzyl alcohols and natural phenolic compounds from plants, e.g. ferulic acid, p-coumaric acid, caffeic acid, and flavonoids (Kim & Cavaco-Paulo, 2011; Rivera-Hoyos et al., 2013; Selinheimo et al., 2008; Stanic et al., 2010). In the laccase-mediator reaction system (LMS), mediators are easily oxidized by laccase and serve as electron shuttles between the enzyme and the substrates of interest resulting in the oxidation of the targeted substrate (Kunamneni et al., 2008).

In protein-related substrates, tyrosine and cysteine residues are the most common sites for laccase-catalyzed oxidative cross-linking (Steffensen et al., 2009). Upon the oxidation catalyzed by laccase, tyrosine residues follow similar pathways as phenolic compounds, where different radicals can be generated via delocalization and coupled to each other (Mattinen et al., 2005) (Scheme 2.2). The cross-linking happens via dityrosine cross-links (C-C) between two radicals at their aromatic rings, or isodityrosine (C-O-C) ether cross-links, between one hydroxyl and one aromatic ring radicals. The latter form was reported to be more prevalent in protein cross-linking (Mattinen et al., 2005). As well, disulfide crosslinks can form between cysteine residues upon oxidation. However, studies reported different opinions about the oxidative-cross-linking mechanism (via direct oxidation by laccase vs LMS) of cysteine residue (Manhivi et al., 2018; Steffensen et al., 2009). Another reaction mechanism involving cysteine was proposed by Steffesen et al., (2009) , where the disulfide bond of cysteine dimer can be disassembled by phenolic mediators in the reaction thus allowing the formation of higher degree of cross-linked product (Scheme 2.3). Tryptophan residues were also reported to be oxidized by laccase into N′- formylkynurenine and further to kynurenine (Steffensen et al., 2008). Aside from cross-linking, proteins can be fragmented by laccase-catalyzed reactions as a result of steric hindrance against the formation of cross-links (Ercili Cura et al., 2009;

Steffensen et al., 2009). The laccase-catalyzed oxidative cross-linking of feruloylated polysaccharides were shown to happen on the ferulic ester functional groups. The dimerization of the polysaccharide was through different diferulic acid cross-links, including 5-5',8-O-4', 8-5' and 8-5' benzofuran dehydrodiferulic acid, and the formation of higher degree of cross-linked product were mainly through 8-O-4' and 5-5' dimer (Scheme 2.4) (Figueroa-Espinoza & Rouau, 1998; Zaidel & Meyer, 2012). In a polysaccharide/protein mixture, Selimheimo et al. (2008) proposed that hetero-conjugation could happen between a tyrosyl radical protein and phenoxy radical of polysaccharide (Scheme 2.5).

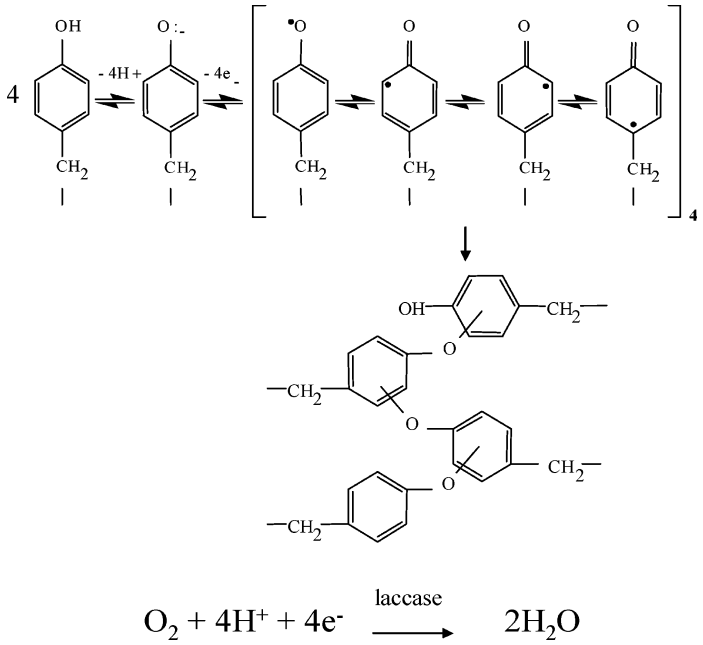

$$O_2 + 4H^+ + 4e^- \xrightarrow{\text{laccase}} 2H_2O$$

Scheme 2.2. Tyrosyl radicals generated by laccase-catalyzed oxidation and delocalization of tyrosyl radicals (Mattinen et al., 2005).

$$2\ PM + R - S - S - R \leftrightarrow 2R - SH + 2PM\bullet$$

Scheme 2.3. Antioxidant mechanism of ferulic acid on di-sulfide linkages (Steffensen et al., 2009). Abbreviation: PM, phenolic mediators.

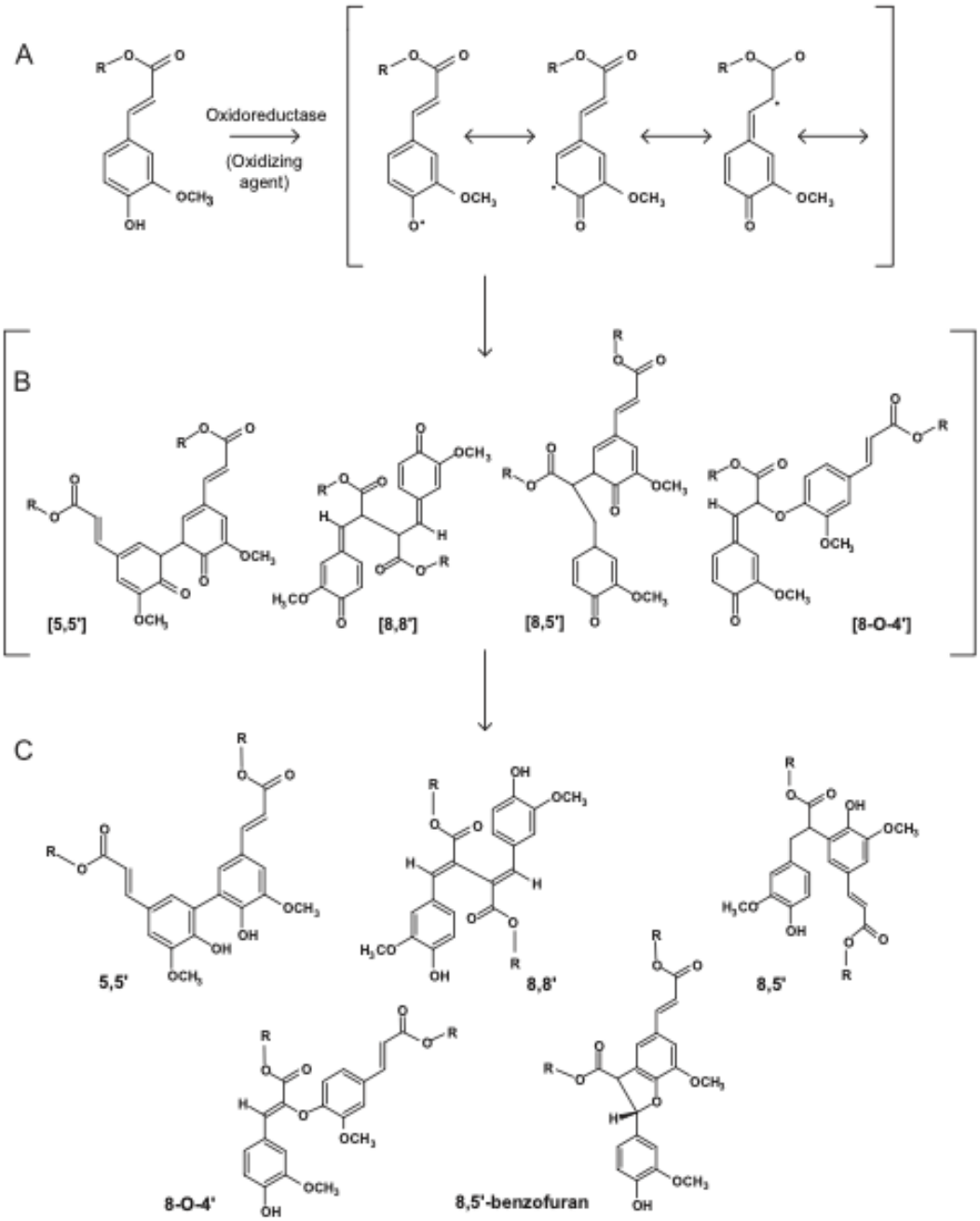

Scheme 2.4. The cross-linking mechanism and identified cross-links of feruloylated polysaccharides (Zaidel & Meyer, 2012).

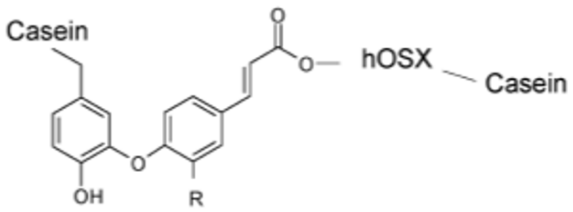

Scheme 2.5. Proposed cross-links for the heteroconjugates of casein and hydrolyzed oat spelt xylan (hOSX) (Selinheimo et al., 2008).

2.3.3. The biocatalysis of laccase: kinetic study

Enzyme kinetic parameters can be used to evaluate the affinity and the catalytic efficiency of the enzyme towards selected substrates. The kinetics of laccase-catalyzed oxidation are commonly shown to obey the *Michaelis-Menten* model as indicated by the hyperbolic shape kinetic curve. Frasconi et al. (2010) have compared the catalytic efficiency of laccases from different sources, including high E^0 laccases (from *T. versicolor and Trametes hirsuta),* and low E^0 laccases (from *Melanocarpus albomyces* and *R. vernicefera*), towards common substrates, such as ABTS, syringaldazine, catechol, dopamine. They stated that syringaldazine and ABTS (K_m=0.034-0.13 mM, k_{cat}/K_m=1024-4780 s^{-1} mM^{-1}) are good substrates for both *Trametes* laccases, whereas catechol and dopamine (K_m=0.031-0.17 mM, k_{cat}/K_m=25.1-2838 s^{-1} mM^{-1}) were shown to be relatively appropriate substrates for both laccases with low redox potential. The kinetic parameters of laccase from *Myceliophthora thermophila sp* in the oxidation of ferulic acid and ethyl ferulate were measured at pH 7.5 (Aljawish et al., 2014). Results showed that *M. thermophila* laccase exhibited higher substrate affinity and specificity towards ethyl ferulate (K_m=0.95 mM, k_{cat}/K_m=0.072 s^{-1} mM^{-1}) than ferulic acid (K_m=1.64 mM, k_{cat}/K_m=0.038 s^{-1} mM^{-1}). The K_m values for selected coumarins ranged from 0.87 to 1.58 μM in the oxidation reaction catalyzed by *T. versicolor* (Wang, Xu, et al., 2019). Among the coumarins, the oxidation of 4-methyl-7,8-dihydroxycoumarin was found to follow a Hill model, which exhibits a sigmoidal shape kinetic curve, and characterised by the lowest K_m with a hill coefficient higher than 1, revealing the presence a substrate activation step (Wang, Xu, et al., 2019). On the other hand, these authors reported an inactivation kinetic model for 7,8-dihydroxy-4-phenylcoumarin and 7,8-dihydroxycoumarin substrates, corresponding to low substrate affinity. The inactivation of laccase by phenolic substrates was reported to be the results of the interactions with reactive species generated during reaction, which were transformation rate dependent (Kurniawati & Nicell, 2009).

2.3.4. The biocatalysis of laccase: molecular modelling study

The advancement of bioinformatic databases and tools increases the possibility and accuracy of the in silico analysis of biocatalytic mechanisms at a molecular level. A number of 3D structures of *Basidiomycete* laccases have been reported, including those from *C. cinereus* (Ducros et al., 1998)*, T. versicolor* (Bertrand et al., 2002; Piontek et al., 2002), *Rigidoporus lignosus* (Garavaglia et al., 2004)*, Lentinus tigrinus* (Ferraroni et al., 2007)*, T. trogii* (Matera et al., 2008)*,* as well as a few of *Ascomycete* laccases, such as laccase from *M. thermophila*

(Ernst et al., 2018). Molecular modelling of an enzymatic reaction not only facilitates the interpretation of experimental data, but also provides a rational basis for directing enzyme engineering and designing new bio-catalytic reactions, especially those with extreme reaction conditions, thereby avoiding expensive and time-consuming experiments (Braiuca et al., 2006; Kazlauskas, 2000). Molecular docking is used to visualize the molecule binding complexes and the interaction between ligands and the active site of enzyme, and further dynamic simulation can provide the calculation of the reaction free energy and reaction modelling, enhancing the understanding of enzyme mechanism (Du et al., 2016; Zheng et al., 2019). The boosting research interest in such aspect led to the increased availability of well-established softwares/algorithms, such as AutoDock, GOLD, DOCK, FlexX, and Glide, for molecular docking and simulation (Du et al., 2016). Mehra et al. (2018) suggested that the laccase-substrate binding was a major contributor to the K_m value, as the correlation between computational binding affinity and K_m was confirmed with common substrates of laccase, while additional electronic properties of the substrates affected the K_m. The presence of ortho-methoxy group on sinapic and ferulic acid was shown to lead to binding modes that favors electron transmission, thus resulting in low K_m of these compounds (Mehra et al., 2018). Through molecular docking, Tadesse et al. (2008) stated that two butyl groups at the meta positions of phenol and aniline obstructed their entrance into the active site of *T. versicolor* laccase and the $\boldsymbol{\pi}$-stacking interaction, limiting its bioconversion. The binding complex from docking of laccase/Triton X-100 showed intense hydrophobic interactions at the active site of laccase, which was speculated to induce conformational changes of laccase and enhance the activity of laccase in the oxidation of aqueous phenol (Zhang et al., 2012). In contrast, the docking results reveal that the predicted hydrogen bonds between formetanate hydrochloride and catalytic amino acid residues (ASP206, CYS453) of *T. versicolor* laccase can interfere the electron transmission; this was used to explain the inhibitory effect of formetanate pesticide on the catalytic efficiency of laccase during bioremediation (Martins et al., 2016). Furthermore, molecular docking and simulation can be used (a) to support the discovery of new substrate scopes or new laccases in bioremediation (Ahlawat et al., 2019; Singh et al., 2016; Singh et al., 2014), and (b) the prediction of the efficiency of the reaction media for the biocatalysis (Stevens et al., 2019) and of the laccase engineering to improve bioconversion for specific substrates (Santiago et al., 2016).

2.3.5. Laccase-catalyzed reaction in protein modification

2.3.5.1. Laccase-catalyzed oxidative modification of amino acid and peptides

Among the investigated amino acids, tyrosine, tryptophan and cysteine can be oxidized by laccase from *T. hirsuta* as indicated by oxygen consumption measurement, with tyrosine being the most reactive substrate (Mattinen et al., 2006). As compared to tyrosine, higher reactivity was observed on tyrosine-containing di- and tri-peptides, whereas the higher polymerization degree was obtained with tyrosine (33<unit of monomer<94, 6-17 kDa) than the peptides (13<unit of monomer<59, 3-14 kDa) (Mattinen et al., 2005). The cross-linked dimer products of peptide Tyr-Ala were detected by liquid chromatography-mass spectrometry (LC-MS), and they showed fluorescent signal at excitation/emission 284/417nm and 325/400nm (Jus et al., 2012). Among the six peptides (molecular weight 700-1400 Da, covering 20 natural amino acids) investigated by Steffensen et al. (2009), oligomerized peptides with up to 5 units of monomer were detected by LC-MS. The MS/MS fragmentation patterns suggested that the cross-linking happened mainly on cysteine or tyrosine residues. Other laccase-catalyzed modifications can happen on amino acids, including tryptophan oxidation generating N′-formylkynurenine, which was assessed through the significant increase in the fluorescence spectrum intensity (excitation/emission 330/370 nm), and the carbonyl of oxidized tryptophan, histidine and methionine, which were detected via amino acid analysis (Steffensen et al., 2008).

The effect of adding ferulic acid into laccase-catalyzed reaction was shown to enhance the cross-linking extent (from dimer/trimer to hexamer) of cysteine-containing peptides via the aforementioned mechanism (Scheme 2.3) (Steffensen et al., 2009). The incorporation of ferulic acid into the product happened via the hetero-conjugation between ferulic acid (in the forms of monomer or dimer) and cysteine/tyrosine residues (Manhivi et al., 2018; Steffensen et al., 2009). On the other hand, Mattinen et al. (2006) and Steffensen et al. (2009) reported that ferulic acid did not act as a mediator in the cross-linking of tyrosine-containing peptides.

2.3.5.2. Laccase-catalyzed protein cross-linking

The activity of laccase in protein oxidation depends on the amino acid composition of the protein substrate, the accessibility of the tyrosine residues and the protein conformation (Mattinen et al., 2006; Steffensen et al., 2008). Small-sized and flexible molecule, α-casein, can be cross-linked efficiently by laccase, whereas protein substrates with a large size and compact structure, such as β-lactoglobulin, bovine serum albumin and wheat gliadin are poor substrates of laccase (Ercili Cura et al., 2009; Selinheimo et al., 2007; Steffensen et al., 2008). The efficiency of laccase in cross-linking could be enhanced by using high enzyme concentration, long incubation time or using appropriate reaction mediators (Ercili Cura et al.,

2009; Selinheimo et al., 2007). The cross-linking of collagen and gelatin was achieved by laccase alone or with the use of catechin as mediator; higher cross-linking efficiency was shown with the latter (Jus et al., 2012; Jus et al., 2011). Digested peptide mapping results showed that the cross-linking of collagen involved tyrosine residues and did not cause other major changes on its amino acid sequence (Jus et al., 2011). Laccase-catalyzed modification of milk proteins (casein, whey proteins, total milk protein) has been extensively studied, and the reactions were carried out with the presence of phenolic mediators (chlorogenic acid, ferulic acid, flavonoids, plant phenolic extracts) for efficient cross-linking (Ercili Cura et al., 2009; Hiller & Lorenzen, 2008; Hiller & Lorenzen, 2009; Hiller & Lorenzen, 2011; Jiang et al., 2017; Ma et al., 2011; Ma, Li, et al., 2020; Sato et al., 2015; Stanic et al., 2010; Yuan et al., 2018). HillerLorenzen (2011) reported an optimized process for the oligomerization of milk proteins (sodium caseinate, whey protein, skim milk powder) with bioconversion yields of 51.3-92%, in which 5% w/w protein substrate, 0.02-0.08 $\boldsymbol{\mu}$mol chlorogenic acid, 0.01U/mg of substrate were incubated at pH 4-5, 40-50 °C for 1 h. As oxidation induced protein unfolding, an improvement in the surface hydrophobicity of the milk proteins (whey proteins, whole milk proteins) was shown upon laccase-catalyzed oxidative cross-linking (Hiller & Lorenzen, 2008; Hiller & Lorenzen, 2009; Jiang et al., 2017; Ma, Li, et al., 2020). Jiang et al. (2017) and Yuan et al. (2018) reported on the secondary structure changes of $\boldsymbol{\alpha}$-lactalbumin and decrease in the $\boldsymbol{\alpha}$-helix content upon laccase-treatment. The cross-linking catalyzed by laccase contributed to gelling ability/gel firmness, water holding capacity and emulsification performance of milk proteins (Ercili Cura et al., 2009; Hiller & Lorenzen, 2009; Jiang et al., 2017; Ma et al., 2011; Ma, Li, et al., 2020; Sato et al., 2015). The treatment of chicken breast myofibril protein by laccase resulted in intermolecular cross-linking of the myosin fraction and the intramolecular cross-linking of the actin fraction and improvements in the thermal stability of the actin and the gel firmness of the myofibril protein (Lantto et al., 2005). Cross-linked potato protein by laccase-ferulic acid reaction system was characterized by a decrease in $\boldsymbol{\beta}$-sheet secondary structure and enhanced thermal stability, while the resulted gel had decreased firmness (Gui et al., 2020).

Attributing to the conformational changes and to the incorporation of the phenolic groups in the cross-linked proteins, cross-linking of proteins by laccase in the presence of phenolic compounds generally led to enhanced antioxidant property (Chung et al., 2003; Hiller & Lorenzen, 2009; Jiang et al., 2017; Tantoush et al., 2011). In addition, this enzymatic cross-linking approach was shown to decrease the allergenicity of the allergen proteins in milk ($\boldsymbol{\beta}$-

casein, ***β***-lactoglobulin) and peanut (Ara h 2) (Mihajlovic et al., 2016; Stanic et al., 2010; Tantoush et al., 2011).

2.3.5.3. Laccase-catalyzed conjugation of protein/polysaccharide

The hetero-conjugation between protein and polysaccharide catalyzed by laccase has also been studied for the generation of new macromolecule structures and modulation of techno-functional and health-promoting properties of the biopolymers (Buchert et al., 2007). Laccase-catalyzed reaction led to the formation of hetero-conjugates between casein and hydrolyzed oat spelt oligosaccharide, as indicated by the appearance of high molecular weight bands on electrophoresis gel detected by glycoprotein specific staining (Selinheimo et al., 2008). The conjugates of sodium caseinate and sugar beet pectin obtained upon laccase-catalyzed reaction exhibited higher heat and acid stability as compared to their electrostatic complexes (Zhang & Wolf, 2019). Bovine serum albumin/sugar beet pectin conjugates from laccase-treatment showed improved emulsifying stability against environmental stress such as salt, pH thermal and freeze-thaw treatment as compared to both parent biopolymers (Chen et al., 2018). The enhancement in stability could be attributed to the unique filamentous connected morphology of the conjugates as observed by the microscopy. Laccase-catalyzed conjugation of ***β***-lactoglobulin with sugar beet pectin conjugates led to improved solubility at pH close to the isoelectric point of ***β***-lactoglobulin (Jung & Wicker, 2012b). The laccase-treated ***β***-lactoglobulin/feruloylated chitosan conjugates were shown to have decreased extent of ordered structure and increased thermal stability as well as higher antioxidant property as compared to the native ***β***-lactoglobulin (Wang, Lv, et al., 2019).

2.3.5. Application of laccase-catalyzed cross-linking/conjugation in food processing

In the processing of bakery products, laccase can be introduced to strengthen the gluten networks via homo-cross-linking or hetero-conjugation among the arabinoxylans and gluten (Labat et al., 2001; Selinheimo et al., 2007; Si, 2001). The effects on dough rheological properties include reduced stickiness and increased the firmness, and on bread include softened crumb and increased volume as well as storage stability (Selinheimo et al., 2007; Si, 2001). The authors also suggested that the combined use of xylanase and laccase optimized the quality of bread by balancing the cross-linking and the hydrolysis mechanisms during processing. Apart from wheat products, treatment with laccase is useful for adjusting the texture and structure of gluten-free products made of oat and amadumbe flours, by constructing biopolymer networks with enhanced viscoelastic properties that can mimic the texture of gluten

(Flander et al., 2011; Manhivi et al., 2018; Renzetti et al., 2010).

Laccase was also identified for its ability in modulating the qualities of dairy products. Due to the unique weak acidic optimum activity of laccase, it is an ideal texturizing reagent for fermented dairy products. Laccase/phenolic mediator treatments (LMS) in the post-fermentation process of yogurt can refine the microstructure of the milk protein gel and enhance its elastic property (Struch et al., 2015). In cheese processing, the cross-linking of milk proteins via LMS prior to the rennet coagulation step can increase the protein content in the milk curd as well as enhance the antioxidant property of the product (Loi et al., 2020; Loi et al., 2018). The sensory characteristic and acceptability of the final cheese product from laccase-ferulic acid treatment were shown to be comparable to those of commercial analogs in a sensory evaluation conducted by 10 trained panelists (Loi et al., 2020).

Strategies of introducing interfacial covalent cross-links via laccase-reactions have been studied for the development of various multilayer emulsion systems and carriers for bioactive compounds. The post-homogenization cross-linking of whey protein isolate by laccase was shown to enhance the storage stability of the oil-in-water emulsion, where particle size distribution of the emulsion was not changed significantly within 3 days and no clear evidence of creaming was observed up to one week (Ma et al., 2011). The laccase-catalyzed conjugation of whey protein isolate/sugar beet pectin complex during the encapsulation of caffeine acid led to the formation of conjugate nano-particles with spherical and homogenous shapes without interacting with encapsulated caffeine acid (Gazme & Madadlou, 2014). The formation of covalent cross-links by laccase in protein/polysaccharides multi-layer emulsions can introduce dense and tight droplet layers and smaller droplets sizes, which enhanced the stability against heat and across a wider range of pH (3.0-8.0) (Azarikia et al., 2015; Zeeb et al., 2012; Zeeb et al., 2013). Laccase-catalyzed reactions were also applied for the construction of gel networks for delivery purpose (Chen et al., 2019; Deng et al., 2018).

2.4. Structural analysis of modified proteins

2.4.1. Size exclusion chromatography (SEC)

SEC is a common analytical technique to obtain important information about average molecular weight and molecular weight distribution of modified protein mixtures (Liu et al., 2017). With the proper selection of column (stationary phase, molecular weight exclusion range, pore size) and mobile phase, proteins can be separated based on their molecular size.

Specific detectors (UV-PDA, fluorescence, refractive index) can be used to monitor the elution for the characterization of selective compounds. Moreover, multiangle laser scattering light detector can provide detailed information for a biopolymer mixture including molecular mass, polydispersity, shape, radius of gyration, concentration and intrinsic viscosity (Liu et al., 2017). The SEC result showed that higher molecular weight fractions appeared in laccase-treated $\boldsymbol{\alpha}$-lactalbumin indicating cross-linking (Jiang et al., 2017). Differently, laccase-treated $\boldsymbol{\beta}$-lactoglobulin was not shown with the increase in molecular weight but exhibited less compact and rod-like shape than the native, as indicated by the slope of the conformation plot (log(root mean square) vs log(molecular weight)) (Jung & Wicker, 2014).

2.4.2. Fluorescence spectroscopy

Intrinsic fluorescence of protein can provide information regarding the polarity of the microenvironment surrounding tryptophan residues thus the tertiary structure of the protein (Liang & Tang, 2013). Among the aromatic residues, tryptophan has the most sensitivity towards the changes in polarity (Wang, Sun, et al., 2017). The intrinsic fluorescence emission spectrum can be obtained by excitation wavelength at 280 nm, where both tyrosine and tryptophan can be excited; by using a higher excitation wavelength at 295-305 nm, tryptophan can be selectively excited. A fully buried tryptophan residue in protein exhibits a $\boldsymbol{\lambda}_{max}$ at around 330 nm while that of a fully exposed tryptophan residue to solvent is around 350 nm (Alavi et al., 2018; Wang, Sun, et al., 2017). A red shift in $\boldsymbol{\lambda}_{max}$ (to higher wavelength) was indicative of an increase in polarity of the tryptophan microenvironment and the loss of the protein tertiary compactness, while a blue shift (to lower wavelength) indicates increase in hydrophobicity surrounding tryptophan or molecular packing and aggregation (Jia et al., 2019; Wang, Sun, et al., 2017). In addition, fluorescence intensity further indicates the changes in the environment; a decrease in fluorescence intensity is the result of the interaction between fluorophore amino acids and quenching reagents in the solvent or in the protein itself (Liu et al., 2012). Red-shift and decrease in intensity was generally reported upon the glycation of protein, which was attributed to protein conformational changes (increase in hydrophilic environment of the tryptophan) and shielding effects of the bound carbohydrate (Ma, Chen, et al., 2020; Wang, Lv, et al., 2019). Differently, the cross-linking of myofibril protein mediated by rutin exhibited a blue shift $\boldsymbol{\lambda}_{max}$ and decrease in intensity, which is ascribed to protein unfolding meanwhile increase in hydrophobic environment of the tryptophan residue (Jia et al., 2019). Whey protein unfolding upon transglutaminase-treatment and urea induced tertiary unfolding of red kidney

bean globulin were characterized by a decrease in fluorescence intensity without shifting the λ_{max} (Carvalho et al., 2019; Liang & Tang, 2013).

The extrinsic fluorescence absorption of protein is also applied to study the protein tertiary structure with the use of fluorescent dyes such as 1-anilinonaphthalene-8-sulfonate (ANS). The extrinsic fluorescence of ANS upon binding with the solvated hydrophobic residues of protein can be used to study the protein unfolding process as well as assess the surface hydrophobicity of protein molecule (Hawe et al., 2008).

2.4.3. Fourier transform infrared spectroscopy (FTIR)

FTIR is a useful tool to analyze the secondary structure composition of proteins to understand the conformational changes caused by protein modification or the changes in microenvironment (Wang et al., 2017). The characteristic IR absorption (absorption frequency/wavenumber and intensity) of a molecule is originated from the vibrational transition of the chemical bonds with the influence from their microenvironment (inter/intramolecular hydrogen-bonding) (Yang et al., 2015). Among the characteristic IR absorption bands of proteins, amide I (1700~1600 cm^{-1}), from C=O stretching vibration coupled with N-H bending of the protein backbone, is the most sensitive spectral region for the detection of secondary structural changes (Yang et al., 2015). Amide I absorption was composed of a mixture of secondary structures, including β-sheet (1620-1640 cm^{-1}) , α-helix (1650-1660 cm^{-1}), β-turns (1670-1690 cm^{-1}) and random coil (~1645 cm^{-1}); the composition can be deciphered using Fourier self-deconvolution or second derivative analysis (Wang, Sun, et al., 2017; Yang et al., 2015). The changes in secondary structural composition can reflect the molecular flexibility of the protein, which is generally related to important functionalities of proteins such as surface activity, protein film rheology and emulsification properties (Liang & Tang, 2013). While β-turn and random coil structures are relatively flexible, the α-helix, β-sheet and β-aggregates (1618-1620 cm^{-1}) indicate protein inflexibility and rigidity (Jarpa-Parra et al., 2015). The conformational changes of lentil protein at air-water interface was characterized by FTIR as increased α-helical/ β-aggregate structure when the bulk phase are at pH 7 and 5, and increased random structure when applied in bulk phase of pH 3. The former was associated with compact/stable interfacial film with high elasticity while the latter was shown to construct a relaxed interface with reduced elasticity over time (Jarpa-Parra et al., 2015). Egg white proteins were shown to have significant increase in α-helix after oxidative cross-linking mediated by AAPH (2,2-azobis(2-amidinopropane) dihydrochloride), while

pulsed electric field treatment destroys the hydrogen bonds in protein which resulted in the decrease in α-helix (Duan et al., 2018; Qian et al., 2016).

Other changes related to the disappearance or formation of chemical bonds in protein structure upon modification can also be characterized by FTIR. Formation of isodityrosine cross-links in tyrosine containing peptide was shown by the appearance of bands at 1010-1027 cm^{-1} , which represented the C-O-C stretching vibration mode of ether bonds (Mattinen et al., 2005). The protein conjugated with ferulic acid was shown by weak bands at 1518 cm^{-1} and the conjugation with feruloylated polysaccharides was characterized by bands at 970-1170 cm^{-1} representing C-C glycosidic bonds (Chen et al., 2012; Mattinen et al., 2005).

2.4.4. Mass spectrometry (MS)

MS can determine the mass-to-charge ratio of ionized protein molecules, which allows the putative identification of the structure. With the use of MS in tandem mode (MS/MS), the targeted ions can be fragmented via collision-induced dissociation and the resulting fragment ions spectrum is used to identify partial or complete amino acid sequence of a protein/peptide (Deutzmann, 2004). This approach is commonly used in the detection of cross-links, glycation or conjugation and their location on protein sequence based on the difference between the fragmentation patterns of the native and modified proteins (Liu et al., 2012; Mckerchar et al., 2019). General strategy in protein/modified protein identification includes the separation of targeted protein, digestion with proteases, extraction of proteolytic peptide, MS or MS/MS analysis of the peptide, peptide mapping with the use of databases (in-house or designed ones according to the modification) (Mckerchar et al., 2019). The vanillic acid-grafted $\boldsymbol{\alpha}$-lactalbumin and grafted $\boldsymbol{\beta}$-lactoglobulin were characterized based on their mass spectra, as indicated by a shift of the deconvoluted mass towards high value (14557 and 18798 Da, respectively) as compared to the native form (14118 and 18481 Da, respectively) (Ma et al., 2011). The difference in mass caused by the modification was used to estimate the number of phenolic moieties grafted on protein. Similarly, the mass profile of glycated $\boldsymbol{\alpha}$-lactalbumin /lysozyme with monosaccharides and the extent of glycation was characterized based on their mass spectra (Seo et al., 2012; Ter Haar et al., 2011). The fragmentation of the ions from cross-linked GLY-LEU-TYR tripeptide from laccase-catalyzed reactions lead to the sequential loss in GLY and LEU residues and a final product of tyrosine trimer (m/z =540.05 Da) which is considered as the cross-link of the reaction product (Mattinen et al., 2006). From the mass spectrum of tryptic-digested peptide mixture of transglutaminase-cross-linked lysozyme, a

distinct compound (monoisotopic mass of 1633.0 Da) was found corresponding to combined lysozyme peptide segments 1-5 (605.4 Da) and 117-125 (1044.5 Da) minus the molar mass of ammonia (17.0 Da). This implied that the cross-linking of lysozyme catalyzed by transglutaminase happened between LYS1 and GLN121 residues via isopeptide bond (Schuh et al., 2010).

2.5. The application prospects of protein modification (cross-linking/conjugation)

Protein modification are applied either in the formulation of proteinaceous matrix or in the synthesis of protein-based ingredients. As the growth in the awareness of healthy diet, there are increasing demands for vegan/vegetarian diets and low fat/sugar products. Cross-linking/conjugation is common tools for texture and structure modulation in these innovative formulations and products (Liu et al., 2017; Zeeb et al., 2017). The choices for protein ingredients in food industry was shifting towards those from renewable/non-conventional sources such as plants, insects and agro-wastes in order to address the issues of sustainability. These new protein ingredients are generally in their modified forms, such as hydrolyzed, phenolic/polysaccharide grafted or cross-linked ones, to offer outstanding stability and/or application values that is comparable to the well-established protein ingredients from animal sources (Fritsch et al., 2017; Sun-Waterhouse et al., 2014). In addition, combining peptide/protein compartments from different sources via cross-linking may provide synergistic effects in amino acid profile, health-promoting effects and functionality, which is promising in the development of plant-based protein functional ingredients with balanced amino acid profile (Dube et al., 2006; Glusac et al., 2018; Glusac et al., 2019; Isaschar-Ovdat & Fishman, 2018). Given their compatibility and biodegradability, cross-linked/polymerized proteins with defined structure are good candidates for innovative biomaterials (e.g. tissues, hydrogels, scaffolds) in medical, pharmaceutical fields and packaging/coating materials (Gupta & Nayak, 2015; James & Numat, 2013; Nicolas et al., 2013) The study of how to modulate the structure and functional profiles of protein via protein modification will contribute to the advancement in the development and application of innovative protein-based ingredients, biomaterials and matrix.

CONNECTING STATEMENT 1

The literature review has discussed about the background of current study in protein modification via laccase-biocatalytic approach. Laccase is a promising green biocatalyst in the generation of novel proteinaceous functional ingredients as well as the modulation of textural and structural quality in various protein-based food formulations. At the starting point of exploring the potential of laccase in the modification of new protein substrates, Chapter III illustrates relevant mechanistic actions of fungal laccase by carrying out model reactions. Laccase-catalyzed oxidative cross-linking was performed on selected substrate models derived from targeted protein substrates (potato protein and lysozyme), from which the enzyme/substrate binding at molecular level, substrate specificity and reaction selectivity was studied.

The results of this chapter were presented at the IFT Annual Meeting & Food Expo-Institute of Food Technologist and submitted to *Enzyme and Microbial Technology*

Li. M, Karboune, S. and Kermasha, S. (2018). *Mechanism Study of Laccase-Catalyzed Oxidative Crosslinking of Protein: Using Tyrosine and Peptides as Model Substrates.* IFT18 Annual Meeting, Chicago, Illinois, July 14–17

Li, M., Liu, L., Kermasha, S., and Karboune, S. (2020). Laccase-Catalyzed Oxidative Cross-linking of Tyrosine and Potato Patatin- and Lysozyme-Derived Peptides: Molecular and Kinetic Study. *Enzyme and Microbial Technology*, (Under review).

CHAPTER III. LACCASE-CATALYZED OXIDATIVE CROSS-LINKING OF TYROSINE AND POTATO PATATIN- AND LYSOZYME-DERIVED PEPTIDES: MOLECULAR AND KINETIC STUDY

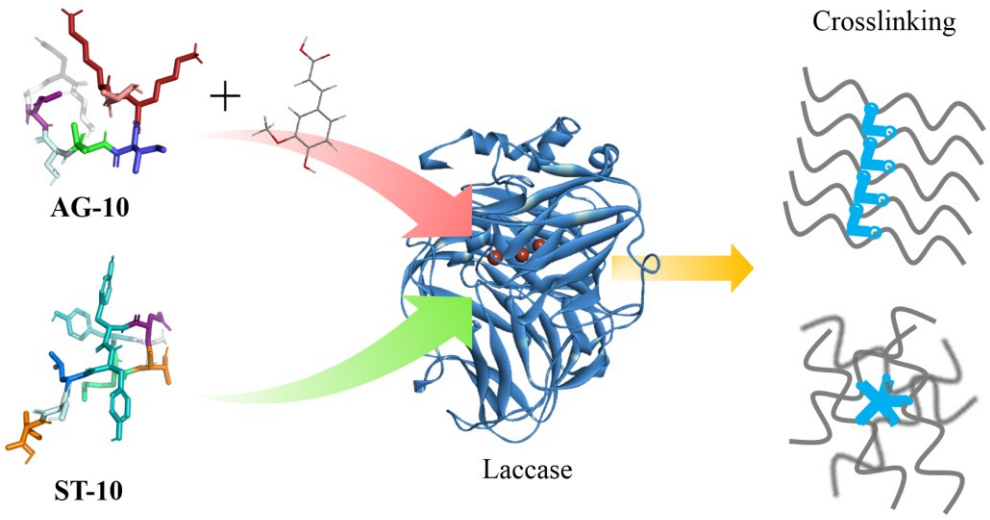

3.1. Abstract

Laccase can catalyze the oxidative cross-linking of peptides, which is useful in the production of proteinaceous materials with enhanced functional properties. However, the kinetics and the pathway of this reaction remain unclear. In the present study, laccase-catalyzed oxidative cross-linking reaction was investigated through a combination of computational analysis, kinetic studies and end-product profiling using selected substrate models, including peptide AG-10 (AKKIVSDGNG) (without tyrosine) derived from lysozyme and tyrosine-containing peptide ST-10 (SYMTDYYLST) from potato protein (patatin), and tyrosine. Both laccases from *Trametes versicolor* (LacTv) and *Coriolus hirsutus* (LacCh) were used as biocatalysts. Laccase exhibited higher binding affinity and catalytic efficiency (k_{cat}/K_m) towards ST-10 and AG-10 than tyrosine. Among the laccases, LacCh showed higher k_{cat} towards ST-10 and AG-10 than LacTv. Through the molecular docking, this result was attributed to the presence of the ASN206 at the cavity of LacCh. The end product profiles reveal the formation of homo-oligomers (> 5 units) of ST-10 in the reaction catalyzed by LacTv, while polymerization was favored by LacCh. These cross-linked products were identified to have a mix of oligo-tyrosine linkages. In contrast, the cross-linking of AG-10 required the presence of ferulic acid as mediator, which resulted in the formation of hetero-oligomers and polymers of AG-10. Ferulic acid was found to promote the cross-linking of limited reactive substrate, AG-10 and tyrosine, while it behaved as a competitor with highly reactive substrate, ST-10, inhibiting their cross-linking. The knowledge obtained in the present study provide insight into an effective reaction for peptide cross-linking.

3.2. Introduction

Laccase (EC 1.10.3.2), one of the oxidoreductases, has attracted a high interest as a potential biocatalyst that can catalyze protein and peptide modification via protein-protein and peptide-peptide crosslinking or protein-polysaccharide and peptide-polysaccharide conjugation due to its broad substrate specificity (Mckerchar et al., 2019; Osma et al., 2010). Indeed, phenols being the common substrates for laccase can be oxidized into reactive radicals that can further undergo non-enzymatic polymerization or depolymerization (Buchert et al., 2010). The oxidation of protein/peptide molecules by laccase happens mainly on their tyrosine residues, which results in the formation of intermolecular di-tyrosine cross-links (Mattinen et al., 2006; Mattinen et al., 2005). When protein substrates are bulky, compact and lack exposed tyrosine residues, phenolic acids can act as reaction mediators to initiate the oxidation of proteins

(Buchert et al., 2010). Laccase can be found in variety sources of fungi (Rivera-Hoyos et al., 2013), plant (Berthet et al., 2012), insects (Yang et al., 2017) and bacteria (Giardina et al., 2010). Fungal laccases have an acidic optimal pH, and exhibit higher redox potential (E^0) and stability than laccases from plant and bacterial sources (Guimarães et al., 2017; Madzak et al., 2006). Among the numerous purified and characterized fungal laccases, those from LacTv and LacCh have been reported to have a distinct high redox potential (Frasconi et al., 2010). The active site of laccase consists of a cluster of four copper atoms, where the redox reactions are carried out (Bertrand et al., 2002). During one redox cycle of laccase, the type 1 copper center coordinating with a histidine residue, HIS458 of LacTv or LacCh, can oxidize four substrate molecules by extracting single electron from each of them; concomitantly, at the type 2 and 3 copper trinuclear center, one molecule of dioxygen is reduced to two water molecules upon receiving the electrons (Bertrand et al., 2002; Giardina et al., 2010; Guimarães et al., 2017; Madzak et al., 2006).

Laccase-catalyzed cross-linking can modify the structural, functional and health-promoting properties of peptides and proteins (Isaschar-Ovdat & Fishman, 2018). Several studies have reported that protein polymerization catalyzed by laccase can improve the gluten network of wheat protein (Selinheimo et al., 2007), alter the rheological properties of milk proteins and dairy products (Hiller & Lorenzen, 2009; Loi et al., 2020; Mokoonlall, Pfannstiel, et al., 2016), and stabilize the protein-polysaccharide based emulsion systems (Chen et al., 2018; Zeeb et al., 2012). In addition, laccase was shown to enhance the biological activities of the proteins, including antioxidant properties (Chung et al., 2003), digestibility and decrease the allergenicity (Stanic et al., 2010; Tantoush et al., 2011). Moreover, laccase-catalyzed the oxidative crosslinking of peptide- and protein-based nanoparticulate systems can enhance their stability and their uses for the controlled delivery of bioactive molecules (Fuchs et al., 2010; Nicolas et al., 2013). However, little insights about kinetics and mechanism of laccase-catalyzed oxidative cross-linking of peptides or proteins are available. Consequently, it remains unclear how exploiting substrate specificity and reaction selectivity of laccase can enable the modulation of the pathway and the end-product pattern of peptide and protein cross-linking, and to what extent mediators play a role in such crosslinking with the reactive substrates. The aim of the present study was to investigate the kinetic and the pathway of laccase-catalyzed oxidative cross-linking reaction of tyrosine and two selected peptides, derived from targeted proteins, including AG-10 (AKKIVSDGNG) from lysozyme and ST-10 (SYMTDYYLST) from potato protein (patatin). Two laccases from selected fungal species, including LacTv and

LacCh, were used as biocatalysts. The binding affinity of laccases towards the substrate models was assessed at the molecular level by molecular docking; while the catalytic efficiency as well as the end-product profile were determined in order to characterize the substrate specificity and the reaction selectivity of laccase reactions. Size exclusion-high performance liquid chromatography and liquid chromatography-mass spectroscopy were used to characterize the end-products in terms of molecular weight profile and oxidative cross-links.

3.3. Materials and Methods

3.3.1. Laccase production

The fungi strain *C. hirsutus* (MYA 828) (ATCC, Manassas, VA) was incubated at 20 °C on malt agar media plates. Circles (diameter=0.5 mm) of *C. hirsutus* mycelium were transferred to the basal liquid media; the incubation and enrichment (2.5 times) were performed at 28 °C, 160 rpm for 7 and 6 days, respectively. During enrichment, 3.6 % (v/v) of pure ethanol was added to the media to induce laccase production. The culture media were filtered with cheese cloth to remove mycelium pellet and then passed through an ultrafiltration system with Prep/Scale TFF cartridge 2.5 ft^2 (Millipore) containing a 10kDa cut-off polyethersulfone membrane under the pressure of 7.5 psi. The obtained enzyme extract from ultrafiltration was precipitated with ammonium sulfate at 80% (w/v) of saturation. The precipitate was recovered via centrifugation at 10000 × g, and redissolved in sodium phosphate buffer (50 mM, pH 5). The partial purified laccase was dialyzed against sodium phosphate buffer (5 mM, pH 5). All enzyme recovery steps were performed at 4 °C. The enzyme dialysate was lyophilized at -40 °C.

3.3.2. Laccase enzymatic assay

A second laccase that was used for this study, LacTv, was obtained from Sigma-Aldrich (St-Louis MO). The enzyme activity of laccases was assayed using 2,2'-azino-bis (3-ethylbenzothiazoline-6-sulphonic acid) diammonium salt (ABTS) as substrate (Niku-Paavola et al., 1990). The oxidation of ABTS was monitored spectrophotometrically at 420 nm, using Beckman DU 650 spectrophotometer (Beckman Instruments Inc.; San Ramon, CA). The reaction mixture was composed of 0.9 mL of enzyme suspension (containing 0.005 - 0.15 mg of protein) and 0.1 mL of 10 mM ABTS in sodium phosphate buffer solution (50 mM, pH 6.5). The reaction rate (v) was estimated from the slope (k) of the linear part of the plots of absorbance versus time, with $v=k/\varepsilon_{ABTS}$ μmol mL^{-1} min^{-1}, where $\varepsilon_{ABTS}=36$ cm^{-1} mM^{-1}. One unit

of laccase activity was defined as the amount of enzyme that oxidize 1 µmol of ABTS per min. The enzyme activity assay was performed in triplicates. The protein content of the enzyme was determined using Hartree-Lowry method (Hartree, 1972). The specific activity was expressed as the laccase activity units per mg protein.

3.3.3. Selection of peptide sequences as substrate models

Crystal structures of laccase (1GYC), patatin (4PK9), the major component of potato proteins, and hen egg lysozyme (4WLT) were submitted to enzyme-protein substrate docking using Z-DOCK as a protein-docking algorithm (Chen et al., 2003). Histidine 458 residue was considered as the electron entrance door of the laccase (Bertrand et al., 2002), Z-DOCK was programmed to block the binding with the non-active site residues of the laccase and instructed HIS 458 as the contact site. The resulted binding poses were viewed and analyzed, using Accelrys Discovery Studio software (DS) (BIOVIA, San Diego, CA), where the shortest distance between HIS458 and the respective protein substrates were measured. From the docking results, the predicted binding sites of the protein substrates were identified. Peptide sequences that include the most appropriate binding sites were synthesized by Genscript (Pistcataway, NJ) and subsequently used as model substrates.

3.3.4. Reaction time course

Laccasse-catalyzed oxidative cross-linking of tyrosine and peptide models was carried out in the presence and absence of ferulic acid over reaction time from 0 to 48 h. The reaction mixtures consisted of 1 mM substrate and 0.22 U per mg substrate of laccase (LacTv or LacCh) prepared in sodium phosphate buffer (50 mM, pH 6.5). Ferulic acid at equal molar concentration to that of the substrate was used as a mediator. The reactions were performed at 28°C under an orbital agitation of 150 rpm. At selected reaction time, the enzymatic reactions were halted by immersing them in a boiling water-bath for 10 min. The enzymatic reactions were carried out in duplicates, along with blank trial containing all reaction components except the enzyme. The consumed substrate concentration was estimated by reverse phase-high performance liquid chromatography (RP-HPLC), meanwhile, the end-product profile was determined by size exclusion-HPLC (SE-HPLC).

3.3.5. Kinetic parameters

The reactions were carried out at substrate concentrations varying from 0.5 to 2.5 mM for tyrosine and from 0.2 to 3.6 mM for peptides in sodium phosphate buffer (50mM, pH 6.5) at

28°C. All the enzymatic reactions were run in duplicates, along with control trials containing the same components except the enzyme. In order to monitor the depletion of the substrate over time, the reaction samples at different time intervals of 0 to 60 min were collected and analyzed by RP-HPLC. The Michaelis-Menten kinetic model was used for the analysis of laccase-catalyzed oxidation of peptides, whereas the Hill model was used for those of tyrosine. Non-linear regression analysis was run by Sigmaplot 12.3 (Systat Software, San Jose, CA) to determine the V_{max}, which is maximum velocity, K_m/K_{50}, which are the substrate concentration at 1/2 V_{max} for the Michaelis-Menten/Hill kinetic models and h, the Hill coefficient.

3.3.6. Molecular docking study

Molecular docking was performed using AutoDock Vina. The peptide substrate models were constructed by PEP-FOLD3 internet server; LacTv (1GYC), LacCh (3FPX) and tyrosine substrate models were downloaded from PDB database. Prior to docking, the experimental structure of laccase was edited by Discovery Studio (DS) to remove the items other than the protein chain, as well, added with polar hydrogen using AutoDock Tools (ADT). Substrate was set with highest torsions using ADT. Designed AutoDock Vina method was used to generate the predicted binding complexes and calculate binding affinity. The best binding complexes was selected for each laccase- substrate model with the criteria of highest binding affinity and shortest distance between HIS458 of laccase and the substrate. The selected binding complexes was analyzed by PyMol (Shrödinger, LLC, Portland, OR) for editing their 3D structures and measuring the distance, as well as by DS for detecting the intermolecular interactions (Martins et al., 2016; Seo et al., 2015).

3.3.7. Characterization of reaction mixture

3.3.7.1. Quantification of bioconversion yield by RP-HPLC

The concentration of enzymatically converted substrates was estimated by RP-HPLC. Reaction samples were eluted on a ZORBAX SB-C18 column (4.6x250 mm) (Agilent, Santa Clara, CA), using HPLC Beckman system, equipped with a programmable solvent module (Model 126), a photodiode array detector (Model 168) and 32 Karat software for data collection (Beckman Coulter, Brea, CA). The elution was carried out at a linear gradient to 60% of solvent B of acetonitrile, containing 0.085% of TFA, at flow rate of 1 mL/min. The elution was monitored at λ 214 nm. The initial reaction rate was calculated on the basis of the polynomial plot of the

substrate concentration versus time. The bioconversion yield was calculated using the equation 3.1:

$$\text{Bioconversion yield (\%)} = ([S]_i - [S]_r) / [S]_i \quad (3.1)$$

where, $[S]_i$ was the initial substrate concentration; and $[S]_r$ was the residual substrate concentration.

3.3.7.2. Determination of end-product profile by SE-HPLC

An isocratic elution was performed using TSKgel G2000SWXL column (Tosoh Bioscience, King of Prussia, PA), with deionized water containing 45% of acetonitrile and 0.1% of TFA at flow rate of 0.5 mL/min. The elution was monitored at λ 214 nm. A standard, containing a mixture of compounds with wide range of molecular weights, including tyrosine (181.2 Da), AG-10 (988 Da), ST-10 (1242.45 Da), lysozyme (14,400 Da) and ovalbumin (44,000 Da), was used for the calibration. The linear correlation between logarithm of molecular weight (MW_{std}) and retention time (RT) was used to estimate the average molecular weight (MW_{pi}) of each end-product (equation 3.2 and 3.3), where std represents the standards for calibration, and pi represents the end-product peaks on the chromatogram. C_{pi}, the concentration (mg/ml) of the compounds at pi, was calculated based on the peak area (mAU) The proportion (P_{pi}%) represents the relative percentage of the compounds in the reaction mixture calculated based on equation 3.4.

$$\log(MW_{std}) = aRT_{std} + b \quad \text{(Eq. 3.2)}$$

$$MW_{pi} = 10^{aRT_{pi}+b} \quad \text{(Eq. 3.3)}$$

$$P_{pi}i\% = C_{pi}/(C_{p1} + C_{p2} + \cdots + C_{pi}) \times 100 \quad \text{(Eq. 3.4)}$$

3.3.7.3. End-product identification by LC-ESI-MS

LC-ESI-MS analysis was performed using a Waters Acquity UPLC system connected with Synapt G2S mass spectrometry. Samples were eluted on Aeris Widepore C8 column (2.1 × 100 mM) using a gradient of 90% of mobile phase A (0.1% of formic acid in water) to 90% of mobile phase B (0.1% of formic acid in acetonitrile) in 12 min. The mass spectra were acquired in both negative and positive ion mode and m/z range from 100 to 3200 was scanned. The potential end products were identified on the basis of the mass spectra. The data was analyzed by Waters MassLynx software.

3.3.8. Characterization of the covalent cross-links

To characterize the covalent cross-links, acid hydrolysis was carried out to break down the peptide bonds in cross-linked products while conserving the covalent enzymatic cross-links. The acid hydrolysis was implemented according to a modification of the procedure of previous described method (Dhayal et al., 2015). Reaction sample was mixed with 10 M HCl at a ratio of 2:3 (v/v) in screwed-cap glass vials. The vials were flushed with a gentle stream of nitrogen for 2 min before incubation at 110ºC for 24 h. The hydrolysate mixture was then dried under nitrogen and reconstituted with 100µL UHPLC-grade water containing 1% acetonitrile and 0.1% formic acid for MS analysis. The acid hydrolysates were analyzed by LC-MS using a Dionex Ultimate 3000 coupled to a Bruker Maxis Impact QTOF in positive ESI mode. Samples were separated on a Phenomenex Luna C18(2) column (5 µM, 100A, 2.0 x 50 mm) using a gradient of 98% mobile phase A (0.1% formic acid in water) and 2% mobile phase B (0.1 % formic acid in acetonitrile) to 20% mobile phase A and 80% mobile phase B in 9 minutes, then kept at 100% mobile phase B for 2 minutes at a flow rate of 0.3 mL/min. The data was processed using the Bruker Data Analysis software version 4.2.

3.4. Results and discussion

3.4.1. Laccase-protein substrate binding and selection of peptide models

The selection of peptide models was assisted by computational analysis. In order to gain an insight of the binding between laccase and substrate proteins, binding complexes of laccase/patatin as well as laccase/lysozyme from Z-DOCK with high docking score were selected and visualized, using Discovery Studio software. Bertrand *et al.* (2002) indicated that, during the oxidation cycle, the HIS458 residue located at laccase's catalytic cavity formed hydrogen bond with substrate, whilst the peripheral residues of the cavity were involved in stabilizing the binding via hydrogen bonding and π-stacking interactions. From the obtained binding complexes of laccase/patatin, it shows that the region of peptide chain SYMTDYYLST (ST-10) in patatin (Fig. 3.1A) is oriented towards the active site and potentially forming hydrogen bond with the residue HIS458 on laccase. Indeed, hydrogen bonding between TYR301 residue of patatin (TYR2 of ST-10) and HIS 458 of laccase was detected, with bond length at 2.6Å, and bond angle at 158.9˚, which indicated that TYR301 of patatin could be the most susceptible site for oxidation by laccase. Other studies have reported similar hydrogen bonding parameters between the reducing substrate and the catalytic histidine residue of laccase from crystal structures (Enguita et al., 2004; Martins et al., 2016). Bertrand

et al. (2002) inferred from the crystal structure of laccase/2,5-xylidine complex that the amino group of 2,5-xylidine formed hydrogen bonds with HIS458 at a distance of 2.6 Å. Euguita *et al.* (2004) reported that in the crystal structure of *Bacillus subtilis* laccase/ABTS complex, the nearest distance between thiazoline rings of ABTS and HIS 497 (equivalent to HIS 458 in LacTv) was 3.3 Å. Contrary to patatin, lysozyme has only four tyrosine residues, all of which are buried in the core of lysozyme. The Z-DOCK results indicate that the tyrosine residues of lysozyme had very limited accessibility to bind and interact with laccase (Fig. 3.1B). In addition, the surface of lysozyme is lacking in residues containing aromatic groups that can support π-stacking interactions with the enzyme. Moreover, steric hindrance from the globular shape of lysozyme molecule can obstruct reactive amino acids from entering the 10.8 Å-wide catalytic cavity of Laccase. Little intermolecular hydrogen-bonding was detected between HIS458 of laccase and lysozyme among their binding complexes. This phenomenon might indicate the relatively low efficiency of laccase-catalyzed oxidation of lysozyme as compared to patatin. However, the docking results revealed that the peptide chain AKKIVSDGNG (AG-10, Fig. 3.1B) on lysozyme was constantly oriented towards the catalytic cavity of laccase, with its GLY102 oriented towards HIS458 of laccase, at a distance of 4.717 Å. Mediators can be used in laccase-catalyzed reaction to overcome the low reactivity due to the steric hindrance of substrate (Tadesse et al., 2008), which may be required for the oxidative cross-linking of lysozyme.

For subsequent investigations, ST-10 (SYMTDYYLST) and AG-10 (AKKIVSDGNG) peptide chains from patatin and lysozyme, respectively, were selected as the model substrates, and their structural and physiochemical properties are shown in Table 3.1.

Table 3.1. Properties of model peptides (provided by GenScript ®, USA)

	ST-10 SYMTDYYLST	AG-10 AKKIVSDGNG
Isoelectric point	3.75	9.53
Net charge	-1	1
Attribute	acidic	basic
Molecular weight	1242.5114	987.5349

Amino acid abbreviation: A-alanine, D-aspartic acid, G-glycine, I-isoleucine, K-lysine, L-leucine, M-Methionine, N-asparagine, S-serine, T-Threonine, V-valine, Y-Tyrosine

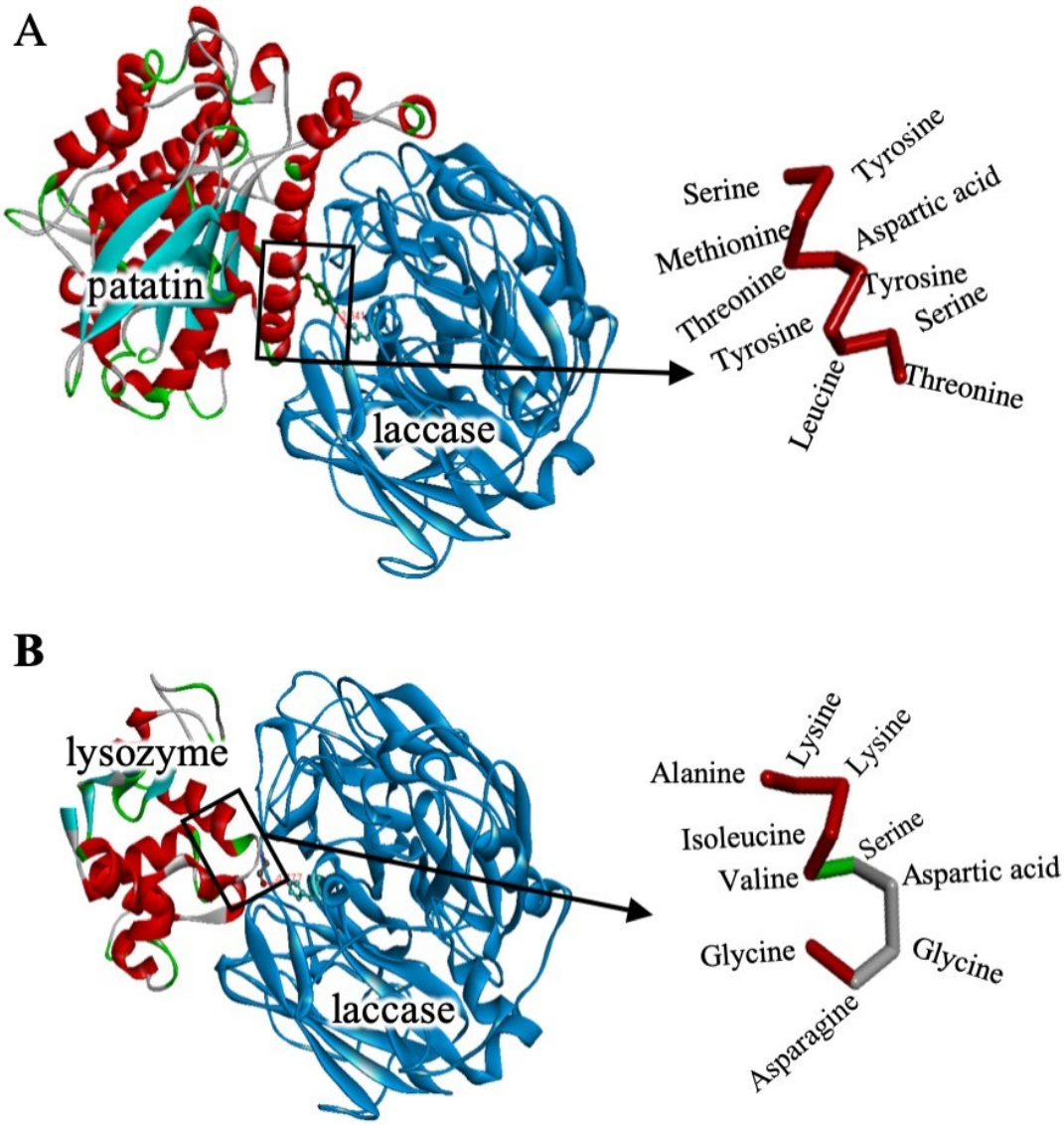

Figure 3.1. Laccase/protein substrate binding; laccase/patatin A, laccase/lysozyme B, and their peptide chain approaching to the active site.

3.4.2. Kinetic parameters and molecular docking

Kinetic parameters of laccase-catalyzed oxidation of selected substrates were determined based on the best-fit kinetic models. Using peptides as substrates, the kinetics of laccase followed the Michaelis-Menten model. In contrast, the laccase-catalyzed oxidation of tyrosine follows a sigmoidal-shape kinetic plot that fits the Hill model with a Hill coefficient of 2.25 and 2.59 for LacTv and LacCh, respectively. These Hill coefficients reveal that the binding affinity between laccase and tyrosine increases as the reaction is progressing. The K_m or K_{50}, k_{cat} and k_{cat}/K_m values were determined (Table 3.2). Laccases exhibit higher specificity towards the peptide models than tyrosine, in terms of binding affinity and catalytic efficiency. However, the catalytic efficiency of LacCh for the oxidation of tyrosine is markedly higher than that of LacTv. The k_{cat} value reflects how fast the oxidation of different substrates could happen. The k_{cat} values for ST-10 were estimated to be 0.35 and 0.43 /s for LacTv and LacCh, respectively, which are the highest among the three investigated substrates. The binding affinity between laccase and the substrate was evaluated by K_m value. The K_m values of LacCh (0.41 mM) and LacTv (0.17 mM) for AG-10 are the lowest as compared to those estimated for ST-10 and tyrosine, indicating the higher affinity of laccases towards AG-10. Previous Z-DOCK results showed that laccase exhibits more binding affinity toward patatin, the mother protein of ST-10, than lysozyme, the mother protein of AG-10. The difference between the peptides and their corresponding mother proteins, in terms of binding affinity to laccase, can be attributed to the difference in their structure and spatial hindrance.

Laccases are known for their ability to oxidize mainly tyrosine residues of proteins. However, no study has reported, so far, the kinetic parameters of laccase-catalyzed oxidation of tyrosine; only K_m value of tyrosinase-catalyzed oxidation of tyrosine was previously reported in literature. The reported K_m value for mushroom tyrosinase towards tyrosine (0.25 mM) is lower than those obtained for laccases (LacTv and LacCh), revealing the expected higher affinity of tyrosinase than laccase toward tyrosine (Fenoll et al., 2002). On the other hand, the reported K_m values of LacTv for ABTS, catechol and lignin were determined to be 0.13, 1.11 and 73 mM, respectively; the K_m value of AG-10 is comparable to that of ABTS, whereas the K_m value of tyrosine is comparable to that of catechol (Frasconi et al., 2010; Perna et al., 2019). The K_m values of LacCh in the oxidation of ferulic acid have been reported to be in the range of 0.0059-0.17 mM, which are lower than those obtained for LacCh toward the selected peptides (AG-10; ST-10) (Gill et al., 2018; Kwang-Soo & Chang-Jin, 1998; Smirnov et al., 2001).

Table 3.2. Kinetic and molecular docking study

Substrate	Laccase	Kinetic parameters				docking parameter	
		K_m or K_{50}	V_{max}	k_{cat}	Catalytic efficiency	Binding affinity	Distance
		(mM)	µmol/min mg of protein	/s	/s mM	Kcal/mol	Å
Tyrosine	LacCh	1.12	0.38	0.34	0.30	-4.7	3
	LacTv	1.10	0.06	0.02	0.01	-4.7	4.4
AG-10	LacCh	0.41	0.37	0.33	0.81	-6.8	3.2
	LacTv	0.17	0.34	0.10	0.56	-7.3	3.3
ST-10	LacCh	0.67	0.48	0.43	0.64	-6.4	2.8
	LacTv	0.50	1.25	0.35	0.70	-6.9	3.0

a. The kinetic study was performed at 0.05M sodium phosphate buffer pH 6.5.
b. At the best binding complexes, the shortest distance between the substrate and HIS458 residue of laccase measured by Discovery Studio.
Abbreviation: LacCh, laccase from *Coriolus hirsutus*; LacTv, laccase from *Trametes versicolor*.

In order to better elucidate the kinetic results, docking was performed by Autodock Vina to visualize the interactions between enzyme and substrates at the molecular level. The docking output included 9 binding complexes for each LacCh/peptide or LacTv/peptide model, 6 for LacCh/tyrosine and 8 for LacTv/tyrosine. The best predicted binding complexes of each combination were selected from the docking results for further analysis of the interactions (Fig.3.2) and determination of the binding affinity (Table 3.2). Tyrosine is well fitted into the laccase's catalytic cavity in terms of size; it is likely to form hydrogen bonds with ASP206 (2.4 Å) and interact with PHE265 via π-π stacking in the cavity of LacTv, and hydrogen-bonds with ASN206 (3.3 Å) and HIS 458 (2.8 Å) in that of LacCh. Even though the sizes of the peptides are larger than the catalytic cavity, both peptide chains are able to orient well towards laccase's active site with intermolecular interactions through multiple residues to stabilize the binding. The distance between TYR2 of ST-10 and HIS458 of both laccases is less than 3.0 Å, which is within the distance range of strong hydrogen-bond. This binding complex is further stabilized by the hydrogen-bond between TYR2 and ASP206 of LacTv (ASN206 of LacCh), π-π stacking between TYR2 and PHE265, as well as interactions between other tyrosine, threonine and serine residues on ST-10 with residues around laccase's active site. Similarly, ASN9 or LYS3 on AG-10 orient towards the center of laccases' active site, respectively, and these binding complexes were stabilized by other intermolecular interactions from multiple residues of AG-10, mainly aspartic acid, valine and glycine. The multiple interactions could contribute to a higher predicted binding affinity for the two peptides (-6.0 to 7.5 kcal/mol) than that for tyrosine (-4.7 kcal/mol) (Table 3.2). This is in good agreement with the K_m values. The key difference between the active sites of these two laccases (LacTv and LacCh) is the amino acid at the position of 206; in the case of LacTv, the position of 206 corresponds to an ASP residue, whereas an ASN residue is positioned at 206 for LacCh. Polyakov *et al.* (2009) suggested that ASN206 plays a key role in the oxidation of organic substrates, and empirically showed that the k_{cat} value for LacCh in the oxidation of catechol is higher than that for other fungal laccases with ASP206 present at the cavity (Polyakov et al., 2009). This can explain the higher k_{cat} values of LacCh towards the investigated model peptide substrates (AG-10, ST-10) as compared to LacTv. Furthermore, through the visualization of the intermolecular interactions, the binding of laccases with peptides were found to be more intensive than that with tyrosine, which may have indirectly contributed to the higher catalytic efficiency in the oxidation of peptides than tyrosine.

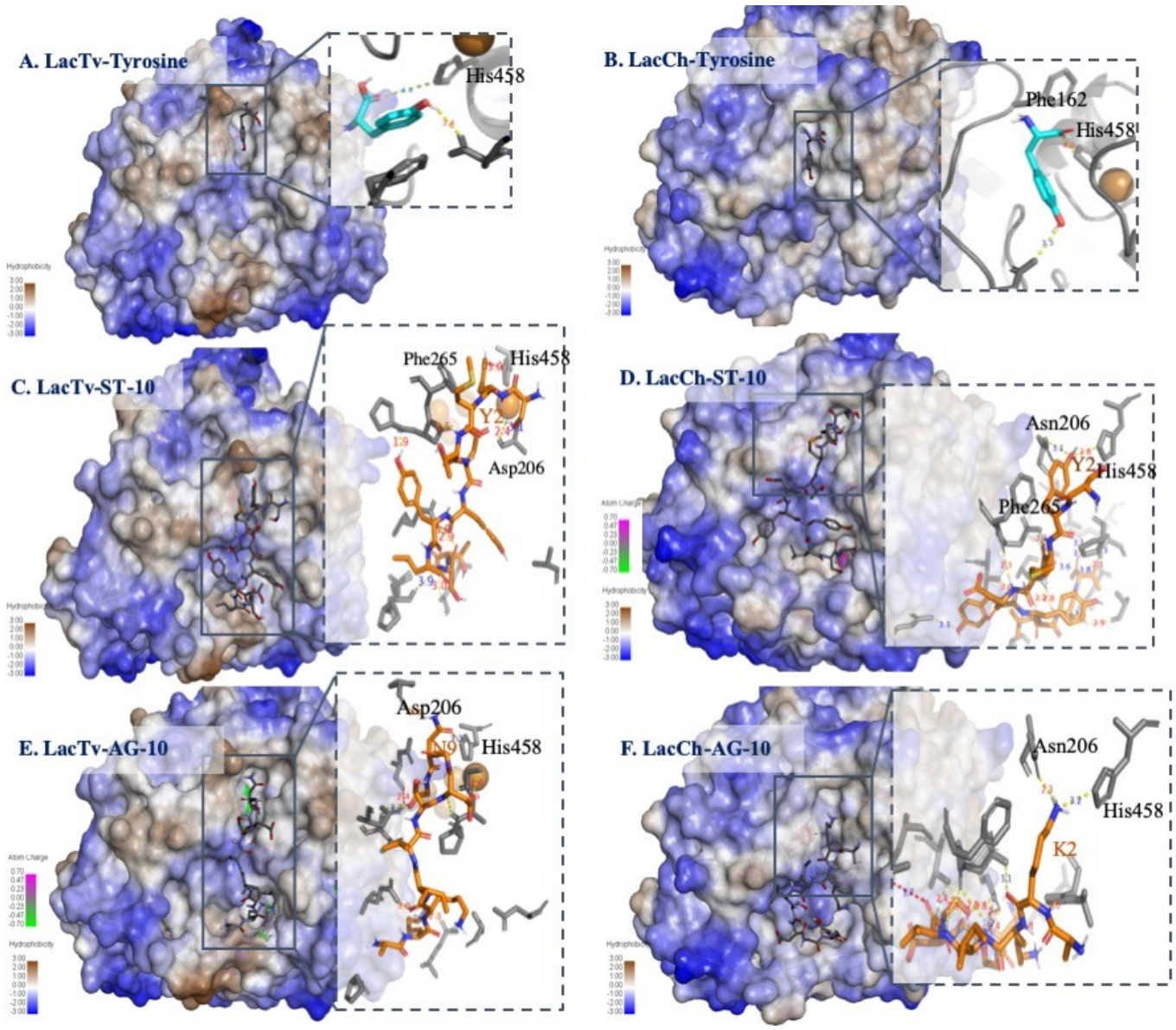

Figure 3.2. Enzyme-substrate interaction predicted by molecular docking study. The general binding poses between laccase and substrate models were shown as a docked substrate on the hydrophobicity surface (blue-brown cover) of laccase where hydrophobic and electrostatic interactions were demonstrated. The inserts is to show hydrogen bonding between laccase and substrate models.

3.4.3. Time courses and end-product profiles of laccase-catalyzed oxidation reactions

The oxidative cross-linking catalyzed by laccase involves two concomitant processes: the enzymatic oxidation, where the substrate is converted to a radical, and non-enzymatic reactions (degradation and cross-linking) producing a mixture of products. The time courses for the bioconversion yield of the oxidation reactions catalyzed by laccase from *T. versicolor* (LacTv) and *C. hirsutus* (LacCh) were investigated (Fig. 3.3). The bioconversion of the model substrates was increased as the reaction proceeded. Peptide ST-10 was bio-converted faster, at a reaction rate of 0.035 and 0.032 μmol/mL min for LacTv and LacCh, respectively, than tyrosine and AG-10 as substrates (Fig. 3.3A & C). The reaction rate for the oxidation of AG-10 was estimated at 0.027 and 0.011 μmol/mL min for LacTv and LacCh, respectively, while that for tyrosine was lower than 0.001 μmol/mL min for both laccases. As a result, a total conversion of peptide ST-10 was achieved within the first hour, while the bioconversion yield of AG-10 reached total conversion within 4 h. Reaction time of 24-48 h was needed for tyrosine to reach 90% of bioconversion. The oxidation rate of the model compounds is in consistence with the V_{max} value obtained from the kinetic study, which is correlated with the reactivity of substrates. The AG-10 peptide from lysozyme is less reactive than ST-10 as a substrate for laccases; this may be attributed to the lack of tyrosine residues on its peptide sequence. Tyrosine is shown to be the least reactive substrate for laccases among the three model substrates, which could be attributed to the inhibitory effects of the end-products (Carunchio et al., 2001). These experimental findings are in agreement with the study reported by Mattinen *et al*. (2005), in which the enzymatic reaction rate was calculated on the basis of the consumption of co-substrate oxygen and they indicated that the reaction rate for tyrosine-containing peptide (GLY and GY) was higher than that for tyrosine itself.

Ferulic acid is a common mediator for laccase-oxidation reaction, in particular for the cross-linking of bulky protein molecules that are not able to access the active site of laccase. Ferulic acid can work as an electron shuttle and/or bridge cross-linking of target substrates, which can improve the efficiency of the enzymatic reaction (Selinheimo et al., 2008). In this study, the effect of ferulic acid on the oxidation of the selected substrates was investigated. Upon addition of ferulic acid, the oxidation rate of AG-10 was enhanced by 50% and 70% with LacTv and LacCh as a biocatalyst, respectively (Fig. 3.3B & D).

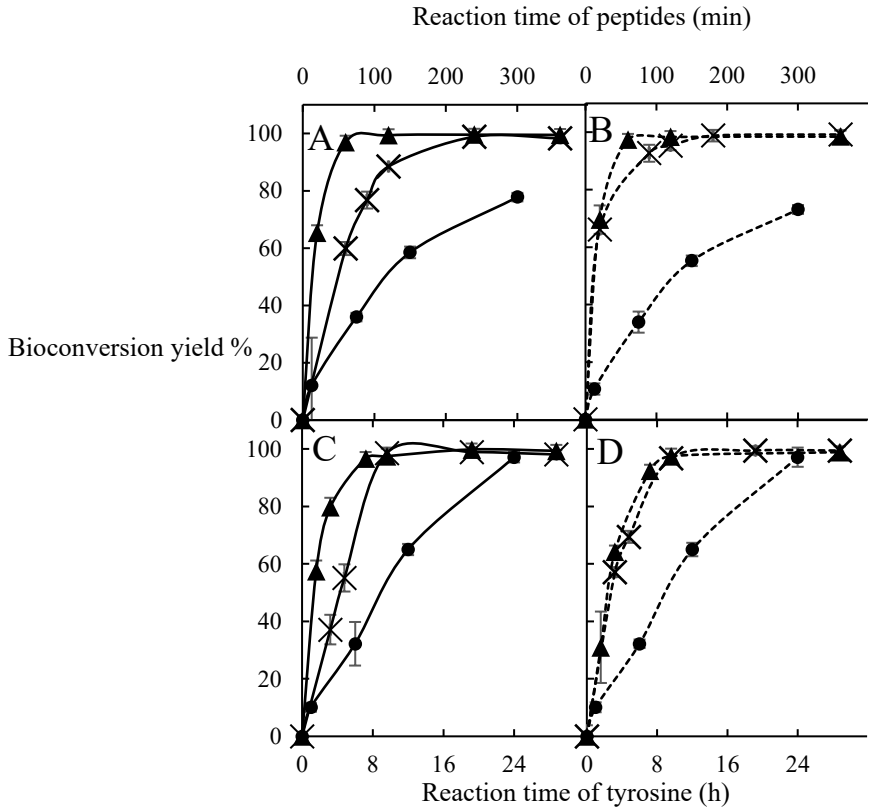

Figure 3.3. Bioconversion yield overtime of the model substrates. Reaction of LacTv A,B and LacCh C,D; solid line are reactions with laccase and model substrate alone and dash lines are those in the presence of ferulic acid. Marker: (●) tyrosine; (▲) ST-10; (×) AG-10.

However, no significant changes in the reaction rate and bioconversion yield were observed in the enzymatic oxidation reactions of ST-10 and tyrosine upon the addition of ferulic acid. Indeed, ferulic acid may have behaved as a competitive substrate to tyrosine and tyrosine-containing ST-10 peptide. It has been reported that the highly reactive ferulic acid can be oxidized to radical prior to tyrosine, resulting in less oligomerization of tyrosine or tyrosine-containing peptides (Steffensen et al., 2009).

The process of oxidative cross-linking was studied through the assessment of the changes in the molecular weight distribution of the products over reaction time. The end-products of the degradation, oligomerization and polymerization of the substrate models were characterized by the molecular weight distribution determined by SE-HPLC (Fig. 3.4) and by the identification of corresponding ions through MS analysis. The results (Figs. 3.5A and 3.5B) show that short-chain oligomers (< 5 units) were the major cross-linked products of tyrosine in the reaction catalyzed by LacTv and LacCh over 48 h time course. The MS analysis (Table 3.3) confirmed the presence of di- and tri-tyrosine in the product mixture. In contrast, higher oligomers of tyrosine, 8-9 units, were identified by Mattinen et al. (2005) in oxidation of tyrosine catalyzed by *T. hirsuta* laccase (Mattinen et al., 2005). For peptide ST-10, derived from patatin, its oxidation resulted in the formation of short-chain (<5 units) oligomers and fragmentation products in the first stage (up to 60 min), and the peak of cross-linked product shifted thereafter towards oligomers (> 5 units) and polymers (> 10 units) (Fig. 3.4A & C). The reaction catalyzed by LacCh contributed to higher proportion of polymerized product. The relative proportion of cross-linked products increased over the reaction time (0-6 h); meanwhile, reduced extent of peptide fragmentation was observed with increased reaction time, indicating that the peptide fragments can be further oxidized and cross-linked by laccase (Fig. 3.5I & J). Among the products, ST-10 dimer $[SYMTDYYLST/SYMTDYYLST]^{2+}$at 1242.5690 m/z was identified in the MS spectra (Table 3.3). Apart from this, product ions with m/z at 1259.4886 can be attributed to the formation of sulfoxide on the methionine residue (Steffensen et al., 2008). The ions at 400.1530, 616.2270, 646.3004 and 862.3723 m/z were identified as $[SYM]^{+}$, $[SYMTD]^{+}$, $[YYLST]^{+}$, $[TDYYLSY]^{+}$ peptide fragments, respectively. These fragments suggest that the oxidation may have occurred at methionine and tyrosine residues of ST-10. In addition, product ions with mass corresponding to cross-linked product of ST-10 oligomer (3-8 units) were detected at low relative abundance (data not shown).

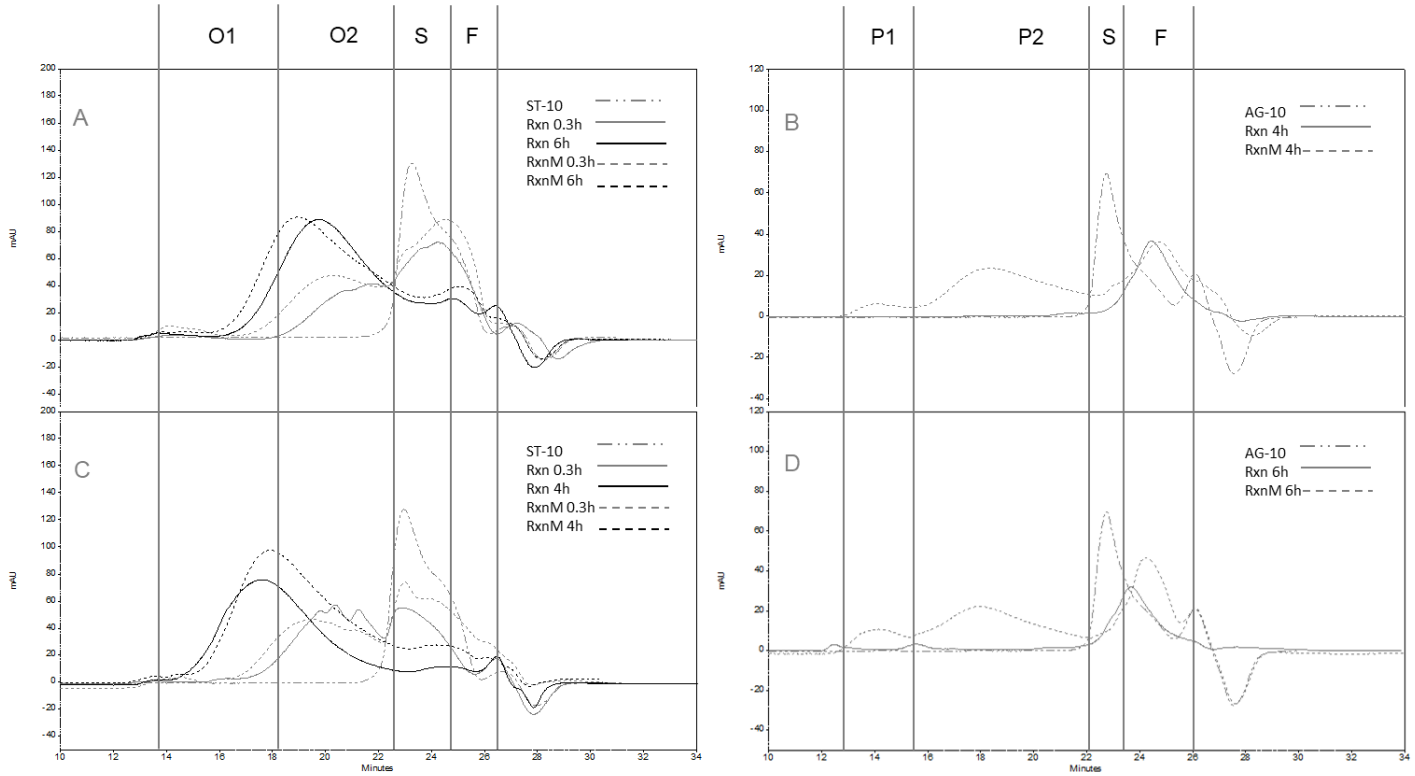

Figure 3.4. Chromatogram of selected reaction samples. Peptide models were incubated with LacTv (A & B) or LacC (C &D) with (rxnM) or without (rxn) the presence of ferulic acid. Different fractions of products were indicated on the chromatogram. Based on their molecular weight: O1, product with more than10 units of ST-10; O2, product with 5-10 units of ST-10; P1, high crosslinked polymers; P2, product with 10 units of AG-10; S, substrate; F, degradation product.

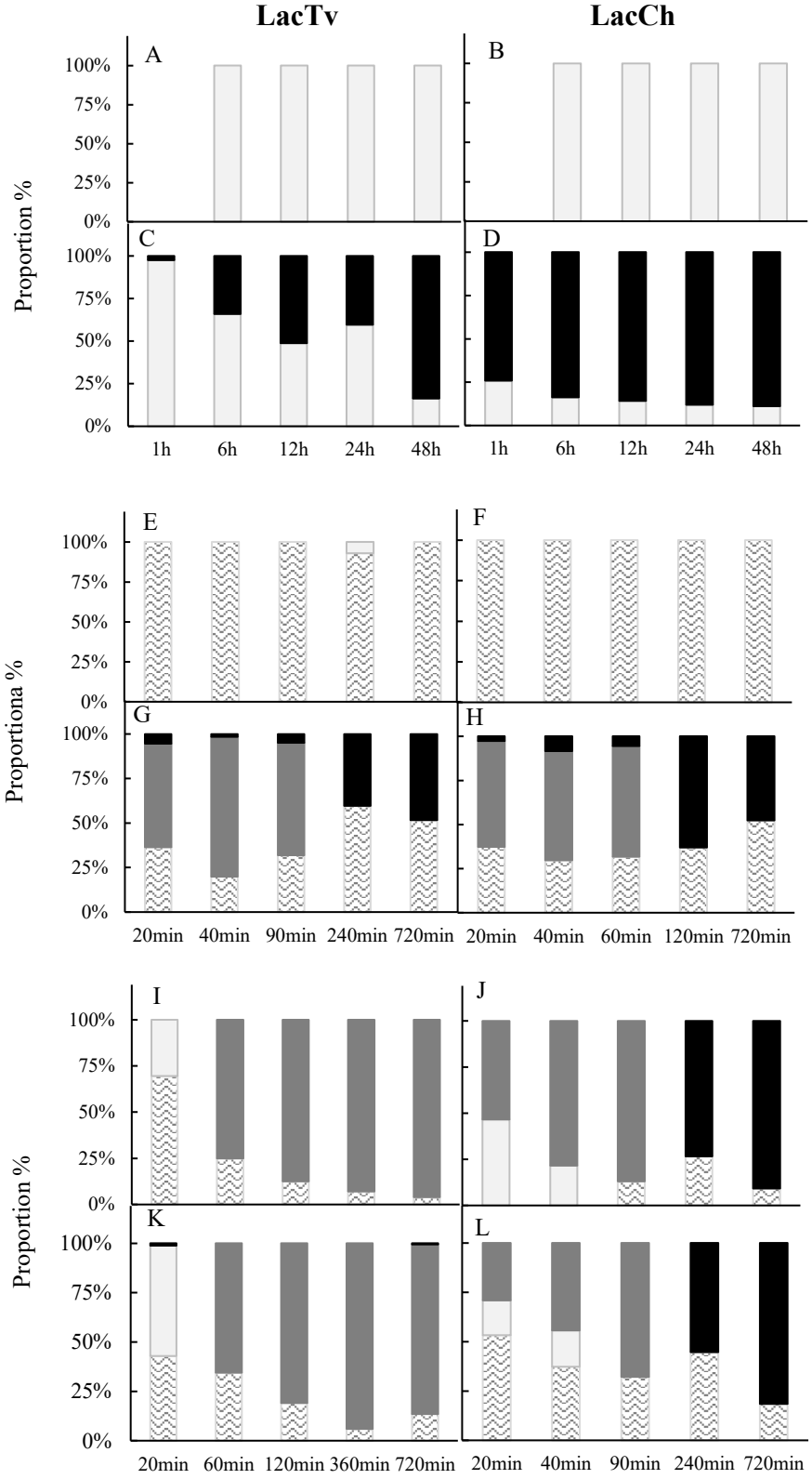

Figure 3.5. End product profiles of laccase-catalyzed oxidation of substrate models. Tyrosine: A, B, without ferulic acid, C, D with ferulic acid; AG-10: E,F without ferulic acid, G, H with ferulic acid; ST-10: I,J, without ferulic acid, K,L with ferulic acid. The end product molecular weight fraction are expressed as: (■) polymer (≥ 10 unit), (■) oligomer (≥5 units), (□) short chain oligomer (≤5 units) and (▨) fragmentation.

The product profile of the AG-10 showed no formation of cross-linked oligomers and polymers over the investigated time course (Fig. 3.4B & D; fig. 3.5E & F), which could be associated with its low reactivity and lack of tyrosine residues. Two degradation products of AG-10, $[AKK+H]^+$ (m/z at 346.2349) and $[IVSDGNG+H]^+$ (m/z at 661.3019), were identified by MS. According to the degradation pattern, lysine residue of AG-10 is likely to be the susceptible site for oxidation. It has been reported that the degradation of peptide upon laccase-catalyzed oxidation can be favored when the neighboring amino acid of the radical residue created steric hindrance against the formation of cross-links (Steffensen et al., 2009).

Ferulic acid was observed to mediate the cross-linking of AG-10 and tyrosine. The cross-linking of AG-10 was notably achieved upon the addition of ferulic acid as a mediator (Figs. 3.5G & H). The main cross-linked product, oligomers (> 5 units) and polymers (≥ 10 units) represent a relative proportion of 47.7-76.4% over the time course of the reaction. The MS analysis (Table 3.3) demonstrated the presence of hetero-oligomers, including AG-10 dimer conjugated with decarboxylated ferulic acid trimer, as well as the ones formed between the AG-10 fragments (AKK or VISDGNG) and ferulic acid tetramer (Table 3.3). The polymerization of tyrosine in the laccase-catalyzed oxidation reaction was also observed to be promoted by the addition of ferulic acid. At the initial stage of enzymatic oxidation of ferulic acid, different types of dimer can be formed including 8-8', 8-5' and 8-O-4'. These dimers can be further oxidized into phenoxy radicals and polymerized (Aljawish et al., 2014; Ward et al., 2001). The MS results (Table 3.3) show the formation of hetero-conjugates of ferulic acid and tyrosine, including dehydro-di-ferulic acid-tyrosine (m/z at 566.1529), decarboxylated tri-ferulic acid-tyrosine (m/z at 716.2263) and dehydro-tetra-ferulic acid-tyrosine (m/z at 948.2227). Conversely, upon addition of ferulic acid to the reaction of ST-10, no increase in the molecular weight and the proportion of the cross-linked products were obtained, but the degradation of the ST-10 was promoted (Figs. 3.4K & L), especially when LacCh was used as a biocatalyst. This confirms that ferulic acid behaved as a competitor to ST-10 peptide substrate rather than a mediator. Apart from these, hetero-conjugates between ST-10, its peptide fragments and ferulic acid were identified from the MS spectra (Table 3.3).The selectivity of the reaction pathways can be determined by the substrate reactivity and the structure of the substrate radicals (Steffensen et al., 2009; Ward et al., 2001).

Table 3.3. Identified end-products from MS

Substrate	Potential compounds	Estimated mass (Da)	Charge state	Estimated m/z	Observed m/z
Y	Y/Y	360.1321	+1	361.1321	361.1408$^{\#\#}$
			+1 ^{Na}	383.1219	383.1226$^{\#}$
	Y/Y/Y	539.1904	+1	540.1904	540.1929$^{\#}$
Y-FA	Y/FA/FA	565.1584	+1	566.1584	566.1529$^{\#}$
	Y/FA/FA/FA[b]	715.2265	+1	716.2343	716.2263$^{\#}$
			+1 ^{Na}	738.2162	738.2007$^{\#\#}$
	TYR/FA/FA/FA/FA[a]	947.2272	+1	948.2272	948.2227$^{\#}$
AG-10	IVSDGNG	660.3079	+1	661.3157	661.3019$^{\#\#}$
			+1 ^{Na}	683.2976	683.2880$^{\#}$
	AKK	345.2376	+1	346.2454	346.2349$^{\#\#}$
			+1 ^{Na}	368.2273	368.2256$^{\#}$
AG-10-FA	AKK/FA/FA/FA/FA [a]	1109.3753	+1	1110.3830	1110.5265$^{\#\#\#\#}$
			+2	555.6877	555.7637$^{\#\#\#\#}$
	IVSDGNG/FA/FA/FA/FA [a]	1424.4456	+1	1425.4530	1425.5916$^{\#\#\#}$
			+1 ^{Na}	1447.4353	1447.578$^{\#\#\#}$
			+2	713.2306	713.2972$^{\#\#\#}$
	AG-10 dimer/FA/FA/FA [b]	2505.1911	+2	1253.6034	1253.6090$^{\#}$
			+2 ^{Na}	1264.5944	1264.6056$^{\#}$
			+3	836.0715	836.0693$^{\#}$

ST-10	ST-10 dimer	2483.0073	+2	1242.4511	1242.5685$^{\#\#\#}$
	SYMTDYYLST^{+o}	1258.5064	+1	1259.5142	1259.4886$^{\#\#}$
	SYM	399.1464	+1	400.1542	400.1530$^{\#}$
	SYM/SYM [a]	794.2615	+1	795.2693	795.2826$^{\#}$
	SYM^{+O}	415.1413	+1	416.1491	416.1484$^{\#}$
	SYMTD	615.2210	+1	616.2288	616.2270$^{\#}$
	YYLST	861.3756	+1	862.3834	862.3723$^{\#}$
	YYLSY/YYLSY [a]	1286.5706	+1	1287.5785	1287.477$^{\#\#\#}$
	TDYYLST	645.3009	+1	646.3088	646.3004$^{\#}$
ST-10-FA	STYMTDYYLST/FA/FA/FA [a,b]	1728.6429	-1	1727.6351	1727.6400$^{\#}$
	SYM/FA	591.1886	+1	592.1964	592.2464$^{\#\#\#}$
	SYM^{+O}/FA [a]	605.1679	+1	606.1757	606.2729$^{\#\#\#\#}$
	SYMTD/FA [a,b]	761.2578	+1	762.2656	762.3836$^{\#\#\#\#}$
	YYLST/FA [a]	835.3276	+1	836.3354	836.3681$^{\#\#}$
	YYLST/FA/FA [c]	1012.3827	+1	1013.3906	1013.313$^{\#\#\#}$
	YYLST/YYLST/FA [c]	1444.6074	+1	1445.6153	1445.6088$^{\#}$

*tyrosine abbreviation: Y, ferulic acid abbreviation: FA;
The deviation range was reported as $^{\#}$ 0-20 ppm, $^{\#\#}$ 20-40 ppm, $^{\#\#\#}$ 40-100 ppm, $^{\#\#\#\#}$ 100-200 ppm.
^{Na} is referred to sodium adducts
a. Oxidative cross-linking involved dehydrogenation; could be related to formation of intramolecular bonds in the cross-linked products/hetero-conjugates;
b. The formation of the hetero-conjugates involved decarboxylation of the ferulic acid;
c. The formation of the hetero-conjugates involved dehydration

A mixture of possible pathways was identified in our study for the substrate models in the reaction catalyzed by laccase. Similarly, the heterogeneity and complexity of the laccase's oxidation products of different peptide substrates have been reported previously (Mattinen et al., 2005; Steffensen et al., 2009). The cross-linking of peptides GY and GLY catalyzed by laccase from *T. hirsuta* resulted in products with 13 to 59 units. Products with low crosslinking degree, such as dimer to pentamer, were observed as the cross-linked product of larger peptides VEPIPY by LacTv (Mattinen et al., 2005; Steffensen et al., 2009). The oxidative degradation of the peptide/protein substrates was also reported and attributed to substrate structure (Lantto et al., 2005; Steffensen et al., 2009). As to the enzymatic reaction mediated by ferulic acid, the heterogeneity was shown to be further enhanced due to the co-existence of homo-cross-linked products and hetero-conjugates (Selinheimo et al., 2008).

3.4.4. Characterization of oxidation-induced cross-links

The oxidative cross-linked products were further structurally analyzed at their cross-links. Among the amino acids, tyrosine was identified to be the primary oxidation site for laccase. Thus, the cross-links of oligomerized product of tyrosine-containing peptides were expected to associate with tyrosine residues. The tyrosyl radicals, generated during the oxidation by laccase, can form C-C bonds between two aromatic rings (dityrosine) or C-O ether bonds via joining a hydroxyl radical and a radical on the aromatic ring (isodityrosine) (Mattinen et al., 2005). Considering the steric hindrance, isodityrosine cross-links could be more favored for the bulky structure of peptide or proteins rather than dityrosine. The MS analysis of the acid hydrolysates of cross-linked ST-10 reaction mixture showed the presence of dehydrotyrosine dimer (Y-Y) with relatively high abundance (Fig. 3.6A). This indicates that the cross-linking happened via dimerization of two tyrosine from two peptide molecules. Since there are three tyrosine residues on ST-10, further oligomerization can be progressively formed via multiple Y-Y cross-links with a proposed structure as scheme 3.1A. In addition, higher tyrosine oligomers (Y_3 -Y_7) were also identified in these hydrolysates from the MS spectrum (Fig. 3.6A, insert), revealing that the cross-linked products were continuously oxidized by laccase on its tyrosine dimer crosslinks and then further condensed with other tyrosyl radicals. Thus, the peptide ST-10 can also be oligomerized via these oligo-tyrosine cross-links, $-(Y)_n-$ ($n>2$) (scheme 3.1B), at less extent as compared to that via Y-Y cross-links.

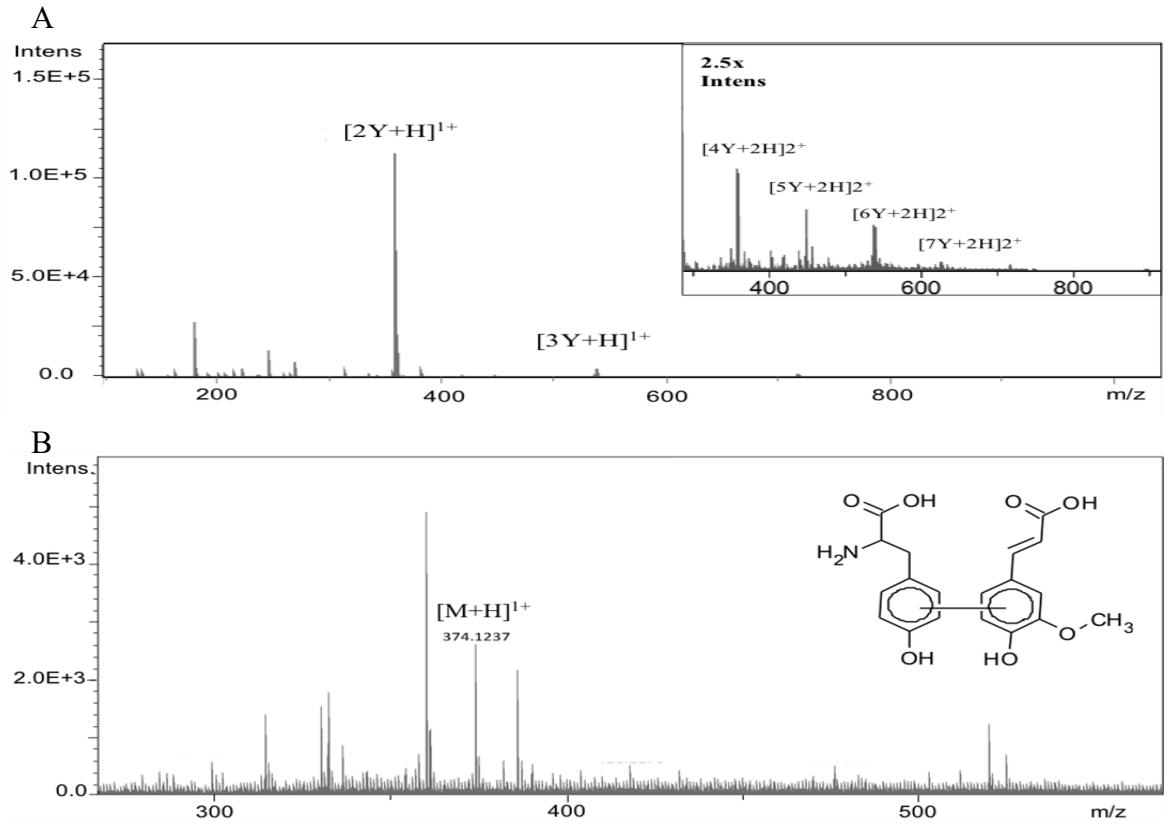

Figure 3.6. Mass spectra of potential cross-links. A. Oligo-tyrosine cross-links; B. tyrosine-ferulic acid cross-link.

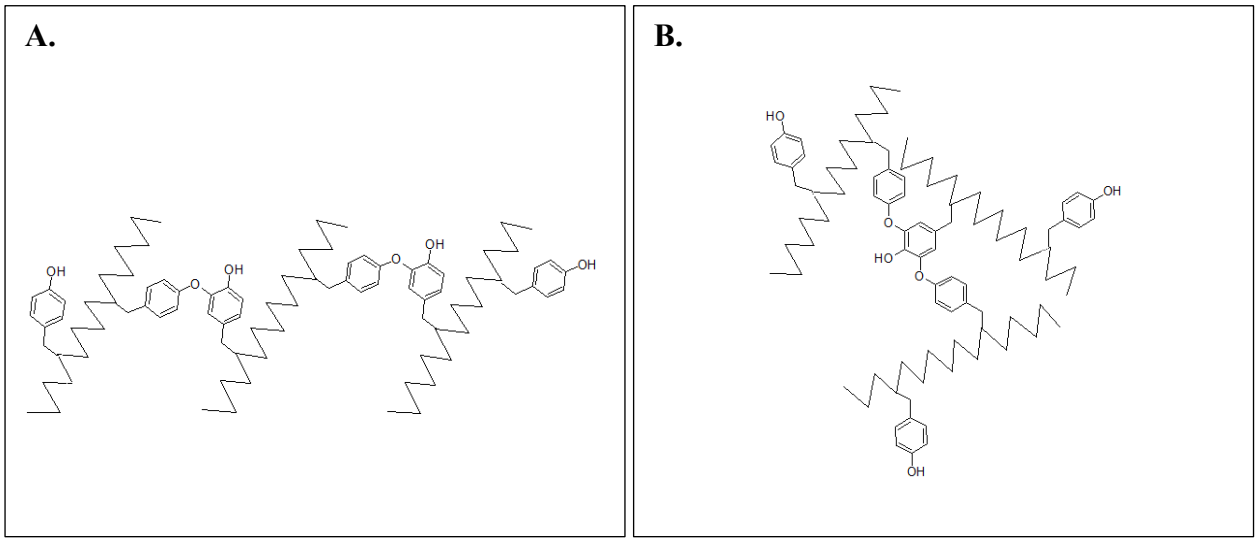

Scheme 3.1. Oligo-tyrosine cross-links for ST-10

From the ST-10 reaction mixture in the presence of ferulic acid, these oligo-tyrosine cross-link structures were also found. Another compound ion with m/z ratio of 374.1237 corresponding to tyrosine-ferulic acid cross-link was identified (Fig. 3.6B). This indicates that the incorporation of ferulic acid to ST-10 is via tyrosine residue. From the hydrolysate of AG-10-FA reaction mixture, no crosslinks between amino acids from AG-10 or amino acid and ferulic acid was found. This could be due to lower stability of amino acid-ferulic acid crosslinks, as compared to that of oligo-tyrosine and tyrosine-ferulic acid cross-links. Another oxidoreductase, peroxidase has been reported for similar pathways in oxidative cross-linking of protein related substrates (Dhayal et al., 2015; Piber & Koehler, 2005). Both peroxidase and laccase catalyzed the oxidative cross-linking via radical formation. Until now, evidence about chemistry and structure was mainly shown for the oxidative cross-linking that involved tyrosine and cysteine residues.

3.5. Conclusion

Laccase-catalyzed oxidation reactions using three substrate models were studied in terms of binding and interaction between enzyme and substrates, oxidation kinetics, the time course and end product profiles of the reactions. The molecular docking study showed that, multiple intermolecular interactions, including hydrogen bonds and π-π stacking, were observed in the stabilization of the binding between laccases and two peptides, while less intermolecular interactions were detected between tyrosine and laccase molecules. The higher binding affinities and k_{cat} value of two peptides, with their lower K_m values collectively indicated that LacTv and LacCh exhibited high catalytic efficiencies toward patatin (ST-10)- and lysozyme (AG-10)-derived peptides than tyrosine. In the enzymatic reaction with the absence of ferulic acid, both tyrosine and ST-10 can be oxidized and crosslinked via Y-Y or $(Y)_n$– cross-links, while the major products for AG-10 were degraded peptide fragments. Ferulic acid was observed to play different roles for different substrates. For non-tyrosine containing peptide AG-10, FA worked as an efficient mediator and enhanced the bioconversion yield/rate and cross-linking extent of AG-10. For the tyrosine-containing peptide ST-10, ferulic acid acted as a competitive substrate, leading to decrease in cross-linked products. Furthermore, the characterization of the end-product profiles and of cross-links revealed the formation of homo- and hetero- oligomerized products. The present study contributed to the understanding of laccase-catalyzed oxidative cross-linking mechanism towards protein-derived substrates. Future work on studying the cross-linking of their parent proteins will be carried out for the development of novel protein functional ingredients.

CONNECTING STATEMENT 2

In Chapter III, the enzyme kinetics and reaction mechanisms of laccase was studied and a mixture of reaction pathways were identified for laccase-catalyzed oxidative cross-linking for selected substrate models. The result implied that the cross-linking of a globular compact protein without exposed tyrosine residue could be prohibited. Chapter IV describes the utilization of a substrate engineering approach to improve the cross-linking efficiency of such proteins in laccase-catalyzed reactions. Egg white lysozyme and ovalbumin were investigated as the substrate proteins. The characterization of product profile and structure, techno-functional properties (Foaming, emulsifying) and allergenicity of the cross-linked products was reported.

Li, M., Liu, L., L'Hocine, L., Achouri, A., Pitre, M., Light, K., Mateo, C., & Karboune, S. (2020). Combining protein surface modification and laccase-catalyzed cross-linking of egg white proteins: structural and functional properties. *Journal of Agricultural and Food chemistry*. (Submitted to the Journal).

.

CHAPTER IV. COMBINING PROTEIN SURFACE MODIFICATION AND LACCASE-CATALYZED CROSS-LINKING OF EGG WHITE PROTEINS: STRUCTURAL, FUNCTIONAL PROPERTIES AND ALLERGENICITY

4.1. Abstract

The efficiency of protein cross-linking catalyzed by laccase can be impacted by the protein structure and the extent of simultaneously competing reactions. In the present study, a substrate engineering approach based on the chemical grafting of ferulic acid (FA) moieties on protein surface was investigated in order to modulate the crosslinking of two different globular proteins with inflexible structure, lysozyme (LZM) and ovalbumin (OVA). The effect of FA grafting extent of protein substrates on *Trametes versicolor* laccase (LacTv)-catalyzed cross-linking was studied. While laccase-catalyzed reactions did not lead to evident cross-linking of native LZM and OVA, oligomeric products (<10 units, up to 16.4%) and polymeric products (>10 units, up to 30.6%) of FA-LZMs and oligomeric FA-OVA (5.1-31.1%) were obtained upon the enzymatic treatments. The cross-linking extent and the cross-linked product profile were affected by the number of grafted FA sites on protein substrate. The molecular structure and the FA-associated covalent linkages of the cross-linked products were characterized. Selected techno-functional properties and the allergenicity of cross-linked LZM and OVA were also evaluated and discussed in relation to the structural properties.

4.2. Introduction

Protein cross-linking has attracted considerable attention as a strategy for modulating structural and mechanical properties of matrix and biopolymer networks as well as for developing biomolecules with targeted functions. Such biomolecules are of great interest in the fields of food, polymer and biomedical science(Benjamin P. Partlow et al., 2016; Hollmann & Arends, 2012; Permana et al., 2020). In particular, due to its safe and mild process and specificity, the enzymatic cross-linking has attracted high interest in food processing to modulate the physiochemical properties of proteins (e.g. solubility, thermal stability, surface hydrophobicity) and to enhance their techno-functional properties (e.g. emulsifying, foaming or gelling performance) (Buchert et al., 2010; Isaschar-Ovdat & Fishman, 2018). Some studies have also shown the ability of protein cross-linking to decrease the protein's allergenicity (Lv et al., 2019; Mihajlovic et al., 2016). Laccase (E.C 1.10.3.2), an oxidoreductase with copper-coordinated redox center, is an effective biocatalyst for protein cross-linking. The oxidative cross-linking of protein catalyzed by laccase is performed mainly through the formation of dityrosine bonds upon oxidation of tyrosine residues, identified as the prime targets in proteins; the formation of disulfide bonds by oxidation of cysteines into cystine can also occur (Mattinen et al., 2006; Steffensen et al., 2009). Laccase-catalyzed oxidation of proteins can also result in several

amino acid modifications, such as the oxidation of tryptophan into N′- formylkynurenine and further to kynurenine and the formation of carbonyl groups upon the oxidation of methionine, as well as in protein fragmentation (Ercili Cura et al., 2009; Steffensen et al., 2008).

Protein cross-linking catalyzed by laccase can be limited by the protein conformation, which can hinder the enzyme accessibility to their reactive residues (Jung & Wicker, 2012b; Mattinen et al., 2006). The use of phenolic acid mediator can promote protein-protein cross-linking, but it may also favor side reactions, such as polymerization of phenolic acid meditoar and the conjugation between phenolics and proteins. (Ma et al., 2011; Steffensen et al., 2009). We hypothesized that the bioconjugation of phenolic moieties on the surface of proteins can create reactive sites for laccase and limit the side reactions, thus allowing a better modulation protein cross-linking. Indeed, the bioconjugation of methoxyphenol groups on whey protein's surface was achieved via chemical amidation with vanillic acid, and the efficiency of laccase-catalyzed cross-linking of whey protein was greatly improved upon such modification (Ma et al., 2011). Alternatively, the modification of proteins to append a tyrosine-containing polypeptide tag was used to direct the site-specific polymerization of proteins catalyzed by laccase/peroxidase, and generate well-structured and highly functional protein polymer assemblies (Minamihata et al., 2011; Permana et al., 2018; Permana et al., 2020). The present study was aimed at the investigation of a substrate engineering approach for the modulation of the protein cross-linking catalyzed by *Trametes versicolor* laccase. Two major proteins from egg white, LZM and OVA, were selected as model protein substrates, and were grafted with controllable and quantifiable feruloyl (4-hydroxy-3-methycinnamoyl) moieties on their surface as new reactive sites for laccase. This approach was based on the modification of protein substrates by grafting controllable and quantifiable feruloyl (4-hydroxy-3-methycinnamoyl) moieties on their surface as new reactive sites for laccase. The relationships between the reactivity of FA-grafted proteins and their enzymatic crosslinking efficiency was discussed with the aim to lay the ground for better modulation of their functionalities. The effect of FA-grafting-LacTv-catalyzed cross-linking on LZM and OVA were assessed by the changes molecular weight profile, the molecular structure of the cross-linked proteins and in selected techno-functional properties and allergenicity.

4.3. Materials and methods

4.3.1. Materials

Lysozyme, ovalbumin, ferulic acid, laccase from *T. versicolor* (LacTv), n-hydroxysuccinimide (NHS), 2,4,6-Trinitrobenzene Sulfonic Acid (TNBS), 2,2'-azino-bis (3-ethylbenzothiazoline-6-sulphonic acid) (ABTS), Folin-Ciocalteu phenol reagent and ethyl acetate were purchased from Sigma Aldrich (St-Louis, MO). 1-ethyl-3-(3-dimethylaminopropyl) carbodiimide hydrochloride (EDCI) was from Tokyo chemical Industry Co. Ltd (Tokyo, JP). Dimethylformamide (DMF) was purchased from Fisher Scientific (Hampton, NH). Serum samples from 6 egg allergic patients were purchase from PlasmaLab (Everett, WA). 3,3′,5,5′-tetramethylbenzidine (TMB) is product of Bioshop (Burlington, ON, Canada). Laccase activity was evaluated using ABTS assay as described by Nikku-Paavola et al., 1990 ABTS per min. One unit activity was defined as the amount of enzyme that oxidize 1 μmol of

4.3.2. Chemical modification of protein substrates

The bioconjugation of FA and protein was performed via a two-step amidation reaction, including NHS-FA ester activation and acylation, according to the modified method of Ma et al., (2011). NHS, EDCI and FA were dissolved in DMF and incubated at 28 °C for 17 h to prepare NHS-FA esters at three concentration levels for each protein. The concentration of FA was maintained in excess at 103 mM, while the concentration of NHS and EDCI was set at 6.1 to 47.3 mM and 6.9 to 54.0 mM, respectively. Protein solution at 10 mg/mL were prepared in sodium phosphate buffer 50 mM at pH 7.0. At second step, acylation reaction mixtures at molar ratios of NHS-FA to protein 1.7:1, 3.2:1 and 6.4:1 were prepared by mixing the activated NHS-FA solution at selected concentrations with protein solution and incubated at 28 °C for 24h. The FA-LZMs and FA-OVAs conjugates were recovered by thorough dialysis and freeze-dried. Protein content of all samples was determined using the Bradford assay (Bradford, 1976).

4.3.3. Chemical characterization of ferulic acid-modified proteins

4.3.3.1. Determination of free amine group content

The free amine content in the native and modified proteins was measured via TNBS assay (Habeeb, 1966). Protein solutions at 0.2 mg/mL were prepared in sodium bicarbonate buffer (pH 8.5, 0.1 M) and mixed with TNBS solution (0.01%, w/v) at a ratio of 2:1 (v/v); the mixture (0.75 mL) was incubated at 37 °C in the dark. After 2 h incubation, 0.25 mL of SDS solution (10%, w/v) was added to prevent precipitation of the protein; 0.125 mL of 1 N HCl was added to stop the reaction. The absorbance of the mixture was measured at 335 nm using a Beckman DU 650 spectrophotometer (Beckman Instruments Inc.; San Ramon, CA). The assay blank

without TNBS reagent and control buffer sample without proteins were run in parallel with the samples. Triplicate measurements were performed for each sample. L-leucine solutions at concentrations ranging from 2 to 16 μg/mL were used for the construction of the calibration curve. The free amine content was expressed as the mole of free amine moiety equivalent per mg of protein.

4.3.3.2. Measurement of total phenolic content

The total phenolic content of native and modified proteins was determined using Folin-Ciocalteu phenol reagent. A mixture of protein solution (0.05-0.2 mg/mL), sodium bicarbonate (250 g/L) and phenol reagent was prepared at ratio of 800/150/50 (v/v/v), and incubated at 40 °C for 30 min. The absorbance was measured at wavelength 765 nm. Measurements were carried out in triplicates. The calibration curve was constructed using gallic acid solutions at concentrations ranging from 0.001 to 0.1 mM. The total phenolic content was expressed as the mole of phenolic moiety equivalent per mg of protein.

4.3.3.3. Mass spectrometry analysis of modified proteins

The mass spectrometry analysis of modified proteins was carried out using a Bruker Maxis electrospray ionization-quadruple-Time-of-Flight-mass spectrometer (ESI-QTOF-MS). Samples were separated on Agilent PLRP-S column (5 μM, 1000Å, 2.1 × 50 mm) using an inline Dionex Ultimate 3000 UHPLC system at 80 °C. The elution was carried out using a gradient from 80% mobile phase A (0.1% formic acid in water)/20% mobile phase B (0.1% formic acid in acetonitrile) to 20% mobile phase A/80% mobile phase B in 12 minutes. The ESI-MS was performed at positive ion mode, and the ESI parameters were set as nebulizer pressure at 0.4-1.0 Bar, temperature at 180-200 °C, 4.0-6.0 l/min of dry gas, capillary voltage at 4500 V. The scanning range was m/z 200-3500. The mass signal of protein was deconvoluted and analyzed using the Bruker Compass Data Analysis software (version 4.2).

4.3.4. Laccase-catalyzed oxidative cross-linking of proteins

Laccase-catalyzed cross-linking was carried out using native and FA-modified proteins as substrates. The reaction mixture consisted of 2 mg/mL of protein and 0.024-0.2 U/mg substrate of enzyme solution prepared in sodium phosphate buffer (pH 6.5, 50 mM). Laccase-mediator reactions were also performed with the native proteins using 0.5 to 1 mM of ferulic acid. The cross-linking reactions were carried out for 48 h time course. At selected time intervals, aliquots of reaction mixture were taken and analyzed by electrophoresis. Control reactions

without laccase or mediator were run in parallel. After halting oxidative reaction, the reaction mixtures were dialysed at 4 °C and lyophilized to recover the cross-linked proteins.

4.3.5. Sodium dodecyl sulfate - polyacrylamide gel electrophoresis (SDS-PAGE)

The electrophoresis was carried out using a mini protein gel apparatus (Bio-Rad, Hercules, CA) following the protocol of Laemmli (1970) . Reaction mixture samples (15 µL) was loaded to 0.75 mm polyacrylamide gels, which consisted of 4% of stacking gel and 12 % of resolving gel for OVA samples or 15 % for LZM samples. The electrophoresis of the protein was run at 120 V. Protein standards with a broad range of molecular weight (6.5 to 200 kDa, Bio-Rad) were used for molecular weight calibration. After Coomassie staining, the electrophoretic patterns were analyzed densiometrically using Red Image system and Alphaview software (version 3.3.1, Cell Biosciences, Santa Clara, CA) to estimate the molecular weight profile of the protein samples. The bioconversion was estimated from the decrease in the proportion of monomer upon the enzymatic treatment. The cross-linking extent was defined as the increase in the proportion of high molecular weight fractions, corresponding to cross-linked products.

4.3.6. Characterization of the ferulic linkages of the cross-linked proteins

The recovery of phenolic compounds (free grafted ferulic acid and ferulic linkages) from the proteins was performed using an optimized alkaline hydrolysis procedure, in which the protein (12.5 mg/mL) was suspended in 4.2 M sodium hydroxide and incubated at 68 °C for 18 h in darkness. The alkaline hydrolysates were acidified to pH 2.0-2.5 using 10 M hydrochloric acid. Phenolic compounds were then extracted three times with ethyl acetate at a ratio of 1:1.5 (v/v); the extracts were evaporated until dryness using a Thermo Scientific AES2010 SpeedVac® System (Waltham, MA) and re-dissolved in methanol/water mixture (50:50 v/v). The characterization and quantification were performed by mass spectrometry using Agilent 1290 Infinity II LC system coupled to the 6545 QTOF -MS (Agilent Technologies, Santa Clara, USA). The sample (1 µL) was eluted on an Agilent poroshell120 EC-C18 analytical column (Agilent Technologies), using a gradient method ramped from 98% of mobile phase A (5 mM ammonium acetate in water)/2% of mobile phase B (methanol/acetonitrile of 1:1, v/v) to 20% of mobile phase A/80% of mobile phase B in 8.5 minutes, at flow rate of 0.3 mL/min. The MS was operated in both positive (ESI+) and negative ion modes (ESI-). The conditions were set as follows: the drying gas temperature was 200 ° C at a flow rate of 10 mL/min, sheath gas temperature was 300 ° C at a flow rate of 12 mL/min, the pressure of nebulizer was 40 psi, the capillary voltage was 3000 V, the nozzle voltage was 0 V, the fragmentor voltage was 125 V

and the skimmer voltage was 65V. For targeted MS/MS fragmentation, collision energy was 20 V. The identification of oligomerized ferulic acid cross-links was based on the accurate mass and the isotopic patterns, as well as the diagnostic fragment ions if available. The consumption of grafted FA sites on proteins was estimated by the difference between the extracted free grafted FA from the control sample and that from the corresponding reaction sample.

4.3.7. Assessment of techno-functional properties of the cross-linked proteins

4.3.7.1 Emulsifying property

The emulsifying ability and stability of LZM samples (native and cross-linked LZM) was investigated. The emulsion was obtained by homogenizing a mixture of the protein solution (0.5 % w/v in 10 mM sodium phosphate buffer, pH 7) and the sunflower oil at a ratio of 3:1 (v/v) using a Fisherbrand™ 850 Homogenizer (Fisher Scientific, Pittsburgh, PA) at 22000 rpm for 90 secs. The initial turbidity of the emulsions and turbidity after 15 min was measured at $\boldsymbol{\lambda}$=500 nm, represented by A_0, A_{15}. The samples were diluted 200 times in 0.1% w/v SDS prior to the turbidity measurement. Emulsifying activity (EA) index and emulsion stability (ES) index were calculated as shown by equation 4.1 and 4.2, respectively.

$$\text{EA index } \left(\frac{\boldsymbol{m^2}}{\boldsymbol{g}}\right)=\frac{\mathbf{2\times 2.303\times A_0\times DF}}{\boldsymbol{c\times\varphi\times 10^4}} \qquad \text{(Eq. 4.1)}$$

$$\text{ES index (min)}=\frac{\mathbf{A_0}}{\mathbf{A_0-A_{15}}} \qquad \text{(Eq. 4.2)}$$

where, DF was the dilution factor of the emulsion (200); c was the concentration of the aqueous solution (0.5 w/v); φ was the oil volume fraction (0.25). In addition, micro-images of the emulsion samples were taken using Zeiss Axio Imager Z1(Zeiss, Jena, Germany) in differential interference contrast (DIC) mode with a 20× magnification objective.

4.3.7.2 Foaming property

Foaming properties of the native and cross-linked ovalbumin were analyzed using a sparging method as described by Waniska and Kinsella (1979) with modifications. Protein solution at 0.5 % w/v was prepared in sodium phosphate buffer (10 mM, pH 7.0) and stirred for 10 min at room temperature (25 °C) for rehydration. A water-jacketed glass condenser foam chamber (70 mL) was loaded with 15 mL of solution via the septum-stoppered inlet. Nitrogen gas was sparged through the solution until the foam chamber was filled, simultaneously liquid was continuously injected to the chamber in order to maintain equal liquid volume as the starting

point. The required time for reaching this volume of foam was recorded (T_f). After 5 min, the volume of the liquid drained from the foam was recorded as (V_d). Parameters related to foaming properties, which were the percentage of gas entrapped in the foam (G_i), the percentage of foam expansion (FE) and the percentage of liquid retained in the foam after 5 min (R_5), were calculated as the following equations (Eq. 4.3-4.5):

$$\mathbf{Gi} = \frac{\mathbf{55} - \boldsymbol{Vi}}{\boldsymbol{FR} \times \mathbf{Tf}} \times \mathbf{100} \quad \text{(Eq. 4.3)}$$

$$\boldsymbol{FE} = \frac{\mathbf{70} - \boldsymbol{V0}}{\boldsymbol{Vi}} \times \mathbf{100} \quad \text{(Eq. 4.4)}$$

$$\mathbf{R}_5 = \frac{\boldsymbol{Vi} - \mathbf{Vd}}{\boldsymbol{Vi}} \times \mathbf{100} \quad \text{(Eq. 4.5)}$$

Where, FR was the nitrogen flow rate (mL/min); V_0 was the initial volume of liquid (15 mL); V_i was the volume of liquid injected during the foaming process.

4.3.8. Assessment of immunoglobulin E (IgE)immunoreactivity

Inhibition enzyme linked immunosorbent assay (ELISA) was used to evaluate the changes in IgE binding capacity of LZM and OVA upon cross-linking. The extracts of native and cross-linked OVAs were prepared in 10 mM phosphate buffer 7.4 with 137 mM NaCl (PBS); that of LZMs were prepared in 50 mM Tris-HCl buffer at pH 7.5 containing 1% w/v SDS. Extracts were then centrifuged (Eppendorf 5430R) at 16 000 x g for 15 min at 4 °C. Soluble proteins were estimated using BCA method (Pierce™BCA Protein Assay Kit, Fisher Scientific). A pool of human sera from individuals with documented egg allergy and containing high level of specific IgE antibodies to LZM and OVA was used for the IgE binding inhibition experiments. Sera containing specific IgE antibody for house dust mite and low total IgE were used as negative controls and non-atopic controls, respectively.

Proteins extracts at 10-fold serial dilution (0.001 to 1000 µg protein/mL) as inhibitors were pre-incubated with pooled sera overnight at 4 °C for OVA samples, and for 2 h at 25 °C for LZM were pre-incubated 2 h at 25 °C. The inhibition experiments were carried out by loading various reagents in sequence; upon the incubation of each loading, a three-time washing process using PBS containing 0.1 % Tween-20 (PBS-T) was applied prior to the next operation. Native OVA or LZM in PBS (25 µg) was first coated on 96-well microplates (Costar™, Corning, NY, USA) and incubated overnight at 4 °C, then blocked by adding 50 µL 5% w/v bovine serum albumin with incubation at 25 °C for 2 h. The coated plates were added with 50 µg of the inhibitor mixtures and incubated for 2 h at 25 °C, followed by loading with secondary

anti-body, peroxidase-labeled mouse anti-human IgE (1:1000 dilution with 1% BSA in PBS-T), and incubated for 1 h at 25 °C. The activity of peroxidase was developed by reacting with 50 µL TMB for 15 min at 25°C and halted by adding 50 µL 1N H_2SO_4. The absorbance at wavelength 450 nm was measured (A). Pooled sera with no inhibitors were used as positive control (100% reactivity) (absorbance recorded as A_0). The percentage inhibition of IgE binding of cross-linked protein were calculated from the absorbance $(\frac{A}{A_0})\%$. IC_{50} was defined as the concentration of the protein samples, where 50% of inhibition of IgE binding was achieved, which was determined via curve-fitting using Gen5 software (Bio-Tek, Winooski, VT, USA). The percentage of IgE binding were determined by the ratio of the IC_{50} of the native protein to the cross-linked protein (Eq.4.6)

$$\%\ \boldsymbol{of\ IgE\ binding} = \frac{\boldsymbol{IC}_{50(\text{native})}}{\boldsymbol{IC}_{50(\text{cross-linked})}} \times \mathbf{100} \qquad \text{(Eq. 4.6)}$$

Experiments were performed in triplicates. A two-way ANOVA followed by mean comparison was performed using the Tukey test. *p*-values ≤ 0.05 were considered to be statistically significant.

4.4. Results and discussion

4.4.1. Surface modification of proteins and their structural characterization

Based on our preliminary results, amidation with selected molar ratios of NHS-FA to protein (1.7:1, 3.2:1, 6.4:1) were performed in order to achieve different content of grafted FA moiety on protein surface. Indeed, NHS-activated FA was first formed in the presence of EDCI, and was then involved in forming stable amide bond with primary amine on protein surface by releasing NHS group (Hermanson, 2013). The amine side chain of lysine residues and the primary amine of N-terminus are the most reactive targeted sites for this modification. It can be assumed that the modification extent was dependent on the position and accessibility of lysine residues. Based on the protein sequences, LZM (PDB: 1DPX) and OVA (PDB: 1OVA), LZM contain in total 6 and OVA has 20 lysine residues, respectively (Stein et al., 1991; Weiss et al., 2000).

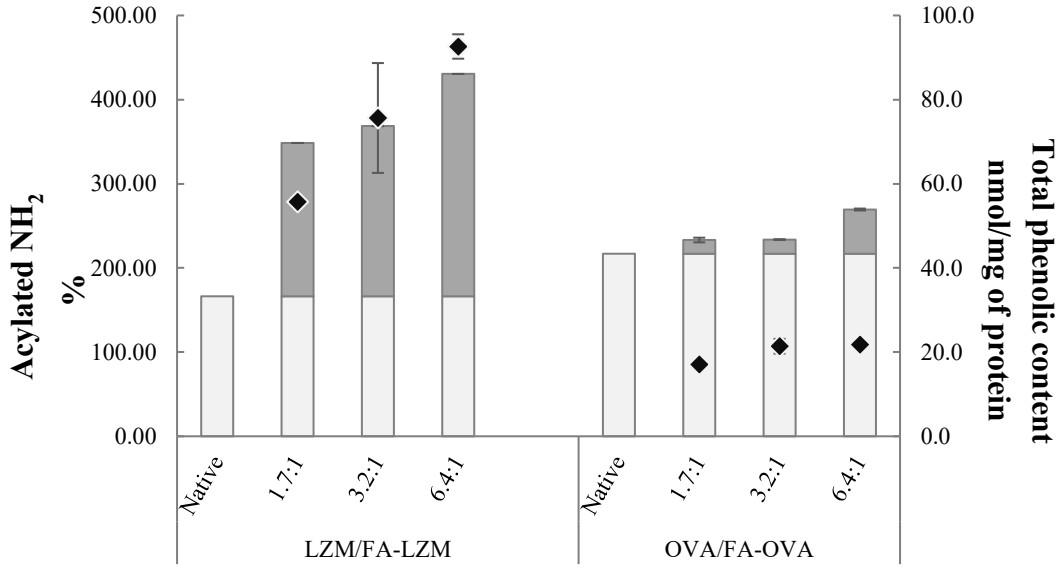

Figure 4.1. The chemical properties of modified protein substrates from amidation at different n-hydroxysuccinimide to protein ratio. Total phenolic content was showed as the bars: phenolic content in native protein (□); increase in phenolic moieties upon acylation (■); percentage of amino groups that were acylated (◆). FA-LZM, ferulic acid modified lysozyme; FA-OVA, ferulic acid modified ovalbumin.

A decrease in the free primary amine content of LZM and OVA was observed upon the amidation reaction. The percentage of acylated amines was estimated by comparing the free primary amine content of modified proteins to the native ones. 55.7 to 92.6 % of free primary amine groups on LZM were acylated upon the amidation, while 17.1 to 21.8% were acylated on OVA (Fig. 4.1). Assuming that all primary amines on proteins were solvent available, it can be estimated that 3-4 out of 7 primary amines (on N-terminus and lysine sidechain) on LZM and of 21 on OVA were acylated with FA at NHS-FA/protein molar ratio of 1.7:1 and 3.2 :1. The number of acylated amine groups on LZM increased to 6 with the increase at the molar ratio to 6.4:1. The acylation percentage of LZM was positively correlated with the reactant molar ratio. Similar correlation has been reported for the modification of gelatin by NHS-esters of different saturated fatty acids and of fish collagen by the NHS-adipic acid derivative (Aewsiri et al., 2011; Shen et al., 2015). Notably, in the case of OVA, a limited increase in the proportion of acylated amines was observed when the molar ratio was increased to 6.4:1. This can be attributed to the limited accessibility of amine groups of some lysine residues of OVA and/or to the changes in the solvation of lysine residues at higher molar ratio of NHS-FA/protein of 6.4:1.

With the increase in the acylation percentage, an increase in the total phenolic content was observed, further reflecting the incorporation of FA in protein molecules (Fig. 4.1). As compared to native LZM, the phenolic content increased by 182.2, 202.3 and 264.2 nmol/mg (2.1-, 2.2- and 2.6-times as the native) upon amidation using NHS-FA/LZM ratio of 1.7:1, 3.2:1 and 6.4:1, respectively. The increase in the content of grafted FA sites was positively correlated with acylated percentage of LZM samples. Depending on the levels of grafted FA sites, these FA-modified LZM samples were defined as low (L-FA-LZM), moderate (M-FA-LZM) and high (H-FA-LZM) modification. Moderate increase (by 52.5 nmol/mg of protein, 1.2-times as the native) in the phenolic content in FA-OVA was achieved upon the modification at NHS-FA/OVA ratio of 6.4:1, while equally low increase (by 16.0 nmol/mg of protein) in the phenolic content was achieved by using NHS-FA/OVA ratios of 1.7:1 or 3.2:1.

The FA-modified OVAs were, therefore, defined by moderate (M-FA-OVA) and low (L1-FA-OVA)/(L2-FA-OVA) modification extent. Although the acylated amine percentage in M-FA-OVA was very close to that of L1-, L2-FA-OVA, its grafted FA level was 2.3-fold higher. These results may be due to conformational changes that happened upon the incorporation of FA moieties, leading either to the underestimation of the acylation percentage or the overestimation of the phenolic content. However, the mass spectrum of M-FA-OVA shows an obviously broader peak with the center of mass signal shifting towards higher molecular weight, as compared to the native and L1/L2-FA-OVA (Fig 4.2). This provides the evidence that higher numbers of FA sites were grafted on M-FA-OVA as compared to L-FA-OVAs.

The profiles of FA-modified LZMs were further characterized by mass spectrometry (Fig. 4.3). Native lysozyme was detected at mass 14,304.70 Da. The incorporation of one FA molecule on protein via amide bond formation will increase the mass of protein by around 176. Upon surface modification with FA, protein peaks with the masses equal to 14,304.70 + 176n Da ($1 \leq n \leq 4$) were present in the mass spectra. By increasing NHS-FA/LZM ratio from 1.7 to 6.4, the mass distribution shifted towards higher molecular weight. The dominant protein peaks shifted from unmodified LZM to LZM+FA and LZM+2FA for L-FA-LZM, and to an additional LZM+3FA for M-FA-LZM. LZM+4FA peak was further detected in the mass spectrum of H-FA-LZM. Since the grafted FA is much smaller than the protein, uniform response factors were assumed for native and modified proteins. From the relative abundance distribution of protein peaks, the percentage of FA-modified LZM was estimated at 39, 59 and 89% for L-, M- and H-FA-LZM, respectively. These results are in agreement with the trend of acylated amine percentage and the increased phenolic content (Figure 4.1).

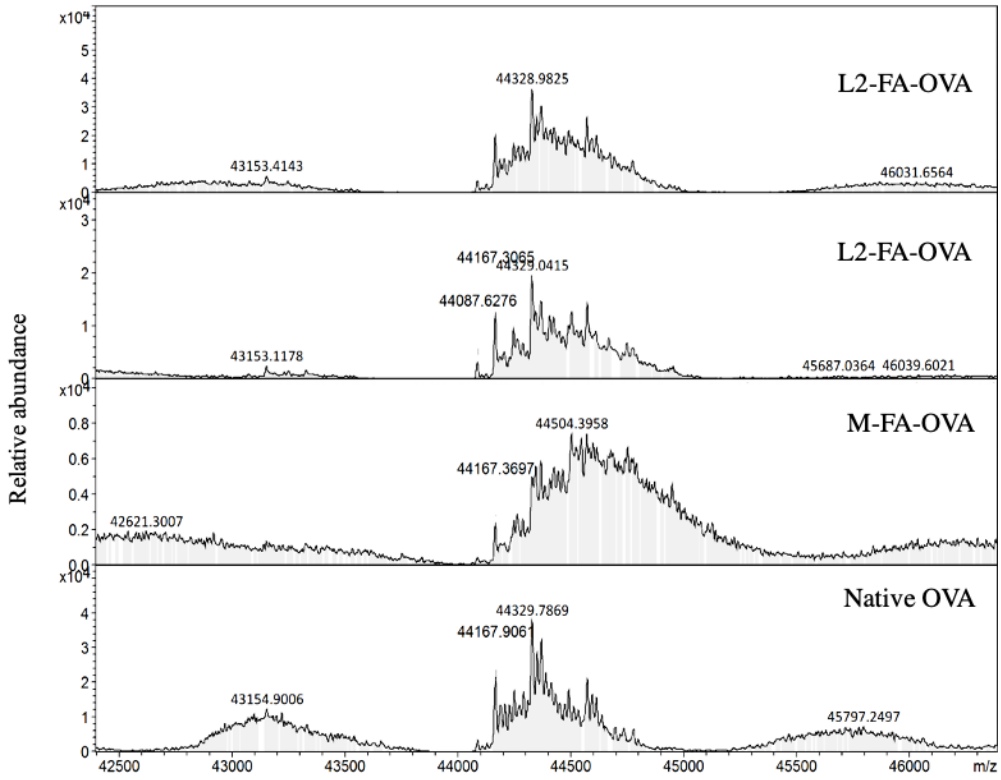

Figure 4.2. Deconvoluted mass spectra of native ovalbumin and ferulic acid (FA) modified ovalbumin (OVA) at different modification degree (L1, L2, M).

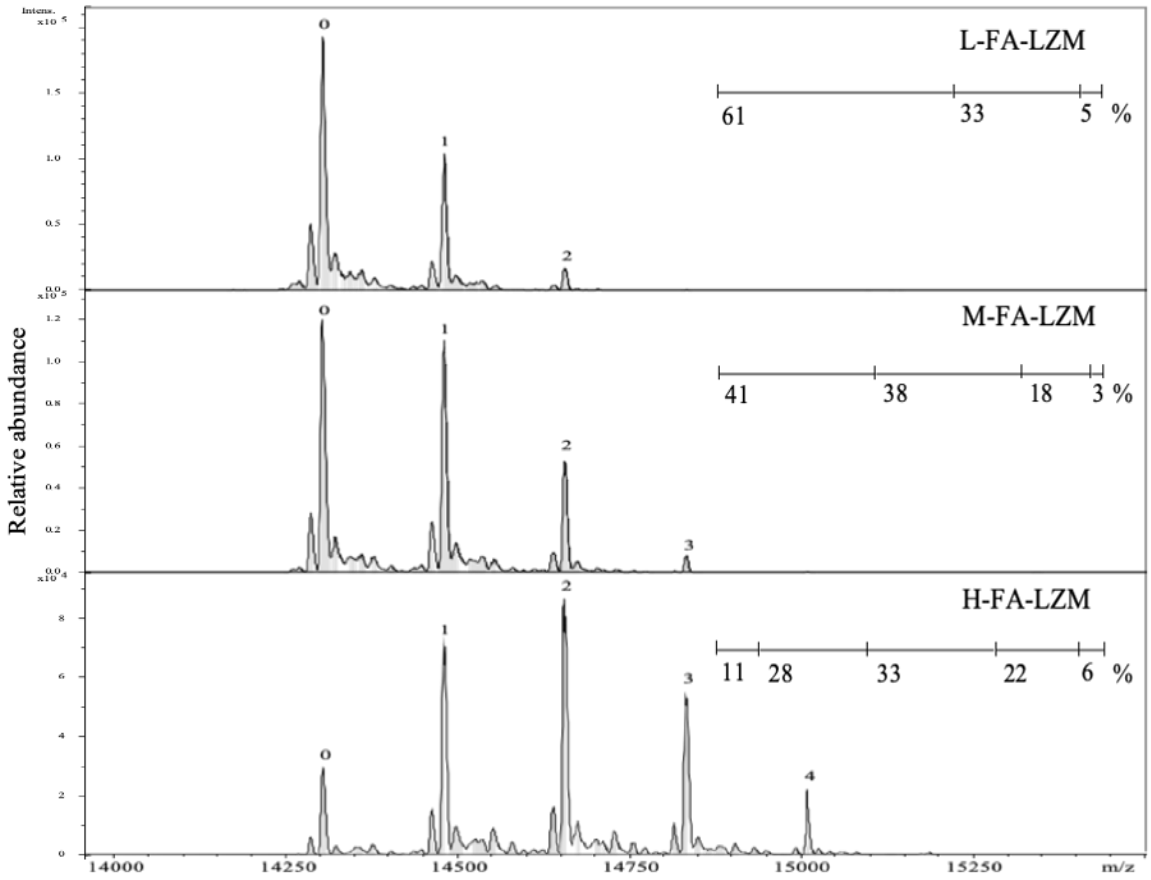

Figure 4.3. Deconvoluted mass spectra (from m/z 1000-2200) of ferulic acid-modified lysozyme (FA-LZM). The mass peaks were marked with numbers, representing the number of FA adduct that were attached on the protein. The calibration scale refers to the relative proportion of each mass peak.

4.4.2. Reactivity and crosslinking of native and modified proteins

The cross-linking of native and FA-modified LZM or OVA by LacTv was carried out. Our previous computational analysis has shown that the catalytic ability of laccase in the oxidative cross-linking of native LZM is limited by the steric hindrance affecting the enzyme-substrate binding (Li et al., 2020). Similarly, the enzymatic cross-linking of native ovalbumin cannot be achieved directly due to its globular shape (Liu, Chen, et al., 2018; Ma et al., 2015). The addition of free ferulic acid mediator for laccase-catalyzed cross-linking of the native protein was also investigated for comparison. The bioconversion of proteins by laccase through oxidation can lead to cross-lining, fragmentation and other type of oxidative modification. The time course for bioconversion of protein monomer and the protein cross-linking product profile were monitored by SDS-PAGE (Fig. 4.5 & 4.6). It is worth noted that FA-modified LZM/OVA samples (lane 2 & 18) and their respective native forms displayed similar electrophoretic patterns prior to cross-linking treatment, indicating the cross-linking was solely induced by laccase-catalyzed reaction (Fig. 4.4).

Little evidence of bioconversion of native LZM by laccase was revealed within the investigated reaction time 0-24 h (Fig 4.4 lane 2-8). Upon the addition of free FA as mediator, the bioconversion of LZM was achieved at a relatively low abundance (7.1-11.1%) as shown by reaction time course (Fig. 4.5A, Fig. 4.4 lane 9-17). For L-, M- and H- FA-LZM, 24.7 to 29.5% of their monomeric proteins were quickly converted within the first 3 h of reaction, where the highest bioconversion rate was observed with H-FA-LZM, followed by M-FA-LZM and then L-FA-LZM. Beyond 3 h, the bioconversion rate slowed down gradually and reached 29.2 to 52.3% at 24 h reaction, with the highest bioconversion obtained with M-FA-LZM. The formation of cross-linked products followed similar trend as the bioconversion, where a high cross-linking efficiency was achieved in the reaction with FA-modified LZM compared to native LZM in the presence of free FA as a mediator (Fig. 4.5A'). The highest cross-linking extent (38.2 %) was obtained upon the use of M-FA-LZM at 24h of reaction rather than H-FA-LZM, although H-FA-LZM contained more grafted FA sites than M-FA-LZM. This result can likely be ascribed to the fact that steric hindrance from multiple FA sites grafted on protein's surface may have limited the cross-linking of H-FA-LZM.

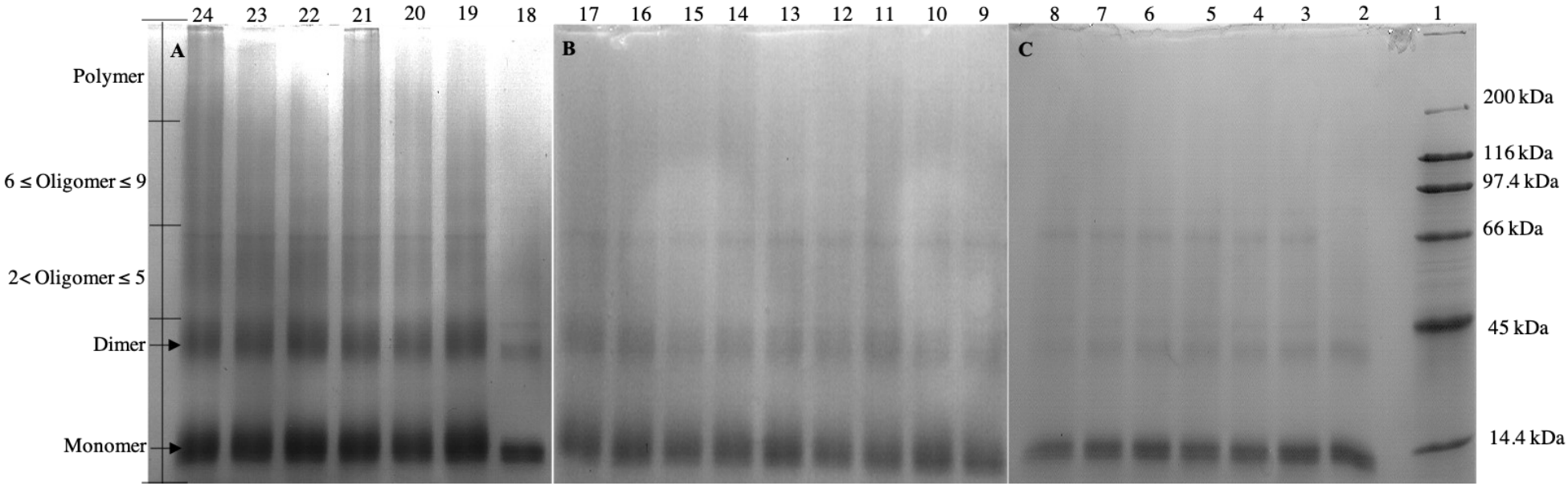

Figure 4.4. SDS-PAGE of enzymatic cross-linking of L-FA-LZM (A), LZM with (B) or without (C) the presence of ferulic acid. Lane 1, molecular weight markers; 2, native LZM; 3 & 6, LacTv-LZM reaction 6h; 4 & 7, LacTv-LZM reaction 12h; 5 & 8, LacTv-LZM reaction 24h; 9-11, LacTv-LZM reaction with 0.5 mM of FA for 6h, 12, and 24h, respectively; 12-14, LacTv-LZM reaction with 0.6 mM FA for 6h, 12, and 24h, respectively; 15-17, LacTv-LZM reaction with 0.6 mM FA for 6h, 12, and 24h, respectively; 18, L-FA-LZM; 19 & 22, LacTv-L-FA-LZM reaction for 6h; 20 & 23; LacTv-L-FA-LZM reaction for 12h; 21 & 24, LacTv-L-FA-LZM reaction for 24h. LZM: lysozyme; FA: ferulic acid and LacTv: laccase from *Trametes versicolor*.

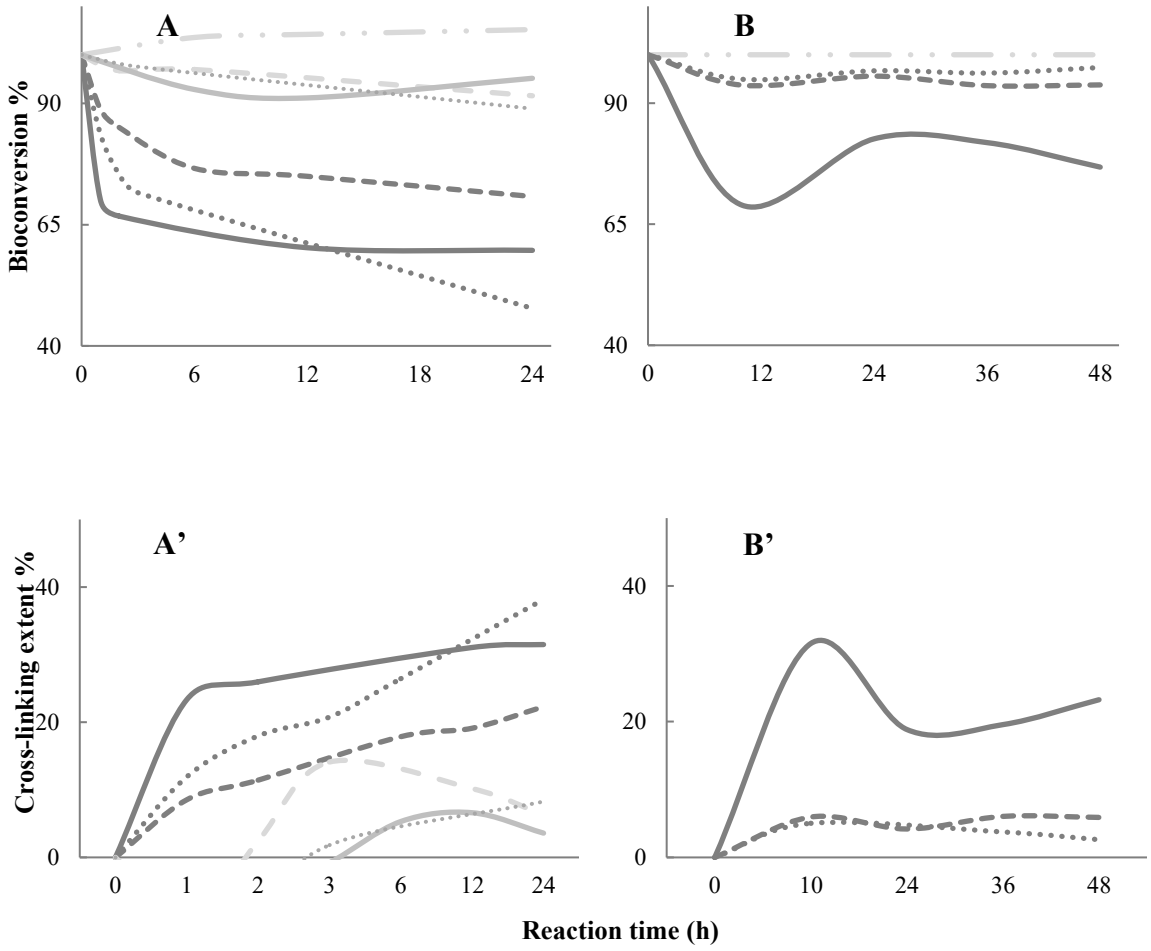

Figure 4.5. Time course for the bioconversion of substrate monomer of and cross-linking extent of lysozyme (LZM) (A) and ovalbumin (OVA) (B) substrate monomer over time. Native (_ . _ . _); Native + 1 mM FA (_____); Native+0.6 mM FA (.....); Native+ 0.5 mM FA (_ _ _ _); H-FA-LZM/M-FA-OVA (_____); M-FA-LZM/L2-FA-OVA (.....); L-FA-LZM/L1-FA-OVA (_ _ _ _).

According to the molecular weight profile of FA-LZM reaction mixtures, the main cross-linked products were dimer, short-chain oligomers (2<unit of monomer ≤ 5) and long-chain oligomer (5<unit of monomer <10) within the first 3 h of reactions; while during 3 to 24 h reaction time, the polymer (unit of monomer ≥10) proportion increased with the concomitant decrease in the dimer and oligomer proportions (Fig. 4.6A, B and C). L-FA-LZM tended to form mainly dimer and oligomers, whereas polymers were formed in M-FA-LZM and H-FA-LZM reaction systems with the highest proportion of polymers (30.6%) was achieved with M-FA-LZM upon 24h of reaction. When the cross-linking of native LZM was mediated by free FA, the formation of dimer and oligomers were less pronounced, and no polymer formation was observed (Figure 4.6A', B' and C').

No clear evidence of bioconversion or cross-linking was detected on the native OVA when treated with LacTv alone or in the presence free FA mediator (data not shown). In contrast, the treatment of FA-OVAs with LacTv led to a bioconversion of 6.3 and 5.1 % at 10 h in L1- and L2-FA-OVA reaction system, respectively, whereas a bioconversion of 31.1 % was achieved with the use of M-FA-OVA as a substrate (Figure 4.5B). Beyond 10 h reaction time, an increase in the proportion of M-FA-OVA monomer fraction was obtained, revealing the oxidative fragmentation of cross-linked OVA proteins at longer reaction time. As the highest bioconversion was achieved with the use of M-FA-OVA, it can be inferred that the relatively high incorporation of FA into OVA in the M-FA-OVA created additional reactive sites for the oxidative cross-linking action of LacTv. The long-chain oligomers were obtained as the major cross-linked product in the reaction with M-FA-OVA, whereas the cross-linking of L-FA-OVAs resulted in mainly formation of short-chain oligomers (Fig. 4.6D, E and F).

The overall results confirmed the enhancement of bioconversion and the modulation of the laccase-catalyzed cross-linking can be achieved efficiently by tailoring the grafted FA sites on protein. The substrate reactivity and the cross-linking extent were positively correlated with the level of grafted FA sites present in LZM. In contrast, no apparent difference in the cross-linking of native LZM with the use of free FA mediator at equivalent concentration to the grafted FA content (0.5, 0.6 and 1 mM) (Fig. 4.4-C, Fig. 4.5A & A').

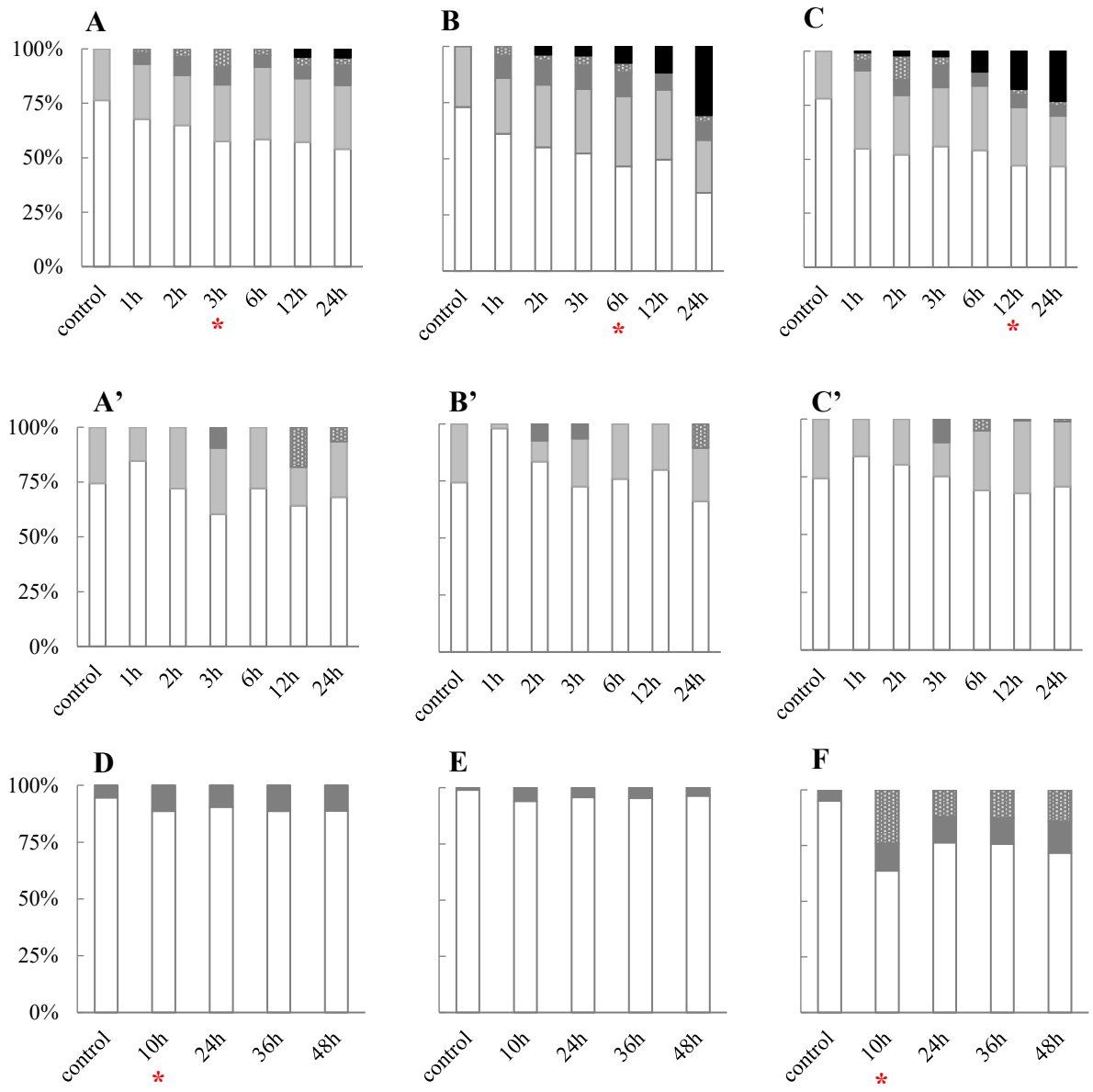

Figure 4.6. Molecular weight profile of reaction mixtures of laccase-catalyzed oxidative cross-linking of modified lysozyme (LZM) and ovalbumin (OVA) over reaction time course: L-FA-LZM (A), M-FA-LZM (B), H-FA-LZM (C), L1-FA-OVA (D), L2-FA-OVA (E) and M-FA-LZM (F) and reaction of native lysozyme with addition of free ferulic acid at 0.5 mM (A'), 0.6 mM (B') and 1 mM (C'). Molecular weight fractions are: Monomer (□), dimer (▒), short chain oligomer ($2 < n \leqslant 5$) (■), oligomer ($n > 5$) (▒), polymer (■). n, represents the units of monomer.

In agreement with our results, Ma et al. (2010) observed a higher cross-linking efficiency in laccase-catalyzed reaction of vanillic acid-modified whey protein isolate as compared to laccase-vanillic acid mediator system. These authors ascribed the relatively low efficiency in protein cross-linking in the presence of free phenolic mediator to the competition between protein and phenolic substrates and/or to the self-polymerization of phenolic compounds (Ma et al., 2010). The oligomerization of LZM up to 5 units of monomer was reported for the cross-linking reaction catalysed by transglutaminase at high hydrostatic pressure as well as for the oxidative reaction with hydroperoxide following microwave treatment (Schuh et al., 2010; Yang & Lesnierowski, 2019). The latter chemical approach resulted in a maximum of 60% of oligomer fractions (Yang & Lesnierowski, 2019). The synthesis of LZM polymeric cross-linked products has not been reported so far with the enzymatic approach. As compared to other OVA samples, the formation of long chain oligomers was only achieved in the reaction with M-FA-OVA, characterised by a high level of grafted FA sites. In literature, the combined use of transglutaminase/heat/high pressure or polyphenol oxidase-caffeic acid mediator system led to the formation of oligomeric product of OVA at estimated molecular weight of 188-250 kDa (4-6 units of monomer) (Giosafatto et al., 2012; Liu, Chen, et al., 2018; Ma et al., 2015). These authors stated that an irreversible partial denaturation process or the use of mediator is necessary to overcome the steric hindrance originated from the protein structure.

Selected cross-linked proteins with well-defined profiles (* in Figure 4.6) were subsequently used for the structural and functional characterization. The selected cross-linked LZM are L-FA-LZM (3), M-FA-LZM (6) and H-FA-LZM (12) characterized by a cross-linking extent of 18.8, 26.4 and 31.1%, and relative proportions of dimer/oligomer/polymer of 26.1/16.4/0 %, 31.3/14.7/7.4% and 26.9/8.4/17.6%, respectively. The selected cross-linked OVA samples, L1-FA-OVA (10) and M-FA-OVA (10), have shown a cross-linking extent of 5.9 % and 31.5 %, with a relative proportion of short/long chain oligomer of 11.3/0% and 24.0/12.3%, respectively.

4.4.3. Characterization of ferulic type cross-links

The laccase-catalyzed cross-linking of proteins can happen via multiple functional groups, including tyrosine, cysteine residues and primary amine groups (Mattinen et al., 2006; Steffensen et al., 2009; Wang, Lv, et al., 2019). Considering the reactivity of grafted FA sites on modified proteins and their accessibility, the cross-linking most likely occurred on FA sites prior to the amino acid residues.

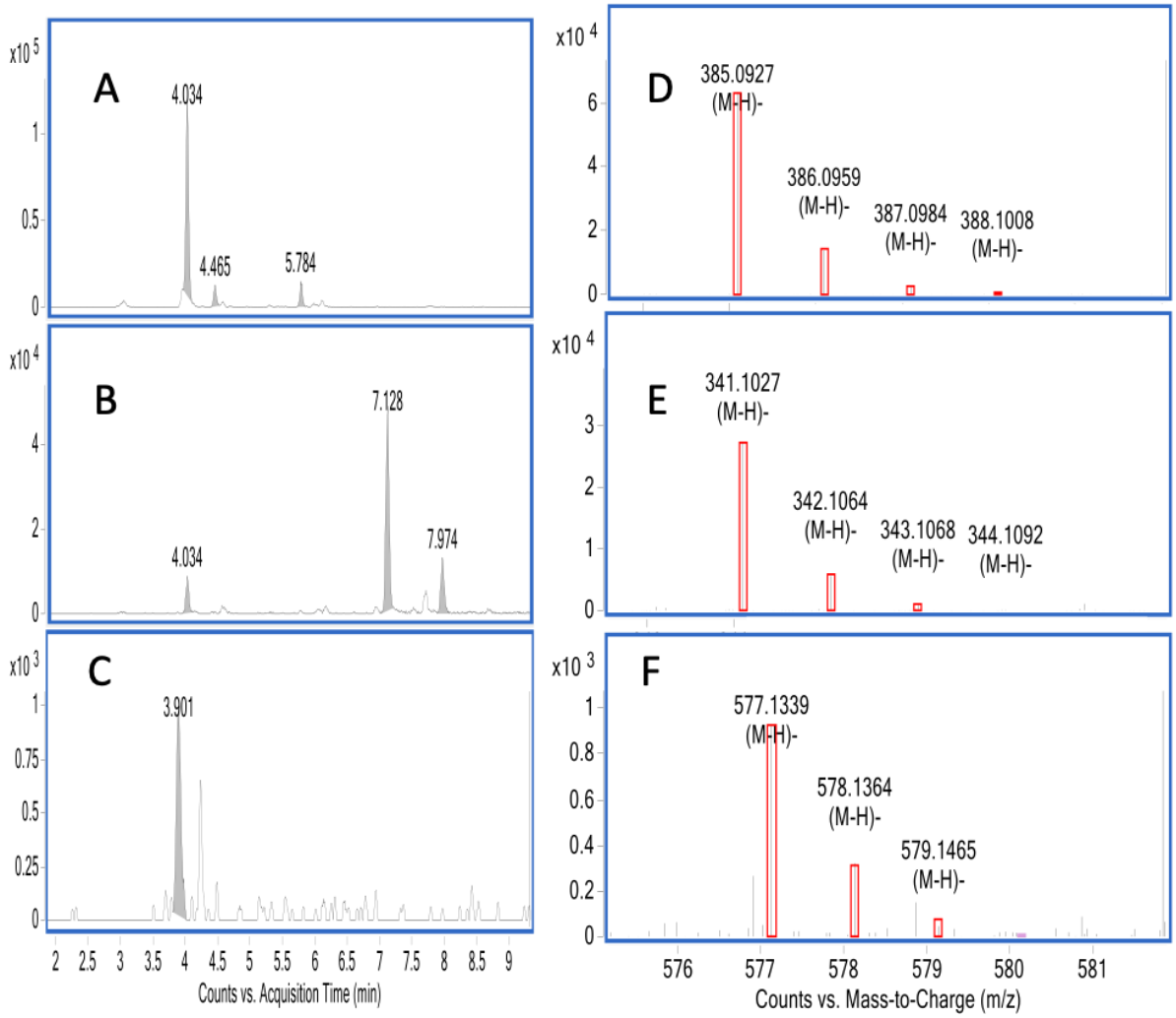

Figure 4.7. Extracted ion chromatograms for detected ferulic acid cross-links from alkaline hydrolysates. A. dehyro-diferulic acid ($C_{20}H_{18}O_8$); B. dehydro-decarboxylated diferulic acid ($C_{19}H_{18}O_6$) and C. dehydro-triferulic acid ($C_{30}H_{26}O_{12}$) and the corresponding mass spectra illustrating the isotope distribution for dehyro-diferulic acid ($C_{20}H_{18}O_8$) at retention time 4.0 min (D), dehydro-decarboxylated diferulic acid ($C_{19}H_{18}O_6$) at retention time 7.1 min (E) and dehydro-triferulic acid ($C_{30}H_{26}O_{12}$) at retention time 3.9 min (F) (red rectangles indicate the theoretical isotope pattern for corresponding chemical formula).

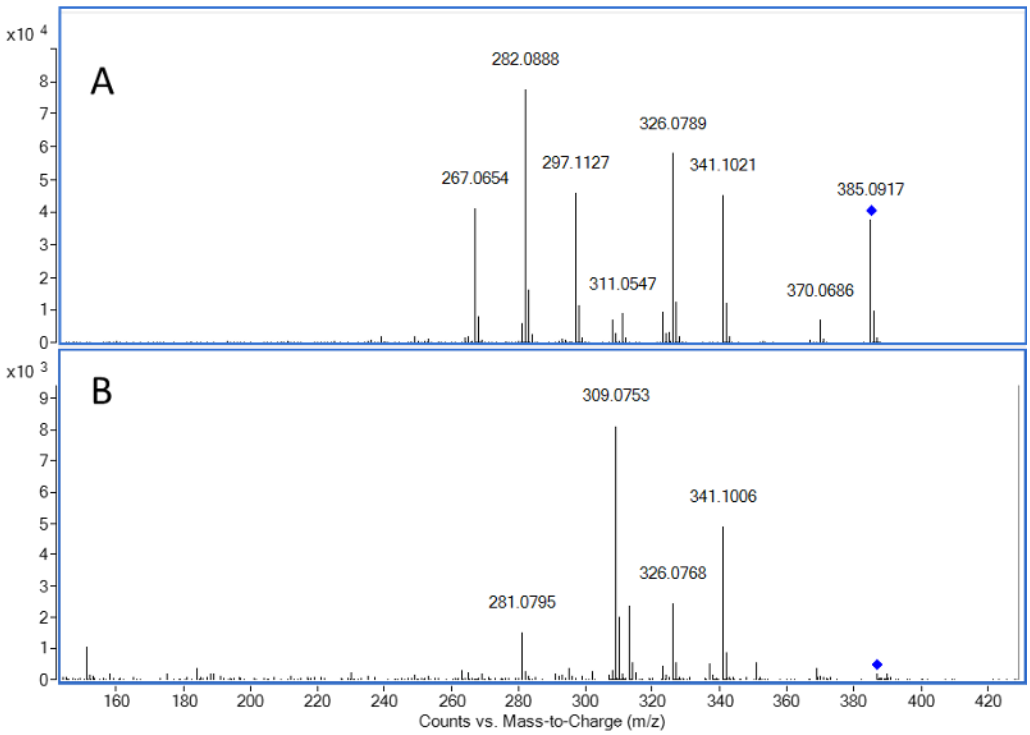

Figure 4.8. Target MS/MS fragmentation mass spectra for $C_{20}H_{18}O_8$ at retention time 4.0 min: (A) in negative ion mode, parent ion with m/z at 385.0923, and (B) positive ion mode, parent ion with m/z at 387.1080. Collision energy was 20 V.

To characterize the FA-type cross-links, alkaline hydrolysis of the selected protein samples coupled with extraction was carried out. Indeed, alkaline hydrolysis can hydrolyze the amide bond formed between FA and amine groups of the protein, while keeping the bonding within FA crosslinks intact. The putative identification of ferulic type cross-links present in the protein alkaline hydrolysate was based on the matching of mass accuracy and the isotope fidelity with the theoretical values (Fig. 4.7). From the hydrolysates of cross-linked FA-LZMs, three different types of ferulic oligomer compounds were identified in negative ion mode: dehydro-diferulic acid ($C_{20}H_{18}O_8$) with m/z at 385.0927, dehydro-decarboxylated diferulic acid ($C_{19}H_{18}O_6$) with m/z at 341.1028, and dehydro-triferulic acid with m/z at 577.1344 ($C_{30}H_{26}O_{12}$) (Bunzel et al., 2006; Ward et al., 2001) (Fig. 4.7). From the hydrolysate of cross-linked FA-OVAs, only dehydro-diferulic acid ($C_{20}H_{18}O_8$) was detected. As well, multiple peaks at different retention times were found for $C_{20}H_{18}O_8$ and $C_{19}H_{18}O_6$ with matching score > 96 (Fig. 4.7A, B and C). This finding is consistent with reported data showing that dehydro-diferulates can be formed with various isomer structures (Bunzel et al., 2006; Ravisankar et al., 2018; Vismeh et al., 2013). Among the compound ions, the major one (m/z 385, retention time around 4.0 min) was further confirmed to be 8-5′noncyclic dehydro-diferulic acid, as indicated by the distinguishing ion detected at m/z 309.0753 yielded by positive mode MS/MS fragmentation (Vismeh et al., 2013; Ward et al., 2001). The product of FA in laccase-catalyzed oxidative cross-linking has been previously identified to be majorly 8-5’ dehydrobenzofuran-diferulic acid, with relatively low extent of other forms including 8-8’, 8-5’ (noncyclic) dehydro-diferulic acid (Aljawish et al., 2014; Carunchio et al., 2001). In the present work, 8-5’(nonclyclic) dehydro-diferulic acid (DiFA(1)) was shown to be the dominant linkage for both crosslinked FA-LZM and FA-OVA samples, which coexisted with other isomers of diferulate cross-links (DiFA(2)) as well as triferulate cross-links at relatively low abundancy.

Quantification of the consumption of grafted-FA sites and characterization of the FA-type cross-links are summarized in Table 1. For all investigated cross-linked FA-modified proteins, more than 88% consumption of grafted FA sites were achieved, confirming that the FA site were efficiently used for cross-linking (Table 4.1). For FA-LZM samples, the content of grafted FA sites in FA-LZM samples that was involved in cross-linking was comparable to that of estimated cross-linked sites based on the corresponding molecular weight distribution (calculation not shown). This suggest that the cross-linking of FA-LZMs happened mainly on the grafted FA sites.

Table 4.1. Identification and quantification of ferulic type linkages from cross-linked proteins

Cross-linked protein samples	Consumed grafted FA sites [a]	DiFA (1) [b]	DiFA (2) [b]	TriFA [c]	Total quantity of FA cross-links
	%		nmol/mg		
L-FA-LZM (3)	95.00±0.00	24.75±0.09	11.83±0.07	0.20±0.00	36.78±0.02
M-FA-LZM (6)	94.48±0.01	27.92±0.71	14.48±0.50	0.32±0.04	42.72±0.25
H-FA-LZM (12)	89.75±0.01	27.24±2.32	19.05±2.09	0.43±0.06	46.72±0.17
L1-FA-OVA (10)	100.00±0.00	1.22±0.00	*N/A*	*N/A*	1.22±0.00
M-FA-OVA (10)	88.30±0.00	8.25±0.00	*N/A*	*N/A*	8.25±0.00

a. The percentage of grafted ferulic acid on protein surface that was consumed during enzymatic cross-linking;
b. Di-ferulate type linkages; DiFA (1) was identified as 8-5' noncyclic dehydrodiferulic aicd whereas DiFA (2) represents of other type of isomers of diferulate linkages;
c. Tri-ferulate linkage;

Abbreviation: FA, ferulic acid; LZM, lysozyme; OVA, ovalbumin.

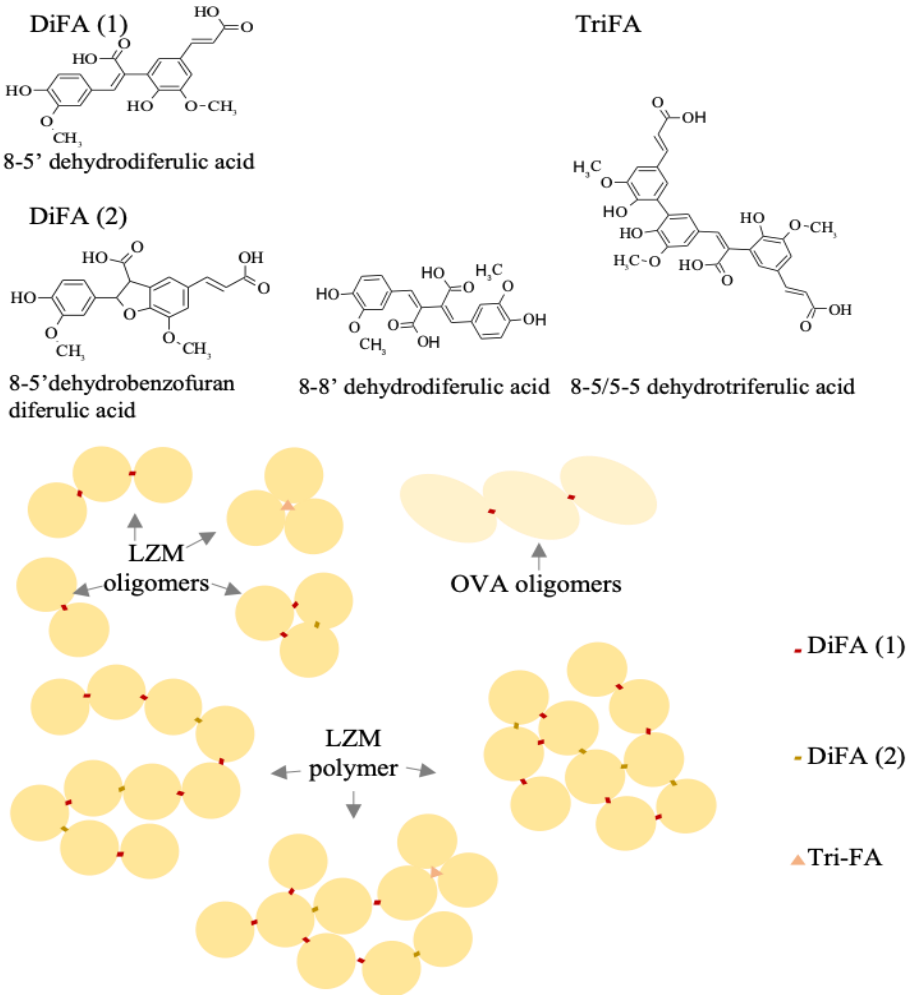

Scheme 4.1. Potential ferulic acid (FA) cross-links and associated oligomeric or polymeric product of lysozyme (LZM), ovalbumin (OVA).

For FA-OVA samples, grafted FA sites corresponded only to 20-40% of the total cross-linked sites (calculation not shown), revealing other types of cross-links may have been involved in the cross-linked FA-OVAs. Indeed, the modification of OVA may have enhanced the exposure of its oxidizable amino acids to laccase action. The composition of the identified FA-type cross-links in each cross-linked protein samples was also characterized (Table 4.1). The relative percentage of di-, tri-ferulate cross-links were estimated by the corresponding signal intensity, assuming that the ionization efficiency of these ferulic compounds were similar. The total quantity of FA cross-links increased with the increase of the LZM FA-grafting and cross-linking extent. M-FA-LZM (6) and H-FA-LZM (12) did not show great difference in the content of DiFA (1) type cross-link (~27.00 nmol/mg); however, H-FA-LZM (12) contained more DiFA (2) (19.05 nmol/mg) and tri-FA (0.43 nmol/mg) than those of M-FA-LZM (6) (14.48 and 0.32 nmol/mg, respectively). As for cross-linked FA-OVAs, much lower quantity of cross-links was seen in FA-OVA samples as compared to FA-LZM, a total of 1.22 and 8.25 nmol/mg DiFA (1) cross-links was obtained for L1-FA-OVA (10) and M-FA-OVA (10), respectively. Upon enzymatic treatment. A total of 1.22 and 8.25 nmol/mg DiFA (1) cross-links was obtained for L1-FA-OVA (10) and M-FA-OVA (10), respectively. Since the most of the ferulic type cross-links are diferulic, the oligomers/polymers should be mainly in chain shapes (single chains and/or branched chains) connected by diferulate cross-links. Extra branches in the product from H-FA-LZM were expected as it consisted of 28% of LZM that are attached with 3-4 FA sites. Taken the consideration of types and proportion of the FA cross-links, postulated structures for cross-linked FA-LZM/OVA via FA-type cross-links can be elucidated as scheme 4.1. It can be seen that the proteins were initially joining via DiFA (1) linkages, whereas the proceeding of the cross-linking and the branching of the oligomeric/polymeric chain involved more of the DiFA (2) or triferulate (tri-FA) type linkages.

As per the authors' knowledge, the cross-linked protein via grafted FA sites and its FA-associated cross-links has not been characterized before. The putative structures of the cross-linked FA-modified proteins were different from the natural proteins cross-linked via tyrosine residues. The polymerized α-lactalbumin obtained from traditional oxidoreductase-catalyzed reaction was reported to connect through shared oligo-tyrosine linkages, forming products in the shape of aggregate cluster (Dhayal et al., 2015). Diferulates are common linkages that are involved in the cross-linking of feruloylated carbohydrate in nature or during food processing, which has important effect on the stability of the biopolymer and texture, and rheology of many food products (Bunzel et al., 2001; Harukaze et al., 2000).

4.4.4. Evaluation of the cross-linked protein as potential functional ingredients

The effect of enzymatic cross-linking on the techno-functional properties of proteins was investigated. The emulsification property of native and cross-linked LZM was evaluated, while foaming property was evaluated for the native and cross-linked OVA. As shown in Figure 4.9, native LZM had limited emulsification performance, in particular the emulsifying stability. This can be explained by its high surface hydrophilicity and inflexible structure (Acton et al., 1990; Blake et al., 1965). L-FA-LZM (3), with low cross-linking extent of 18.8 %, exhibited similar emulsification performance to that of native LZM. With high cross-linking extent (26.4 and 31.4%) of M-FA-LZM (6) and H-FA-LZM (12), an enhancement in the emulsification property was observed. Indeed, the emulsifying ability of cross-linked M-FA-LZM (6) was two times higher than that of the native form, and its emulsion micrograph (Fig. 4.9C) was also characterized by smaller oil droplets with more homogenous size than emulsions of other LZM samples. The presence of LZM dimer and oligomers in M-FA-LZM (6) may have favored its adsorption at oil-water interface. H-FA-LZM (12) led to the highest emulsifying stability among all LZM samples. High proportion of polymeric LZM present in H-FA-LZM (12) are likely to promote the formation of protective layer around the oil droplets, limiting the creaming and coalescence (Ma et al., 2011). The emulsifying property of lysozyme was shown to positively correlate with the surface hydrophobicity (Kato et al., 2014). The cross-linking of FA-modified LZM probably contributed to the enhancement of the surface hydrophobicity thus its adsorption at oil-water interface and stability of the interface (Li et al., 2019; Yang & Lesnierowski, 2019). Similar to polymerization, the thickening of the interfacial protein layers was achieved by the conjugation of LZM with various oligo/polysaccharide molecules, which can also strengthen the stabilization effect of LZM as emulsifier (Hamdani et al., 2018; Seo et al., 2013).

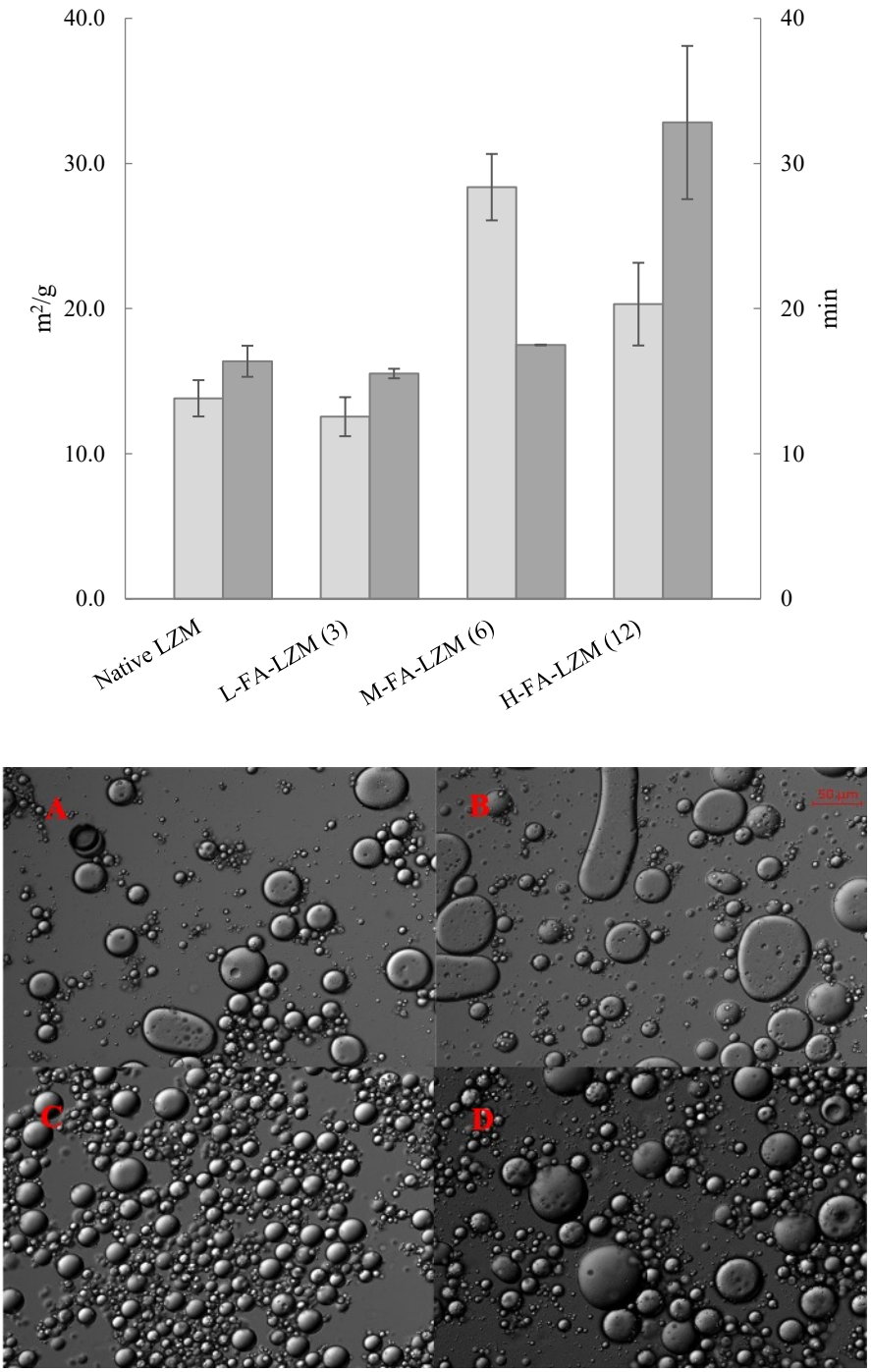

Figure 4.9. Emulsifying property of native and cross-linked lysozyme (LZM) and the micro-images of emulsions. Emulsifying ability (m2/g) (□) ; emulsifying stability (min) (■) . Micro-images A, native LZM; B, L-FA-LZM (3); C, M-FA-LZM (6); D, H-FA-LZM (12).

The foaming capacity of native and cross-linked OVA was assessed by measuring the percentage of gas entrapped (G_i) and foam expansion (FE), while the foam stability was assessed by estimating the percentage of liquid retained after 5 min (R_5) (Figure 4.10). Slightly higher foaming capacity was observed with the cross-linked OVA (98.4, 99.7%) than the native one (94.3%) as indicated by the G_i (Fig. 4.10A). As well, both cross-linked OVA exhibited higher foam expansion than the native one, especially for L1-FA-OVA (10) with relatively low cross-linking extent (6.1%), the FE value of which was 1.5-fold of that for the native (Fig. 4.10B). On the other hand, both cross-linked FA-OVAs showed impaired foam stability as indicated by R_5 value (Fig. 4.10C); but a greater decrease was shown in M-FA-OVA (10) sample with relatively high cross-linking extent (31.1%). Overall, the cross-linked OVA exhibited higher foaming capacity, while producing less stable foam than native OVA. The enhanced foaming capacity is most likely associated with low cross-linking extent and relatively low molecular weight cross-linked products (short-chain oligomer, 2<monomer units≤5). It has been previously shown that a proper hydrophobicity-hydrophilicity balance of the protein structure due to structural unfolding contributes to better foaming performance of OVA upon oxidative cross-linking treatment, whereas the loss in this balance as a result of prolonged treatments could impair foaming performance (Li et al., 2019). In contrast with our observation, the increase in molecular size of OVA upon heat treatment was associated with foam stabilization against bubble aggregation and interfacial drainage (Sheng et al., 2019). The decrease in the foam stability for cross-linked FA-OVAs may be ascribed to the presence of FA phenolic moiety, which could either disrupt the intra- or inter- molecular hydrophobic interaction of OVA that is responsible for film viscoelasticity upon adsorption or weaken the electrostatic repulsion between bubbles resulting in faster drainage (Aewsiri et al., 2009; Wu et al., 2007).

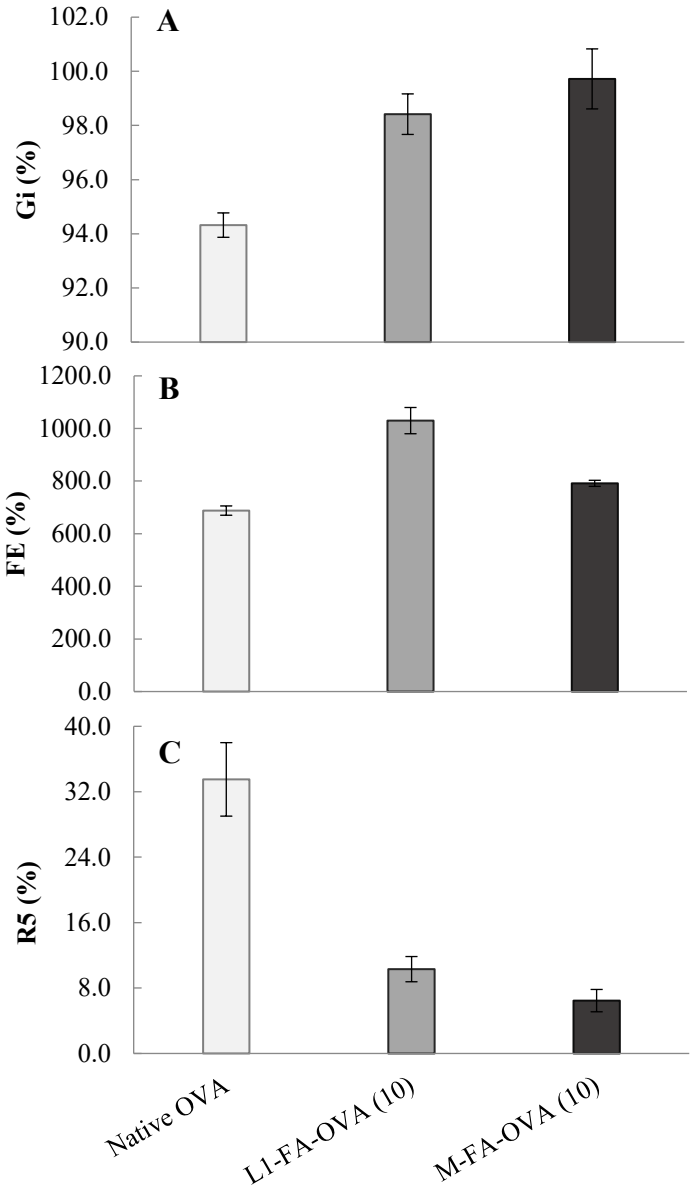

Figure 4.10. Foaming property of native and cross-linking ovalbumin (OVA). GI represents the foaming capacity (A), FE represents the foam expansion (B) and R_5 (C) indicates the foam stability.

Cross-linking can alter the distribution of epitope on protein thus affecting the allergenicity of the protein ingredients. The effect of cross-linking on the allergenicity of OVA and LZM was evaluated by assessing the changes in specific IgE antibody binding capacity (Fig. 4.11). A decrease in IgE binding capacity was observed for all three cross-linked FA-LZMs, indicating the potential of the investigated approach for reducing the allergenicity of LZM (Fig. 4.11A). In addition, the decrease in IgE binding capacity was positively correlated with the FA-grafting/cross-linking extent. H-FA-LZM (12), containing more branched cross-linked product and 17.6% of polymers, showed the highest reduction (~51%) in IgE binding capacity. Similarly, the IgE binding capacity of LZM was reported previously to decrease upon glycation and carboxymethylation (Mine & Zhang, 2002; Seo et al., 2013). On the contrary, urea-induced denaturation of LZM led to a significant increase in allergenicity, as multiple epitope regions of LZM was revealed upon disulfide bonds reduction (Jimenez-Saiz et al., 2014; Mine & Zhang, 2002). No significant difference was shown in IgE binding capacity of the native and cross-linked OVA (Fig. 4.11B). It can be concluded that the cross-linking did not effectively alter the IgE binding capacity of OVA as compared to LZM. It has been reported that the sequential epitopes of OVA are majorly responsible for the binding with human anti-OVA IgE, while anti-LZM IgE interacts with both conformational and sequential epitopes (Mine & Zhang, 2002). Laccase-catalyzed cross-linking of FA-modified OVA seems to not have affected the sequential epitope of OVA on the protein surface due certainly to limited modification and cross-linking. Ma et al., (2015) attributed the insignificant changes in IgE binding capacity of OVA upon transglutaminase-catalyzed cross-linking of low cross-linking extent. On the other hand, the cross-linking of OVA using polyphenol oxidase-caffeic acid reaction system was reported to significantly decrease specific IgE binding capacity and other immunostimulatory responses (Liu, Chen, et al., 2018; Tong et al., 2018). In literature, the effect of protein cross-linking by laccase-phenolic mediator reaction system on allergenicity was protein-dependent. Lower IgE binding capacities of fish allergen protein and peanut protein by 34.8% and 50.4 %, respectively, were observed upon laccase-catalyzed cross-linking (Lv et al., 2019; Mihajlovic et al., 2016). The laccase-cross-linking approach was potential in mitigating the allergenicity of milk allergen **β**-casein, while it can promote the allergic sensitization of **β**-lactoglobulin (Stanic et al., 2010; Stojadinovic et al., 2014).

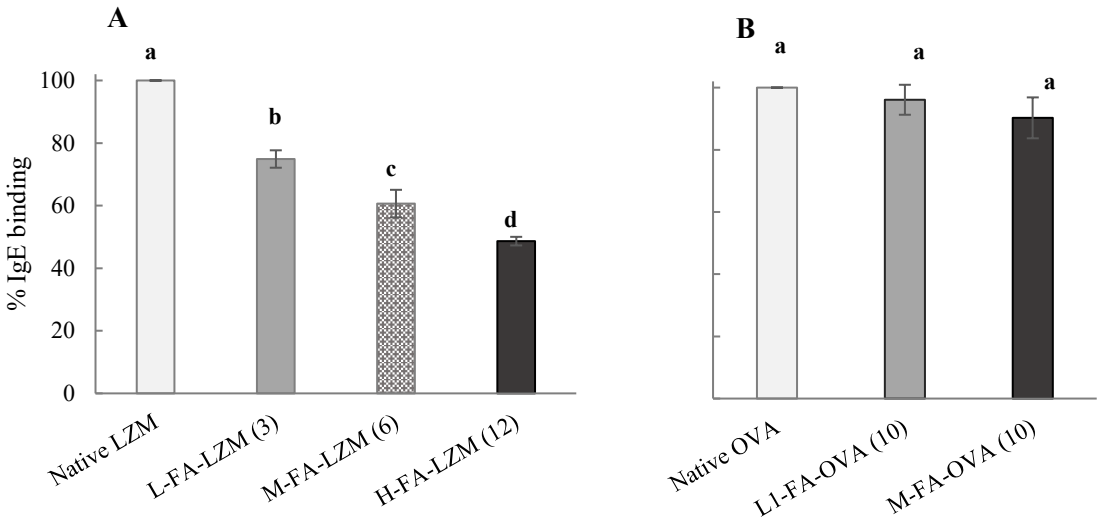

Figure 4.11. The ability in binding Specific IgE of the native and cross-linked lysozyme (LZM, A) and ovalbumin (OVA, B) as determined by inhibition ELISA Different letters indicate significant differences ($p < 0.05$).

4.5. Conclusion

The cross-linking of egg white lysozyme and ovalbumin were efficiently achieved by *T. versicolor* laccase upon the grafting of ferulic acid sites on their surface, especially for lysozyme, in which polymerization happened. The extent of grafted-FA sites was positively correlated with substrate reactivity/cross-linking efficiency. The cross-linking of the proteins on their grafted FA sites occurred via the formation of di- and/or tri-ferulate, with 8-5′noncyclic dehydro-diferulate being the main ferulic type linkage, resulting in chain-shape molecular assemblies. The cross-linked FA-LZM exhibited enhanced emulsifying property, while the cross-linking of FA-OVA, particularly at low extent and with low molecular weight product, was shown to improve the foaming capacity. Furthermore, the FA-grafting-laccase-catalyzed cross-linking modification approach resulted in decreased protein allergenicity, which was found to be associated with the modification/cross-linking extent. Our results suggested that current cross-linking approach is promising one for the production of hypoallergenic protein ingredients with enhanced functionalities.

CONNECTING STATEMENT 3

Chapter IV demonstrated an efficient approach to cross-link egg white lysozyme or ovalbumin via laccase-catalyzed reaction and the potential of laccase-catalyzed protein cross-linking in the production of hypoallergenic functional ingredients. The importance of accessible phenolic moieties of protein substrates for its cross-linking in catalyzed by laccase was noted. In fact, the results from Chapter III has inferred that accessible tyrosine residues on potato patatin surface could favor the oxidative cross-linking catalyzed by laccase, which also showed that model peptide ST-10 of potato patatin exhibited higher reactivity as substrate of laccase than AG-10 from lysozyme. Chapter V focuses on the investigation of laccase-catalyzed cross-linking in the modification of potato protein. The kinetic property of fungal laccases in the oxidation of potato proteins were investigated in the coming chapter to provide complementary evidence for the previous findings. Both direct (treated by laccase alone) and indirect (with the presence of ferulic acid as mediator) cross-linking of potato protein were carried out and compared for their product profile. In addition, the effects of laccase-catalyzed cross-linking on the secondary structure and emulsifying, foaming and antioxidant property were evaluated.

The results of this chapter were presented at the 14th International Symposium of Biotransformation and Biocatalysis (Biotrans).

Li, M., Karboune, S., and Light, K. (2019) Enzymatic cross-linking of potato proteins by laccase. Biotrans2019, Groningen, the Netherlands, July 7-11th.

Li, M. & Karboune, S. (2020) Oxidative cross-linking of potato proteins by fungal laccases: modification efficiency, structural and functional properties of modified proteins (To be submitted)

CHAPTER V. OXIDATIVE CROSS-LINKING OF POTATO PROTEINS BY FUNGAL LACCASES: MODIFICATION EFFICIENCY, STRUCTURAL AND FUNCTIONAL PROPERTIES OF MODIFIED PROTEINS

5.1. Abstract

In order to expand the application potato proteins as functional ingredients, their oxidative cross-linking using fungal laccases (from *Trametes versicolor* (LacTv) or *Coriolus hirsutus* (LacCh)) was investigated. Current study included the enzyme kinetic analysis, the study of oxidation reaction time course, the characterization of cross-linked products profile, and the assessment of structural and techno-functional properties of selected cross-linked products. Fungal laccases exhibited higher specificity towards the oxidation of patatin-containing potato proteins, while smaller-sized potato protease inhibitors proceeded faster in the formation of cross-linked products. The cross-linking extent and the composition of cross-linked proteins were modulated by the use of specific laccase and the ferulic acid mediator. The effects of the modification on selected functionalities (foaming, emulsifying and antioxidant properties) of potato proteins were correlated with the cross-linked product profile, the extent of cross-linking, the rearrangement in the secondary structure and the incorporation of ferulic acid. The laccase-catalyzed cross-linking led to the improvement in emulsifying property of both potato proteins, Enhanced foaming property was observed in mildly cross-linked patatin-containing potato protein. This biocatalytic approach has major potential in tailoring the cross-linking of potato proteins and hence enhancing their techno-functional/health-promoting properties.

5.2. Introduction

With ever-growing attention turning to climate change and sustainability, plant-based proteins are well positioned to replace animal-sourced proteins in consumers' diets and food formulations. In this regards, potato proteins provide superior amino acid profile, composed of a high proportion of lysine, threonine, tryptophan and methionine, compared to other vegetable/cereal proteins (Gorissen et al., 2018; Waglay & Karboune, 2016b). In addition to their low allergenicity, potato proteins exhibit some health-promoting properties such as antioxidant and anti-carcinogenic capacities (David & Livney, 2016). Potato proteins are also known for their diverse techno-functional properties, including foaming, emulsifying and gelling properties, allowing their broad application in various food formulations (Creusot et al., 2011; Romero et al., 2011). Potato proteins can be isolated from the tuber itself, although another source includes the by-product from the potato starch industry known as potato fruit juice (Waglay & Karboune, 2016b).

Potato proteins consist of three main protein fractions: high-molecular weight potato protein (10%, w/w), patatin (50%, w/w) and protease inhibitors (40%, w/w) (Schmidt et al., 2018).

Among them, patatin and protease inhibitors are the main contributors to functionalities. Patatin, a glycoprotein with molecular weight around 40-45 kDa, is the major storage protein in potato and offers biological lipid acyl hydrolase and acyltransferase activities (David & Livney, 2016). It is thermally stable up to 45℃ with an isoelectric point around pH 4.9 and minimum solubility at pH 4.0 (Ralet & Guéguen, 2001). Protease inhibitors are a mixture of proteins ranging from 5-25 kDa, including serine protease inhibitor, cysteine protease inhibitor, carboxylpeptidase inhibitor, and show higher hydrophilicity than patatin (Glusac et al., 2017; Schmidt et al., 2018). The functional properties of potato proteins are greatly affected by the recovery process, which may hamper their applications.

Protein modification is a common strategy to modulate the structural (secondary, tertiary) and physicochemical properties (net charge, isoelectric point, hydrophobicity) to yield modified proteins, which have more appealing techno-functional properties than the parent proteins (Heck et al., 2013; Sun-Waterhouse et al., 2014). For this purpose, modification techniques have been applied to potato proteins, including high hydrostatic pressure (Elahi & Mu, 2017), hydrolysis (Miedzianka et al., 2014; Waglay & Karboune, 2016a), acetylation (Miedzianka et al., 2012) and glycation (Seo et al., 2014; Seo et al., 2012). As far as the authors are aware, modulation of the functional properties of potato proteins via protein cross-linking have rarely been explored (Heck et al., 2013). The oxidative cross-linking of proteins catalyzed by laccase is mainly through the formation of dityrosine bonds upon the oxidation of tyrosine residues which are identified as the prime targets in proteins; the formation of disulfide bonds through the oxidation of cysteines can also occur (Buchert et al., 2010; Heck et al., 2013). When the tyrosine residues are not accessible, food-grade phenolic compounds (e.g. vanillic acid, ferulic acid) can be used as reaction mediators to achieve the protein cross-linking (Kim & Cavaco-Paulo, 2011; Ma et al., 2011; Steffensen et al., 2008). The redox-related cross-linking mechanism of laccase is a “green” process, which takes the dissolved oxygen as electron donor and generates water as the only by-product (Buchert et al., 2010). So far, laccase-catalyzed oxidative cross-linking has been investigated on milk protein (Ercili Cura et al., 2009; Hiller & Lorenzen, 2008; Tantoush et al., 2011), meat protein (Lantto et al., 2005) and cereal proteins (Flander et al., 2011; Selinheimo et al., 2007). These studies revealed that protein cross-linking by laccase could modulate the rheological property, enhance the antioxidant activity and digestibility, as well as reduce the allergenicity. However, the complex reaction kinetic of laccase-catalyzed cross-linking of protein still needs to be elucidated. In the present study, the catalytic efficiency of two laccases from *Trametes versicolor* and *Coriolus hirsutus* towards

potato proteins was investigated. The reaction time courses for the oxidative cross-linking by two laccases were studied in order to characterize the reaction pathways, including direct cross-linking of potato proteins by laccase alone and indirect one through the use of ferulic acid (FA) mediator. The understanding of the structure-function relationships was achieved through the comparison of the modified proteins in terms of their techno-functional, chemical and structural properties.

5.3. Materials and methods

5.3.1. Laccase enzymes and potato proteins substrates

Two types of fungal laccases were investigated as biocatalysts for the oxidative cross-linking of potato proteins, including *T. versicolor* laccase (Sigma-Aldrich, St-Louis, MO) and *C. hirsutus* laccase. LacCh was produced as described previously by Gill et al. (2018) with an additional ammonium sulfate precipitation (80% saturation) step to obtain partially purified laccase. The enzyme activity was determined using the 2,2'-azino-bis(3-ethylbenzothiazoline-6-sulfonic acid (ABTS) assay; one unit of enzyme activity was defined as the mg of enzyme that oxidize one µmol of ABTS in one minute; while the protein content was measured using the Hartree-Lowry assay(Hartree, 1972; Niku-Paavola et al., 1990). The potato protein extracts were obtained from Avebe (Veedam, The Netherlands). Potato protein Solanic 206P, containing around 40 % of patatin fraction, was referred as PAT, while Solanic 306P contained mainly protease inhibitors (~95%) and was referred as PIs.

5.3.2. Kinetic study of laccase-catalyzed oxidation of potato proteins

Laccase-catalyzed oxidation of potato proteins was investigated by monitoring the decline in the fluorescence signal of aromatic amino acids over time using SpectroMax® i3x plate reader (San Jose, CA). Potato protein substrates, ranging from 0.1 to 1.6 mg/ml in sodium phosphate buffer (50 mM, pH 6.5), were incubated with laccase at enzymatic units ranging from 0.0083 to 0.3595 U/ml. The reactions were carried out at 28 ºC and monitored at excitation/emission wavelengths of 260/310 nm for 100-240 min, and the signals were recorded every 10 to 15 min. The initial velocity of the oxidation was estimated from the exponential trendline of the fluorescence decline curve. The laccase enzyme activity was expressed as µmol of equivalent tyrosine of the protein substrate that was oxidized per min per mg of laccase protein. The laccase enzyme activities were plotted versus the substrate concentration using SigmaPlot 12.3 (Systat Software, San Jose, CA), from which the best kinetic model and kinetic parameters

were determined. All reactions were performed in duplicate. Control reactions without laccase enzymes were carried out in parallel with the enzymatic reactions.

5.3.3. Oxidation time course

In order to assess the formation of oxidation products, resulted from tryptophan (e.g. N-formylkynurenine) and tyrosine (e.g. di-tyrosine**)** oxidation, the reaction was monitored by fluorescence detection at excitation/emission wavelength of 325/415 nm. Reaction mixtures in sodium phosphate buffer (50 mM pH 6.5) were composed of potato protein substrates at concentrations of 2 K_m, K_m or ½ K_m and fungal laccases at 0.04 U/ml. The mixtures were incubated at 28 ºC under the orbital agitation at 150 rpm. Aliquots of 200 µL were taken at selected time intervals over 48h of reaction, and their fluorescence intensity was measured. All reactions were performed in duplicate. Control samples with potato protein and without the addition of laccases were run in parallel with the corresponding reaction samples. The content of oxidation product was expressed as the intensity RFU/mM of equivalent tyrosine.

5.3.4. Enzymatic oxidative cross-liking of potato proteins

Potato proteins at a concentration of 0.8 mg/ml in sodium phosphate buffer (50 mM, pH 6.5) were incubated with 0.04 U/ml of LacCh or LacTv, with or without the presence of 1 mM ferulic acid. The enzymatic reactions were performed at 28°C under an agitation of 150 rpm using a New Brunswick Scientific shaker. Aliquots of the reaction mixtures were taken at selected reaction times for the characterization of the molecular weight profile over the time course.

5.3.5. Characterization of end-product profiles

The reaction mixture samples recovered at selected reaction times were loaded on a Superdex 200 Increase 10/300 GL column (GE Healthcare, Piscataway, NJ) using an ÄKTA purifier system (GE Healthcare). The elution was carried with the mobile phase that consisted of sodium phosphate buffer (50 mM, pH 7.0) containing 0.15 M NaCl and 0.1% (w/v) SDS at a flow rate of 0.5 mL/min. The elution was monitored by UV detector at 280 nm. A mixture of standards, including thyroglobulin (670 kDa), ovalbumin (44 kDa), ribonuclease A (13.5 kDa) and vitamin B12 (1.35 kDa), was used to construct the molecular weight calibration curve. The relative proportion of each fraction was estimated based on their peak area on the chromatograms. The collected fractions were also examined for their ferulic acid content and

the oxidation product content by measuring the absorbance at 310 nm and the fluorescence intensity at excitation/emission wavelength of 325/415 nm, respectively.

5.3.6. Protein secondary structure: Fourier transform infrared spectroscopy (FTIR)

FTIR spectra of modified and non-modified potato proteins were obtained using a Varian FTIR instrument. The potato protein suspensions (100 mg/ml) were prepared in deuterium oxide (D_2O). 9 µL of each sample was loaded between two CaF_2 windows separated by a 25 µm spacer. The spectrum was obtained at wavenumber from 4000 to 400 cm^{-1} by taking 256 scans. Fourier self-deconvolution at wavenumber protein amide I region 1700-1600 cm^{-1} was performed using OMNIC 8.0 software (Thermo Electron Corporation, Madison, WI) at bandwidth 23 cm^{-1} and enhancement parameter of 2.3. The deconvoluted spectra was subjected to peak fitting using half bandwidth of 6 cm^{-1}, and the relative proportion of the protein secondary structure was calculated based on the peak area identified by peak fitting. The bands were assigned as follows: region 1615-1610 cm^{-1}, side chain group vibration; 1620-1616 cm^{-1}, intermolecular anti-parallel β-sheet; 1630-1622 cm^{-1} and 1690-1680 cm^{-1}, antiparallel β-sheet; 1640-1630 cm^{-1}, parallel β-sheets; 1660-1650 cm^{-1}, α-helix; 1670-1660 cm^{-1}, β-turns (Li & Xiong, 2015; Waglay et al., 2019; Yang et al., 2015).

5.3.7. Assessment of techno-functional properties

5.3.7.1. Solubility

The percentage of solubility of the modified and non-modified potato proteins was determined gravimetrically as described by Haar et al., (2011). Protein solutions at 5 mg/ml was prepared in sodium phosphate buffer (10mM, pH 7), and allowed hydration for 1h. Samples of 1 mL were then centrifuged (10000 × g, 10 min), decanted, washed with 1 ml of water, decanted and then lyophilized. The weight of the insoluble solid was determined as w_{in}. The solubility was referred as the percentage of soluble weight in the total weight of sample w_t (5mg), calculated as equation 5.1:

$$\boldsymbol{solubility}\ \% = \frac{w_t - w_{in}}{w_t} \times \mathbf{100} \qquad \text{(Eq. 5.1)}$$

5.3.7.2 Foaming property

Foaming property was measured using the modified protocol of Houde et al. (2018). Foam was produced via a whipping method. Modified and non-modified potato proteins solution at 0.5% (w/v) was prepared with sodium phosphate buffer (10 mM, pH 7.0). The protein solutions (2

mL were foamed in a 10 ml calibrated test tube, using a PowerGen 125 homogenizer (Fisher scientific, Pittsburg, PA) with the speed setting corresponding to 30000 rpm, for 70 seconds. The volume of foam ($V_{f\,t=0}$) was calculated by subtracting liquid volume (V_l) from the total volume (V_t). The foaming capacity was the percentage of increase in total volume after whipping, calculated as equation 5.2-5.3:

$$\mathbf{V}_{f\,t=0} = \mathbf{V}_t - \mathbf{V}_l \quad \text{(Eq. 5.2)}$$

$$\boldsymbol{Foaming\ capacity}\% = \frac{\mathbf{V}_{f\,t=0}}{\boldsymbol{V}_i} \times \mathbf{100} \quad \text{(Eq. 5.3)}$$

where, V_i is the initial volume of protein solution before whipping.

The foam was allowed to stand at room temperature for 30 min where the foam volume was measured again ($V_{f\,t=30}$). Foam stability was the percentage of remaining foam after 30 min as shown by equation 5.4:

$$\boldsymbol{Foam\ stability}\ \% = \frac{V_{f\,t=30}}{V_{f\,t=0}} \times \mathbf{100} \quad \text{(Eq. 5.4)}$$

5.3.7.3. Emulsifying properties

Modified and non-modified protein solutions at 0.5% (w/v) was prepared with sodium phosphate buffer (10 mM, pH 7.0) and mixed with sunflower oil at a ratio of 1:3 (v/v). The mixtures were homogenized at 22,000 rpm for 1 min 30 s using a Fisherbrand™ 850 Homogenizer (Fisher Scientific, Pittsburgh, PA). The absorbance of the initial turbidity of the emulsions and turbidity after 15 min was measured at 500 nm using Beckman DU 650 spectrophotometer (Beckman Instruments Inc.; San Ramon, CA), represented by A_0, A_{15}. Samples were diluted 200 times in 0.1% w/v SDS solution to obtain a clear solution prior to turbidity measurement. The emulsifying capacity, indicated by emulsifying activity index (EAI) and emulsifying stability (ESI) was calculated using the equations:

$$\text{EA Index } \left(\frac{\boldsymbol{m^2}}{\boldsymbol{g}}\right) = \frac{\mathbf{2 \times 2.303 \times A_0 \times DF}}{\boldsymbol{c \times \varphi \times 10^4}} \quad \text{(Eq 5.5)}$$

$$\text{ES Index (min)} = \frac{\mathbf{A_0}}{\mathbf{A_0 - A_{15}}} \quad \text{(Eq. 5.6)}$$

where, DF is the dilution factor of the emulsion (200), c is the concentration of the aqueous solution (0.5% w/v%), φ is the oil volume fraction (0.25). In addition, the morphology of the emulsion droplets was observed using Zeiss Axio Imager Z1(Zeiss, Jena, Germany) in differential interference contrast (DIC) mode. One drop of emulsion sample (6 µL) was placed on a microscopic glass slide and covered. Micro-images were taken using the in-line camera.

5.3.7.4. Antioxidant activity

The ABTS+ radical scavenging activity of potato protein samples was investigated as described by Tantoush et al. (2011). Ascorbic acid ranging from 0.03 to 0.6 mM was used as calibration. The scavenging activity of the modified potato proteins was expressed as equivalent of ascorbic acid per mg of protein. The radical scavenging activity of the proteins was determined in triplicate.

5.4. Results and discussion

5.4.1 Kinetic properties of Laccase-catalyzed oxidation of potato proteins

Direct oxidation of proteins catalyzed by laccase can happen on tryptophan, tyrosine and cysteine amino acids, with the highest residue reactivity shown by tyrosine (Mattinen et al., 2006); the radical based reaction could also later lead to the oxidation of methionine and histidine (Steffensen et al., 2008). Our previous computational analysis indicated that binding and interaction between laccase and potato patatin occurred mainly on tyrosine residues, because of their availability and accessibility. It can be assumed that the conversion of tyrosine residues by laccase provides an estimation of early oxidation of potato proteins. In order to evaluate the catalytic efficiency of laccases from *T. versicolor* and *C. hirsutus*, the oxidation reaction was monitored by quantifying the decrease in the intrinsic fluorescence signal of potato proteins, which correlates with the oxidation of aromatic amino acid residues (e.g. phenylalanine, tyrosine and tryptophan). No significant change in the fluorescence signal of proteins due to the non-enzymatic modification was detected during the time course of the oxidation reaction. The specific activity was expressed as equivalent molar of tyrosine and plotted against substrate concentration (Fig. 5.1). As expected, at the initial stage of the kinetic plots, the specific activities of laccase-catalyzed oxidation of potato proteins increased as the concentrations of the potato proteins increased; upon a selected substrate concentration, the increase extent of specific activities was limited (Fig. 5.1). This can be explained by the substrate saturation and/or the substrate/product inhibition. With LacTv, no obvious saturation phase was detected within the investigated substrate concentration range (Fig. 5.1A & C). Conversely, the specific activity of LacCh reached a saturation at around 1.5 mg/ml of PAT (Fig. 5.1B), while the PIs-LacCh reaction system showed an enzyme inhibition at concentrations higher than 0.8 mg/ml (Fig. 5.1D).

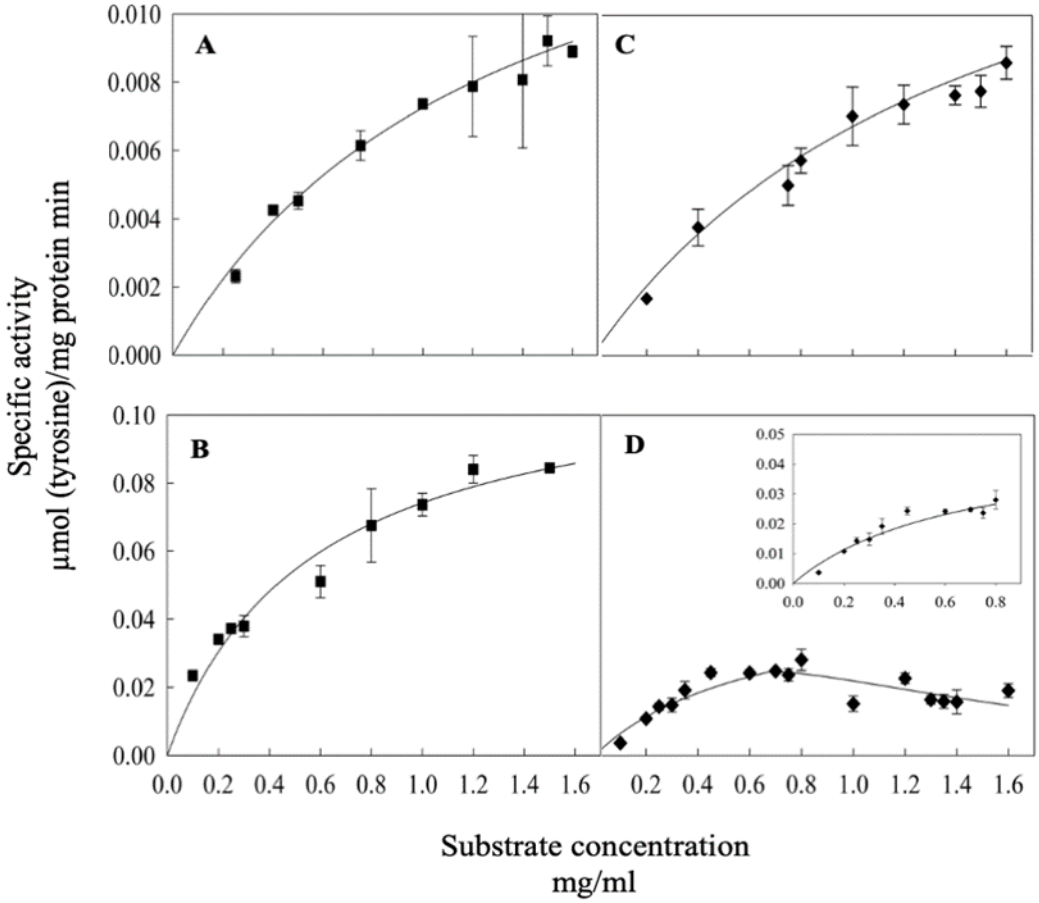

Figure 5.1. Kinetics of laccase-catalyzed oxidation of potato proteins: the specific activity of laccase from T. versicolor in the oxidation of PAT (A) and PIs (B), and that of laccase from C. hirsutus in the oxidation of PAT (C) and PIs (D) as a function of substrate concentration. The insert in D represents the kinetic plot of LacCh-PIs reaction at substrate concentration 0.0-0.8 mg/ml.

Table 5.1. Kinetic parameters for laccase-catalyzed oxidation of potato proteins

Enzyme	**Substrates**	K_m mM[a]	V_{max} μmol[a]/mg protein min	k_{cat} S^{-1}	**Catalytic efficiency** (k_{cat}/K_m) $mM^{-1}S^{-1}$
Laccase from *T. versicolor*	PAT	0.507 ± 0.072	0.017 ± 0.001	0.005	0.010
	PIs	0.594 ± 0.123	0.017 ± 0.002	0.005	0.008
Laccase from *C. hirsutus*	PAT	0.222 ± 0.004	0.116 ± 0.010	0.166	0.748
	PIs	0.255 ± 0.079	0.049 ± 0.008	0.047	0.184

a. Tyrosine equivalent mM or μmol.
Abbreviations: PAT, patatin-containing potato protein; PIs, potato protease inhibitors.

As an overall, LacCh from *C. hirsutus* exhibited higher enzyme specific activity towards both potato proteins with values that were 3 to 10 times higher than those of LacTv from *T. versicolor*.The results also reveal that the oxidation reaction of potato proteins catalyzed by the two selected laccases can fit the Michaelis-Menten kinetic model with p-value <0.001. The kinetic parameters estimated from regression analysis, are summarized in Table 5.1. LacCh exhibited a higher substrate binding affinity (K_m value of 0.222~0.255) and specificity towards potato proteins than LacTv (K_m value of 0.507~0.594). The substrate binding affinity towards PAT and PIs are comparable in the reaction catalyzed by each laccase. This result reveals that the substrate binding at the active site of laccase is not sterically hindered by the presence of high molecular weight patatin (~40 kDa) in PAT substrate. The highest catalytic efficiency was shown by PAT-LacCh reaction system (k_{cat}/K_m 0.748 mM^{-1} s^{-1}) followed by PIs-LacCh one (k_{cat}/K_m 0.184 mM^{-1} s^{-1}) and much lower for those with LacTv ((k_{cat}/K_m ~0.01 mM^{-1} s^{-1}). The high substrate reactivity of laccase can be attributed to the non-steric hindrance of the protein substrates, when interacting with the active site of laccase, and to the accessibility of the oxidizable sites (tryptophan, tyrosine, cysteine) (Mattinen et al., 2006; Steffensen et al., 2008). As per the author's knowledge, no kinetic parameters were determined for laccase-catalyzed oxidation of proteins. However, K_m values for LacTv/LacCh catalyzing the oxidation of ABTS and catechol were reported to be 0.13/0.041 and 1.11/0.16 mM (Frasconi et al., 2010). Similar to our results, LacCh showed higher affinity towards these substrates than LacTv. LacTv exhibited higher affinity towards potato proteins as compared to catechol, whereas LacCh showed lower affinity towards potato proteins than both ABTS and catechol.

5.4.2. The formation of oxidation products over the reaction time course

Protein oxidation catalyzed by laccase go through complex reaction pathways resulting in tyrosine associated cross-links, disulfide linkages, tryptophan oxidation product *N'*-formylkynurenine, carbonyl formation on tryptophan, methionine and histidine residues (Steffensen et al., 2008). The decline in aromatic amino acid fluorescence signal was observed to be accompanied with the increase in signal between 350-450 nm when excited at around 320 nm. This could be attributed to the formation of dityrosine and *N'*-formylkynurenine related oxidation products according to the previous studies (Ma, Li, et al., 2020; Malencik & Anderson, 2003; Steffensen et al., 2008). Figure 5.2 shows the time courses for the formation of oxidation products, expressed as the ratio of fluorescence intensity RFU to equivalent tyrosine concentration of the protein, at 3 concentrations of the substrates, ½K_m, K_m and 2K_m.

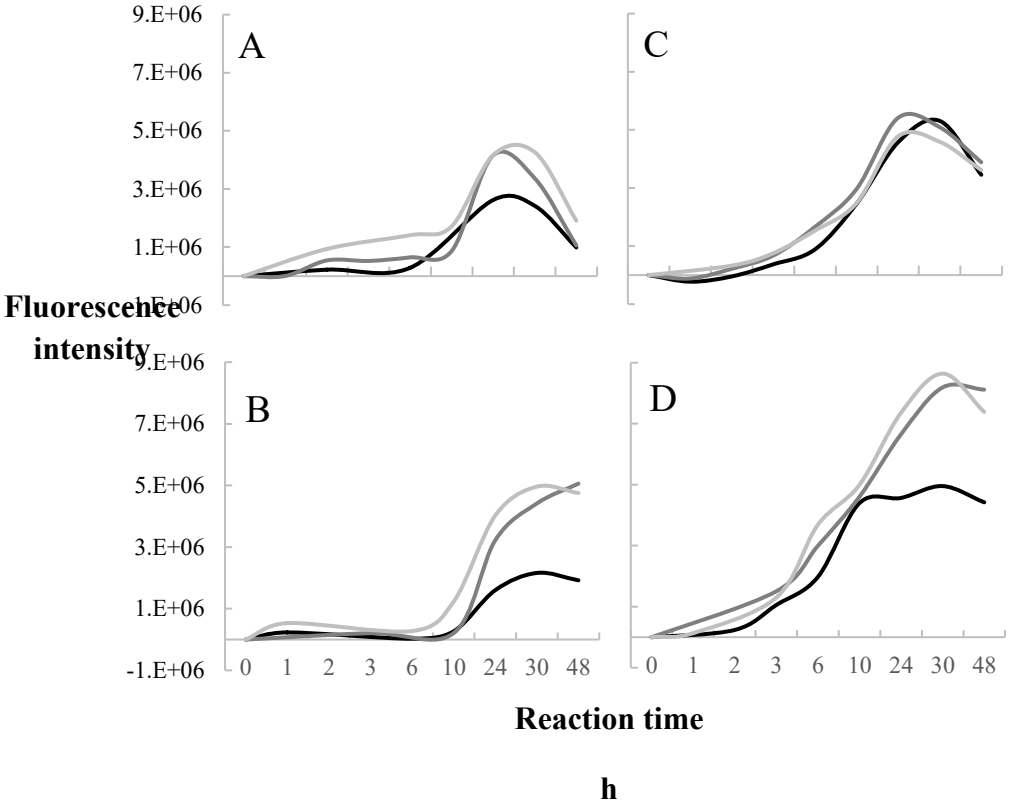

Figure 5.2. Time courses of oxidation product in reaction systems of LacTv-PAT (A), LacCh-PAT (B), LacTv-PIs (C) and LacCh-PIs (D) reactions. Curves in each graph shows time courses at different substrate concentrations: $2K_m$ in black, K_m in dark grey and $1/2K_m$ in light grey.

It can be seen that the product formation follows the same trend at substrate concentration of ½K_m and K_m, whereas a lower level of the oxidation products is formed at higher substrate concentration of 2K_m. The time courses for PAT are different (Fig. 5.2A & B) from those determined for PIs (Fig. 5.2C &D). The formation of oxidation products occurred faster in PIs reaction systems as indicated by a clear increase in the fluorescence signal at the initial stage of the reaction time courses (1 to 3 h); while PAT reaction systems showed a lag stage prior to showing obvious formation of oxidation products (at around 10 h). As well, higher extent of the product was formed with PIs than PAT, especially at low substrate concentrations (½K_m and K_m) treated by LacCh. The relatively high efficiency of PIs in forming *N'*-formylkynurenine or di-tyrosine could be attributed to their smaller molecular size. At the later stage of oxidation, a decline in the fluorescence signal was observed in the reaction catalyzed by LacTv, starting at 30 h and 22 h in the PAT and PIs reaction systems, respectively (Fig. 5.2A & C). This could be an indication of the saturation in forming dityrosine or *N'*-formylkynurenine related oxidation products followed by their condensation (e.g. dityrosine to oligo-tyrosine cross-links; *N'*-formylkynurenine to kynurenine) (Dhayal et al., 2015; Ehrenshaft et al., 2015). Similar trends were reported for the cross-linking reaction of tyrosine-containing peptide by tyrosinase and for the oxidation reaction of gelatin by laccase (Isaschar-Ovdat & Fishman, 2017; Jus et al., 2012).

5.4.3. Molecular and structural properties of cross-linked potato proteins

Oxidative cross-linking reactions with or without the presence of ferulic acid were performed on both potato proteins and characterized by size exclusion chromatography. Higher molecular weight fractions appeared in both PAT and PIs upon enzymatic treatments. An apparent increase in the UV response of the total peak area of the chromatograms were observed in the reaction with ferulic acid due to the incorporation of phenolic moieties to the protein fractions (data not shown). In order to evaluate the changes in the composition of potato proteins during oxidative cross-linking reaction time course, the relative proportion of different populations was estimated. Figure 5.3 shows the estimated molecular weight profiles of potato proteins over 48 h of oxidative crosslinking reaction. The profile comprises of highly cross-linked protein (MW>135 kDa), oligo-patatin (80-135 kDa), large potato protein and others (60-80 kDa), patatin (40-60 kDa), oligo-protease inhibitors (30-40 kDa) and protease inhibitors (1-30 kDa). The PAT control sample is comprised of fractions of large potato protein, patatin and protease inhibitors at a ratio of 15.2/39.1/45.7% (w/w/w%), whereas the control sample of PIs mainly contains protease inhibitors (~95%, w/w%).

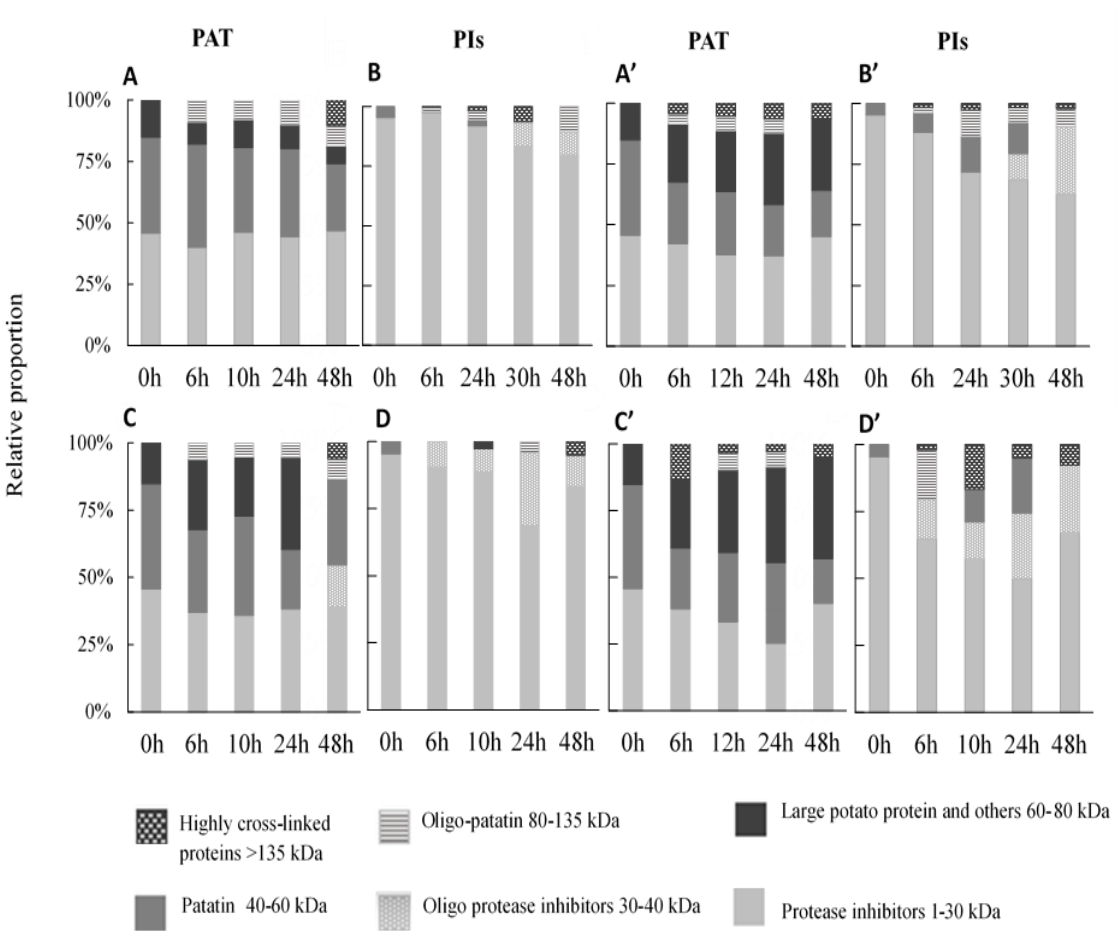

Figure 5.3. Changes in molecular weight profiles of potato proteins during oxidative cross-linking catalyzed by LacTv (A, B, A', B') and LacCh (C, D, C', D'), graphs with apostrophe indicates the enzymatic reactions with the presence of ferulic acid.

As expected, the overall molecular weight profile of cross-linked products varies by the reaction systems. The cross-linking of PAT catalyzed by LacTv resulted in the formation of oligo-patatin (80-135 kDa) and highly cross-linked proteins (MW>135 kDa) at relative proportion of 8-10.5% (Fig. 5.3A). The highest cross-linking extent of PAT by LacTv was observed at 48h, at which the cross-linked proteins represented a total relative proportion of 18.7%. Molecular weight profiles of PAT obtained upon the reaction with LacCh were different from those of LacTv. LacCh-PAT reaction system led to low oligo-patatin (5.2-6.0 % w/w) proportion over 6 to 24 h reaction time course, while 6.8-19.1% increase in the relative proportion of fraction at 60-80 kDa was observed (Fig. 5.3C). This last fraction is equivalent to the molecular weight of the hetero-cross-linked product of patatin/protease inhibitors. For the potato protein PIs, no significant changes (2-8% of cross-linked product) in the profile was observed within the first 24 h reaction catalyzed by LacTv (Fig. 5.3B); prolonging to 30 and 48h resulted in an increase in the cross-linked products to 17-20%. Among the cross-linked products, 10% were identified to be oligo-PIs (30-40 kDa) that corresponded to homo- and hetero-cross-linked products of Kunitz serine protease inhibitors (~16.5 kDa), cysteine protease inhibitor or aspartic protease inhibitor (~20 kDa) (Fig. 5.3B); while 6-10% were characterized by higher molecular weight (>80 kDa). As compared to LacTv, LacCh-PIs reaction system led to higher extent of cross-linking, within the first 24 h of reaction, with the oligo-PIs (27.3%) being the most abundant cross-linked products (Fig. 5.3D). For both PAT and PIs, at 48h of reaction catalyzed by LacCh, a decrease in the relative proportion of major cross-linked products was noted and accompanied by an increase in fractions at lower molecular weight (< 60kDa in PAT/<30 kDa in PIs). This may be ascribed to the precipitation of highly cross-linked proteins or to the oxidative fragmentation of the protein at longer reaction time. At extended reaction time, LacCh, characterized by a higher catalytic efficiency, showed more evidently increase in low molecular weight fractions. It has been reported that casein, gelatin and some small peptides containing tyrosine residues can go through direct oxidative cross-linking catalyzed by laccase (Jus et al., 2012; Jus et al., 2011; Steffensen et al., 2008). Similar to potato proteins, high molecular weight cross-linked products and precipitates due to excessive cross-linking were obtained upon the oxidative cross-linking of gelatin by laccase (Kato et al., 2014). Oxidative fragmentation of proteins can also happen upon the enzymatic treatment by laccase (Lantto et al., 2005; Mokoonlall, Pfannstiel, et al., 2016). Another oxidoreductase, tyrosinase, showed higher substrate reactivity and selectivity towards protease inhibitors than patatin, in which the molecular weight profile of cross-linked potato protein was different from what we have observed for LacTv and LacCh (Glusac et al., 2017).

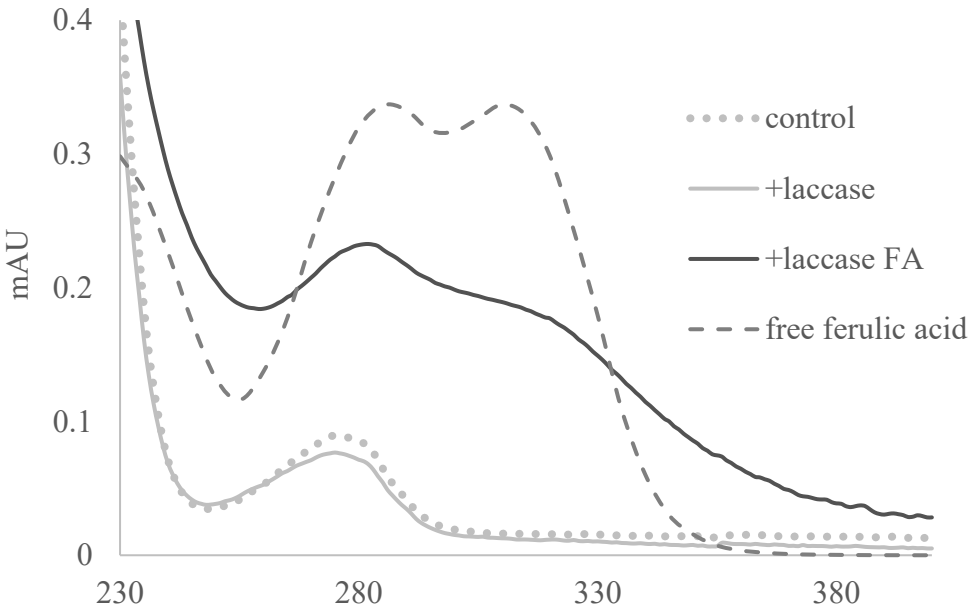

Figure 5.4. Spectra of protein incorporated with ferulic acid. FA: ferulic acid

Table 5.2. Formation of fluorescent oxidation product and ferulic acid incorporation in time course

		Oxidation product		Incorporation of ferulic acid	
		Intensity/mM of tyrosine		µmol/mg of protein	
Substrate	**Reaction time**	**LacTv-reaction**	**LacCh-reaction**	**LacTv-FA reaction**	**LacCh-FA reaction**
Patatin-containing potato protein (PAT)	6h	973530	275893	0.072	0.079
	10/12	904118	1233074	0.085	0.096
	24h	3350200	4025359	0.082	0.092
	48h	1498365	4753197	0.14	0.1334
Potato protease inhibitors (PIs)	6h	1581317	3031991	0.008	0.048
	10/12h	4819625	4647414	-	0.060
	24h	-	7626230	0.015	0.132
	30h	3621275	-	0.032	-
	48h	4042718	7388787	0.045	0.082

Abbreviations: LacTv, laccase from *T. versicolor*; LacCh, laccase from *C. hirsutus*

In the ferulic acid-based reaction systems, the incorporation of ferulic acid (0.008-0.14 μmol/mg) into the proteins was detected by the UV absorption band at 310-350 nm (Fig.5.4, Table 5.2). Highly cross-linked products >135 kDa (4.4 % in LacTv-reaction, 13.3% in LacCh-reaction) appeared upon 6h of reaction in PAT-ferulic acid system, indicating that the presence of ferulic acid accelerated the cross-linking (Fig. 5.3A' and C'). In addition, the molecular weight profile of cross-linked proteins in the presence of ferulic acid was different from those obtained from the reaction with laccase alone. In the PAT-ferulic acid reaction system, end-products with molecular weight of 60-80 kDa were accumulated, suggesting that ferulic acid mainly promoted the hetero-cross-linking between patatin and protease inhibitors. While the cross-linked products of PIs-ferulic acid reaction system was shifted towards higher molecular weight (>40kDa) (Fig. 5.3B' and D'). As a whole, ferulic acid increased the cross-linking extent of both PAT and PIs. Phenolic compounds are commonly used to overcome the limited accessibility of laccase to tyrosine residues in a protein and the steric hindrance caused by the tridimensional structure of protein. However, these compounds can also prohibit the cross-linking of a protein and undergo undesired self-polymerization (Jus et al., 2011; Mokoonlall, Pfannstiel, et al., 2016; Steffensen et al., 2008; Tantoush et al., 2011). Our results demonstrated that potato proteins can be oxidized by laccase directly and/or with the use of ferulic acid. Ferulic acid promoted the cross-linking of potato proteins by accelerating the reaction rate of cross-linking and by shifting the end-product profile towards hetero-cross-linking and high molecular weight for PAT and PIs, respectively.

The effect of oxidative cross-linking on the secondary structural properties of potato proteins was studied using the modified proteins recovered at the early (6h) and late (24h) stages of the reaction in comparison with the non-modified ones (Table 5.3). In spite of the fact that native and modified potato proteins (PAT and PIs) are made of a mix of proteins, FTIR was used to study the relative changes in overall secondary structures and in molecular interactions associated with the enzymatic modifications. The spectrum of the amide I region of PIs includes bands at 1622/1684, 1639, 1653 and 1670 cm^{-1} which were assigned to antiparallel β-sheets, parallel β-sheet, α-helix and β-turn structures, respectively. The secondary structure of non-modified PIs is composed with majorly β structures, 87.7% (14.0 % of antiparallel β-sheet, 59.4 % of parallel β-sheet, 14.2 % of β-turns) and 12.9% of α-helix, which is consistent with the literature (Pouvreau et al., 2004) (Table 5.3). The LaTv-6h and all LacCh enzymatic reactions caused an apparent loss of 2.7-18.2% in anti-parallel β-sheet structure with a concomitant increase (3.4-8.0%) in the antiparallel β-sheet structure of PIs samples (Table 5.3),

Table 5.3. Secondary structural composition of the native and modified potato proteins as determined by FTIR and cross-linking extent

	Enzymatic reactions	**Secondary structure** (%)						**Crosslinking extent (%)** [a]
		Side chain	Intermolecular β-sheet	Anti-parallel β-sheet	Parallel β-sheet	α-helix	β-turn	
PAT	Non-modified	-	5.8	5.0	36.2	41.2	11.7	N/A
	LacTv-6h	-	5.5	6.4	37.5	39.7	10.9	8.9
	LacTv-24h	-	3.6	5.1	39.1	43.2	9.1	10.0
	LacTv-FA-6h	-	4.1	6.2	33.5	43.7	12.5	17.3
	LacTv-FA-24h	-	-	6.1	39.4	40.4	14.1	21.2
	LacCh-6h	-	-	6.6	48.2	37.0	8.3	17.1
	LacCh-24h	12.0	-	4.4	41.0	31.4	11.2	24.4
	LacCh-FA-6h	-	1.0	3.3	39.1	44.6	11.9	23.8
	LacCh-FA-24h	-	1.3	3.5	38.6	43.9	12.7	29.3
PIs	Non-modified	-	-	14.0	59.4	12.3	14.2	N/A
	LacTv-6h	-	-	19.4	51.1	14.9	14.5	7.2
	LacTv-24h	-	-	13.6	56.7	17.0	12.7	5.7
	LacTv-FA-6h	-	-	12.3	58.7	12.2	16.9	17.2
	LacTv-FA-24h	-	-	12.7	58.5	14.2	14.7	26.7
	LacCh-6h	-	-	17.4	53.3	14.6	14.7	9.6
	LacCh-24h	-	-	17.5	51.7	16.1	14.8	31.4
	LacCh-FA-6h	-	-	22.0	41.2	18.2	18.6	35.3
	LacCh-FA-24h	-	-	21.3	42.4	19.4	17.0	45.5

a. Crosslinking extent was the sum of increase in the relative proportion of higher MW fractions after enzymatic treatment as compared to the non-modified proteins;

b. "-" represents no observation; "N/A" represents not applicably; Abbreviations: PAT, patatin-containing potato protein; PIs, potato protease inhibitors; LacTv, laccase from *T. versicolor*; LacCh, laccase from *C. hirsutus.*

indicative of protein unfolding induced by these oxidative cross-linking treatments (Liu et al., 2011). In addition, the α-helix structures increased by 1.8-7.0% upon laccase treatments; higher extent of such changes was observed in PIs-LacCh reaction systems than those of PIs-LacTv. The rearrangement of β structures into α-helix due to oxidative cross-linking was also reported previously for β-lactoglobulin (Alavi et al., 2018). An increase of 2.6-4.4% of β-turns was also noted in PIs samples treated by laccase-FA systems.

The non-modified PAT contains a mixture of anti-parallel β-sheet (1686 cm^{-1}), parallel β-sheet (1637), α-helix (1653 cm^{-1}) and β-turn (1671 cm^{-1}) with relative proportion of 5.0/36.2/41.2/11.7%. Another band of non-modified PAT spectrum at around 1620 cm^{-1}, corresponded to 5.8% of the secondary structure composition, was assigned as intermolecular antiparallel β-sheet. This intermolecular β structure was previously reported for patatin-containing potato proteins, which was attributed to denaturation during the extraction process (Seo et al., 2014; Waglay et al., 2019). The changes in the PAT secondary structure upon crosslinking are shown by the decrease in its inherent intermolecular β-sheet structure, which was completely eliminated upon LacCh-6h/24h and LacTv-24h-FA treatments. As well, a decrease in helical structure was observed in some PAT reaction systems, including LacTv-6h and LacCh-6h/24h (Table 5.3). Similarly, the disruption of α-helical structures of myosin has been reported to be the result of oxidation and cross-linking (Li & Xiong, 2015). A new band at lower wavenumber region (1614 cm^{-1}) appears in PAT samples obtained from LacCh-24h treatment, which was assigned to amino acid side chain vibration (Liu et al., 2011). The appearance of this new band may indicate major conformational changes relating to protein excessive unfolding thus aggregation in PAT-LacCh-24h sample (Eissa et al., 2006; Li & Xiong, 2015). In laccase-ferulic acid reaction systems, the main conformational changes of PAT are shown to be the reduction in the inherent intermolecular β-sheets structure, while only limited disruption in its α-helical structures was observed. Such results may imply that the use of phenolic mediator could protect the structural integrity of PAT.

5.4.4. Techno-functional properties and antioxidant activity

The effects of the enzymatic cross-linking of potato proteins on their foaming and emulsifying properties were investigated. The changes in solubility were first evaluated since the foaming and emulsification ability of protein can be affected by their solubility. The solubility of potato proteins at pH 7 was not significantly affected by oxidative cross-linking (Fig. 5.5A); the percentage of solubility of non-modified and modified PAT and PIs represented more than 80%.

Except, modified PIs obtained upon LacCh-catalyzed reactions exhibited lower solubility (57.1-76.5%) than that of non-modified PIs (80.7%).

The foaming property of non-modified and modified potato proteins were studied by determining their foaming capacity (Fig. 5.5C) and the stability of the foam (Fig. 5.5D). In general, the foaming capacity is dependent on the ability of proteins to migrate towards the interface, to unfold/rearrange and to form an elastic film to entrap the air bubbles, whereas the foam stability can be attributed to the rheological property of the film constructed by protein, the interaction between the protein molecules and the viscosity of the continuous phase (Wouters et al., 2016). The foaming capacity of non-modified PAT and PIs was estimated at 43.1% and 42.5 %, respectively. All enzymatic crosslinking of PAT and PIs catalyzed by LacTv lowered their foaming capacity (12.5%-27.5%), whereas LacCh-catalyzed cross-linking contributed to the enhancement of the foaming capacity of the potato proteins recovered in the following reaction systems : LacCh-6h (82.0%) and LacCh-FA-6h (74.2%) for PAT, LacCh-6h (45.4%) for PIs. This enhancement can be attributed to the abundance of hetero-cross-linked products made of patatin/protease inhibitor (60-80 kDa) in the modified PAT and of oligo-PIs (30-40 kDa) in the modified PIs as compared to the corresponding modified proteins from LacTv systems and non-modified proteins. The increase in the cross-linking extent as shown in the PAT-LacCh-24h reaction system did not further promote the foaming capacity of PAT. In contrast, the presence of cross-linked PIs at high extent (9.6-31.4%) in the LacCh-6h/24h reaction system tended to enhance the foaming capacity more than cross-linked PIs with low to moderate extent (5.7-9.6%), recovered upon LacTv-6h/24h reactions. The enhancement in foaming property can be ascribed to the protein unfolding and/or to the increased surface hydrophobicity (Baier & Knorr, 2015; Hiller & Lorenzen, 2008). However, over exposure of hydrophobic residues and an increase in molecular size were reported to decrease the foaming capacity (Hunter et al., 2008; Partanen et al., 2009; Ter Haar et al., 2011).

The foaming stability of non-modified PAT and PIs was estimated at 68.9 and 89.7%, respectively. Comparing to non-modified proteins, an enhancement in the foam stability was achieved by the following reaction systems: PAT-LacTv-24h, PAT-LacCh-6h/24h and PIs-LacTv-24h. Although ferulic acid mediator promoted the cross-linking, its incorporation into the cross-linked potato proteins (LacTv or LacCh-FA-reactions) impaired the foam stability. This could be due to the fact that crosslinked FA-potato proteins exhibited conformations, which may have disfavored the re-organization of protein molecules around air bubbles and their interaction required for forming a viscoelastic film (Jarpa-Parra et al., 2015).

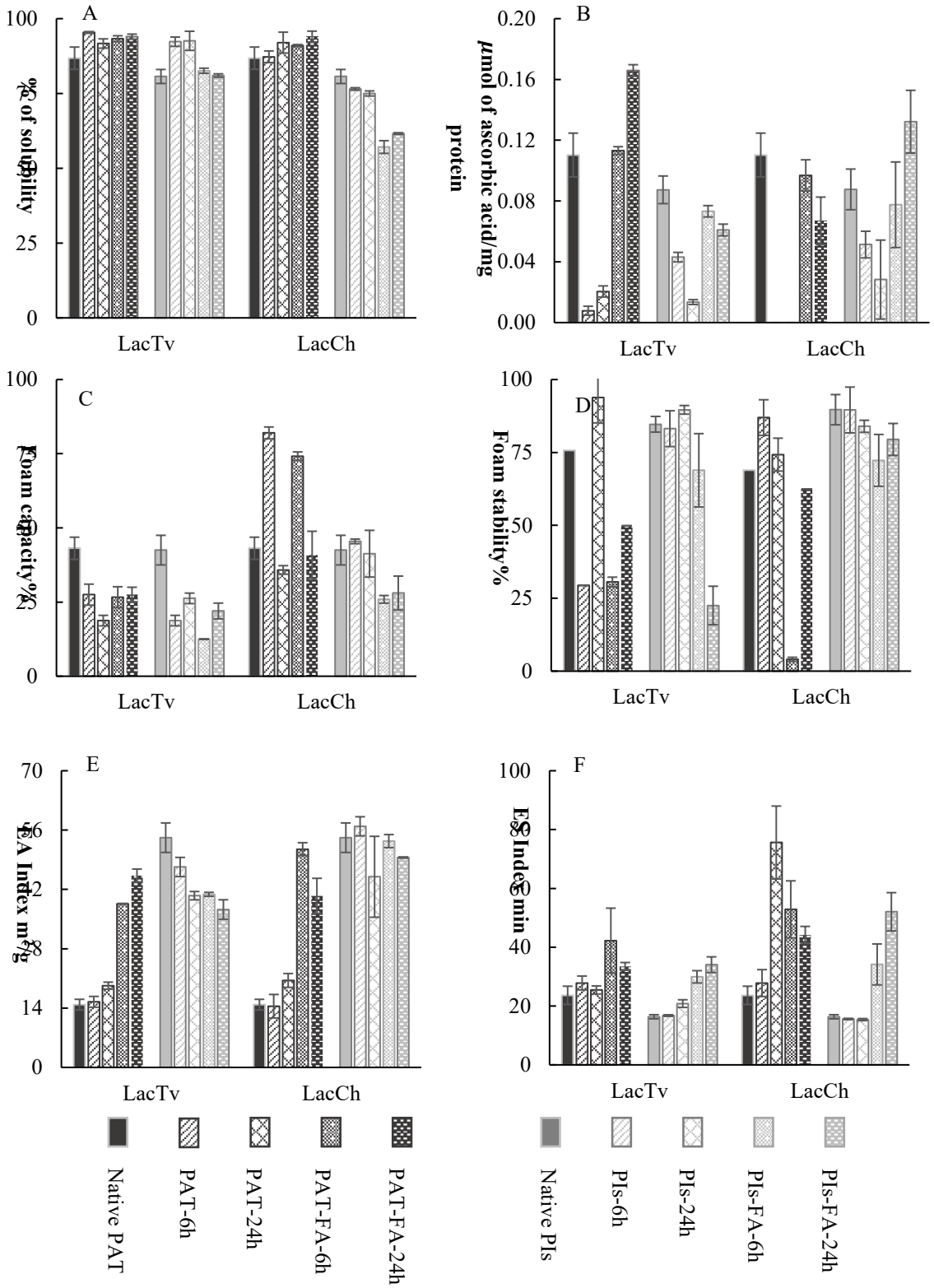

Figure 5.5. Assessment of solubility (A), antioxidant property (B), foaming capacity (C), foam stability (D) emulsifying ability (E) and emulsion stability (F) of native and cross-linked potato protein containing patatin fraction (PAT), protease inhibitor potato protein fraction (PIs). LacTv: laccase from *T.versiolor*; LacCh: laccase from *C. hirsutus*

Our study showed that LacCh-6h-reaction system was able to improve the foaming capacity and stability of PAT. Indeed, cross-linked PAT recovered from this reaction system, was characterized by disappeared β-intermolecular and lower content of α-helix structures than the native and other modified PATs. These structural characteristics may have supported the high mobility of modified PAT to the interface (Table 5.3). In addition, this PAT was moderately cross-linked (17%) (Table 5.3) with low degree of oxidation product (dityrosine, *N'*-formylkynurenine) formation (Table 5.2) and a molecular weight of 60-80 kDa (Fig. 5.3C). These modifications may have led to better hydrophobicity-hydrophilicity balance for the protein, thus contributing to its network forming ability and foam stability. The same reaction LacCh-6h also in some extent contributed to the foaming property of PIs; this cross-linked PIs was characterized as moderate extent of cross-linking and low α-helix structures as compared to PIs from other reaction systems.

Similar to foaming, the emulsifying performance of protein is associated with the mobility, the conformational changes and the surface activity property of protein (Kato et al., 2014). However, to enhance emulsifying performance, higher exposed hydrophobicity and higher degree of conformational changes in protein are required when comparing to foaming performance (Yu et al., 2019). Changes in emulsifying properties of potato proteins upon modification were evaluated based on the emulsifying activity index (Fig. 5.5E) and stability index (Fig. 5.5F). The EA index/ES index of unmodified PAT and PIs were estimated at 14.8/23.6 and 52.4/16.3 (m^2/g/min), respectively. Differently from the result of foaming property, laccase-catalyzed cross-linking greatly improved the emulsifying activity and stability of PAT. The EA index of PAT increased to 20 m^2/g after treatment with laccase-24h reactions. More than 2 times increase in the EA index was achieved upon the use cross-linked PATs from LacTv-FA-6h/24h and LacCh-FA-6h/24h reaction systems. The enhancement in emulsifying activity was associated with moderate to high cross-linking extent of PAT (10.0-29.3%) (Table 5.3). In addition, according to the micro-images, the cross-linked PATs with enhanced emulsifying capacity were shown to form relatively small and homogenous droplets as compared to the non-modified PAT (Fig. 5.6). Previous studies have attributed the increase in emulsifying activity via enzymatic cross-linking to the increased surface hydrophobicity, the formation of intramolecular linkages and the protein unfolding (Berton-Carabin et al., 2016).

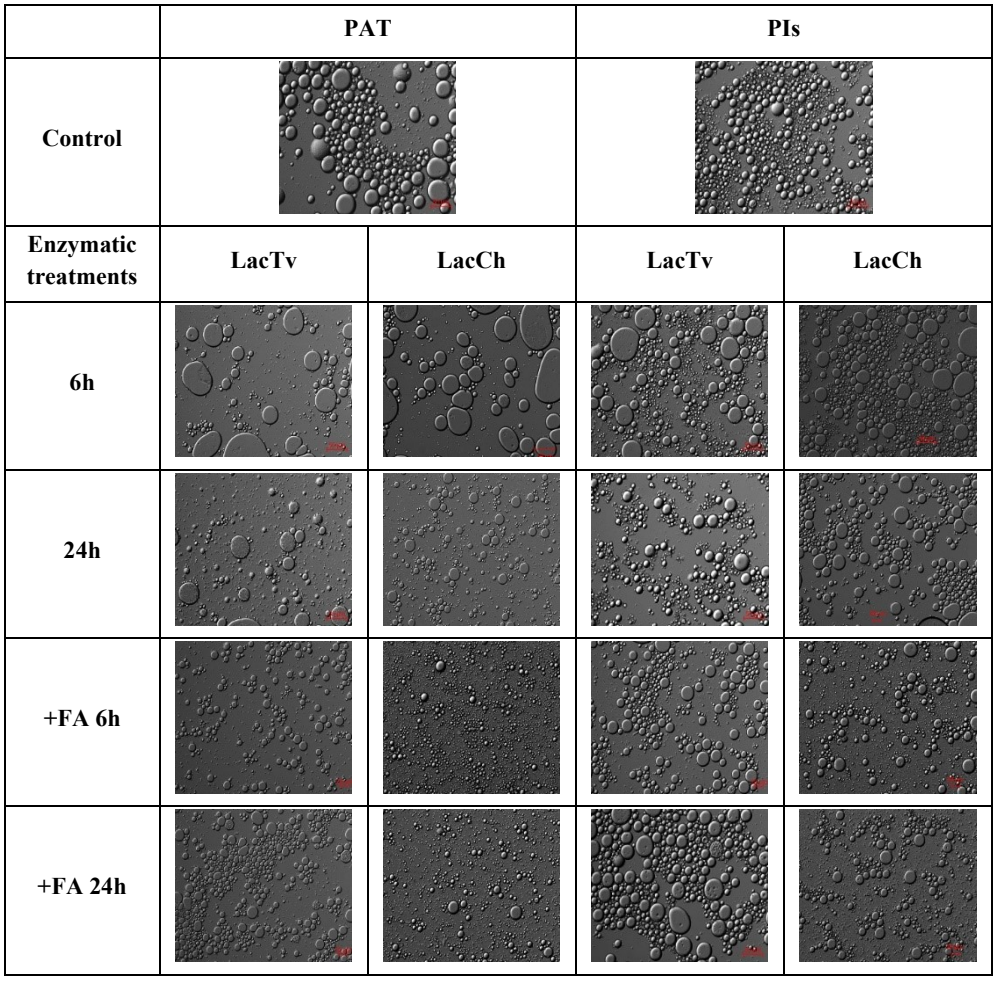

Figure 5.6. Micro-images of oil-in-water emulsions stabilized by potato protein samples

In addition, obvious improvement in the emulsifying stability of PATs was achieved with the use of LacTv-FA-6h/24h, LacCh-24h, LacCh-FA-6h/24h reaction systems. Although the cross-linking of PIs did not affect significantly its emulsifying activity, it resulted in 1.1 to 2.2-fold increase in the emulsion stability, especially with the presence of ferulic acid. The micro-images of emulsion samples made with modified PIs from LacCh-FA-6h/24h reaction systems showed less adhesion between droplets as compared to non-modified PIs, implying less droplet coalescence thus better stabilization effect. The improvement in PIs emulsifying stability upon cross-linking could be associated with its unfolding and the rearrangement of its secondary structure as indicated by the FTIR result (Table 5.3). Cross-linked PAT and PIs have larger molecular size, which generally form a more rigid film around the oil droplet, retarding their coalescence and destabilization (Wang et al., 2018). The larger sized protein can also contribute to the higher extent of repulsion force and the steric hindrance between the oil droplets, hence limiting the destabilization of the system (Sato et al., 2015). Other effects from protein cross-linking contributing to emulsion stability includes shifting hydrophobic-hydrophilic balance and altering molecular flexibility (Alavi et al., 2019; Yu et al., 2019).

The changes in the antioxidant activity after cross-linking was evaluated using the ABTS+ radical scavenging assay. The antioxidant activity of unmodified PAT and PIs were estimated at 0.110 and 0.087 μmol equivalent to ascorbic acid/mg of protein (Fig. 5.5B). The antioxidant activity of PAT was greatly impaired by the oxidative cross-linking treatment (Fig. 5.5B). However, the radical scavenging activity of PIs was less affected by the laccase-catalyzed oxidation. The ability of protein in radical scavenging relies on the amino acid composition and conformation for quenching and stabilization of the radicals (Chi et al., 2015; Wang & Xiong, 2005). Aromatic amino acids (e.g. tyrosine, tryptophan), cysteine and methionine residues are important sites associating with the antioxidant activity of protein molecules (Chi et al., 2015; Medina-Navarro et al., 2010), which are susceptible to laccase catalyzed oxidation. The decrease in scavenging activity of potato proteins could be a result of reducing effective sites, as well as conformational changes. Conversely, the oxidative cross-linking with the presence of ferulic acid has less negative effects on the antioxidant activity of potato proteins than cross-linking using laccase alone. Higher radical scavenging activity than the control was obtained when PAT was treated in LacTv-FA-6h/24h reaction systems, and PIs in LacCh-FA-24h reaction systems. The increase in the antioxidant activity of protein due to incorporation of phenolic compounds during laccase-catalyzed cross-linking have been reported previously (Tantoush et al., 2011).

5.5. Conclusion

In conclusion, laccase can directly or indirectly catalyze the oxidative cross-linking of both patatin-containing potato protein (PAT) and potato protease inhibitors (PIs). The cross-linking caused a combination of modification in the molecular and structural properties of the protein and resulted in varied functionality profiles of potato proteins. Mild oxidative-cross-linking of PAT and increased proportion of cross-linked proteins at 60-80kDa were associated with enhanced foaming performance, whereas for PIs, relatively high cross-linking extent with high proportion of oligo-PIs (30-40 kDa) favored its foaming performance. The cross-linking generally improved the emulsifying performance of PAT, and an obvious increase in the emulsifying stability was achieved upon the use of cross-linked PIs. The oxidative cross-linking in the presence of ferulic acid did not contribute to foaming property; however, it resulted in higher emulsifying performance and antioxidant property, as compared to the cross-linking achieved using laccase alone. As overall, this comprehensive kinetics-structure-function study contributes to the understanding of laccase-biocatalytic approach and will help with the efficient production of cross-linked potato proteins with desired properties.

CONNECTING STATEMENT 4

Chapter V reported the laccase-catalyzed oxidation with or without the presence of ferulic acid in the cross-linking of potato proteins. Potato proteins were shown to be a promising substrate for laccase-catalyzed modification. In Chapter VI, further investigation of the conjugation of potato protein with selected pectic polysaccharides via laccase-catalyzed reactions were carried out. Response surface methodology was used to model the enzymatic conjugation and study the effect from important reaction parameters on conjugation extent and emulsification performance of the products .

This work was submitted to *Food Chemistry*

Li, M., & Karboune, S. (2020). Laccase-catalyzed conjugation of potato protein with selected pectic polysaccharides: conjugation efficiency and emulsification properties. *Food Chemistry*. (Under review)

CHAPTER VI. LACCASE-CATALYZED CONJUGATION OF POTATO PROTEIN WITH SELECTED PECTIC POLYSACCHARIDES: CONJUGATION EFFICIENCY AND EMULSIFICATION PROPERTIES

6.1. Abstract

The current study focused on the investigation of laccase-catalyzed conjugation of potato protein (PPT) with selected pectic polysaccharides (PPS) and modulation of the conjugation in order to obtain desired functional ingredients. PPS, including sugar beet pectin/arabinan, apple/citrus pectin and potato galactan, were evaluated as substrates in the conjugation reaction-catalyzed by laccases (*Trametes versicolor*-LacTv, *Coriolus hirsutus*-LacCh). LacCh exhibited a higher catalytic efficiency than LacTv. The reactivity of PPT/PPS and their ratio were determinants for their heteroconjugation. Both laccases exhibited the highest specificity towards the conjugation of PPT/sugar beet pectin. Predictive models were developed for conjugation efficiency and emulsification performance. The conjugation extent was negatively affected by the protein ratio and the protein ratio/enzyme concentration interaction; while the emulsification performance was positively correlated with the protein ratio and the protein ratio/reaction time interaction. This study contributed to the understanding of laccase-catalyzed conjugation reaction for controlled synthesis of conjugated-PTT as functional ingredients.

6.2. Introduction

Proteins and polysaccharides are two common biopolymer ingredients that can exhibit a wide range of techno-functional and health-promoting properties. These biopolymers are often used synergistically to construct various colloidal systems for food and pharmaceutical applications (Liu et al., 2017). Indeed, proteins being amphiphilic compounds are well-positioned as good candidates for emulsifying and foaming purposes, whereas polysaccharides being hydrophilic components can exhibit thickening and gelling properties and stabilize the emulsion systems (K & Bandyopadhyay, 2012). For instance, pectic polysaccharides (PPS), which are abundant in the cell wall of by-products, may have unique chemical characteristics, as results of the acetylation and/or methylation on the galactorunic acid residues of homogalacturonan (HG) and the feruloylation of neutral sugar side chains of rhamnogalactorunan I (RGI) region. These characteristics modulate the techno-functional properties of PPS (Patova et al., 2014).

Conjugating proteins with polysaccharides via covalent linkages has been identified as a potential strategy to overcome limitations of each of these biopolymers and to generate novel protein/polysaccharide conjugates with synergistic properties (Liu et al., 2017; Seo et al., 2014). This strategy has been explored in the design of food colloidal systems that offer high pH and thermal stability, resistant against freeze-thaw treatment, as well as a controlled-release as food delivery systems (Gazme & Madadlou, 2014; Zeeb et al., 2017). The development of strategies

for the production of protein/polysaccharide conjugates has become of substantial importance in many fields. The conjugation via Maillard reaction has been studied extensively due to the high prevalence and achievability of this chemical conjugation, in which covalent bonds between free amine groups of protein and carbonyl groups of carbohydrate are formed (De Oliveira et al., 2016; Seo et al., 2014). However, the protein/polysaccharide conjugation via Maillard reaction may require a long time of incubation and elevated temperatures; more importantly, Maillard reaction can be difficult to control and to limit its advanced stages that can lead to undesired side products (Flanagan & Singh, 2006). Alternatively, the protein/polysaccharide conjugation can be achieved via laccase-based enzymatic approach as a green process (Gazme & Madadlou, 2014). Indeed, laccase (E.C1.10.3.2), an oxidoreductase, can catalyze the oxidation of protein and polysaccharide on their phenolic functional groups, and can result in the formation of covalent conjugates via the reactive phenolic moieties. Protein's tyrosine residues and ferulic ester on the α-(1-5)-arabinan or β-(1,4)-galactan side chains of the RGI region of PPS are the common reactive sites for laccase-catalyzed oxidation (Patova et al., 2014; Selinheimo et al., 2008). Laccase-catalyzed protein/polysaccharide conjugation has been performed with limited protein models, such as casein, β-lactoglobulin and bovine serum albumin (Chen et al., 2018; Selinheimo et al., 2008; Wang, Lv, et al., 2019; Zeeb et al., 2017). It has been reported that such conjugation can strengthen the oil-water interfacial layer that is made of protein and polysaccharide (Gazme & Madadlou, 2014). Furthermore, the improvements in protein's solubility (Jung & Wicker, 2012b), heat stability (Wang, Lv, et al., 2019), and emulsifying stability (Chen et al., 2018) were achieved upon conjugation with polysaccharides via laccase-catalyzed reactions. However, these improvements require a better modulation of the laccase action, which remains to be better elucidated.

As far as the authors are aware, only limited plant-based proteins have been modified through this approach. To our knowledge, to date, no literature has investigated the conjugation of potato protein (PPT) with polysaccharides through laccase-catalysed reaction. There is an increasing demand for the use of plant-based proteins as an alternative to animal proteins. PTT is of great potential because of its high nutritional quality, its ability to reduce food intake by increasing the circulation of cholecystokinin levels and its techno-functional properties (Glusac et al., 2017; Komarnytsky et al., 2011). However, functional limitations of PPT have been seen, including limited solubility/gel forming efficiency at increased ionic strength, lower denaturation temperature than animal and soy protein as well as susceptibility to process

conditions (Creusot et al., 2011; Miedzianka et al., 2012). It can be hypothesized that the conjugation of PPT with PPS through laccase-catalyzed reaction can improve their use as a functional ingredient and broaden its application. The present study was aimed at the investigation of laccase-catalyzed conjugation of PPT with five different PPS, including sugar beet pectin, citrus pectin, apple pectin, potato galactan and sugar beet arabinan. The conjugation was assessed by determination of the catalytic efficiency of laccases as it is related to the structural property of PPS and bioconversion of the biopolymers. In addition, the effect of enzymatic conjugation of PPT with sugar beet pectin on the emulsification performance of the biopolymers was modulated using response-surface methodology (RSM), where predictive models were developed to better understand the interactions between key reaction parameters.

6.3. Materials and Methods

6.3.1. Materials

Potato protein Solanic 206P (PPT) was kindly provided by Solanic (Avebe ®, Veendam, NL). Sugar beet pectin, GENU® BETA pectin was obtained from CPKelco (Groβenbrode, Germany). *Trametes versicolor* laccase, citrus pectin, apple pectin, 2,2'-azino-bis-3-ethylbenzothiazoline-6-sulfonic acid (ABTS) were purchased from Sigma-aldrich (St-Louis, MO), while potato galactan and sugar beet arabinan were purchased from Megazyme (Wicklow, Ireland).

6.3.2. Laccase enzymes

Two types of fungal laccases were investigated as biocatalysts for the oxidative conjugation, including *T. versicolor* laccase and *Coriolus hirsutus* laccase. LacCh was produced as described previously by Gill, *et al.* (2018), with an additional ammonium sulfate precipitation (80% saturation) step. Laccase activity was determined using ABTS assay. One unit of laccase activity was defined as the amount of enzyme that oxidizes 1 µmol of ABTS per min. Protein content of enzyme was determined using Hartree-lowry method.

6.3.3. Spectral and chemical characterization of pectic polysaccharide

The fluorescence spectra of the PPS at pH 6 and 10 were determined using SpectroMax® i3x 96-well microplate reader (San Jose, CA). 2 to 25 mg/ml of PPS were prepared using sodium phosphate buffer (50 mM, pH 6) and sodium carbonate buffer (50 mM, pH 10). The excitation spectra at 250-400 nm were taken by setting the emission wavelength at 450 nm; whereas the

emission spectra at 400-600 nm were taken at excitation wavelength of 355 nm. The spectra were compared with those of ferulic acid and methyl ferulate at pH 6 and 10.

The content of ferulic ester in PPS (% w/w) was determined spectrophotometrically at 325 nm using methyl ferulate as a standard. Polysaccharide solutions (triplicates) and methyl ferulate in sodium phosphate buffer (50 mM, pH 6.5) at concentrations varying from 0.005 to 0.2 mM were prepared. The content of ferulic ester of PPS was determined from the slope of absorbance versus concentration using the extinction coefficient of 9.29 $mM^{-1} \cdot cm^{-1}$ estimated from methyl ferulate standard curve.

6.3.4. Oxidation of biopolymers by laccases

The oxidation of PPS by laccases was examined by measuring the decrease in the absorbance of their ferulic ester at 325 nm. The initial concentration of PPS in the reaction mixture was set at 2.4, 7.1, 27, 13.3 and 30 mg/ml sodium phosphate buffer (50 mM, pH 6.5) for sugar beet pectin, citrus pectin, apple pectin, potato galactan and sugar beet arabinan, respectively, in order to maintain an initial absorbance of one at 325 nm. The oxidation reactions were initiated by the addition of LacTv or LacCh to achieve an enzyme concentration ranging from 0.004-0.01 mg protein/ml. The absorbance of the reaction mixtures was measured over a time course of 15 to 60 min at 28 °C. The oxidation reactions catalyzed by laccases were also carried out in the co-presence of PPS and PPT protein (2.4 mg/ml) as substrates. The specific activity of laccases (LacTv, LacCh) towards selected biopolymers were estimated from the initial slope of the absorbance over the reaction time. The absorbance of the control samples, which contains the same reactants composition without enzyme added, was monitored in parallel. All measurements were conducted in triplicates.

6.3.5. Laccase-catalyzed conjugation reaction

Selected PPS/PPT reaction systems were further investigated for conjugation efficiency, including sugar beet pectin/PPT, citrus pectin/PPT and sugar beet arabinan/PPT. The concentration of PPS/PPTwas set at 0.05 μmol of ferulic ester equivalent of PPS polysaccharide per mg PPT protein. The enzyme concentrations (LacCh/LacTv) used for the reaction systems with sugar beet pectin, citrus pectin and sugar beet arabinan were 0.004/0.05, 0.008/0.10 and 0.004/0.05 mg protein/ml respectively. The conjugation reactions were carried out at 28°C for 2h and 12 h under orbital agitation of 150 rpm, using a New Brunswick Scientific shaker. Control samples with polysaccharide/protein mixture and without the

addition of laccase were run in parallel with the corresponding reaction mixtures. The control samples and the reaction mixtures were characterized by anionic exchange chromatography on a MonoQ 5/50 GL column (GE Healthcare, NJ) using a ÄKTA fast protein liquid chromatography (FPLC) system (GE Healthcare) with fraction of 1ml collected from the elution. The elution was carried out at flow rate 1 ml/min with a gradient of 1 M NaCl (B) in the potassium phosphate buffer (50 mM, pH 6): 0% of B for 2 column volume (CV), increased to 25% of B within 10 CV and stabilized at 25% of B for 5 CV, then increased to 40% of B within 5 CV and stabilized for 5 CV and at the end increased to 100% of B within 5 CV. The protein and carbohydrate contents of each fraction were quantified using Bradford assay and phenol test, respectively. The bioconversion was calculated as the sum of percentage of consumed protein and polysaccharide.

6.3.6. Experimental design for the enzymatic conjugation of potato protein and sugar beet pectin

A 5-level central composite rotatable design (CCRD) was used to optimize the conjugation of PPT/sugar beet pectin catalyzed by LacCh. The independent variables and their actual levels were: X_1: PPT proportion over the sum concentration of PPT and sugar beet pectin, 20-80%; X_2: reaction time, 2-12 h; X_3: enzyme concentration, 0.0050-0.0200 U/ml. A total of 16 randomized experimental trials were carried out including 2 replicates of central point, 8 axial points (level ±1) and 6 factorial points (level ± 1.68). Duplicate was run for each trial. The conjugation extent, the solubility index and the emulsification properties were assessed as responses.

Analysis of variance (ANOVA) of the model was performed by using Design Expert Software (Stat-Ease, Inc. MN, USA), where two-factor and quadratic regression were used to model the responses according to the model fitness, as indicated by *F* value, *p*-value, lack of fit and R^2. A generalized equation the models were shown as equation 6.1 :

$$Y=\beta_0+\sum \beta_i X_i+\sum \beta_{ij} X_i X_j+\sum \beta_{ii} X_i^2 \qquad \text{(Eq. 6.1)}$$

where, Y is the response, X_i and X_j are the independent variables, and polynomial coefficients are $\boldsymbol{\beta}_0$ (constant term), $\boldsymbol{\beta}_i$ (linear coefficient), $\boldsymbol{\beta}_{ij}$(interaction coefficient) and $\boldsymbol{\beta}_{ii}$ (quadratic coefficient).

6.3.7. Characterization of potato protein/sugar beet pectin conjugates

6.3.7.1. Conjugation extent

In order to determine the conjugation extent, the molecular weight (MW) distribution of the reaction mixture was analyzed by high performance size exclusion chromatography (SE-HPLC). A Waters HPLC system equipped with a 1525 binary pump, Breeze™ 2 Software and with both UV diode-array detector (Model 2998) and refractive index (RI) detector (Model 2489) was used for the analysis. The reaction mixtures were eluted on three size exclusion columns in series, TSK gel G5000, G4000 and G3000 PWXL columns (0.78 × 30 cm) (Tosoh Bioscience, PA). An isocratic elution was performed with sodium phosphate buffer (10 mM, pH 7) containing 0.15 M of NaCl, at flow rate 0.5 mL/min. A mixture of compounds including Thyroglobulin, ovalbumin, vitamin B12 and dextran standards were used for MW calibration. The MW distribution of conjugates was determined in the UV and RI chromatograms. The conjugation extent was estimated as the relative proportion of conjugation product in the reaction mixtures

6.3.7.2. Solubility index

The solubility index of PPT/sugar beet pectin reaction mixtures was defined as the ratio of solubility of reaction mixture over that of the control sample. The PPT/sugar beet pectin mixtures were centrifuged at 12.5 rpm for 5 min. The insoluble fractions were recovered, dried and weighed. The solubility index was calculated as shown by equation 6.2.

$$\boldsymbol{solubility\ index} = \frac{(w_t\text{-}w_r)\%}{(w_t\text{-}w_c)\%} \qquad \text{(Eq. 6.2)}$$

where w_t is the total weight of the dry substrate mixture, w_r is the weight of insoluble solid of the reaction mixture; w_c is the weight of insoluble solid of the control samples.

6.3.7.3 Emulsification performance and emulsion stability

The emulsification performance of the conjugated PPT/sugar beet pectin mixtures were evaluated by estimating the emulsifying activity index (EAI) and the particle size distribution. Emulsions were prepared by homogenizing the mixture of conjugated PPT/sugar beet pectin solution (5% w/v, in sodium phosphate buffer (10mM, pH 7)) and commercial sunflower oil at a ratio of 3:1 (v/v), using a Fisherbrand™ 850 Homogenizer (Fisher Scientific, Pittsburg, PA) at 22,000 rpm for 1.5 min. Samples were taken from each emulsion and diluted 200 times with 0.1% w/v SDS solution and the absorbance A_0 was recorded at 500 nm. The EAI was calculated as equation 6.3:

$$\text{EAI } (\frac{m^2}{g}) = \frac{2 \times 2.303 \times A_0 \times DF}{c \times \varphi \times 10^4} \quad \text{(Eq. 6.3)}$$

where DF, dilution factor; c, emulsifier concentration; φ, oil volume fraction= 0.25. The droplet size of the emulsion was measured by dynamic light scattering (DLS) using a NanoBrook Omni particle size analyzer (Brookhaven Instruments, NY). The average diameter of the droplet and polydispersity indices were determined from 6 measurements.

The prepared emulsion samples were allowed to stand in room temperature for 15 min, where the absorbance of the diluted samples was measured again as A_{15}. The emulsion stability (ES) index was calculated as equation 6.4:

$$\text{ES Index} = \frac{A_0}{A_0 - A_{15}} \quad \text{(Eq. 6.4)}$$

6.4. Results and discussion

6.4.1. Structure and ferulic ester content of pectic polysaccharides

As the structural properties of biopolymers determine the conjugation efficiency via laccase-catalyzed reaction and the beneficial characteristics of conjugates, these properties need to be characterized and modulated. In the present study, five different PPS were selected including sugar beet pectin, citrus pectin, potato galactan, apple pectin and sugar beet arabinan. The structural properties of the selected PPS varied greatly, in terms of fraction type, monosaccharide profile, linkages, MW distribution and feruloylation extent. Sugar beet pectin (300-800 kDa) and apple pectin (1050 kDa) contain relatively diverse fractions of HG and RGI, whereas the citrus pectin (478 kDa) is characterized by lower dispersity with HG being the main fraction (Jung & Wicker, 2012a; Ma, Chen, et al., 2020; Qi et al., 2019; Yapo et al., 2007). Potato galactan (>500 kDa) and sugar beet arabinan (~1.3 kDa), mainly made of neutral monosaccharides, consisted of arabinan- and galactan-substituted RGI of the corresponding PPS, respectively (Khodaei & Karboune, 2013; Zaidel et al., 2011). Apple pectin and citrus pectin are known for their thickening, stabilizing and gelling effects, whereas sugar beet pectin has outstanding emulsification property as compared to the other PPS (Guo et al., 2018; Leroux et al., 2003). Sugar beet arabinan and potato galactan are commonly proposed to be used as prebiotic ingredients due to the profile of their neutral-rich RGI branches, aside from techno-functional properties (Holck et al., 2011; Khodaei & Karboune, 2013).

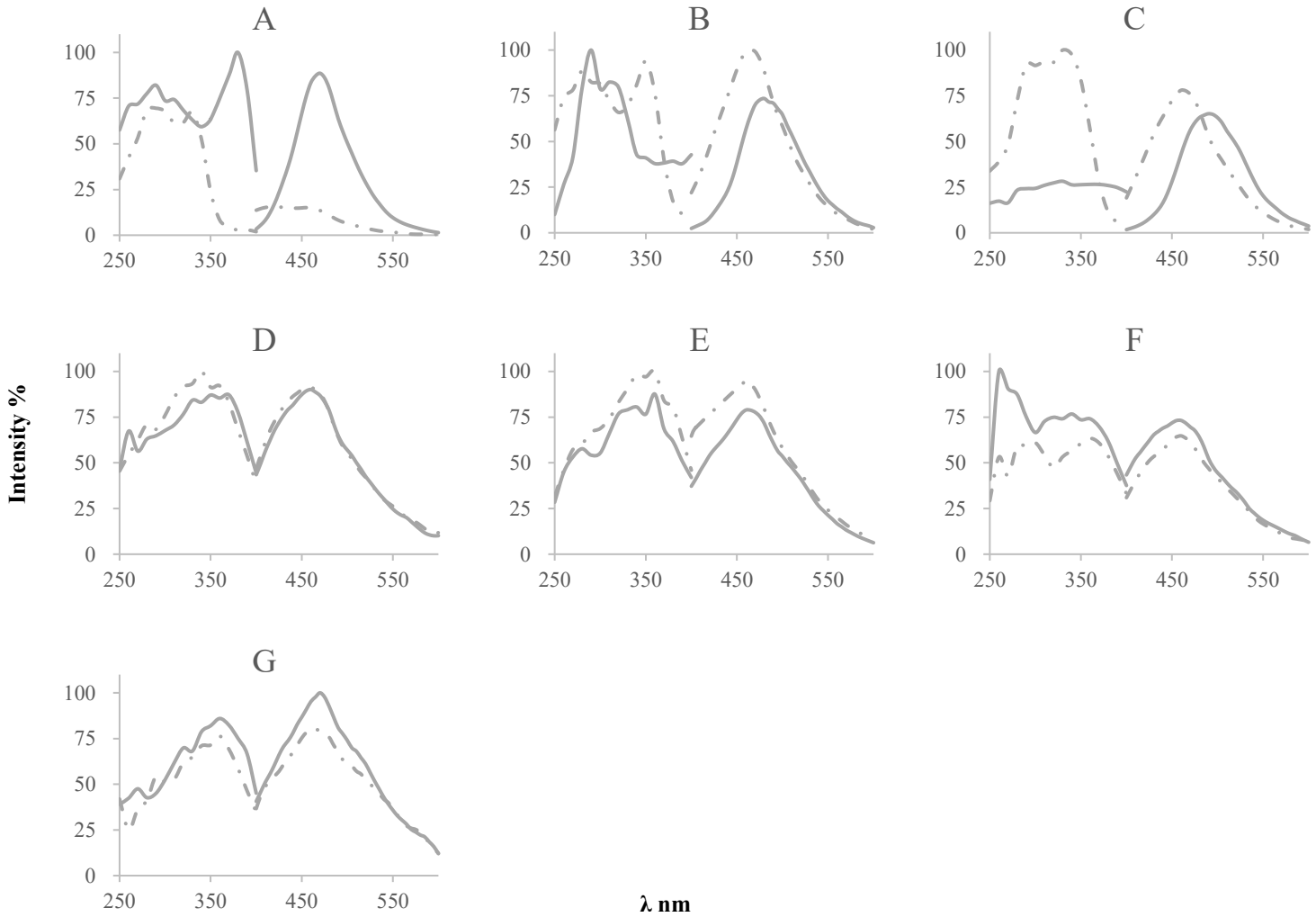

Figure 6.1. Fluorescence emission and excitation spectra of ferulic acid (A), methyl ferulate (B) and polysaccharides, including sugar beet pectin (C), citrus pectin (D), sugar beet arabinan (E), potato galactan (F) and apple pectin (G). pH 6: - - - -, pH 10: ——— . λ 450 and 335 nm was used to acquire excitation and emission spectra, respectively.

In addition to the structural properties of the PPS, the presence and the accessibility of their ferulic ester residues can determine the oxidoreductase's catalytic reactivity (Oosterveld et al., 2001; Patova et al., 2014). It can be hypothesized that the oxidative conjugation of PPT with PPS depends on the feruloylation extent of PPS and the availability of their ferulic ester residues, which can vary depending on the source, the extraction method and the structural composition.

To assess the presence and the accessibility of ferulic ester residues, the fluorescence spectral characterization of PPS was carried out. The spectra of PPS were compared to those of free ferulic acid (Fig. 6.1A) and methyl ferulate (Fig. 6.1B). Indeed, the main difference between free ferulic acid and ferulic ester is the number of ionization state. When shifting pH from 6 to 10, ferulic acid can change from single ionized state to double ionized; this change was accompanied with an obvious increase in the fluorescence intensity (Meyer et al., 2003). In contrast, the ester linked ferulic group does not show such increase at pH 10 as it can only be singly ionized. The results indicate that the spectra of sugar beet pectin and arabinan exhibited the characteristics of ester linked ferulic group as in methyl ferulate (Fig. 6.1C & E), whereas those of apple pectin and potato galactan are similar to free ferulic acid (Fig. 6.1F & G). In addition, ferulic ester present in polysaccharides from cell walls exhibits a unique right shift of the λ_{max} in the emission spectra from blue (455-492 nm) to green (492-577nm) region in alkaline condition (Fincher, 1976). This emission shift can be seen in methyl ferulate but not in free ferulic acid. Among the PPS, this shift was observed in the spectrum of sugar beet pectin. Other PPS did not show such spectral characteristic, which could be attributed to limited ferulic ester content and/or to the steric hindrance, affecting their accessibility.

Table 6.1 summarizes ferulic ester content of selected PPS. Sugar beet pectin contains the highest amount of ferulic ester residues (0.872%, w/w) as compared to the other PPS. This result is consistent with that of previous studies and was attributed to the relatively high proportion of RGI fraction (52%) and neutral sugar content (20-38%) in sugar beet pectin (Guo et al., 2018; Leroux et al., 2003; Oosterveld et al., 2001; Voragen et al., 2009). It has been also reported that the ferulic ester residues of sugar beet pectin are evenly distributed among the multiple RGI fractions of the polysaccharide chain (Oosterveld et al., 2001).

Table 6.1. Specific activity of laccases-catalyzed oxidation in pectic polysaccharides (PPS) and potato protein(PPT)/pectic polysaccharides (PPS) reaction systems

	Ferulic ester content (%, w/w)	Specific Activity [a] PPS- Reaction System		Specific Activity [a] PPT/PPS- Reaction System	
		LacTv	LacCh	LacTv	LacCh
Sugar beet pectin	0.872±0.038	19.5±1.8	107.3±9.9	14.4±0.5	197.2±0.3
Citrus pectin	0.275±0.007	1.6±0.3	18.1±0.0	2.8±0.3	28.7±1.1
potato pectic galactan	0.156±0.005	9.6±0.6	109.6±6.5	1.1±0.2	72.1±5.8
Apple pectin	0.068±0.003	10.7±0.2	17.9±0.4	N/A [b]	N/A [b]
Sugar beet arabinan	0.069±0.002	9.5±1.1	29.8±4.8	4.4±0.3	70.2±7.6

Abbreviations: PPS: pectic polysaccharide; PPT: potato protein, FE: ferulic ester content, LacTv: laccase from *Trametes versicolor*; LacCh: laccase from *Coriolus hirsutus*

a. The specific activity of laccase was defined as the nmol of oxidized ferulic ester on pectic polysaccharide per mg laccase and min of reaction. It was measured at pH 6.5.

b. Not applicable.

The results also show that 0.275 % w/w of ferulic ester residues are present in citrus pectin; this is within the 0.12-0.34% range as reported for citrus pectins by Maria et al. (2012). Low ferulic ester extent of citrus pectin is likely to be associated with its low proportion of RG I (~10%) (Yapo et al., 2007). Potato galactan was estimated with 0.156% w/w of ferulic ester residues, whereas apple pectin and sugar beet arabinan exhibited the least amount of ferulic ester residues (~0.070% w/w) compared to the other selected PPS. The feruloylation extent of apple pectin was reported to be relatively low, though it has comparable RGI region (48%) than sugar beet pectin (Voragen et al., 2009). Zaidel et al, (2011) reported higher ferulic ester content of sugar beet arabinan (0.48-0.94 % w/w) than our study (0.069% w/w); this discrepancy could be due to the use of different extraction process. Apart from the structural characteristics, the accessibility of the ferulic ester residues could also be affected by the flexibility of PPS, which is related to the stretchy region constructed by rhamnose, and the molecular size (Axelos & Thibault, 1991; Zaidel et al., 2011).

6.4.2. The catalytic efficiency of laccases

The catalytic efficiency of laccase-catalyzed the oxidative cross-linking of selected PPS polysaccharides was first investigated. Indeed, oxidation of the hydroxyl functional groups of ferulic ester residues present in PPS can result in reactive intermediates, which can couple with each other, or other reactive species in the reaction mixture via covalent cross-links (Selinheimo et al., 2008). Selected concentrations of PPS were used to achieve equal level of initial ferulic ester content in the reaction system. The catalytic activity of laccase in the oxidation of PPS was estimated from the decreased extent of their ferulic ester residues. Table 6.1 shows that LacCh exhibited higher specific activities towards the oxidation of PPS than LacTv. This can be attributed to the side debranching activity of LacCh, which may have improved the accessibility and hence the oxidation of ferulic residues (Rytioja et al., 2014). The highest specific activity of LacCh was observed towards sugar beet pectin and potato galactan (107.3 and 109.6 nmol/mg protein min, respectively), followed by that towards sugar beet arabinan (29.8 nmol/mg protein min); while the use of apple pectin and citrus pectin led to the lowest catalytic activity of LacCh (18.1 nmol/mg protein min). LacTv showed different substrate specificity than LacCh. The specific activity of LacTv towards sugar beet pectin (19.5 nmol/mg protein min) was the highest as compared to other PPS, followed by that towards apple pectin, potato galactan and sugar beet arabinan (9.5-10.7 nmol/mg protein min). The specific activity towards citrus pectin (1.6 nmol/mg protein min) was the lowest. Similarly, Littoz et al., (2012) have reported a lower laccase activity of LacTv towards citrus pectin as

compared to sugar beet pectin and attributed this result to the low feruloylation extent of citrus pectin. Additionally, Zaidel et al., (2011) have shown that at equal molar of ferulic ester content, the initial rate of horseradish peroxidase-catalyzed cross-linking of sugar beet arabinans was negatively affected by the length of arabinans.

To assess the contribution of the presence of PPT protein to the specific activity of laccases, the cross-linking reactions of PPS polysaccharides were carried out in the presence of this protein. Such addition of PPT protein in the PPS reaction systems can either enhance the PPS oxidation by promoting the coupling of substrate radicals or limit this oxidation as a result of substrate competitive inhibition of laccases. The results (Table 6.1) show that the specific activity of LacTv and LacCh in the oxidation of citrus pectin in the presence of PPT was 1.8 and 1.6-fold higher, respectively, as those without PPT. The specific activity of LacCh towards sugar beet pectin and arabinan also increased upon the addition of PPT by 1.8 and 2.4-fold, respectively, whereas that of LacTv was reduced by 26.1 and 53.7%. The oxidation of potato galactan by LacTv or LacCh significantly decreased upon the addition of PPT in the reaction mixture by 34.2 and 88.5%, respectively. It is worth to note that the specific activity of both laccases-catalyzed oxidation of apple pectin could not be determined accurately upon addition of PPT in this reaction system. Indeed, the catalytic activity of laccase may have been interfered and/or hindered by the high viscosity of reaction mixture of apple pectin/PPT. Contrary to our results, laccase from *Trametes hirsuta* was reported to exhibit similar activity towards the $\boldsymbol{\alpha}$-casein/oat spelt oligosaccharide mixture than each of the mono-component of this mixture (Selinheimo et al., 2008). For our subsequent study, sugar beet pectin, citrus pectin and sugar beet arabinan were selected as the best candidates for laccase-catalyzed conjugation reaction of PTT with PPS.

6.4.3. Conjugation efficiency of laccase-catalyzed oxidation reaction

Conjugation efficiency of laccase-catalyzed oxidation reaction was investigated in PPT/sugar beet pectin, PPT/citrus pectin and PPT/sugar beet arabinan reaction systems. As PPT/PPS conjugates exhibit different surface negative charge than their respective biopolymers, they were separated by anionic exchange chromatography, and the decrease in the relative proportion of PPT and PPS upon reaction was quantified (Fig. 6.2). Among the reaction systems, PPT/sugar beet pectin system was shown to be the most effective one for laccase-catalyzed reaction; indeed, relatively high bioconversion of PPT and sugar beet pectin (13.3~26.2%) by LacCh at 12 h was observed. In the PPT/sugar beet pectin reaction system,

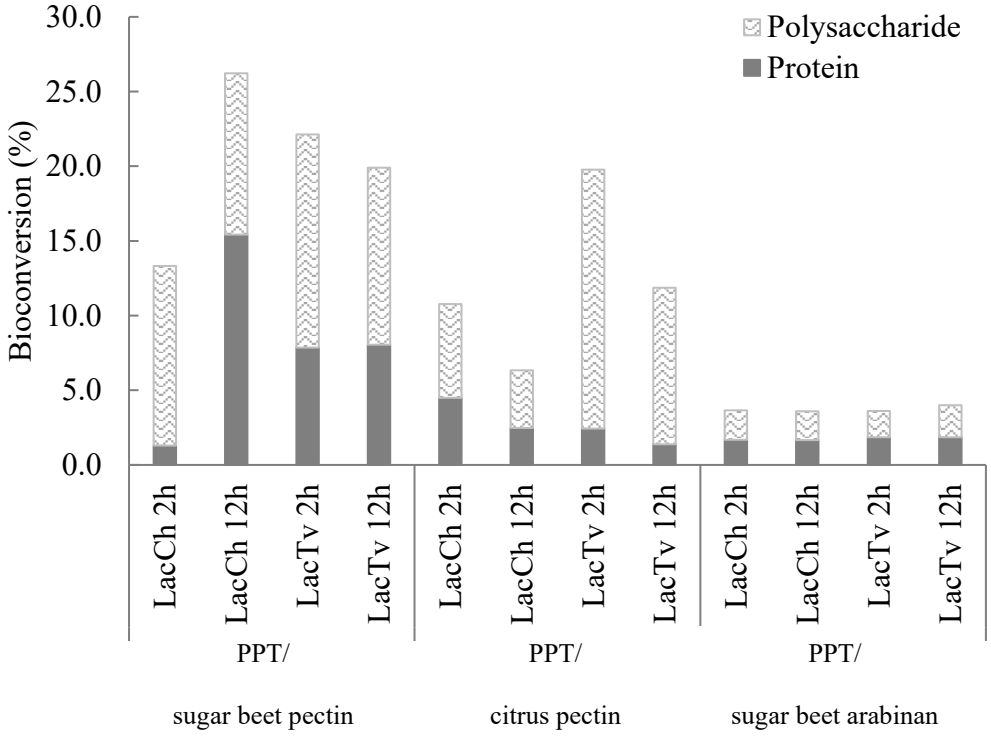

Figure. 6.2. The bioconversion of biopolymers (potato protein (PPT) and different pectic polysaccharides) in conjugation reactions for 2h and 12h catalyzed by laccase from *T. versicolor* (LacTv) or from *C. hirsutus* (LacCh).

both biopolymers were modified with a considerable extent, which may have promoted the formation of protein/polysaccharide hetero-conjugates. Although the PTT/sugar beet arabinan reaction system led to the lowest bioconversion, its biopolymers were converted by both laccases at the same extent, revealing the production of hetero-conjugates. In contrast, in the PPT/citrus pectin reaction system, there was more bioconversion of polysaccharide (up to 17.9%) than protein (up to 4.5%). The results also show that although LacCh has shown a higher specific activity towards PPT/citrus pectin compared to LacTv (Table 6.1), less conjugation extent was obtained with LacCh (Fig. 6.2). These results may be due to the substrate/product inhibition of LacCh and/or to the multi-site actions of LacCh on the same citrus pectin polymer, which may have limited the number of biopolymer substrates being oxidized and conjugated.

The oxidative conjugation of proteins with polysaccharides depends on the reactivity of each of these biopolymers as substrates for laccases. For instance, compact globular proteins, such as bovine serum albumin or $\boldsymbol{\beta}$-lactoglobulin, were reported to be less reactive substrates for laccase than sugar beet pectin; their hetero-conjugation with polysaccharides could be favored by partial denaturation or oxidation of these proteins prior to the addition of polysaccharide (Chen et al., 2018; Jung & Wicker, 2012b). On the other hand, $\boldsymbol{\alpha}$-casein, with flexible structure, exhibited comparable reactivity than oat spelt oligosaccharides in laccase-catalyzed reaction; as a result, the hetero-conjugation of $\boldsymbol{\alpha}$-casein with oat spelt oligosaccharides was achieved directly without pre-treatment and was favored at high polysaccharide to protein ratio, at which the protein homo-cross-linking was limited (Selinheimo et al., 2008). Specific activity of LacTv and LacCh towards PPT at substrate concentration 2.4 mg/ml were determined to be 11.1 and 93.9 nmol of equivalent tyrosine per mg protein per min, respectively (data not shown). These results reveal that the investigated laccases exhibited slightly lower reactivity towards PPT than sugar beet pectin, but higher than citrus pectin and sugar beet arabinan (Table 6.1). The relatively high hetero-conjugation efficiency of PPT/sugar beet pectin reaction system can be attributed to the comparable reactivity of its respective biopolymers. While the use of high polysaccharide proportion (~92% w/w) in the PPT/ sugar beet arabinan reaction system may have favored their hetero-conjugation.

Table 6.2. Design and experimental results of conjugation extent, solubility index and emulsification performance

Run No.	PPT ratio [a] %	Reaction time h	[E][b] U/ml	Conjugation extent [c] %	Solubility index [d]	EAI [e] m2/g	Particle size [f] nm	PDI [g]
11	20.0	7.0	0.0125	30.8±8.1	1.06±0.08	19.0±0.4	35236	0.59
1	32.2	4.0	0.0080	13.6±0.4	0.97±0.08	13.9±2.1	27529	0.56
2	32.2	10.0	0.0080	24.6±4.7	0.90±0.03	16.4±3.1	28039	0.51
12	32.2	4.0	0.0170	37.7±6.0	0.95±0.04	23.6±1.0	23726	0.50
5	32.2	10.0	0.0170	43.0±1.0	0.78±0.00	21.3±0.0	28058	0.42
4	50.0	7.0	0.0050	18.5±1.1	1.06±0.04	23.5±1.2	29909	0.53
9	50.0	2.0	0.0125	16.3±1.7	1.00±0.04	29.1±4.4	24390	0.52
16	50.0	7.0	0.0125	17.5±1.9	0.99±0.05	31.1±2.2	18856	0.48
13	50.0	7.0	0.0125	20.3±4.5	0.97±0.15	28.9±0.9	13035	0.46
6	50.0	12.0	0.0125	14.2±2.3	0.95±0.04	18.6±1.1	10477	2.11
15	50.0	7.0	0.0200	12.6±3.7	0.90±0.18	31.7±8.4	22100	0.43
3	67.8	4.0	0.0080	12.4±1.1	1.21±0.00	28.3±2.8	22146	0.50
14	67.8	10.0	0.0080	9.5±1.3	0.97±0.00	19.3±0.0	11057	2.34
8	67.8	4.0	0.0170	10.3±1.7	1.15±0.09	29.7±7.5	15253	0.42
7	67.8	10.0	0.0170	9.8±0.2	1.21±0.09	18.7±0.0	6950	0.84
10	80.0	7.0	0.0125	5.1±1.1	1.15±0.00	28.3±10.1	11818	0.42

The experimental results were obtained from averages of duplicate measurements; the enzymatic conjugation was performed at pH 6.5; emulsification performance of the conjugation product was evaluated at pH 7.

a. Potato protein ratio, which represented the percentage of protein over the sum of protein and polysaccharide (w/w);
b. Enzyme concentration;
c. The relative proportion of conjugation products which was calculated according to the size exclusion chromatograms of the reaction mixture;
d. The percentage (w/w) of soluble content in the protein/polysaccharide mixture upon enzymatic reaction over that of the corresponded control samples;
e. Emulsifying activity index
f. Average particle size of the emulsion droplets obtained from 6 measurements
g. Polydispersity index

The efficiency of laccase-catalyzed conjugation reaction system was evaluated in other reported studies by measuring related reactive groups in the biopolymer mixture (Jung & Wicker, 2012b; Wang, Lv, et al., 2019). Complete loss in the total phenolic content and 32% reduction in the amine content were reported for LacTv-catalyzed conjugation of ***β*** -lactoglobulin with feruloylated chitosan (Wang, Lv, et al., 2019); while 41 % reduction in the tyrosine residue content was obtained in the ***β***-lactoglobulin/sugar beet pectin mixture upon treatment with by laccase from Rhus vernificera (Jung & Wicker, 2012b).

6.4.4. Enzymatic conjugation of potato protein and sugar beet pectin

The PPT/sugar beet pectin reaction system was selected in order to investigate the effect of the enzymatic conjugation on the techno-functional properties. Using RSM, the reaction parameters (X_1 protein ratio % over total substrate; X_2 reaction time; X_3 enzyme concentration) were studied for their effects on the conjugation extent and the emulsification performance of the reaction mixture. The experimental design was performed based on the CCRD. The levels of the selected parameters were set based on preliminary trials (data not shown). The solubility index, conjugation yield and emulsification efficiency (EAI, particle size, PDI) were measured as responses (Table 6.2). The conjugation extent, estimated by SE-HPLC (UV & RI chromatograms), varied from 5.1 to 40.9% depending on the conditions. The highest conjugation extents were achieved at low protein ratio (20-32.2%). Increasing reaction time at low protein ratio enhanced the conjugation extent, as indicated in runs n° 2 vs 1 and 5 vs 12. The solubility of proteins was reported to be enhanced by conjugation with polysaccharides (Jung & Wicker, 2012b; Seo et al., 2014). However, extensive cross-linking by laccase can lead to the formation of insoluble high MW aggregates. The results show that the solubility index values at high protein ratios (68.8-80%) were mostly higher than 1, reflecting increased solubility. However, low solubility index values (< 1) were observed in the conditions (runs n° 5;6;15) with longer reaction time or high enzyme concentration; these results revealed the formation of high MW insoluble aggregates.

The changes in structural/physicochemical properties of biopolymers upon conjugation can affect their emulsification properties. To investigate the emulsification properties, EAI, particle size and PDI of PPT/sugar beet pectin conjugates were assessed. Contrary to the conjugation extent, high EAI values were observed at higher protein ratio than 50%. The combined effect of high protein ratio (≥50%) and shorter reaction time (≤ 7h) (runs n° 3;8;10;13;16) resulted in relatively high EAIs ranging from 28.3 to 31.7 m^2/g. The changes in the particle size were

consistent with those in EAI, where smaller average droplet size (11000~24000 nm) were observed at protein ratio ≥50% treated for ≤ 7h reaction time. The overall results may be attributed to the fact that the enzymatic conjugation of PPT/sugar beet pectin mixture affects the surface property of the biopolymers, hence their emulsifying behavior (Ma et al., 2020). Although some trials with l0 and 12h of reaction time (n° 6;7;14) are shown with relatively small average droplet size, their polydispersity indices are higher than 0.7, indicating that the droplet sizes of these emulsion systems are highly heterogeneous (Danaei et al., 2018).

6.4.4.1. Regression model analysis

Multiple regression analysis was performed in order to evaluate how the changes in conditions can affect conjugation extent, EAI and particle size. The best-fitted model was developed for each response; the significance of the models was determined by *F* value, *p*-value, lack of fit and R^2 (Table 6.3). A two-factor model was found to best represent the conjugation extent, with *F* value of 10.46 and *p*-value of 0.001, indicating the statistical significance as well as the non-significant lack of fit (*p*-value 0.3). The results also show that the conjugation extent is strongly affected by the linear term of protein ratio (X_1) (*F* value 49.15; *p*-value <0.0001), followed by the interactive term of protein ratio and enzyme concentration ($X_1 \times_3$) (*F* value 5.45; *p*-value 0.044). Quadratic models were determined to be the most appropriate for EAI (*F* value 7.4; *p*-value 0.012) and particle size (*F* value 12.07, *p*-value 0.003), and the lack of fit of these models were shown to be insignificant (*F* value/p-value 3.21/0.399, 0.413/0.808, respectively). All linear terms were shown to be significantly correlated with EAIs and particle size, with *F* value of 6.3-67.7, *p*-value of 0.000-0.046, among which the protein ratio (X_1) and reaction time (X_2) seem to be more relevant. Among the interactive effects, that between protein ratio and reaction time ($X_1 \times_2$) was significant to both EAI and particle size (*F* value/*p*-value 7.47/0.034 and 8.14/0.029, respectively). However, EAI was significantly affected by the quadratic terms of protein ratio and reaction time (X_1^2; X_2^2) (*F* value 12.3, 11.7; *p*-value 0.013, 0.014), whereas the particle size was by enzyme concentration (X_3^2) (*F* value 9.28; *p*-value 0.023).

The R^2 of the models for conjugation extent, EAI and particle size were 0.87, 0.91 and 0.95, respectively and their adjusted R^2 were 0.79, 0.79 and 0.87, which indicated that the models were satisfactory to be used for prediction. Equations (Eq. 6.5-6.7)of predictive models were generated by regression analysis in which the statistically non-significant terms were not considered.

$$\text{Conjugation extent (\%)} = 17.21 - 7.66X_1 - 3.33X_1X_3 \quad \text{(Eq. 6.5)}$$

$$\text{EAI } (m^2/g) = 30.32 + 2.66X_1 - 2.74X_2 + 2.12X_3 - 2.53X_1X_2 - 3.02X_1^2 - 2.94X_2^2 \quad \text{(Eq. 6.6)}$$

$$\text{Particle size (nm)} = 16173.58 - 6687.46X_1 - 2778.76X_2 - 2044.08X_3 - 3029.11X_1X_2 + 3005.85X_3^2 \quad \text{(Eq.6.7)}$$

6.4.4.2. Interactive effects of reaction parameters

The most significant interactive effects of reaction parameters are shown in contour plots (Fig. 6.3). Figure 6.3a-c illustrates the effects of protein ratio and enzyme concentration on the predicted conjugation extent at fixed reaction time (2, 7, 12h). These two independent variables display an adverse interactive effect on the conjugation extent, where the conjugation extent increased by a concomitant decrease of protein ratio and an increase of enzyme concentration. At high enzyme concentration (>0.013 U/ml), the increase in conjugation extent by lowering the protein ratio was more pronounced than at low enzyme concentration. High conjugation extent (>30%) can be achieved at protein ratio lower than 35%. The conjugation may have been favored when sugar beet pectin was dominating in the reaction mixture. Protein ratio of 5-50% was used in the previous studies to prepare protein/polysaccharide conjugates via oxidoreductase-catalyzed reaction (Chen et al., 2018; Liu, Qiu, et al., 2015; Selinheimo et al., 2008; Wang, Lv, et al., 2019). In addition, it has been shown that low protein ratio (< 10%) contributed to higher conjugation extent between protein/polysaccharide than high protein ratio (20-83%) (Liu, Qiu, et al., 2015; Selinheimo et al., 2008). In the predictive model of conjugation extent, the positive effect of reaction time can also be seen at lower enzyme concentration.

The interaction (X1×2) between protein ratio and reaction time was identified as the most important one in the predictive models of EAI (Fig. 6.3d-f) and particle size (Fig. 6.3g-i). This interaction is shown at enzyme concentration of 0.008 (Fig. 6.3d & g), 0.013 (Fig. 6.3e & h) and 0.017 (Fig. 6.3f & i) U/ml. EAI, reflecting the ability of the biopolymers adsorbing around the oil droplets, increased as the protein ratio was increased and the reaction time was decreased. In the lower range of reaction time (<7h), positive correlation between EAI and protein ratio up to 60% was observed (Fig 6.3d-f). When the reaction was run for longer time (> 7h), the reaction with increased protein ratio did not show tendency in increasing the EAI of the resulted emulsion. Although the reactions with low protein ratio were obtained with relatively low EAI, its EAI value could be improved by applying longer reaction time as well as higher enzyme concentration.

Table 6.3. Analysis of variances of fitted predictive models for conjugation extent, emulsifying activity index and particle size

	Conjugation extent [a] Two-factor		EAI [b] Quadratic		Particle size [c] Quadratic	
	F value	*p*-value	F value	*p*-value	*F* value	*p*-value
Model	10.460	0.001	7.400	0.012	12.070	0.003
X_1-(Protein ratio)	49.150	< 0.0001	14.070	0.010	67.710	0.000
X_2-(Reaction time)	1.210	0.299	14.950	0.008	11.690	0.014
X_3-(Enzyme concentration)	1.260	0.291	8.950	0.024	6.330	0.046
$X_1 \times_2$	4.320	0.067	7.470	0.034	8.140	0.029
$X_1 \times_3$	5.450	0.044	3.440	0.113	0.721	0.428
$X_2 \times_3$	1.340	0.277	0.842	0.394	0.605	0.466
X_1^2			12.260	0.013	4.660	0.074
X_2^2			11.650	0.014	0.001	0.981
X_3^2			3.570	0.108	9.280	0.023
Lack of fit	1.690	0.536	3.210	0.399	0.439	0.808

Terms with F-value >1 and p-value < 0.05 were considered as significant;

a. R^2=0.87
b. Emulsifying activity index, R^2=0.91
c. R^2=0.95

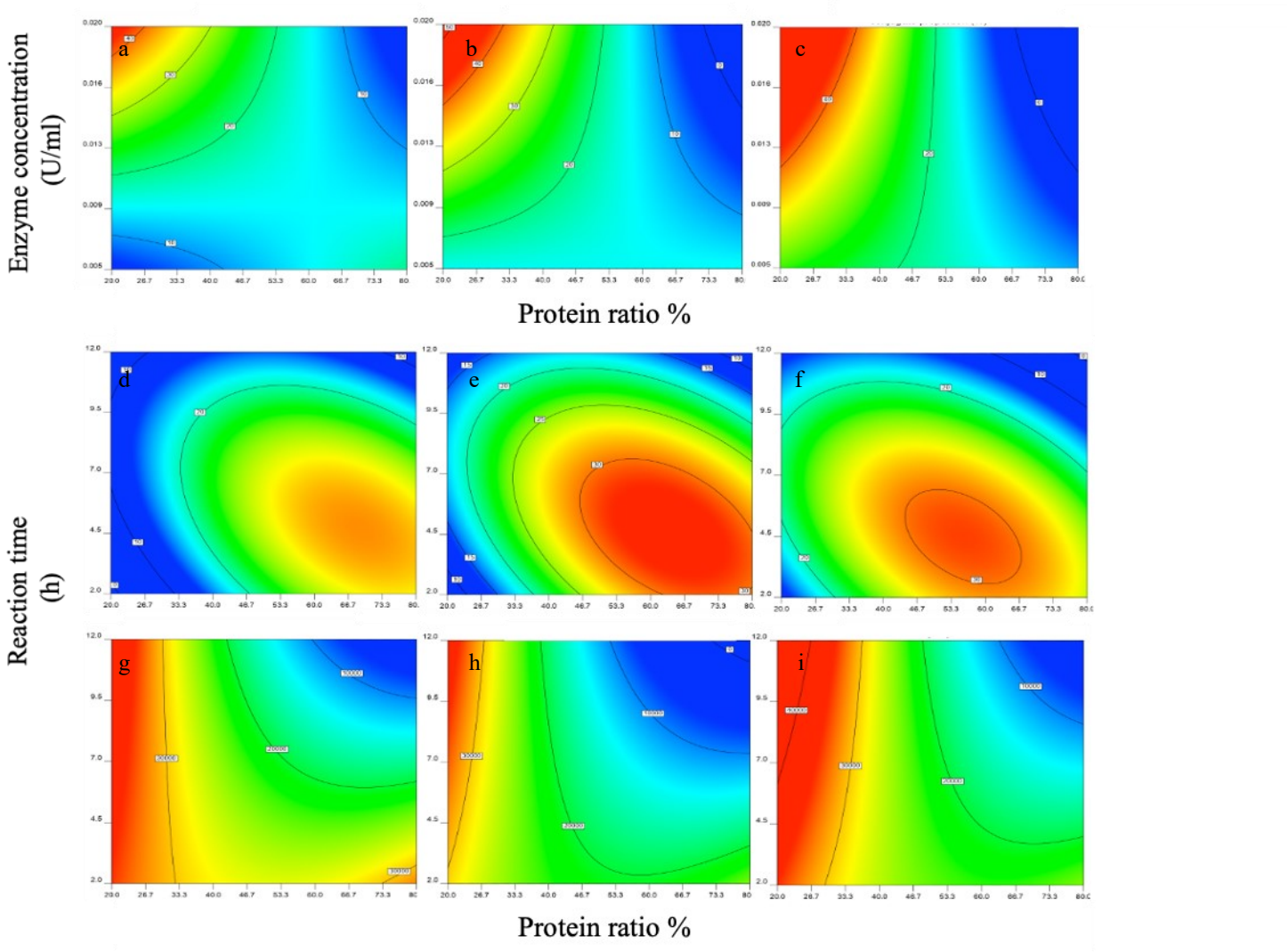

Figure 6.3. Contour plots. a-c are showing the response of conjugation extent, d-f are for those of emulsifying activity index (EAI) and g-I are for those of particle size.

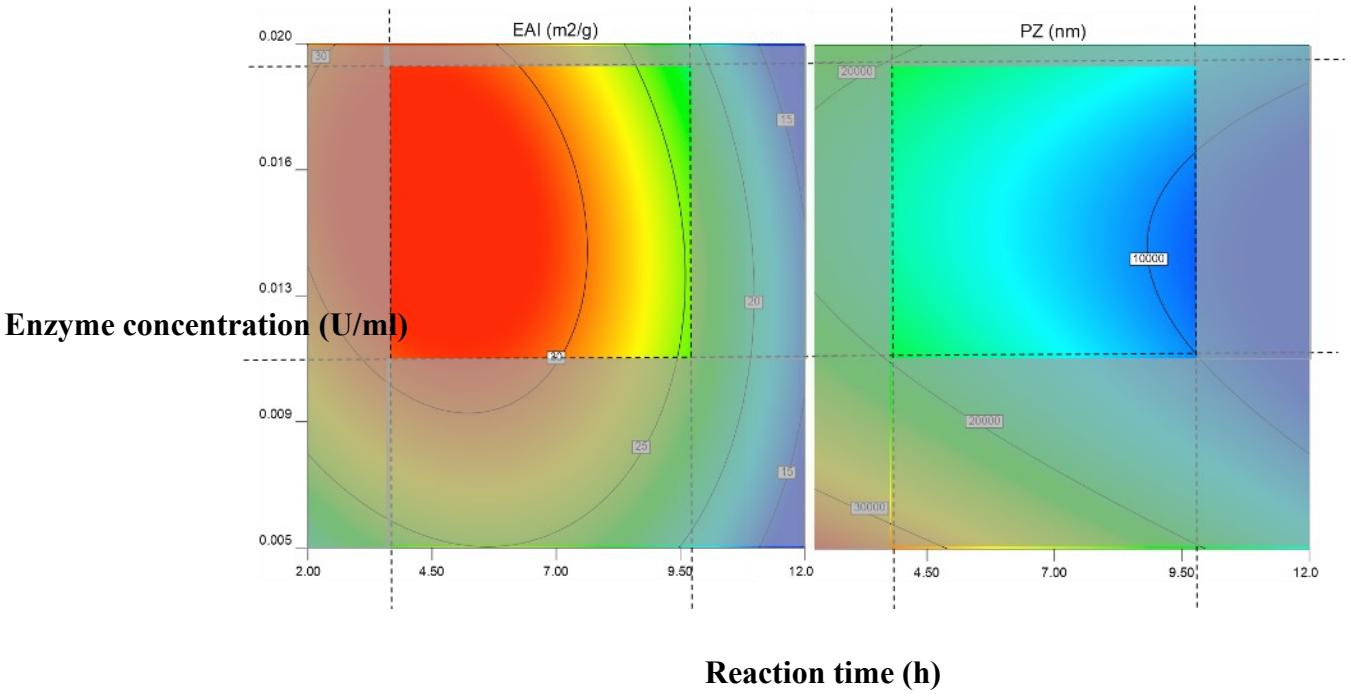

Figure. 6.4. Overlapped optimum conditions for high emulsifying activity index (EAI) and small particle size (PZ). Contour plots were generated at PTT protein ratio of 60%.

When looking at the contour plots of Figure 3d,3e and 3f together, there is an observable increase in EAI at low protein ratio as the enzyme concentration was increased from 0.008 to 0.013 U/ml; while further increase in the enzyme concentration to 0.017 U/ml shifts slightly the optimum region of EAI towards lower protein ratio. The region of protein ratio around 60% and 4.5 h of reaction time can achieve the most desirable results for EAI (around 30 m^2/g). Good emulsification performance was expected to be correlated with high EAI and small droplet size; the droplet size is reduced by the increase of protein ratio, which is consistent with the increase in EAI. Contrary to EAI model, the interactive effect of protein ratio and reaction time was synergistic in the particle size predictive model (Fig. 6.3g-i). In addition, the decrease in the particle size at high protein ratios was more apparent upon conjugation for longer reaction time (>7); while the positive effect on EAI at high protein ratios was more pronounced at shorter conjugation reaction time (<7). Relatively small droplet size (~10000 nm) is predicted to be obtained from treatments with protein ratio higher than 60% and reaction time longer than 7h. At moderate enzyme concentration (0.013 U/ml) (Fig. 6.3h), smaller droplet size was predicted as compared to low and high values (Fig. 6.3g & i). The overlapped area, representing a good emulsion system with high EAI and small particle size, is located at around protein ratio of ~ 60% reaction time of 3-9.5h and enzyme concentration of 0.011-0.019 U/ml (Fig. 6.4).

6.4.4.3. Optimization and validation of models

Using the predicted models, 3 optimum conditions for enzymatic conjugation, Opt A (maximizing the conjugation extent and EAIs), Opt B (maximizing the conjugation extent, EAI while minimizing the particle size) and Opt C (maximizing EAI while minimizing particle size) were selected (Table 6.4). The experimental results of the responses were compared to the predicted ones. The difference between them was determined to be not statistically significant (p-value <0.05) and all the experimental data were within the predicted intervals of 95% confidence. This confirms the validity of the established models for predicting conjugation extent and its effect on the emulsification performance in terms of EAI and particle size. Opt C conditions (protein ratio of 63.53%, reaction time of 3.7 h, enzyme concentration of 0.018U/ml), were designed for producing a good emulsion system with relatively high EAI of 30.0 m^2/g and small particle size of 16755 nm, with a mild conjugation extent 10.3%. When the conjugation extent is required to be optimized together with EAI and particle size (Opt B),

Table 6.4. Optimization of the conjugation and the emulsifying performance and model verification

	Opt A		Opt B		Opt C		Native PPT
Protein ratio %	27.04		44.19		63.53		-
Reaction time (h)	8.3		6.0		3.7		-
[E] [a] U/ml	0.020		0.019		0.018		-
	experimental	*predicted*	*experimental*	*predicted*	*experimental*	*predicted*	*experimental*
Conjugation extent [c] %	35.5±3.2	39.8	20.8±0.4	19.0	10.3±0.2	8.7	-
EAI [b] m^2/g	22.9±0.3	23.6	27.4±1.3	29.4	30.0±2.5	31.9	14.8±1.3
Particle size (nm)	35181 (0.573)[d]	36419	22194 (0.511)[d]	19178	16755 (0.469)[d]	18008	32413 (0.576) [d]
Emulsion stability (min)	25.1±0.8		27.5±1.8		31.0±1.4		23.6±3.1

The experimental values were from averages of triplicate measurements, emulsifying property was evaluated at pH 7.

a. Enzyme concentration

b. Emulsifying activity index

c. The relative proportion of conjugation products which was calculated according to the size exclusion chromatograms of the reaction mixture, indicating the conjugation extent;

d. Polydispersity index of the particle size measurement

lower protein ratio of 44.19% combined with relatively high enzyme concentration (0.019 U/ml) and increased reaction time (6h) were identified by the predicted models. This confirms that relatively low protein ratio was required to promote conjugation, while an increase in reaction time or enzyme concentration could favor the emulsification performance at low protein ratio. The Opt B treatment can double the conjugation extent (20.8%) with slight compromise in the emulsifying performance (EAI of 27.4 m^2/g; particle size of 22194 nm) as compared to Opt C. When only conjugation extent and EAI were taken into consideration for optimization, lower protein ratio (27.04%), higher enzyme concentration (0.02 U/ml) and increased time (8.7 h) were suggested (Opt A). The reaction conditions of Opt A resulted in the highest conjugation extent (35%), with EAI of 22.9 m^2/g and particle size of 35181 nm. Similarly, Seo et al., (2014) reported that the conjugation extent of potato proteins with different galactose-based carbohydrates via Maillard reaction was ranged from 19 to 48%.

The results (Table 6.4) also show that the conjugation of PPT with sugar beet pectin via treatment Opt B and Opt C resulted in higher emulsifying capacity and smaller particle size than the native PPT (EAI of 14.8 m^2/g, particle size of 32413 nm). In addition, an improvement in the emulsion stability was observed upon the conjugation of PPT with sugar beet pectin as indicated by the ESI value (Table 6.4). The EAI values of native PPT were reported to be in the range of 4.5-32.3 m^2/g with a particle size varying from 10 to 50 μm (Glusac et al., 2017; Schmidt et al., 2018; Waglay et al., 2019), whereas sugar beet pectin led to emulsions with particle size of 0.74-6.6 μm (Chen et al., 2018; Maravić et al., 2019). These large variations may be attributed to the differences in the emulsion preparation and in the concentration of biopolymer. The PPT conjugated with galactose was reported to show enhanced emulsifying capacity, which was attributed to the improvement of the hydrophobic-hydrophilic balance of PTT adsorbed at the water-oil interface (Seo et al., 2014). Furthermore, it has been reported high MW conjugates can lead to larger emulsion particle size reflecting lower emulsifying capacity as compared to the parent biopolymers (Maravić et al., 2019). However, the emulsion-stabilizing effect of the protein/polysaccharides conjugates was attributed to the enhanced thickness of bioconjugate films formed at the water-oil interface (Chen et al., 2018; Gazme & Madadlou, 2014; Leroux et al., 2003; Ma, Chen, et al., 2020). As shown in our study, a compromise between emulsion capacity and emulsion stabilization can be achieved through the modulation of the conjugation by controlling the reaction parameters.

6.5. Conclusion

The conjugation of PPT with selected PPS was carried out through laccase-catalyzed oxidative reaction. LacCh exhibited a higher catalytic efficiency in the protein/polysaccharide reaction systems than LacTv. Among the investigated PPS, sugar beet pectin was the most efficient in conjugating with PPT as indicated by the reactivity and the bioconversion of both biopolymers as well as the conjugation extent. The conjugation extent was negatively correlated with the protein ratio. While emulsification performance was favored by the increase in the protein ratio, where improved solubility of the biopolymer mixture was seen. The most important interactive effect on the conjugation extent was that between protein ratio and enzyme concentration, whereas protein ratio and reaction time exhibited the significant interactive effect on emulsification performance. The importance of controlling the enzymatic conjugation extent in achieving desirable emulsification performance was demonstrated. Overall, the study can serve as a stepstone to develop new biopolymer-based emulsion system using laccase-catalyzed reaction.

CONNECTING STATEMENT 5

Chapter V and VI studied the modification of potato proteins using different laccase-catalyzed reactions. Modified proteins, including cross-linked potato proteins, cross-linked potato proteins with the incorporation of ferulic and potato proteins conjugated with sugar beet pectin, were varied from the native potato proteins in molecular, structural and techno-functional properties. Chapter VII continues to understand the protein structure in the correlation with the interfacial properties of these modified potato proteins. The effects of laccase-catalyzed modification on the tertiary structure stability, air-water interfacial adsorption kinetics and film rheological property of the potato proteins were discussed in this chapter.

Li, M., Blecker, C., & Karboune, S. (2020). Molecular and air-water interfacial properties of potato protein upon modification via laccase-catalyzed cross-linking and conjugation with sugar beet pectin. *Food Hydrocolloids*. (Under review).

.

CHAPTER VII. MOLECULAR AND AIR-WATER INTERFACIAL PROPERTIES OF POTATO PROTEIN UPON MODIFICATION VIA LACCASE-CATALYZED CROSS-LINKING AND CONJUGATION WITH SUGAR BEET PECTIN

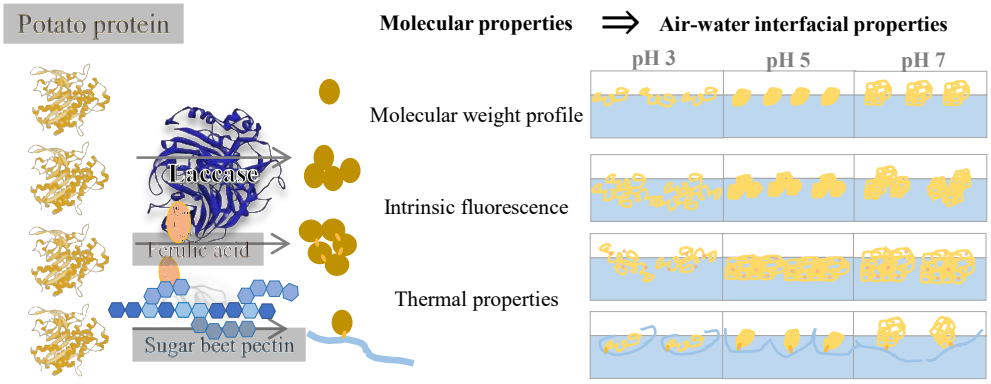

7.1. Abstract

Foaming-related functionalities of potato proteins are important for the development of innovative food products. The main purpose of current study was to investigate the effects of laccase-catalyzed modifications on the molecular properties, the air-water interfacial adsorption kinetics and the interfacial rheological characteristics of potato protein at selected pH values. The cross-linking of potato protein (PPT) with or without the presence of ferulic acid (FA) as mediator and its conjugation with sugar beet pectin were biocatalyzed by fungal laccases (*Trametes versicolor* or *Coriolus hirsutus*). As compared to the native potato protein, all modified cross-linked proteins showed a decrease in intrinsic fluorescence intensity and total enthalpy changes during thermal denaturation, indicating tertiary unfolding due to modification. The conjugation of potato protein with sugar beet pectin (PPT-SBP-H/-L) resulted in lower equilibrium surface tension at pH 7 than the native potato protein by facilitating the protein late-stage adsorption. Cross-linked potato proteins (MPPT24h, MPPT24hFA, MPPT48h and MPPT48hFA) were associated with enhanced surface dilatational elasticity of the interfaces. In addition, the susceptibility of potato protein to acid pH in thermal denaturation or interfacial adsorption was shown to be reduced upon laccase-cross-linking treatments. This study provided insights into the impact of laccase-catalyzed modifications on the functionalities of potato protein from molecular and mesoscopic aspects.

7.2. Introduction

Surface and interfacial properties govern foaming and emulsifying properties of proteins and hence determine the quality of protein-stabilized food systems, which are keys to a wide range of food products, such as ice-creams, cakes, breads, meringues, beers, cheese and spreads. Because of their surface activity, selected proteins lower the surface tension at the air-water interface. To carry this function, proteins rely on amphiphilic feature, which is associated with their molecular properties, including molecular weight, flexibility, exposed hydrophobicity and net charge (De Jongh et al., 2004; Dickinson, 1999). As compared to low molecular weight surfactant foaming agents, proteins tend to self-assemble into a viscoelastic film at the interface in addition to their higher nutritional value and consumer acceptance (Felix et al., 2019; Van Koningsveld et al., 2001). Protein's interfacial association is governed by a balance of molecular interactions rather than one dominant force; such balance can be affected by extrinsic parameters such as pH, temperature, ionic strength and processing history (Ercili-Cura et al., 2015). Protein modification can help to modulate the balance of molecular

interactions, hence altering the interfacial properties of protein to achieve the desired functionality (Hiller & Lorenzen, 2009; Murray, 2002). However, the relationship between protein modification and the interfacial properties still needs to be better elucidated. Indeed, this relationship was found to be greatly dependent on the nature of the native protein, the modification extent and approach as well as the protein microenvironment (Gharbi & Labbafi, 2019; Mirmoghtadaie et al., 2016).

Enzymatic modifications are of a high interest given their mild reaction conditions, specificity, and high consumer acceptance. For instance, protein cross-linking catalyzed by laccase (E.C. 1.10.3.2), an oxidoreductase, can modify interfacial properties. Previous studies have reported protein cross-linking by laccase led to increased surface hydrophobicity and foam formation of whey protein isolate (α-lactalbumin) and total milk protein (Hiller & Lorenzen, 2008; Hiller & Lorenzen, 2009; Jiang et al., 2017). The stability and rheological properties of polymer networks in different food/non-food complexes using laccase-catalyzed cross-linking/conjugation of biopolymers were also studied (Azarikia et al., 2015; Chen et al., 2018; Gazme & Madadlou, 2014; Loi et al., 2020; Struch et al., 2015). However, information is still lacking regarding the effects of laccase-catalyzed cross-linking/conjugation of proteins on their interfacial behavior, which can provide insight into how to modulate the techno-functional properties of proteins such as foaming properties.

There are three mechanisms by which protein modification can be achieved by laccase. First, proteins are directly oxidized by laccase acting on exposed tyrosine residues where cross-links are formed (Mattinen et al., 2006). Second, phenolic compounds are added as mediators to indirectly cross-link protein biomolecules through hetero-conjugation (Steffensen et al., 2008). The third pathway consisted of covalently linking protein with feruloylated polysaccharides to form protein-polysaccharide conjugates (Selinheimo et al., 2008). The latter two pathways were used more often than direct oxidative cross-linking because of the steric hindrance from the protein at laccase's active site.

Potato proteins are distinguished from other plant-based proteins by their amino acid profile, that is equivalent to a whole egg and superior to many vegetable/cereal proteins, and by a wide range of techno-functional properties (Miedzianka et al., 2012). However, the techno-functional properties of potato proteins can be affected by processing and extrinsic conditions of food systems. To improve and expand the application of potato proteins, direct cross-linking, indirect cross-linking with FA as mediator and the conjugation with sugar beet pectin (SBP)

catalyzed by fungal laccases were explored. The present study is part of our effort to understand the impacts of laccase-catalyzed modifications on the structure and composition of proteins as they are related to techno-functionalities. In particular, this study aimed at investigating the interfacial and structural properties of the modified proteins. The interfacial properties of native and modified proteins were evaluated at three different pH conditions: pH 3 (below the isoelectric points (pI) of potato protein), 5 (close to the pI) and 7 (above the pI). Our study is expected to contribute to the understanding of the ability of laccase in modifying the techno-functional properties of potato protein ingredient as a foaming agent.

7.3. Materials and methods

7.3.1. Materials

Potato protein solanic 206P, containing ~40% patatin and ~50% of protease inhibitors, was obtained from Avebe (Veedam, The Netherlands). Two types of fungal laccases from *Trametes versicolor* (LacTv) and *Coriolus hirsutus* (LacCh), were used as biocatalysts. LacCh was produced as described by Gill et al., 2018, with an additional ammonium sulfate precipitation (80% saturation) step for partial purification. LacTv was purchased from Sigma-Aldrich. The activity of laccase was determined by 2,2'-azino-bis (3-ethylbenzothiazoline-6-sulphonic acid) diammonium salt (ABTS) assay; one unit (U) of enzyme activity was defined as the mg of enzyme that oxidizes one μmol of ABTS in one minute. The protein content of the enzyme suspension was determined using Hartree-Lowry assay. Sugar beet pectin (GENU® BETA pectin) was obtained from CPKelco (Groβenbrode, Germany).

7.3.2. Laccase-catalyzed protein modifications

All reaction mixtures were prepared in sodium phosphate buffer (pH 6.5, 50 mM), and the enzymatic reactions were carried out at 28℃ with an orbital agitation of 150 rpm. Direct oxidative cross-linking of potato protein was carried out by mixing 2 mg/ml of potato protein and 0.096 U/ml (~0.08 mg protein/ml) of LacTv. The reaction mixture was incubated for 24h or 48h to obtain modified potato proteins MPPT24h and MPPT48h, respectively. The oxidative cross-linking was carried out with the presence of ferulic acid as a mediator at 1 mM for 24h or 48h to yield modified potato proteins, named MPPT24hFA and MPPT48hFA. In addition, two conjugates of potato protein/sugar beet pectin (PPT-SBP) with high and low conjugation extent, PPT-SBP-H and PPT-SBP-L were prepared using LacCh. PPT-SBP-H was obtained upon the conjugation reaction in which 2.2 mg/ml of potato protein, 2.8 mg/ml of

polysaccharide, 0.019 U/ml (~0.013 mg protein/ml) of LacCh were mixed and incubated for 6 h. To obtain PPT-SBP-L, 3.2 mg/ml of protein, 1.8 mg/ml of polysaccharides and 0.019 U/ml (~0.013 mg protein/ml) of LacCh were mixed and incubated for 3.7 h. After inactivating the enzymes, the reaction mixtures were stored at -20°C, and the modified proteins were recovered by dialysis (cut-off 10 kDa) and lyophilised.

7.3.3. Characterization of molecular weight profile

The molecular weight profile of MPPT samples (MPPT24h, MPPT24hFA, MPPT48h and MPPT48hFA) was determined using size exclusion (SE)- fast protein liquid chromatography (FPLC), whereas the PPT-SBP conjugates were analyzed by SE-high performance liquid chromatography (HPLC). SE-FPLC was carried out using an ÄKTA FPLC system (GE Healthcare) equipped with a Superdex 200 column (10/300 GL, GE-Healthcare, Piscataway, NJ), eluted with sodium phosphate buffer (50 mM, pH 7) containing 0.15 M NaCl and 0.1% w/v SDS, at flow rate of 0.5 ml/min. The elution was monitored at 280 nm by a UV detector. The SE-HPLC was carried out using a Waters HPLC system (Model 1525) equipped with three TSK gel PWXL columns in series (TSK gel G5000, G4000 and G3000, 0.78 × 30 cm) following a TSK gel PWXL guard column (0.6 × 4 cm), coupled with both UV diode-array detector (Model 2998) and refractive index (RI) detector (Model 2489). Conjugate samples were eluted with sodium phosphate buffer (10 mM, pH 7) containing 0.15 M NaCl at flow rate of 0.5 mL/min. The elution was monitored by UV (280 nm) and RI detectors. Thyroglobulin (669 kDa), ovalbumin (44 kDa), ribonuclease A (13 kDa), vitamin B12 (1.35 kDa) and dextran standards (50, 150, 410 and 670 kDa) were used for molecular weight calibration. The relative proportion of the molecular weight fractions were estimated from the peak areas detected at 280 nm. The cross-linking extent was defined as the increase in the proportion of high molecular weight fractions, corresponding to cross-linked products

7.3.4. Fluorescence spectroscopy

The microenvironment of the aromatic amino acid residues was analyzed using fluorescence spectroscopy. Protein suspensions 0.1 to 1 mg/ml were prepared at selected pH values: trisodium citrate buffer (30 mM, pH 3), sodium acetate buffer (22 mM, pH 5) or sodium phosphate buffer (25 mM, pH 7). The suspensions were shaken gently for 30 min. Emission spectra from 305 to 500 nm (slit of 5 nm) were recorded by a SpectraMax® i3x plate reader (San Jose, CA) with an excitation wavelength set at 280 nm. The protein content of the potato protein samples was measured by Bradford assay, and the fluorescence spectra were

normalized according to the protein content. All the measurements were carried out in duplicates.

7.3.5. Differential scanning calorimetry

Thermograms of the samples at different pH conditions (pH 3, 5 and 7) were obtained using differential scanning calorimeter (DSC) Q1000 TA Instruments (New Castle, Delaware, USA). Sample solution was prepared on aluminum hermetic pans, by adding 9 mg of buffer to 1 mg of samples, then covered, sealed and left at 4°C overnight before analysis. During measurement, samples were heated from 0 to 150 °C at a rate of 5 °C/min. The denaturation temperature (T_d) and denature enthalpy (ΔH) were calculated using Universal analysis software (version 4.3).

7.3.6. Dynamic adsorption kinetics

The adsorption kinetics of the native and modified potato proteins were evaluated by maximum bubble pressure and drop volume method. The analysis of the protein samples was conducted at pH 7, 5 and/or 3. Prior to each measurement, the tensiometers were cleaned with MilliQ water. A value of 72 mN/m ± 0.5 mN/m for the blank (MilliQ water) was maintained throughout the measurements.

7.3.6.1. Maximum bubble pressure method

Maximum bubble pressure method was used to analyze the initial adsorption kinetics of the native PPT, MPPTs and PPT-SBP conjugates at air-water interface at 25 °C. The protein contents in native and MPPT samples were estimated at ~0.9-1 mg protein/mg, whereas the conjugates contains protein/polysaccharide at ratios of 0.78:1 and 1.78:1. Sample solutions at 1 mg/mL were prepared using Milli-Q water, and adjusted to pH 3, 5 or 7, using 0.1 M NaOH and HCl solutions. Air bubble were generated in a Bubble Pressure Tensiometer BP100 (Krüss GmbH - Hamburg, Germany) at constant speed through the protein solution (1 mg/ml) using S180 capillary (diameter 0.2 mm). When the bubble radius reached that of the capillary, the pressure was at the maximal level. The surface tension was monitored overtime from the bubble formation to when bubble pressure reached the maximum. The adsorption kinetic curves were constructed by plotting the surface tension versus surface age (from 5 ms to 200 s), from which the lag time was estimated as the time at which the surface tension decreased to 95% of the initial value; the slope of the decrease in surface tension after lag phase was calculated as the adsorption rate. The measurements were done in triplicates.

7.3.6.2. Drop volume method

Automatic drop volume tensiometer TVT1 (Lauda, Königshofen, Germany) was used to perform dynamic measurement for surface tension. The samples were prepared as described in the maximum bubble pressure method. Drops were formed in an empty optical glass cuvette, at the tip of a 1.055 mm-radius capillary which was connected to a 2.5 ml syringe. Continuous formation of drops at creation rate from 0.07 to 0.8 s/µL was analyzed to determine the surface tension as function of formation time. A total of 8 drops was recorded and analyzed. From the kinetic curves, equilibrium surface tension was estimated by the intercept of the plot of surface tension versus $1/\sqrt{t}$ (t=time). The experiments were carried out at 25°C. The measurements were done in triplicates.

7.3.7. Protein film mechanical and rheological properties

7.3.7.1. Oscillating pendant drop method

Surface tension of the protein samples was measured in an oscillating mode in order to study surface dilatational elasticity of the protein samples. The experiment was performed at 25 °C in triplicates. Prior to each measurement, the instrument was cleaned and verified as discussed in section 2.6. The surface tension of 1 mg/ml of sample solution was measured by Tracker™ tensiometer (IT Concept, Longessaigne, France) via a formation of a pendant drop of 5 µL at the tip of a capillary. After an equilibrium time of 2400 s, the surface tension ($\boldsymbol{\gamma}$) was recorded against surface area (A) under sinusoidal oscillating mode operated at an amplitude of 0.5 µl and a period of 10 s. Images of the drops were recorded during oscillation. From the drop shape analysis, the surface dilatational elastic modulus (E') was determined, as shown by equation 7.1:

$$\boldsymbol{E' = \frac{d\gamma}{dInA}} \qquad \text{(Eq. 7.1)}$$

7.3.7.2. Film compression isotherms

The compression isotherms were measured using a Langmuir film balance (KSV NIMA Instruments Ltd., Espoo, Finland). Protein solutions were prepared at 2 mg/ml in MilliQ water (~ pH 7) and stored overnight at 4 °C. To favor spreading, a 0.05 % (v/v) solution of amyl alcohol was added as recommended by Sanchez-Gonzalez et al. (2003) then 80 $\boldsymbol{\mu}$L of solution was spread evenly on the surface in the trough, and the system allowed to equilibrate for 30 min. Compression was carried out at rate of 10 mm/min for 5 min, during which the surface

area and surface pressure ($\boldsymbol{\pi}$) were recorded. All measurements were carried out at 25 °C in triplicates. The balance was cleaned based on the standard protocol and the cleanness was verified by less than ± 0.5 mN/m change in surface pressure during compression/expansion cycle of MilliQ water. The elasticity ($\boldsymbol{\varepsilon}$) of the monolayer film during compression was calculated as per equation 7.2:

$$\boldsymbol{\varepsilon} = -\boldsymbol{A}\frac{\boldsymbol{d\pi}}{\boldsymbol{dA}} \quad \text{(Eq. 2.2)}$$

7.3.8. Statistical analysis

Statistical analyses were performed using XLSTAT software (Addinsoft, New York, NY, USA) and Microsoft Excel (Microsoft, Redmond, WA, USA). One-way analysis of variance (ANOVA) and the Tukey's honest significant difference (HSD) test were performed to detect significant differences ($P < 0.05$).

7.4. Results and discussion

7.4.1. Assessment of protein modification by crosslinking and conjugation

The potato protein was modified through laccase-catalyzed oxidative cross-liking and conjugation reactions. These enzymatic reactions can lead to homo-cross-linking, hetero-conjugation of biopolymers, or fragmentation when extensive radical-based enzymatic modification occurs (Ercili Cura et al., 2009; Mokoonlall, Sykora, et al., 2016; Steffensen et al., 2008). Upon our preliminary trials, the appropriate conditions for production of well-defined modified proteins were determined and applied. Table 7.1 summarizes the modification extent (conjugation/cross-linking and fragmentation extents). The molecular weight (MW) distribution profiles of native potato protein and MPPTs are shown in figure 7.1. Native potato protein contains a mixture of large potato protein (60-80 kDa) /patatin (40-60 kDa)/protease inhibitors (1-30 kDa) fractions at a ratio of 10/40/50 (w/w, %) (Fig. 7.1). The highest cross-linking extent (43.1%) was achieved at 24 h in the laccase-ferulic acid mediator reaction system (MPPT24hFA). Increasing the reaction time of this reaction system to 48 h (MPPT48hFA) resulted in a decrease in the cross-linking extent to 4.2% and an increase in the fragmentation one (43.5%). In contrast, no significant change in the cross-linking extent was observed in the laccase reaction system (MPPT24h; MPPT48h) upon increasing the reaction time from 24 h to 48 h (~13.5%), with an estimated fragmentation extent at 29.6 % for MPPT48h.

Table 7.1. Modification extent of potato proteins upon treatment thought different laccase-catalyzed reactions.

	Cross-linking or conjugation extent (%)	Fragmentation extent (%)	Modification extent* (%)
MPPT24h	13.5±5.6	N/A	13.5±5.6
MPPT48h	13.5±1.5	29.6±11.1	43.0±9.6
MPPT24hFA	43.1±4.1	N/A	43.1±4.1
MPPT48hFA	4.2±0.0	43.5±0.1	47.6±0.0
PPT-SBP-H	25.1±3.6	N/A	25.1±3.6
PPT-SBP-L	17.9±2.3	N/A	17.9±2.3

*The sum of cross-linking/conjugation and fragmentation extent;
N/A non-applicable
Abbreviations: PPT, potato protein; MPPT24h, MPPT48h are modified protein obtained from laccase-catalyzed reaction for 24h and 48h respectively; MPPT24hFA, MPPT48FA are modified protein obtained from laccase-ferulic acid mediator reaction for 24h and 48h, respectively; PPT-SBP-H and PPT-SBP-L are PPT/sugar beet pectin conjugates with high and low conjugation extent; respectively.

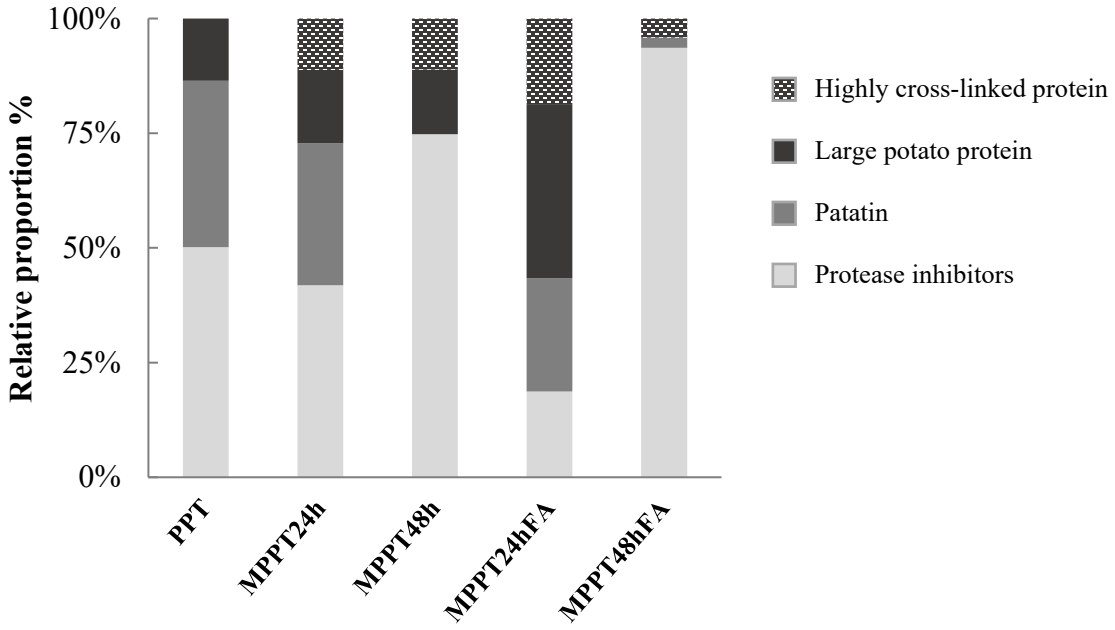

Figure 7.1. Molecular weight distribution of native and modified potato protein treated with laccase: PTT, native potato protein; MPPT24hPPT, treated by laccase-catalyzed direct cross-linking for 24h; MPPT48h, PPT treated by laccase-catalyzed direct cross-linking for 48h; MPPT24hFA, PPT treated by laccase-ferulic acid mediated reaction for 24h; MPPT48hhFA, PPT treated by laccase-ferulic acid mediated reaction for 48h.

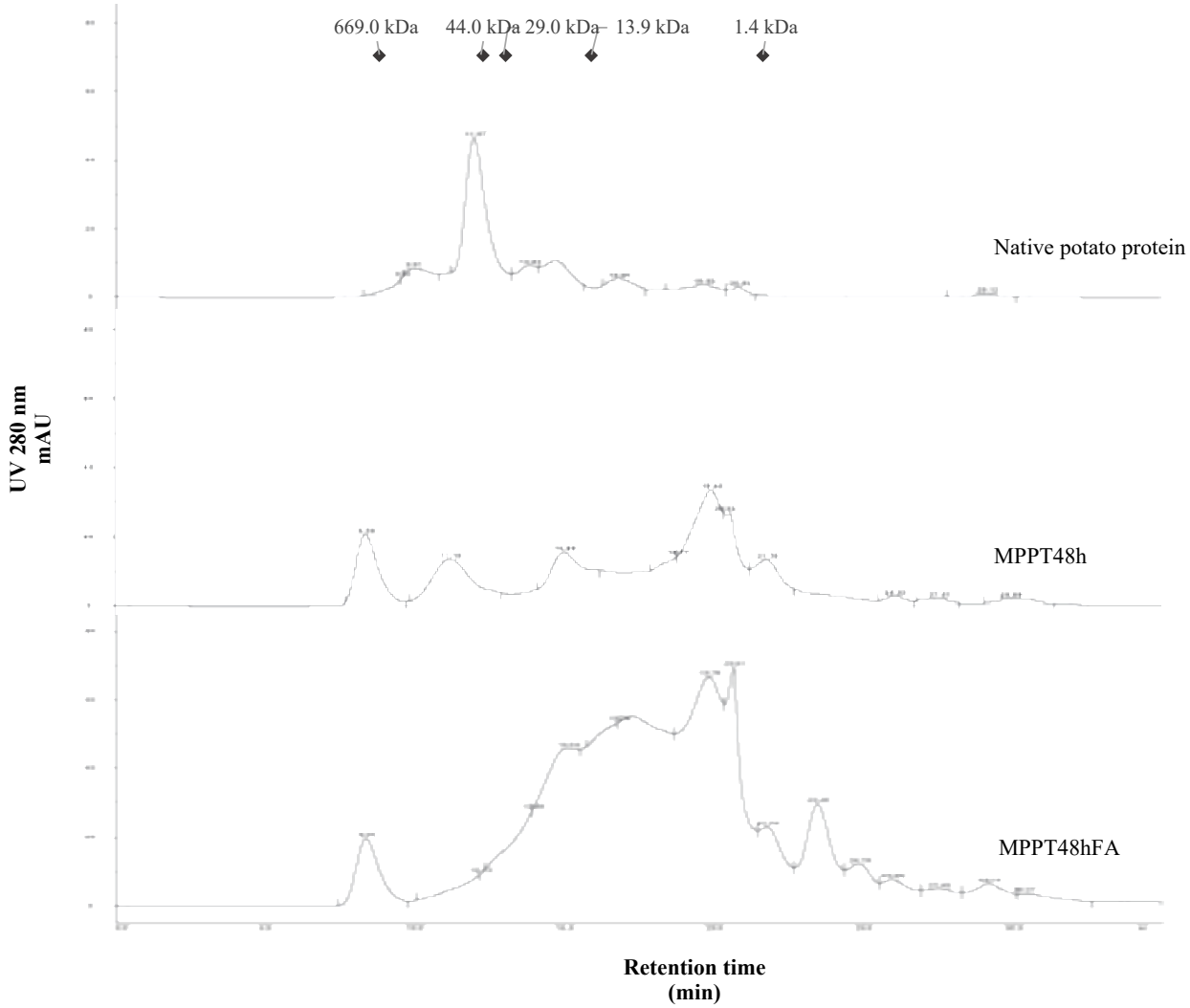

Figure 7.2. Size exclusion chromatograms on Superdex 200 10/300 GL colum at UV 280 nm.

As expected, ferulic acid mediator enhanced the crosslinking of potato protein by overcoming the limited accessibility of selected amino-acid side chains (e.g. tryptophan, cysteine, and tyrosine) to laccase and the substrate steric hindrance due to the protein's inflexibility (Jung & Wicker, 2014; Kim & Cavaco-Paulo, 2011; Mattinen et al., 2006; Steffensen et al., 2008). As shown by the high extent of fragmentation in the MPPT48hFA, the presence of ferulic acid mediator may have also led to the generation of more radicals that promoted the fragmentation of proteins. This observation aligns with the results reported for laccase-phenolic mediator system in the modification of milk protein (Mokoonlall, Pfannstiel, et al., 2016). In addition, spectral characterization indicated the incorporation of ferulic acid moiety to the protein upon reaction (data not shown). The MW profile (Fig. 7.1) reveals the presence of cross-linked proteins with MW of > 135 kDa and 60-80 kDa, corresponding to trimer-patatin oligomer and cross-linked patatin/protease inhibitor, respectively, in both MPPT24h and MPPT24hFA. The MW profile of the products, MPPT48hFA or MPPT48h, contains 94.5 and 77.3% of fragmentation MW fraction at 1-30 kDa, respectively. In addition, the reaction mixtures at 48h were fairly turbid as compared to those at 24h; this indicates protein aggregation as a result of excessive oxidation. Indeed, relatively broader peaks were observed in the SEC chromatograms (Fig. 7.2), confirming the formation of intramolecular cross-links (Lantto et al., 2005). Cura et al., (2009) have shown that sodium caseinate can be cross-linked either directly by laccase at high enzyme concentration or in combination with ferulic acid. Another study showed that the polymerized products of $\boldsymbol{\alpha}$-lactalbumin in the reaction catalyzed by laccase from *Aspergillus* with the presence of ferulic acid increased in proportion and molecular size as a function of incubation time (0-24h) (Jiang et al., 2017).

Both potato protein and sugar beet pectin were found to exhibit comparable specific activity in the laccase-catalyzed oxidative crosslinking reaction system, which promoted their hetero-conjugation (Li & Karboune, 2020). The use of selected ratios of protein to sugar beet pectin (1:1.27; 1.78:1 w/w) resulted in different hetero-conjugation extents. The high and low conjugated PPT-SBP showed distinct size exclusion chromatograms (Fig. 7.3). Sugar beet pectin (Rt 31-46 min), which was highly feruloylated (0.87%, w/w), were detected by both RI and UV detectors and included populations with MW ranging from 0.25 to 6 MDa, with an average MW of 1.3 MDa. On the other hand, the main fraction of potato protein, patatin, was identified at 48-57 min in the SEC chromatogram, with average MW of ~80 kDa, which is consistent with the fact that patatin exists in the form of dimer in non-reducing environment.

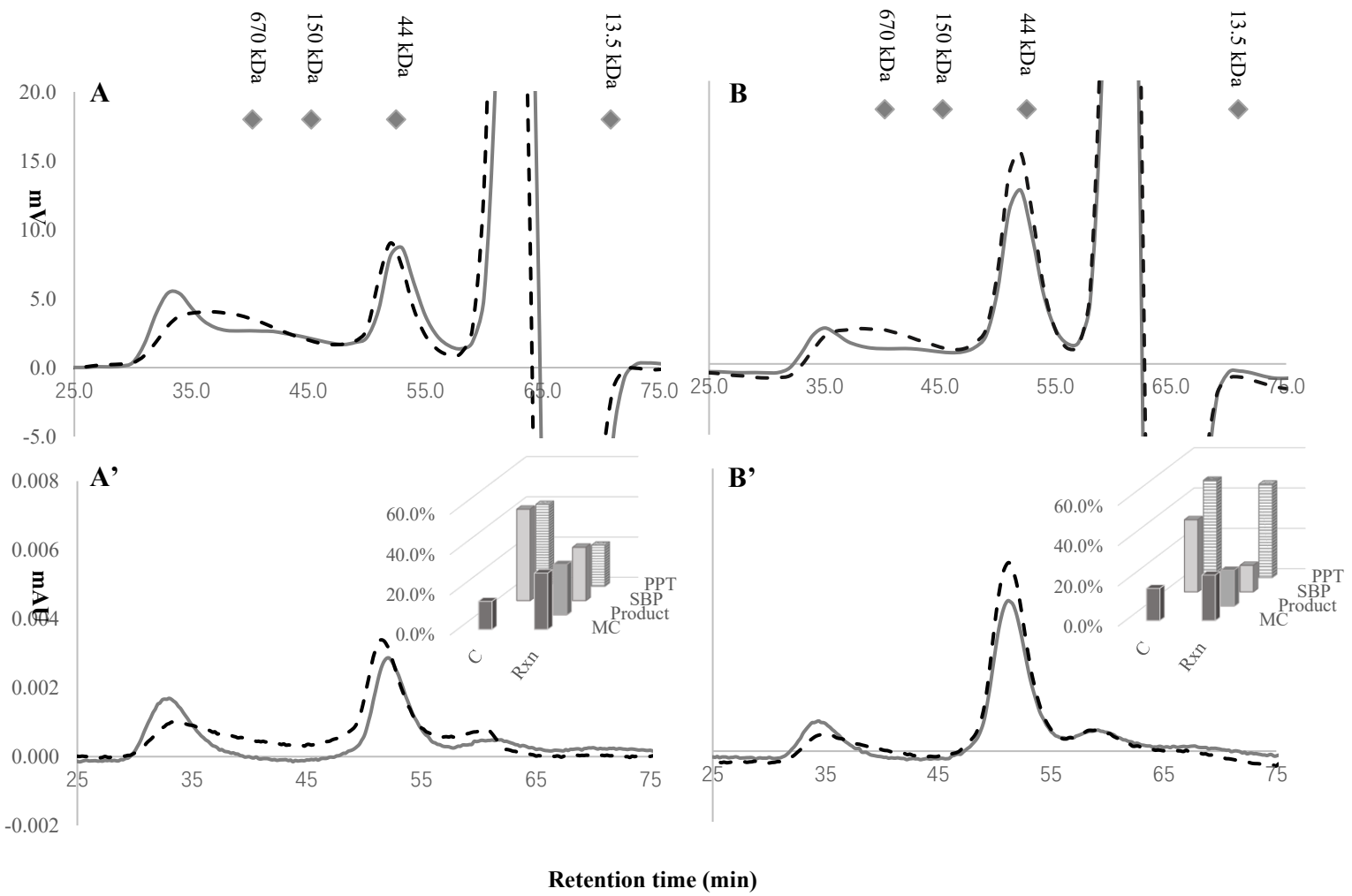

Figure 7.3. Molecular weight distribution of laccase-catalyzed conjugation of potato protein (PPT) and sugar beet pectin (SBP). The chromatograms at UV 280 nm (A'&B') and refractive index (A&B) of highly conjugated PPT-SBP-H (A&A') and low conjugated PPT-SBP-L (B&B') . Chromatograms of the conjugates (—) and corresponded controls (…) were aligned; the insert is representing the relative proportion of each component in reaction mixture (Rxn) & control (C): Potato protein (PPT), sugar beet pectin (SBP), multiconjugates/aggregate (MC).

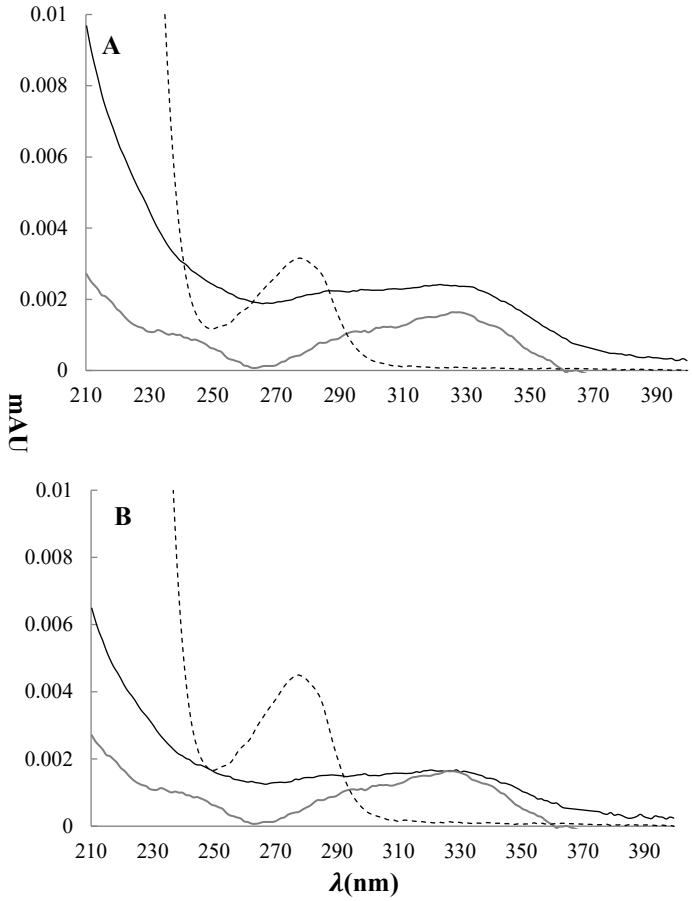

Figure 7.4. Comparison of UV spectra of conjugates, PPT-SBP-H (A) and PPT-SBP-L (B), potato protein and sugar beet pectin. Black line, conjugates; grey line, sugar beet pectin; dash line, potato protein.

A new peak that exhibited the spectral characteristics from both PPT and SBP was detected at 29-38 min in both RI and UV chromatograms. The appearance of this new peak was accompanied by a decrease in the peak areas of sugar beet pectin and protein, which was attributed to PPT-SBP conjugates as shown by spectral characteristics (Fig. 7.4). It is important to note that the insoluble fraction of the reaction mixtures increased upon conjugation and was attributed to the excessive multi-conjugation and/or to the aggregation of the biopolymers. At a protein to sugar beet pectin ratio of 1:1.27, 25.1% of soluble PPT-SBP conjugates with a MW of 3.8 MDa and 14.0% of insoluble multi-conjugates/aggregates were obtained in the PPT-SBP-H reaction mixture. The PPT-SBP-L reaction mixture corresponds to that at the protein to sugar beet pectin ratio of 1.78:1. As compared to PPT-SBP-H, relatively lower conjugation extent of 17.9% and MW of the conjugates (2.7 MDa) were obtained in the PPT-SBP-L reaction system in which only 6.7 % multi-conjugates/aggregates were generated. Similarly, bovine serum albumin conjugated with sugar beet pectin catalyzed by laccase was characterized by the appearance of peaks at high MW region and decrease in the concentration in parent biopolymer (Chen et al., 2018)

7.4.2. Structural characterization and thermal denaturation properties

Fluorescence spectroscopy was used to analyze the tertiary conformational changes in the microenvironment of aromatic amino acid residues upon modification. A decrease in fluorescence signal and increase in wavelength of maximum emission intensity (λ_{max}) is correlated with exposure of aromatic amino acid (mainly tryptophan) residues to hydrophilic solvent environment and the presence of compounds with shielding effect (Jia et al., 2019). The fluorescence spectral characteristics of proteins were shown at pH 3, 5, and 7 (Fig. 7.5A). Native potato protein exhibited λ_{max} at 345 nm at all three pH conditions, which falls within the range of reported λ_{max} for patatin (335nm) and protease inhibitors (347nm) (Pots et al., 1999; Pouvreau et al., 2004). In agreement with our results, Waglay et al. (2016) have reported λ_{max} of 345 at pH 4-9 for native potato protein. A blue shift of the λ_{max} to 330-340 nm was noticed in MPPT24hFA at all pH conditions. This indicates an increase in the hydrophobicity surrounding the aromatic amino acids, which could be attributed to the incorporation of the FA in the protein structure as hydrophobic patches. In addition, the λ_{max} of PPT-SBP conjugates shifted towards 350 nm at pH 3 as compared to the native potato proteins, while the λ_{max} at pH 5 and 7 remained unchanged from the native.

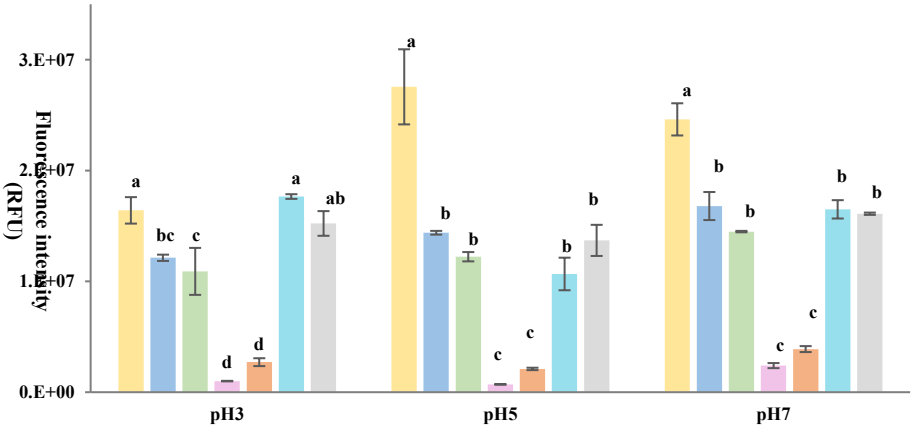

Figure 7.5. Fluorescence intensity at λ_{max}. Samples were color-coded as yellow-native potato protein, blue-MPPT24h, green-MPPT48h, pink-MPPT24hFA, orange-MPPT48hFA, cyan-PPT-SBP-H and grey-PPT-SBP-L Letter indicates significant difference at the same pH conditions.

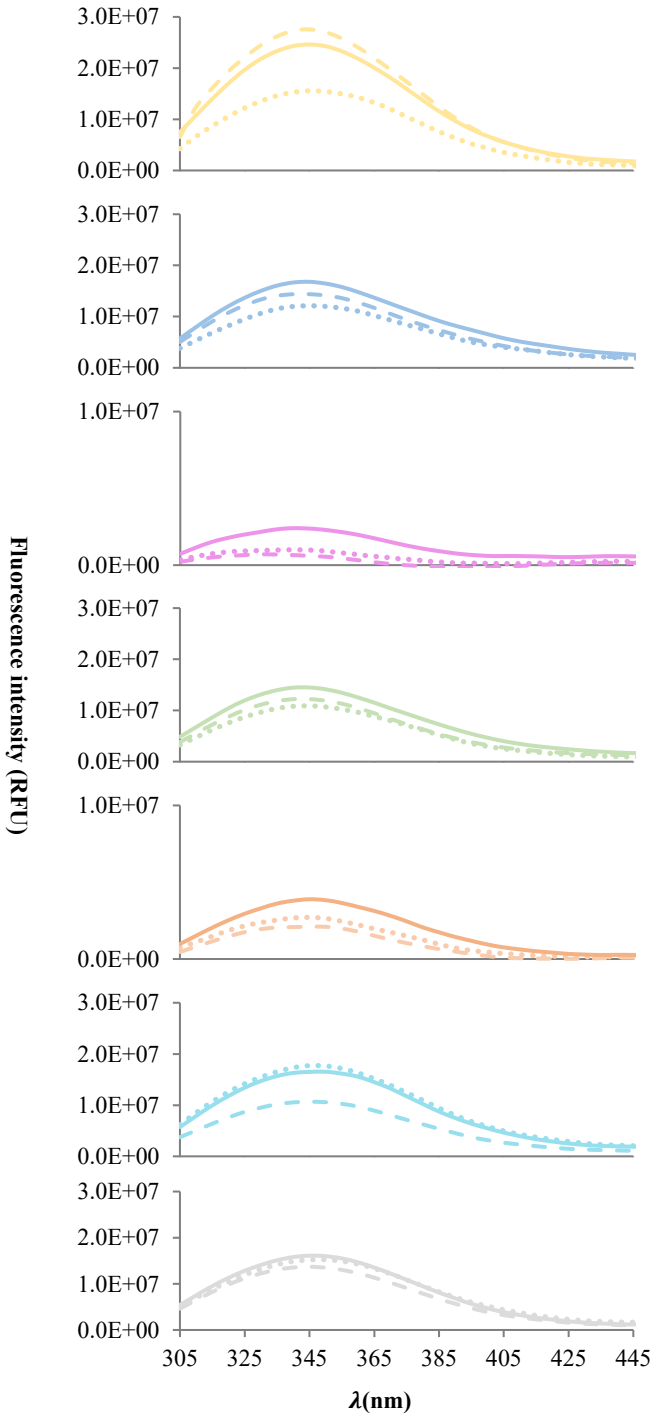

Figure. 7.6. Fluorescence spectra of native and modified potato proteins. Spectra was determined at pH 3 (dash line), pH 5 (dotted line) and pH 7 (solid line). Samples were color-coded as yellow-native potato protein, blue-MPPT24h, green-MPPT48h, pink-MPPT24hFA, orange-MPPT48hFA, cyan-PPT-SBP-H and grey-PPT-SBP-L.

A red shift was indicative that the microenvironment surrounding the potato protein molecule in PPT-SBP conjugates is more hydrophilic (Ma, Chen, et al., 2020; Seo et al., 2014; Wang, Lv, et al., 2019).

Lower fluorescence intensity than the native one was seen for all modified proteins at pH 7 (*p-value* < 0.0001) (Fig. 7.5). Among the modified proteins, cross-linked MPPT24h/48h and PPT-SBP-L/H conjugates exhibited relatively high fluorescence intensity. This indicates that the direct cross-linking or the steric effect from polysaccharide upon conjugation caused less structural unfolding effect as compared to the reaction with phenolic mediator.The conjugated ovalbumin with pullulan was shown to undergo conformational changes associated with less exposure of the aromatic amino acid residues as compared to the heated ovalbumin (Sheng et al., 2020). Tertiary structural changes of protein unfolding and enhanced surface hydrophobicity were generally caused by oxidative cross-linking and augmented by the extent of oxidative treatment (Hiller & Lorenzen, 2008; Li et al., 2012; Wu et al., 2009). The prolonged oxidation and fragmentation of MPPT48h were expected to result in lower fluorescence intensity than MPPT24h due to the exposure of tryptophan, being the most fluorescent, to polar environment and loss in aromatic fluorophore. But the decrease was not significant (p-value = 0.201). The significantly low intensity of cross-linked MPPT24hFA and MPPT48FA with ferulic acid mediator suggested a major change in the protein conformation took place upon modification. The decrease in the fluorescence intensity in combination with blue shift in spectral characteristics were reported for the other cross-linked proteins mediated by phenolic compounds and attributed to the penetration of water molecules and the interaction between the aromatic amino acid residues (e.g. tryptophan) of protein and the incorporated phenolic moieties (Jia et al., 2019). Aside from protein unfolding, the decrease in the fluorescence intensity upon protein modification arises from many other factors that can influence chemical characteristics, such as the loss in aromatic amino acids, formation of disulfide bonds and protein dissociation/degradation (Alavi et al., 2018; Jarpa-Parra et al., 2015; Wu et al., 2009).

The modification of potato protein also resulted in different pH dependent-unfolding responses (Fig. 7.5&7.6). Among the investigated pH conditions, a significant decrease in the fluorescence intensity was observed at pH 3 for native protein and MPPT24h, and at pH 3 and pH 5 for MPPTs-FA (p-value < 0.05). The apparent decrease in fluorescence intensity at the indicated pH conditions implies that tertiary unfolding of the proteins was promoted, possibly due to the electrostatic repulsions at acidic pH as well as the pH-dependent deprotonation of

incorporated ferulic acid moieties (Alavi et al., 2018; Ghigo et al., 2020). In contrast, the fluorescence intensity of PPT-SBP-L was shown to be unaffected by the change in pH condition, whereas an apparent decrease in fluorescence intensity of PPT-SBP-H was observed at pH 5 (p-value < 0.05), rather than pH 3. In fact, at pH 3, relatively high fluorescence intensity of PPT-SBP conjugates as compared to MPPTs was noted (p-value <0.05). In the PPT-SBP conjugates, both electrostatic and covalent interactions may have influenced the folding states of the potato proteins (Chen et al., 2019; Zeeb et al., 2012). The pI of native potato patatin was reported to be at pH 4.5 - 5.2; those of protease inhibitors was ranged from pH 5.1 to 9.0 (Bárta et al., 2012; Pouvreau et al., 2001). At pH 3, electrostatic attractions may have happened between the positively charged protein and the anionic polysaccharides, a relatively high fluorescence intensity of the conjugates could be attributed to the limited protein unfolding and forming compact complexes.

The thermal denaturation properties of native and modified potato protein were studied by DSC to provide further information about tertiary structural property (Table 7.2). Although the structural changes are not related to a single protein, but rather a complex mixture, it was still worthwhile to estimate denaturation temperature (T_d) and enthalpy change (ΔH) that reflect protein's thermostability and molecular compactness/content of undenatured structure, respectively (Wang et al., 2014). An understanding of such characteristics of modified potato protein are necessary for better modulation of the extent of their modification and for the evaluation of their potential application. At pH 5 and 7, the native potato protein showed T_d at 70.2-70.4℃ and ΔH of 10.1-11.2 J/g. The T_d of potato protein measured in our study is slightly higher than those reported in other studies (~ 66℃), whereas ΔH was lower than others (20~25 J/g) (Elahi & Mu, 2017; Van Koningsveld et al., 2001). These variations in T_d and ΔH could be due to the use of different extraction and purification methods as well as DSC methods. The modifications lowered ΔH values, which may indicate the loss in protein's compactness and decrease in inherent non-covalent interactions that stabilize the potato protein (Li et al., 2012). These results align with the fluorescence spectra reflecting protein unfolding upon modification.

Table 7.2. Thermal properties of native and modified potato proteins samples

		Endothermic			Exothermic		
		pH 3	**pH 5**	**pH 7**	**pH 3**	**pH 5**	**pH 7**
Native	Td ℃	62.85	70.26	70.33			
	ΔH(J/g)	9.29	10.13	11.14			
MPPT24h	Td ℃	64.48	69.44	68.40			
	ΔH(J/g)	5.064	5.924	7.095			
MPPT+FA24h	Td ℃	63.71	67.73	66.65			
	ΔH(J/g)	2.1	2.8567	3.868			
MPPT48h	Td ℃	60.4	69.93	69.4			
	ΔH(J/g)	5.179	9.002	8.366			
MPPT+FA48h	Td ℃	62.81	68.98	67.82			
	ΔH(J/g)	1.654	3.289	3.897			
PPT-SBP-H	Td ℃	59.40	70.23	70.50	27.90	31.03	37.70
	ΔH(J/g)	1.10	1.83	2.34	1.44	1.45	3.38
PPT-SBP-L	Td ℃	57.07	70.16	70.61		33.09	34.41
	ΔH(J/g)	2.31	4.56	4.53		2.19	0.18

Abbreviations: PPT, potato protein; MPPT24h, MPPT48h are modified protein obtained from laccase-catalyzed reaction for 24h and 48h respectively; MPPT24hFA, MPPT48FA are modified protein obtained from laccase-ferulic acid mediator reaction for 24h and 48h, respectively; PPT-SBP-H and PPT-SBP-L are PPT/sugar beet pectin conjugates with high and low conjugation extent; respectively.

At pH 5 and 7, the T_d indicating thermal stability of the two PPT-SBP conjugates are similar to native potato protein, followed by cross-linked MPPT24h/48h and then cross-linked MPPT24hFA/48hFA in the presence of ferulic acid mediator. Relatively high thermal stability was shown by PPT-SBP conjugates as compared to other modified proteins at pH 5 and 7, which could be ascribed to the stabilizing effects of polysaccharides on protein, while the total enthalpy values of these conjugates were lower than the other modified proteins. The phenomenon of the decrease of total enthalpy with increasing T_d was reported for sunflower globulins and peanut proteins, which was associated with protein exothermic coagulation with the temperature increase (Colombo et al., 2010; Rouilly et al., 2003). Another thermal characteristic of the PPT-SBP-H/L samples that is worth noted is the presence of exothermic peak between 30 and 40 °C, indicating the conjugated protein might have undergone folding at this temperature. Such thermal changes may come from the disruption of the hydrophilic interaction between protein and polysaccharide with the temperature increase (Tang et al., 2007). The results (Table 7.2) also show that at pH 5 and 7, the cross-linked proteins MPPT48h/48hFA obtained after 48h reaction exhibited a higher thermal stability and content of ordered structure than those corresponding 24h reactions (MPPT24h/24hFA) as shown by the T_d and ΔH values. The increase in the thermal/structural stability upon advanced cross-linking at longer reaction time confirms the formation of intramolecular cross-links, regardless of the protein fragmentation that did happen. When comparing between the modified proteins from laccase-catalyzed reaction with (MPPT24hFA, MPPT48hFA) and without (MPPT24h, MPPT48h) ferulic acid, the latter exhibits higher values of both thermal parameters, especially the ΔH values. This indicates that less stable and compact structure of the cross-linked proteins were obtained in the presence of ferulic acid.

Native potato protein showed lower T_d (62.89℃) and ΔH (9.29 J/g) at pH 3 than at pH 5 and 7, implying that protein assumed a less stable conformation at acidic conditions. Cross-linked MPPTs24/24FA, characterized with high MW profiles, exhibited a higher thermal stability at acidic condition than the native as indicated by their T_d values (64.48/63.71℃). On the other hand, both PPT-SBP-L/-H conjugates had the lowest T_d values (59.40/57.07℃) at pH 3 compared to the other modified proteins. It was reported previously that the electrostatic attraction of protein/polysaccharide could promote protein thermal denaturation (Xu et al., 2019; Yang et al., 2020). It can be hypothesized that at acidic pH excessive macromolecule interactions may have occurred upon conjugation with polysaccharide than crosslinking, resulting in thermal denaturation of potato protein.

The fluorescence spectra and DSC results reveal that potato protein assumes selected conformations with specific unfolding and ordered structures upon their cross-linking and conjugation through laccase-catalyzed reactions. The use of different pH values and the cross-linking in the presence of ferulic moieties allowed us to assess the significance of intermolecular interactions and the non-covalent forces (e.g. hydrophobic, hydrogen, electrostatic) in the maintenance of stable structure. Similar modification effects on protein tertiary structure have been reported previously (Hiller & Lorenzen, 2008; Hiller & Lorenzen, 2009; Lantto et al., 2005). As compared to the native form, milk proteins treated by oxidoreductase-catalyzed reactions were reported to exhibit less stable and extended secondary/tertiary structure with higher surface hydrophobicity and lower thermal stability (Hiller & Lorenzen, 2008), whereas the formation of inter-/intra-molecular cross-links in protein upon transglutaminase-treatments was associated with less unfolded/extended structure and higher stability (Hiller & Lorenzen, 2008; Lantto et al., 2005). In addition, protein that is conjugated covalently with polysaccharides via Maillard reaction was reported to show generally more buried tryptophan residues and overall enhanced tertiary stability with higher T_d and lower ΔH (Liu et al., 2012; Sheng et al., 2020).

7.4.3. Assessment of air-water interfacial properties

7.4.3.1. Interfacial adsorption kinetics

Dynamic surface tension measurements were performed to evaluate the changes in the adsorption kinetics of protein at the air-water interface upon laccase-catalyzed modifications. The comparison was also evaluated at different pH conditions. The maximum bubble pressure method allows the instant measurement of surface tension at initial stage adsorption (Fig. 7.7A-G). From the initial adsorption kinetic results, the lag time and the initial adsorption rate were evaluated (Table 7.3). Lag time reflects the process of sufficient protein that are adsorbed at interface to allow molecular interactions, which is associated with the flexibility and susceptibility to conformational changes of the protein molecules (Ruíz-Henestrosa et al., 2007). At neutral pH, native potato protein (7.6 s) had the shortest lag time, followed by MPPT24h (19.1s), MPPT24hFA (37.7 s), MPPT48hFA (42.9 s) and PPT-SBP-L (51.2 s). Relatively longer lag times than the other samples were seen for MPPT48h and PPT-SBP-H (90-120 s), which may be ascribed to their relatively compact structures and high MW, respectively.

Table 7.3. Adsorption kinetic parameters: lag time, rate of adsorption and equilibrium state surface tension

	pH 3	pH 5	pH 7
	Lag time (s)		
Native PPT	3.6 ±0.4^{c}	30.0 ±0.1^{b}	7.6 ±0.0^{d}
MPPT24h	10.4 ±1.4^{bc}	N/A	19.1 ±0.1^{cd}
MPPT48h	15.2 ±0.0^{bc}	219.5 ±27.3^{a}	118.9 ±0.1^{a}
MPPT24hFA	44.1 ±5.5^{bc}	N/A	37.7 ±0.1^{bcd}
MPPT48hFA	149.2 ±0.1^{a}	-	42.9 ±6.9^{bc}
PPT-SBP-H	211.2 ±35.9^{a}	37.9 ±0.1^{b}	93.5 ±0.3^{b}
PPT-SBP-L	37.9 ±0.1^{b}	28.0 ±3.5^{b}	51.2 ±6.9^{bcd}
	Initial adsorption rate (mN/(m ms))		
Native PPT	5.5 ±0.3^{c}	8.4 ±0.2^{a}	9.5 ±0.3^{bc}
MPPT24h	5.9 ±0.1^{c}	N/A	10.1 ±0.1^{abc}
MPPT48h	6.0 ±0.1^{c}	8.8 ±0.7^{a}	9.1 ±0.5^{c}
MPPT24hFA	9.3 ±0.6^{ab}	N/A	10.5 ±0.5^{abc}
MPPT48hFA	10.9 ±2.3^{a}	-	11.4 ±1.6^{ab}
PPT-SBP-H	8.1 ±1.7^{abc}	8.9 ±0.4^{a}	12.2 ±1.0^{a}
PPT-SBP-L	7.5 ±0.2^{bc}	8.4 ±0.3^{a}	11.0 ±0.7^{abc}
	Equilibrium surface tension (mN/m)		
Native PPT	55.8 ±0.6^{f}	55.1 ±0.1^{e}	50.7 ±0.3^{e}
MPPT24h	56.7 ±0.2^{e}	N/A	54.5 ±0.5^{d}
MPPT48h	57.3 ±0.3^{de}	64.2 ±0.1^{b}	63.3 ±0.5^{a}
MPPT24hFA	57.6 ±0.1^{d}	N/A	58.3 ±0.6^{c}
MPPT48hFA	60.3 ±0.1^{c}	66.5 ±0.2^{a}	61.7 ±0.2^{b}
PPT-SBP-H	67.3 ±0.2^{a}	61.6 ±0.3^{c}	51.5 ±0.3^{e}
PPT-SBP-L	64.6 ±0.2^{b}	59.8 ±0.2^{d}	48.7 ±0.3^{f}

All values are expressed as mean ± SD.

Within the same column, means with different letters are significantly different at $P \leq 0.05$

"N/A": non-applicable

"-": non-applicable, The decrease in surface tension was very slow, as a result the calculation for lag time and adsorption rate was not valid.

Abbreviations: PPT, potato protein; MPPT24h, MPPT48h are modified protein obtained from laccase-catalyzed reaction for 24h and 48h respectively; MPPT24hFA, MPPT48FA are modified protein obtained from laccase-ferulic acid mediator reaction for 24h and 48h, respectively; PPT-SBP-H and PPT-SBP-L are PPT/sugar beet pectin conjugates with high and low conjugation extent; respectively.

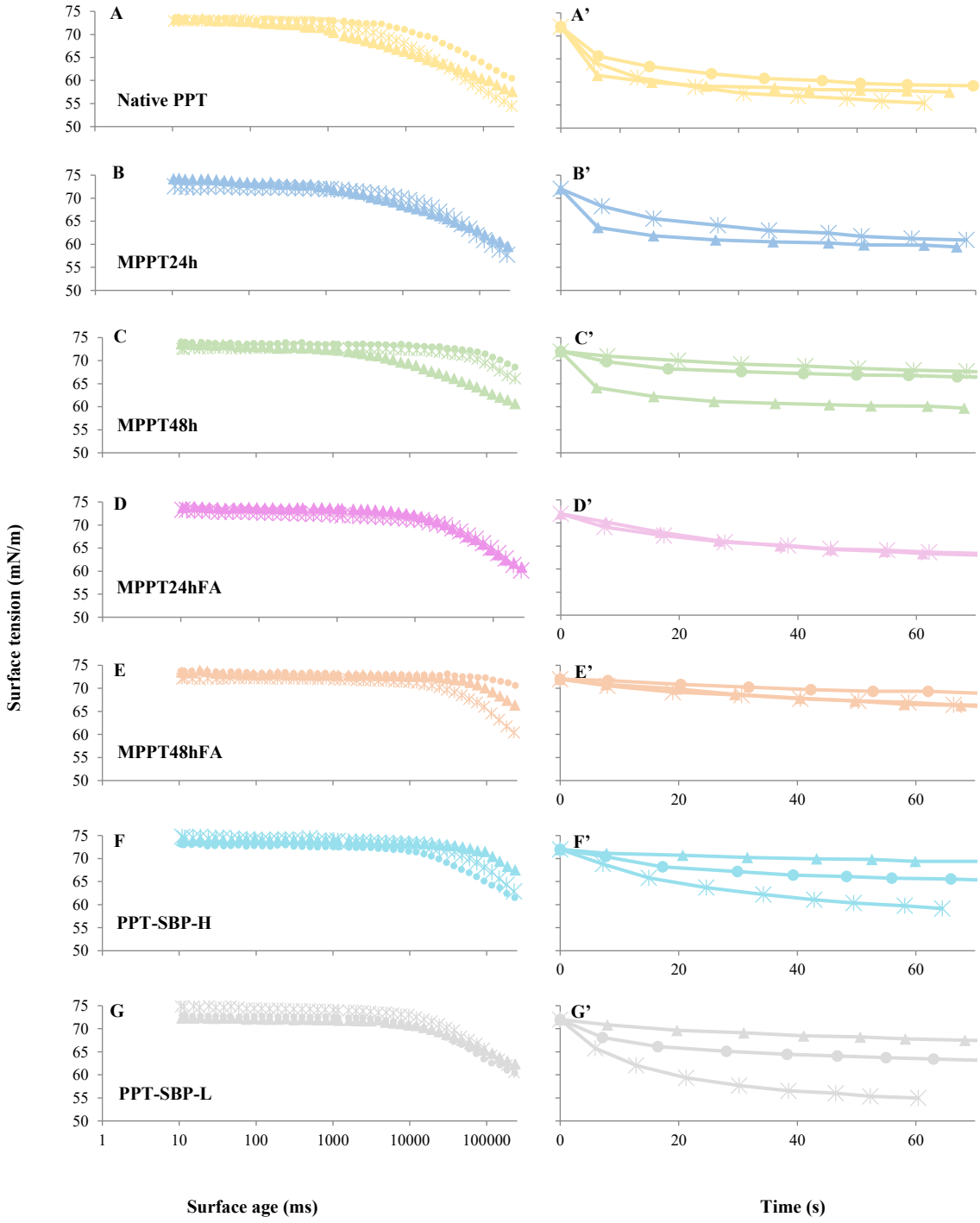

Figure 7.7. Adsorption kinetics at air-water interface with selected bulk phase pH conditions. pH 3:▲, pH 5:●, pH 7:✳. Transient adsorption kinetics: A-G; long term adsorption kinetics: A'-G'.

As expected, the lag phase is affected by pH of the bulk phase, as pH governs the extent and type of intermolecular interactions. Among the investigated pH, the lag times of the native and MPPT24h/48h decreased significantly at pH 3, whereas those of PPT-SBP conjugates achieved the lowest lag time at pH 5 (p-value < 0.05). The short lag times tend to be achieved at the conditions where the proteins were the most unfolded or had the least interactions with the conjugated polysaccharides, as depicted by the result of fluorescence and DSC, and likely associated with a high molecular flexibility (Jarpa-Parra et al., 2015; Rodriguez Patino et al., 2007). The cross-linked MPPT24hFA/48hFA did not show a decrease in the lag time at pH 3 as observed with MPPT24h/48h. This could be due to the great loss in the tertiary stability of MPPTs-FA that may have limited their conformational changes under acidic conditions. The results also show an obvious increase in the lag time at pH 5 for the native protein and the cross-linked MPPTs, while PPT-SBP-H conjugated showed relatively long lag time (>200 s) at pH 3. The increase in lag time at these pH conditions may be attributed to the folding and repacking of the structure of protein due to low surface charge and/or aggregation (Yang et al., 2018).

Following the lag phase, surface tension started to decrease and the slope was defined as the initial adsorption rate (Table 7.3). At pH 7 and 3, relatively high initial adsorption rates were seen for PPT-SBP conjugates and MPPT24hFA/48hFA; the native and MPPT24h/48h showed the lowest adsorption rates. At pH 5, the initial adsorption rates of the investigated samples were not varied significantly. The effect of pH conditions on the initial adsorption of potato proteins is determined by the competition between exposed hydrophobicity and the protein net charge due to partial unfolding (Schmidt et al., 2018). The native and MPPT24h/48h samples exhibited lower initial adsorption rates at pH 3 than that at pH 7 (p-value <0.05), whereas the rates of MPPT24hFA/48hFA were not affected by the pH variations. For the native and MPPT24h/48h samples, the increase in net charge may have counterbalanced the exposed hydrophobicity at pH 3 resulting in a decrease in initial adsorption rates. The initial adsorption rates of native protein and the conjugates at pH 5 were also lower than that at pH 7 (p-value < 0.05), which was most likely associated with the compact structure and low exposed hydrophobicity at the condition near the pI of the protein. Such decrease was not shown by MPPT48h, as the exposure of hydrophobic segments due to oxidative fragmentation may have counteracted the conformational effects of pI.

Long-term adsorption kinetics (0-60 s) was studied via drop volume method (Fig. 7.7 A'-G') to complement the initial adsorption kinetic results and to extrapolate the equilibrium surface

tension (Table 7.3) of the native and modified potato proteins. At pH 7, the surface tension of native potato protein and cross-linked MPPTs decreased gradually and no equilibrium was observed within 60 s; the trend of decrease was the fastest in the native followed by modified proteins obtained from 24 h treatment than those from 48 h treatments (Figure 7.7A', B' and C'). The results also showed that PPT-SBP-L conjugates were more active in decreasing the surface tension than PPT-SBP-H and all MPPTs at pH 7. As compared to the native protein, the decrease trend line of surface tension of PPT-SBP-L proceeded through two stages characterized by a moderate and higher capacity at the first 20 s and thereafter, respectively; as a result, a lower equilibrium surface tension was achieved by PPT-SBP-L. The relatively high surface activity of the conjugates could be ascribed to the deeper penetration of the protein in the bubble at late adsorption state supported by the polysaccharide parts (Perez et al., 2010). Overall, as suggested by the value of equilibrium surface tension, the capacity of the potato protein in native and modified forms in reducing surface tension at pH 7 was as the following order: PPT-SBP-2 > native, PPT-SBP-1 > MPPT24h > MPPT24hFA > MPPT48hFA > MPPT48h (p-value < 0.05) (Table 7.3). The capacity of ovalbumin, $\boldsymbol{\beta}$-lactoglobulin, $\boldsymbol{\alpha}$-casein and bovine serum albumin in reducing surface tension were negatively impacted by oxidation or cross-linking as reported by Duan et al., (2018), Ercili-Cura et al., (2015) and Steffensen et al., (2008). Differently from pH 7, the kinetic curves of the native, MPPT24h and MPPT48h at pH 3 were characterized by a significant decrease at the first 20s followed by an almost horizontal trend line (Fig. 7.7 A'-C'), implying that, at acidic pH, these proteins adsorbed faster; however, the adsorption reached the equilibrium more quickly. The use of acidic pH had little or no impact on the adsorption kinetic of MPPT24hFA/48hFA. The adsorption barrier of potato protein and low interfacial packing density due to strong electrostatic repulsion was suggested as the reason for the low surface activity at pH 3 (Dachmann et al., 2020). Decrease in surface activity was observed for the native and MPPT24h when pH was changed from 7 to 3 as indicated by the equilibrium surface tension which can be associated with reduced adsorbed proteins at the interface due to the extended and unfolded protein conformation. In contrast, lower equilibrium surface tension of MPPT48h/48hFA was observed at pH 3 than other pH conditions ($p < 0.0001$); indicative that the acidic conditions promoted the adsorption of the proteins with more compact structure. Among the investigated pH conditions, the least efficient adsorption was observed at pH 3 or 5 for the native and crosslinked MPPTs, while pH 3 for the conjugates. These results could be associated with long lag time, low exposure of the hydrophobic residues of protein and/or molecular inflexibility at indicated conditions.

7.4.3.2. Film rheological characteristics

The surface dilatational elastic moduli of the native and laccase-catalyzed modified potato proteins were evaluated at three pH conditions by oscillating pendant drop method. The results (Table 7.4) show that the E' of all the samples are relatively high at pH 3, followed by pH 5, whereas relatively low E' value was obtained at pH 7. These results reveal that the dominant molecular interactions at the interfaces were dependent on the bulk phase pH conditions. Similar relationship of pH and surface dilatational elasticity of potato protein was reported by Dachmann et al. (2020) and by Chang, et al. (2015) for other plant proteins. MPPT24h/24hFA/48h (42.9/38.5/35.0 mN/m) resulted in high E' values at pH 7, while at pH 3, MPPT48hFA/48h (66.1/62.1 mN/m) led to high E' values. Brückner-Gühmann et al. (2018) have studied the foaming property of oat protein isolate and reported that bulky protein molecules and their steric effects promoted the formation of a strong viscoelastic interface at neutral pH condition, while size reduction of protein through partial hydrolysis to increase the exposed hydrophobicity is the key for the film formation at acidic pH. This aligns with our observation on the E' values of modified potato proteins at pH 7 and 3. At pH 5, the E' values of the native and modified proteins were not significantly different, except MPPT48h, which showed a decrease in E' as compared to the native (p-value of 0.009). The increased surface load and the formation of multi-layer film because of the low electrostatic repulsion may have favored the surface dilatational elasticity at pH close to protein's isoelectric point (Bos & Van Vliet, 2001; Jarpa-Parra et al., 2015; Pezennec et al., 2000). However, for the fragmented MPPT48h proteins, they have most likely being charged and exhibited repulsions at the interface. The PPT-SBP conjugates showed relatively low E' value as compared to the native and MPPTs, possibly due to the co-adsorption of polysaccharide parts at the interface which could disrupt the intermolecular interactions at the surface (Liu, Selig, et al., 2018). Similarly, A decrease in surface dilatational elasticity was also reported by Zhu et al., (2020) on soy proteins.

Table 7.4. Elasticity modulus measured by oscillating pendant drop method

	Elasticity modulus mN/m		
	pH 3	**pH 5**	**pH 7**
Native PPT	57.16±1.32^{abc}	46.42±2.36^{a}	29.32±1.83^{b}
MPPT24h	49.84±2.52^{bc}		42.86±2.18^{a}
MPPT48h	62.11±5.17^{ab}	31.37±0.84^{b}	34.95±0.98^{ab}
MPPT 24hFA	46.12±1.65^{c}		38.45±1.75^{ab}
MPPT 48hFA	66.10±2.40^{a}	48.39±7.17^{a}	32.21±3.02^{b}
PPT-SBP-H	55.05±9.54^{abc}	40.25±1.97^{ab}	29.78±3.02^{b}
PPT-SBP-L	44.94±0.23^{c}	40.20±4.79^{ab}	30.08±4.29^{b}

All values are expressed as mean ± SD;
Within the same column, means with different letters are significantly different at $P \leq 0.05$. the first section of letter indicates the difference between treatments; the second section indicates the difference between pH conditions of the same sample
N/A: non-applicable;
Abbreviations: PPT, potato protein; MPPT24h, MPPT48h are modified protein obtained from laccase-catalyzed reaction for 24h and 48h respectively; MPPT24hFA, MPPT48FA are modified protein obtained from laccase-ferulic acid mediator reaction for 24h and 48h, respectively; PPT-SBP-H and PPT-SBP-L are PPT/sugar beet pectin conjugates with high and low conjugation extent; respectively.

The characteristics of the spread monolayer films at pH 7 was further investigated through their compression isotherms (Fig. 7.8). A0 value, the initial surface area, was used to indicate the monolayer expansion (Fauconnier et al., 2000). Although the protein samples (except PPT-SBP-H) may have encountered interfacial oversaturation, it was still worthwhile to indirectly compare A0 according to the surface pressure at the initial of compression. It is as the following order of magnitude: native potato protein > MPPT24h/24hFA > MPPT48hFA, PPT-SBP-L, MPPT48h > PPT-SBP-H. These reveal that the modifications of potato protein resulted in a decrease in the coverage of surface per milligram of protein. An inflection was observed at 0.137 m2/mg for native potato protein and MPPT24h, and at 0.123 m2/mg for MPPT48h and PPT-SBP-L, indicating that these modified proteins can adapt to the compression via rearrangement of their structures (Wouters et al., 2016). At a further compression (surface area < 0.08 m2/mg), an apparent increase in the slope of the isotherms suggested film elasticity. Relatively higher elasticity was observed for the cross-linked proteins (MPPTs), especially MPPT24hFA, as compared to that of the native (Fig. 7.8 insert). A second inflection at the end of the compression was observed for the native protein, MPPT24hFA and MPPT48hFA, which indicated the collapse of the protein films (Barka et al., 2018). No clear collapse behaviour was seen for the other samples. The maximal surface pressure of the non-collapsed samples reflects their film stability (Fauconnier et al., 2000), which follows the order of MPPT24h/48h > PPT-SBP-L > PPT-SBP-H. In general, the observations from the compression isotherms align with the results obtained upon oscillating pendant drop analysis.

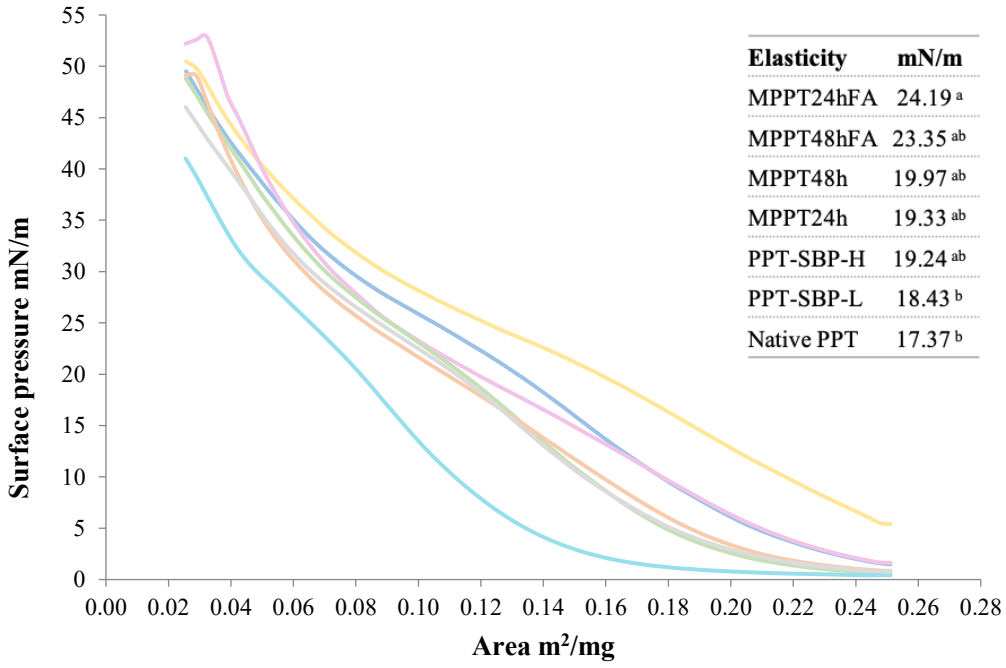

Figure 7.8. Compression isotherms for native and modified potato proteins. Samples were color coded as yellow- native potato protein, blue-MPPT24h, green-MPPT48h, pink-MPPT24hFA, orange-MPPT48hFA, cyan-PPT-SBP-H and grey-PPT-SBP-L. The isotherms were determined at pH 7.

Insert represents the elasticity, which was calculated from 0.03-0.08 region of the surface area.

Note: surface area is expressed as m2 per mg of samples. the native and cross-linked proteins (Native PPT, MPPTs and MPPTFAs) contains 0.8-1 mg protein/mg. The protein to polysaccharide ratios in the conjugates are 0.78:1 and 1.78 to 1 for PPT-SBP-H and PPT-SBP-L, respectively.

7.4.3.3. Impacts of protein modification on interfacial property

Interfacial properties of proteins, including the adsorption kinetics, the capacity in reducing surface tension and interfacial elasticity, are the mesoscopic details connected to protein foam formation and stabilization. In order to modulate and enhance the interfacial properties of proteins via modification, the selection of appropriate modification approach (conjugation vs crosslinking) and the quantification of key molecular properties of the modified proteins are essential. For cross-linked proteins, the balance between molecular size, flexibility and exposed surface hydrophobicity were found to be determinant for the interfacial property. The presence of high MW cross-linked products slowed down the adsorption of MPPT24h/24hFA due to their bulkiness and large molecular size, whereas it enhanced the surface dilatational elasticity via intensifying molecular interactions at interface (Davis & Foegeding, 2004). MPPT48h/48hFA were less surface active than its corresponding 24h MPPTs, due to its higher structural stability, which may have caused structural constrains against their adsorption (Ercili-Cura et al., 2015; Ercili-Cura et al., 2012). On the other hand, MPPT48h/48hFA tend to show better interfacial performance at the acidic pH than other pH conditions, and higher surface dilatational elasticity at acidic condition than the other modified protein. These may imply that the structural stability may be crucial for the interfacial properties of protein at acidic pH condition. The conjugation with SBP can enhance the surface activity of potato proteins at neutral pH condition. Indeed, the electrostatic repulsions from the polysaccharide tail may have facilitated the protein rearrangement and the penetration at the interface at the late adsorption stage (Liu, Selig, et al., 2018). However, conjugation did not favor the elastic property. The modulation of conjugation extent and the control of the protein/polysaccharide distribution at the interface may improve the elasticity and stability of protein interface via conjugation (Bertsch et al., 2019; Perez et al., 2010). When it goes to macroscopic level, a fast adsorption kinetic and high capacity in lowering the surface tension are keys for good foamability, and high film elasticity is critical for a stable foam (Srinivasan, 1994). Among the investigated modification approaches, the conjugation with SBP is likely to enhance the foaming ability of potato protein at pH 7, while the cross-linking could favor the stabilization of the potato protein-based foams. At pH 3, modified proteins MPPT48h/48hFA, characterized by reduced molecular size and high structural stability, may exhibit higher foam stability than other proteins.

7.4. Conclusion

Laccase-catalyzed modification approaches, including direct cross-linking, indirect cross-linking using ferulic acid mediator and conjugation with polysaccharide, was investigated for its effects on the tertiary structure, thermal stability and air-water interfacial property of potato proteins. The conjugation of potato protein with sugar beet pectin promoted the late stage adsorption, thus lowering equilibrium surface tension as compared to the native protein at neutral pH, which may contribute further to the foaming ability. The cross-linked potato protein (MPPT24h/24hFA) with increased molecular weight exhibited improved elastic properties at neutral pH condition, while extended oxidative cross-linking treatment (MPPT48h/48hFA) contributed to surface dilatational elasticity at acidic pH. These revealed the potential of cross-linked potato proteins as good foam stabilizer at indicated conditions. In addition, the low susceptibility of the interfacial performance of modified proteins MPPT48h/48hFA/24hFA to acidic pH allows the expansion of the application of potato proteins to low-pH formulations. Future work to understand the changes in relation to the techno-functional properties may help modulate better the application of potato protein via laccase-biocatalytic approaches.

CHAPTER VIII. GENERAL SUMMARY AND CONCLUSIONS

Research is providing a better understanding of protein functionalities and their limitations in processing. To explore the unique capabilities of proteins in various food formulations, it is important to develop novel approaches for protein modifications. The main objective of the present research was to investigate protein modifications catalyzed by laccase to produce protein-based ingredients with enhanced techno-functional properties. Changes upon protein modifications can occur at the molecular (amino acid sequence, secondary/tertiary structure, molecular weight, shape, flexibility and etc.) and/or physicochemical (solubility, hydrophobicity, isoelectric points, net charge) levels. Tailoring protein functionality towards specific applications requires the modulation of protein modification. The present research covers the mechanistic insights of laccase-catalyzed reactions with protein and protein related substrates and characterization of the modified proteins with the aim to modulate the catalytic action of laccases towards well-defined modifications.

The presence of tyrosine residues in the peptide sequence contributed to its reactivity in laccase-catalyzed oxidative cross-linking reaction. The laccase-catalyzed reaction resulted in cross-linked oligomer/polymer of potato patatin peptide model ST-10 (containing tyrosine) and oligomer < 5 units of tyrosine. Lysozyme peptide model AG-10, which does not contain tyrosine, can only be cross-linked in the presence of ferulic acid mediator, forming oligomer/polymer. The cross-linked product profile is affected by the reaction time, the type of biocatalyst and the use of ferulic acid mediator. Tyrosine is the main target site for oxidative cross-linking of ST-10, which forms di- and oligo-tyrosine cross-links upon laccase-treatment. Effect of ferulic acid on cross-linking is substrate dependent; it promoted cross-linking of less reactive substrate like AG-10, but inhibited that of reactive tyrosine-containing peptide ST-10.

Lysozyme upon grafted with ferulic acid reactive sites was subjected to laccase catalyzed reactions, and the polymerization of lysozyme was achieved mostly via the cross-linking on grafted ferulic acid sites. Similar approach was successfully applied to ovalbumin leading to its oligomerization. The extent of grafted ferulic acid sites was positively correlated with the substrate reactivity and the cross-linking extent, and it dictated the profile of cross-linked protein. The cross-linking was shown to contribute to the emulsifying property; however, the increase in molecular weight and the incorporation of ferulic acid moiety could lead to negative impact on the foaming property. Furthermore, the ferulic acid-grafting-laccase-catalyzed cross-linking decreased the allergenicity of lysozyme and ovalbumin. Overall, ferulic acid grafting followed by laccase cross-linking is a promising way to cross-link compact globular proteins.

In contrast with lysozyme or ovalbumin, the oxidative cross-linking of potato proteins can be

achieved directly or with the presence of ferulic acid as mediator. Laccase exhibited comparable binding affinity towards potato protein fraction containing patatin and potato protease inhibitors fraction, while the highest catalytic efficiency was achieved in the reaction with the former. The cross-linked product profile was affected by the type of biocatalyst and the use of ferulic acid mediator. Laccase with a high catalytic efficiency in oxidation led to a high extent of modification (cross-linking or fragmentation). In addition to promoting the cross-linking of potato protein, ferulic acid was incorporated to the cross-linked products, contributing to the antioxidant activity of the protein. Obtaining cross-linked potato proteins with well-defined oxidative cross-linking extent, molecular weight profile and secondary structural changes is important for the improvement of the foaming and emulsifying property.

Additionally, laccase-catalyzed reactions were explored for the conjugation of potato protein with polysaccharides. Sugar beet pectin with high content of ferulic ester and high substrate reactivity was shown to be the most efficient in forming hetero-conjugates with potato protein. The modulation of the conjugation was studied using RSM. Among the reaction parameters, the protein ratio in the potato protein-sugar beet pectin mixture was shown to be the most significant parameter affecting both conjugation extent and emulsifying ability of the biopolymer system; protein ratio/enzyme concentration had the most important interactive effect on conjugation extent, while the interaction of protein ratio/reaction time was the most important for emulsifying ability. With the use of developed predictive models, the conjugation extent can be controlled to obtain conjugates with desired emulsification performance.

The modified potato proteins obtained from different laccase-catalyzed reactions were shown to have unfolded structures with reduced compactness, and they were comparatively studied for their air-water interfacial properties. The conjugation with sugar beet pectin promoted its adsorption at the interface and led to increased surface activity at neutral pH, while increased film elasticity at neutral pH was favored by the increase in molecular size via cross-linking. Extended enzymatic cross-linking treatment led to relatively high structural stability as compared to the short time one and reduced the susceptibility of potato protein to acid condition in its performance at air-water interface.

As an overall, the current research contributes to the scientific knowledge for the effective application of the biocatalytic approach based on laccase in protein modifications. The understanding of the complex kinetics of the oxidative cross-linking and conjugation reactions catalyzed by laccases would allow the generation of well-defined cross-linked and conjugated proteins.

CHAPTER VIII. CONTRIBUTIONS TO KNOWLEDGE AND RECOMMENDATIONS FOR FUTURE STUDIES

9.1. Contributions to knowledge

The major contributions to knowledge are

(1) It was the first study about the mechanistic actions of laccase in the oxidation of protein related substrates, from enzyme/substrate binding and kinetics to bioconversion and cross-linking time course. As well, for the first time, molecular docking of laccase and protein related substrates was performed to elucidate these enzyme/substrate binding at molecular level.
(2) It was the first study reporting laccase-catalyzed cross-linking of egg white lysozyme and ovalbumin in the combination with phenolic grafting of the substrate protein. The relationship between protein surface phenolic extent and reactivity as a substrate for laccase and cross-linking efficiency was studied for the first time.
(3) For the first time, the cross-linked product profiles of potato proteins in laccase-catalyzed reactions were characterized. As well, it was the first study reporting the structure-functionality relationship of laccase-catalyzed modified potato proteins.
(4) The laccase-catalyzed conjugation between potato protein and pectic polysaccharides was studied for the first time, in which response surface methodology was used to model the enzymatic conjugation for the development of conjugated potato protein with desired emulsification performance.
(5) For the first time, the interfacial properties of various modified potato proteins were studied from the mesoscopic level.

9.2. Recommendation for future research

(1) Assessment of antioxidant property and antimicrobial spectrum of the cross-linked lysozyme to extend its application as innovative protein-assembly biomaterials.
(2) Investigation of laccase-catalyzed cross-linking of fractionated potato patatin and protease inhibitors to gain further insight about structure-function relationship of the modified patatin/protease inhibitors
(3) Development of stable potato protein/sugar beet pectin delivery system using laccase-catalyzed conjugation reaction.
(4) Discovery of laccase with high binding affinity and catalytic efficiency in the oxidative cross-linking of protein substrates using molecular docking and dynamic simulation.

REFERENCES

Acton, J. C., Kropp, P. S., & Dick, R. L. (1990). Properties of Ovalbumin, Conalbumin, and Lysozyme at an Oil-Water Interface and in an Emulsion System1. *Poultry Science, 69*(4): 694-701.

Aewsiri, T., Benjakul, S., Visessanguan, W., Eun, J.-B., Wierenga, P. A., & Gruppen, H. (2009). Antioxidative activity and emulsifying properties of cuttlefish skin gelatin modified by oxidised phenolic compounds. *Food Chemistry, 117*(1): 160-168.

Aewsiri, T., Benjakul, S., Visessanguan, W., Wierenga, P. A., & Gruppen, H. (2011). Improvement of foaming properties of cuttlefish skin gelatin by modification with N-hydroxysuccinimide esters of fatty acid. *Food Hydrocolloids, 25*(5): 1277-1284.

Ahlawat, S., Singh, D., Virdi, J. S., & Sharma, K. K. (2019). Molecular modeling and MD-simulation studies: Fast and reliable tool to study the role of low-redox bacterial laccases in the decolorization of various commercial dyes. *Environmental Pollution, 253*: 1056-1065.

Akbari, N., Mohammadzadeh Milani, J., & Biparva, P. (2020). Functional and conformational properties of proteolytic enzyme-modified potato protein isolate. *Journal of the Science of Food and Agriculture, 100*(3): 1320-1327.

Alavi, F., Emam-Djomeh, Z., Momen, S., Mohammadian, M., Salami, M., & Moosavi-Movahedi, A. A. (2019). Effect of free radical-induced aggregation on physicochemical and interface-related functionality of egg white protein. *Food Hydrocolloids, 87*: 734-746.

Alavi, F., Momen, S., Emam-Djomeh, Z., Salami, M., & Moosavi-Movahedi, A. A. (2018). Radical cross-linked whey protein aggregates as building blocks of non-heated cold-set gels. *Food Hydrocolloids, 81*: 429-441.

Aljawish, A., Chevalot, I., Jasniewski, J., Paris, C., Scher, J., & Muniglia, L. (2014). Laccase-catalysed oxidation of ferulic acid and ethyl ferulate in aqueous medium: A green procedure for the synthesis of new compounds. *Food Chemistry, 145*: 1046-1054.

Axelos, M. A. V., & Thibault, J. F. (1991). Influence of the substituents of the carboxyl groups and of the rhamnose content on the solution properties and flexibility of pectins. *International Journal of Biological Macromolecules, 13*(2): 77-82.

Azarikia, F., Wu, B. C., Abbasi, S., & McClements, D. J. (2015). Stabilization of biopolymer microgels formed by electrostatic complexation: Influence of enzyme (laccase) cross-linking on pH, thermal, and mechanical stability. *Food Research International, 78*: 18-26.

Baier, A. K., & Knorr, D. (2015). Influence of high isostatic pressure on structural and functional characteristics of potato protein. *Food Research International, 77*: 753-761.

Barka, A., Amira, A. B., Francis, F., & Blecker, C. (2018). Physicochemical characterization of colored soluble protein fractions extracted from Spirulina (Spirulina platensis). *Food Science and Technology International, 24*(8): 651-663.

Bárta, J., Bártová, V., Zdráhal, Z., & Šedo, O. (2012). Cultivar Variability of Patatin Biochemical Characteristics: Table versus Processing Potatoes (Solanum tuberosum L.). *Journal of Agricultural and Food Chemistry, 60*(17): 4369-4378.

Benjamin P. Partlow, Matthew B. Applegate, Fiorenzo G. Omenetto, & Kaplan, D. L. (2016). Dityrosine Cross-Linking in Designing Biomaterials. *ACS Biomaterial Science & Engineering, 2*(12): 2108-2121.

Berthet, S., Thevenin, J., Baratiny, D., Demont-Caulet, N., Debeaujon, I., Bidzinski, P., Leple, J.-C., Huis, R., Hawkins, S., Gomez, L.-D., Lapierre, C., & Jouanin, L. (2012). Role of Plant Laccases in Lignin Polymerization. In *Lignins - Biosynthesis, Biodegradation and Bioengineering* (pp. 145-172).

Berton-Carabin, C. C., Schröder, A., Rovalino-Cordova, A., Schroën, K., & Sagis, L. (2016). Protein and lipid oxidation affect the viscoelasticity of whey protein layers at the oil-water interface. *European Journal of Lipid Science and Technology, 118*(11): 1630-1643.

Bertrand, T., Jolivalt, C., Briozzo, P., Caminade, E., Joly, N., Madzak, C., & Mougin, C. (2002). Crystal structure of a four-copper laccase complexed with an arylamine: insights into substrate recognition and correlation with kinetics. *Biochemistry, 41*(23): 7325-7333.

Bertsch, P., Thoma, A., Bergfreund, J., Geue, T., & Fischer, P. (2019). Transient measurement and structure analysis of protein-polysaccharide multilayers at fluid interfaces. *Soft Matter, 15*(31): 6362-6368.

Bilal, M., Rasheed, T., Nabeel, F., Iqbal, H. M. N., & Zhao, Y. (2019). Hazardous contaminants in the environment and their laccase-assisted degradation – A review. *Journal of Environmental Management, 234*: 253-264.

Blake, C. C. F., Koenig, D. F., Mair, G. A., North, A. C. T., Phillips, D. C., & Sarma, V. R. (1965). Structure of Hen Egg-White Lysozyme: A Three-dimensional Fourier Synthesis at 2 Å Resolution. *Nature, 206*(4986): 757-761.

Bos, A. M., & van Vliet, T. (2001). Interfacial rheological properties of adsorbed protein layers and surfactants: a review. *Advances in Colloid and Interface Science, 91*(3): 437-471.

Bouferkas, Y., Haddi, A., Mehedi, N., Saidi, D., Kheroua, O., , & (2019). Enzymatic treatment of gliadins triggers anaphylactic reaction in a murine model of wheat allergy- in vivo and ex vivo study. *Bioscience Research, 16*(2): 1377-1390.

Bradford, M. M. (1976). A rapid and sensitive method for the quantitation of microgram quantities of protein utilizing the principle of protein-dye binding. *Analytical Biochemistry, 72*: 248-254.

Braiuca, P., Ebert, C., Basso, A., Linda, P., & Gardossi, L. (2006). Computational methods to rationalize experimental strategies in biocatalysis. *Trends in Biotechnology, 24*(9): 419-425.

Buchert, J., Ercili Cura, D., Ma, H., Gasparetti, C., Monogioudi, E., Faccio, G., Mattinen, M., Boer, H., Partanen, R., Selinheimo, E., Lantto, R., & Kruus, K. (2010). Crosslinking food proteins for improved functionality. *Annual Review of Food Science and Technology, 1*: 113-138.

Buchert, J., Selinheimo, E., Kruus, K., Mattinen, M.-L., Lantto, R., & Autio, K. (2007). Using crosslinking enzymes to improve textural and other properties of food. In *Novel Enzyme Technology for Food Applications* (pp. 101-139).

Bunzel, M., Ralph, J., Bruning, P., & Steinhart, H. (2006). Structural identification of dehydrotriferulic and dehydrotetraferulic acids isolated from insoluble maize bran fiber. *Journal of Agricultural and Food Chemistry, 54*(17): 6409-6418.

Bunzel, M., Ralph, J., Marita, J. M., Hatfield, R. D., & Steinhart, H. (2001). Diferulates as structural components in soluble and insoluble cereal dietary fibre. *Journal of the Science of Food and Agriculture, 81*(7): 653-660.

Caillard, R., Remondetto, G. E., Mateescu, M. A., & Subirade, M. (2008). Characterization of amino cross-linked soy protein hydrogels. *Journal of Food Science, 73*(5): C283-291.

Carunchio, F., Crescenzi, C., Girelli, A. M., Messina, A., & Tarola, A. M. (2001). Oxidation of ferulic acid by laccase: identification of the products and inhibitory effects of some dipeptides. *Talanta, 55*(1): 189-200.

Carvalho, N. C. d., Pessato, T. B., Negrão, F., Eberlin, M. N., Behrens, J. H., Zollner, R. d. L., & Netto, F. M. (2019). Physicochemical changes and bitterness of whey protein hydrolysates after transglutaminase cross-linking. *LWT - Food Science and Technology, 113*.

Cassie, N., Anderson, R. L., Wilson, D., Pawsey, A., Mercer, J. G., & Barrett, P. (2017). Body weight loss, effective satiation and absence of homeostatic neuropeptide compensation in male Sprague Dawley rats schedule fed a protein crosslinked diet. *Appetite, 117*: 234-246.

Chang, C., Tu, S., Ghosh, S., & Nickerson, M. T. (2015). Effect of pH on the inter-relationships between the physicochemical, interfacial and emulsifying properties for pea, soy, lentil and canola protein isolates. *Food Research International, 77*: 360-367.

Chen, B., Li, H., Ding, Y., & Suo, H. (2012). Formation and microstructural characterization of whey protein isolate/beet pectin coacervations by laccase catalyzed cross-linking. *LWT - Food Science and Technology, 47*(1): 31-38.

Chen, H., Gan, J., Ji, A., Song, S., & Yin, L. (2019). Development of double network gels based on soy protein isolate and sugar beet pectin induced by thermal treatment and laccase catalysis. *Food Chemistry, 292*: 188-196.

Chen, H., Ji, A., Qiu, S., Liu, Y., Zhu, Q., & Yin, L. (2018). Covalent conjugation of bovine serum album and sugar beet pectin through Maillard reaction/laccase catalysis to improve the emulsifying properties. *Food Hydrocolloids, 76*: 173-183.

Chen, R., Li, L., & Weng, Z. (2003). ZDOCK: an initial-stage protein-docking algorithm. *Proteins, 52*(1): 80-87.

Chi, C. F., Hu, F. Y., Wang, B., Li, Z. R., & Luo, H. Y. (2015). Influence of Amino Acid Compositions and Peptide Profiles on Antioxidant Capacities of Two Protein Hydrolysates from Skipjack Tuna (Katsuwonus pelamis) Dark Muscle. *Marine Drugs, 13*(5): 2580-2601.

Chung, J. E., Kurisawa, M., Uyama, H., & Kobayashi, S. (2003). Enzymatic synthesis and antioxidant property of gelatin-catechin conjugates. *Biotechnology Letters, 25*(23): 1993-1997.

Colombo, A., Ribotta, P. D., & Leon, A. E. (2010). Differential scanning calorimetry (DSC) studies on the thermal properties of peanut proteins. *Journal of Agricultural and Food Chemistry, 58*(7): 4434-4439.

Creusot, N., Wierenga, P. A., Laus, M. C., Giuseppin, M. L., & Gruppen, H. (2011). Rheological properties of patatin gels compared with beta-lactoglobulin, ovalbumin, and glycinin. *Journal of the Science of Food and Agriculture, 91*(2): 253-261.

Dabrowska, A., Bajzert, J., Babij, K., Szoltysik, M., Stefaniak, T., Willak-Janc, E., & Chrzanowska, J. (2020). Reduced IgE and IgG antigenic response to milk proteins hydrolysates obtained with the use of non-commercial serine protease from Yarrowia lipolytica. *Food Chemistry, 302*: 125350.

Dachmann, E., Nobis, V., Kulozik, U., & Dombrowski, J. (2020). Surface and foaming properties of potato proteins: Impact of protein concentration, pH value and ionic strength. *Food Hydrocolloids, 107*.

Daliri, E. B., Oh, D. H., & Lee, B. H. (2017). Bioactive Peptides. *Foods, 6*(5).

Danaei, M., Dehghankhold, M., Ataei, S., Hasanzadeh Davarani, F., Javanmard, R., Dokhani, A., Khorasani, S., & Mozafari, M. R. (2018). Impact of Particle Size and Polydispersity Index on the Clinical Applications of Lipidic Nanocarrier Systems. *Pharmaceutics, 10*(2).

David, S., & Livney, Y. D. (2016). Potato protein based nanovehicles for health promoting hydrophobic bioactives in clear beverages. *Food Hydrocolloids, 57*: 229-235.

de Jongh, H. H., Kosters, H. A., Kudryashova, E., Meinders, M. B., Trofimova, D., & Wierenga, P. A. (2004). Protein adsorption at air-water interfaces: a combination of details. *Biopolymers, 74*(1-2): 131-135.

de Oliveira, F. C., Coimbra, J. S., de Oliveira, E. B., Zuniga, A. D., & Rojas, E. E. (2016). Food Protein-polysaccharide Conjugates Obtained via the Maillard Reaction: A Review. *Critical Reviews in Food Science and Nutrition, 56*(7): 1108-1125.

Deng, C., Liu, Y., Li, J., Yadav, M. P., & Yin, L. (2018). Diverse rheological properties, mechanical characteristics and microstructures of corn fiber gum/soy protein isolate hydrogels prepared by laccase and heat treatment. *Food Hydrocolloids, 76*: 113-122.

Deutzmann, R. (2004). Structural Characterization of Proteins and Peptides. In J. Decler & U. Reischl (Eds.), *Molecular Diagnosis of Infectious Diseases* (pp. 269-297). Totowa, NJ: Humana Press.

Dhayal, S. K., Sforza, S., Wierenga, P. A., & Gruppen, H. (2015). Peroxidase induced oligo-tyrosine cross-links during polymerization of alpha-lactalbumin. *Biochimica et Biophysica Acta, 1854*(12): 1898-1905.

Díaz-Rodríguez, A., & Davis, B. G. (2011). Chemical modification in the creation of novel biocatalysts. *Current Opinion in Chemical Biology, 15*(2): 211-219.

Dickinson, E. (1999). Adsorbed protein layers at fluid interfaces: interactions, structure and surface rheology. *Colloids and Surfaces B: Biointerfaces, 15*(2): 161-176.

Drago, S. R., & González, R. J. (2000). Foaming properties of enzymatically hydrolysed wheat gluten. *Innovative Food Science & Emerging Technologies, 1*(4): 269-273.

Du, X., Li, Y., Xia, Y. L., Ai, S. M., Liang, J., Sang, P., Ji, X. L., & Liu, S. Q. (2016). Insights into protein-ligand Interactions: mechanisms, models, and methods. *International Journal of Molecular Sciences, 17*(2).

Duan, X., Li, M., Shao, J., Chen, H., Xu, X., Jin, Z., & Liu, X. (2018). Effect of oxidative modification on structural and foaming properties of egg white protein. *Food Hydrocolloids, 75*: 223-228.

Dube, M., Schäfer, C., Neidhart, S., & Carle, R. (2006). Texturisation and modification of vegetable proteins for food applications using microbial transglutaminase. *European Food Research and Technology, 225*(2): 287-299.

Ducros, V., Brzozowski, A. M., Wilson, K. S., Brown, S. H., Ostergaard, P., Schneider, P., Yaver, D. S., Pedersen, A. H., & Davies, G. J. (1998). Crystal structure of the type-2 Cu depleted laccase from Coprinus cinereus at 2.2 A resolution. *Nature Structural & Molecular Biology, 5*(4): 310-316.

Ehrenshaft, M., Deterding, L. J., & Mason, R. P. (2015). Tripping up Trp: Modification of protein tryptophan residues by reactive oxygen species, modes of detection, and biological consequences. *Free Radical Biology and Medicine, 89*: 220-228.

Eissa, A. S., Puhl, C., Kadla, J. F., & Khan, S. A. (2006). Enzymatic cross-linking of beta-lactoglobulin: conformational properties using FTIR spectroscopy. *Biomacromolecules, 7*(6): 1707-1713.

Elahi, R., & Mu, T. H. (2017). High Hydrostatic Pressure (HHP)-Induced Structural Modification of Patatin and Its Antioxidant Activities. *Molecules, 22*(3).

Enguita, F. J., Marcal, D., Martins, L. O., Grenha, R., Henriques, A. O., Lindley, P. F., & Carrondo, M. A. (2004). Substrate and dioxygen binding to the endospore coat laccase from Bacillus subtilis. *Journal of Biological Chemistry, 279*(22): 23472-23476.

Ercili Cura, D., Lantto, R., Lille, M., Andberg, M., Kruus, K., & Buchert, J. (2009). Laccase-aided protein modification: Effects on the structural properties of acidified sodium caseinate gels. *International Dairy Journal, 19*(12): 737-745.

Ercili-Cura, D., Miyamoto, A., Paananen, A., Yoshii, H., Poutanen, K., & Partanen, R. (2015). Adsorption of oat proteins to air–water interface in relation to their colloidal state. *Food Hydrocolloids, 44*: 183-190.

Ercili-Cura, D., Partanen, R., Husband, F., Ridout, M., Macierzanka, A., Lille, M., Boer, H., Lantto, R., Buchert, J., & Mackie, A. R. (2012). Enzymatic cross-linking of β-

lactoglobulin in solution and at air–water interface: Structural constraints. *Food Hydrocolloids, 28*(1): 1-9.

Ernst, H. A., Jorgensen, L. J., Bukh, C., Piontek, K., Plattner, D. A., Ostergaard, L. H., Larsen, S., & Bjerrum, M. J. (2018). A comparative structural analysis of the surface properties of asco-laccases. *PLoS One, 13*(11): e0206589.

Fan, H. Y., Duquette, D., Dumont, M. J., & Simpson, B. K. (2018). Salmon skin gelatin-corn zein composite films produced via crosslinking with glutaraldehyde: Optimization using response surface methodology and characterization. *International Journal of Biological Macromolecules, 120*(Pt A): 263-273.

Fauconnier, M.-L., Blecker, C., Groyne, J., Razafindralambo, H., Vanzeveren, E., Marlier, M., & Paquot, M. (2000). Characterization of Two Acacia Gums and Their Fractions Using a Langmuir Film Balance. *Journal of Agricultural and Food Chemistry, 48*(7): 2709-2712.

Feeney, R. E. (1977). Chemical Modification of Food Proteins. In *Food Proteins* (Vol. 160, pp. 3-36): AMERICAN CHEMICAL SOCIETY.

Felix, M., Yang, J., Guerrero, A., & Sagis, L. M. C. (2019). Effect of cinnamaldehyde on interfacial rheological properties of proteins adsorbed at O/W interfaces. *Food Hydrocolloids, 97*: 105235.

Fenoll, L. G., Rodriguez-Lopez, J. N., Varon, R., Garcia-Ruiz, P. A., Garcia-Canovas, F., & Tudela, J. (2002). Kinetic characterisation of the reaction mechanism of mushroom tyrosinase on tyramine/dopamine and L-tyrosine methyl esther/L-dopa methyl esther. *The International Journal of Biochemistry & Cell Biology, 34*(12): 1594-1607.

Ferraroni, M., Myasoedova, N. M., Schmatchenko, V., Leontievsky, A. A., Golovleva, L. A., Scozzafava, A., & Briganti, F. (2007). Crystal structure of a blue laccase from Lentinus tigrinus: evidences for intermediates in the molecular oxygen reductive splitting by multicopper oxidases. *BMC Structural Biology, 7*(1): 60.

Figueroa-Espinoza, M. C., & Rouau, X. (1998). Oxidative Cross-Linking of Pentosans by a Fungal Laccase and Horseradish Peroxidase: Mechanism of Linkage Between Feruloylated Arabinoxylans. *Cereal Chemistry, 75*(2): 259-265.

Fincher, G. B. (1976). FERULIC ACID IN BARLEY CELL WALLS: A FLUORESCENCE STUDY. *Journal of the Institute of Brewing, 82*(6): 347-349.

Flambeau, M., Redl, A., & Respondek, F. (2017). Proteins From Wheat. In *Sustainable Protein Sources* (pp. 67-78).

Flanagan, J., & Singh, H. (2006). Conjugation of sodium caseinate and gum arabic catalyzed by transglutaminase. *Journal of Agricultural and Food Chemistry, 54*(19): 7305-7310.

Flander, L., Holopainen, U., Kruus, K., & Buchert, J. (2011). Effects of tyrosinase and laccase on oat proteins and quality parameters of gluten-free oat breads. *Journal of Agricultural and Food Chemistry, 59*(15): 8385-8390.

Foegeding, E. A., & Davis, J. P. (2011). Food protein functionality: A comprehensive approach. *Food Hydrocolloids, 25*(8): 1853-1864.

Frasconi, M., Favero, G., Boer, H., Koivula, A., & Mazzei, F. (2010). Kinetic and biochemical properties of high and low redox potential laccases from fungal and plant origin. *Biochimica et Biophysica Acta, 1804*(4): 899-908.

Fritsch, C., Staebler, A., Happel, A., Cubero Márquez, M., Aguiló-Aguayo, I., Abadias, M., Gallur, M., Cigognini, I., Montanari, A., López, M., Suárez-Estrella, F., Brunton, N., Luengo, E., Sisti, L., Ferri, M., & Belotti, G. (2017). Processing, Valorization and Application of Bio-Waste Derived Compounds from Potato, Tomato, Olive and Cereals: A Review. *Sustainability, 9*(8).

Fuchs, S., Kutscher, M., Hertel, T., Winter, G., Pietzsch, M., & Coester, C. (2010). Transglutaminase: new insights into gelatin nanoparticle cross-linking. *Journal of Microencapsulation, 27*(8): 747-754.

Gao, Y., Li, J., Chang, C., Wang, C., Yang, Y., & Su, Y. (2019). Effect of enzymatic hydrolysis on heat stability and emulsifying properties of egg yolk. *Food Hydrocolloids, 97*.

Garavaglia, S., Teresa Cambria, M., Miglio, M., Ragusa, S., Iacobazzi, V., Palmieri, F., D'Ambrosio, C., Scaloni, A., & Rizzi, M. (2004). The Structure of Rigidoporus lignosus Laccase Containing a Full Complement of Copper Ions, Reveals an Asymmetrical Arrangement for the T3 Copper Pair. *Journal of Molecular Biology, 342*(5): 1519-1531.

Gazme, B., & Madadlou, A. (2014). Fabrication of whey protein–pectin conjugate particles through laccase-induced gelation of microemulsified nanodroplets. *Food Hydrocolloids, 40*: 189-195.

Gharbi, N., & Labbafi, M. (2019). Influence of treatment-induced modification of egg white proteins on foaming properties. *Food Hydrocolloids, 90*: 72-81.

Ghigo, G., Vione, D., & Berto, S. (2020). Experimental and theoretical study of the fluorescence emission of ferulic acid: Possible insights into the fluorescence properties of humic substances. *Spectrochimica Acta Part A: Molecular and Biomolecular Spectroscopy, 228*.

Giardina, P., Faraco, V., Pezzella, C., Piscitelli, A., Vanhulle, S., & Sannia, G. (2010). Laccases: a never-ending story. *Cellular and Molecular Life Sciences, 67*(3): 369-385.

Gill, J., Orsat, V., & Kermasha, S. (2018). Optimization of encapsulation of a microbial laccase enzymatic extract using selected matrices. *Process Biochemistry, 65*: 55-61.

Giosafatto, C. V. L., Rigby, N. M., Wellner, N., Ridout, M., Husband, F., & Mackie, A. R. (2012). Microbial transglutaminase-mediated modification of ovalbumin. *Food Hydrocolloids, 26*(1): 261-267.

Glusac, J., Davidesko-Vardi, I., Isaschar-Ovdat, S., Kukavica, B., & Fishman, A. (2018). Gel-like emulsions stabilized by tyrosinase-crosslinked potato and zein proteins. *Food Hydrocolloids, 82*: 53-63.

Glusac, J., Davidesko-Vardi, I., Isaschar-Ovdat, S., Kukavica, B., & Fishman, A. (2019). Tyrosinase-crosslinked pea protein emulsions: Impact of zein incorporation. *Food Research International, 116*: 370-378.

Glusac, J., Isaschar-Ovdat, S., Kukavica, B., & Fishman, A. (2017). Oil-in-water emulsions stabilized by tyrosinase-crosslinked potato protein. *Food Research International, 100*(Pt 1): 407-415.

Gomes, M. H. G., & Kurozawa, L. E. (2020). Improvement of the functional and antioxidant properties of rice protein by enzymatic hydrolysis for the microencapsulation of linseed oil. *Journal of Food Engineering, 267*.

Gómez-Estaca, J., Gómez-Guillén, M. C., Fernández-Martín, F., & Montero, P. (2011). Effects of gelatin origin, bovine-hide and tuna-skin, on the properties of compound gelatin–chitosan films. *Food Hydrocolloids, 25*(6): 1461-1469.

Gorissen, S. H. M., Crombag, J. J. R., Senden, J. M. G., Waterval, W. A. H., Bierau, J., Verdijk, L. B., & van Loon, L. J. C. (2018). Protein content and amino acid composition of commercially available plant-based protein isolates. *Amino Acids, 50*(12): 1685-1695.

Gui, Y., Li, J., Zhu, Y., & Guo, L. (2020). Roles of four enzyme crosslinks on structural, thermal and gel properties of potato proteins. *LWT - Food Science and Technology, 123*.

Guimarães, L. R. C., Woiciechowski, A. L., Karp, S. G., Coral, J. D., Zandoná Filho, A., & Soccol, C. R. (2017). 9 - Laccases. In *Current Developments in Biotechnology and Bioengineering* (pp. 199-216): Elsevier.

Gunnoo, S. B., & Madder, A. (2016). Bioconjugation - using selective chemistry to enhance the properties of proteins and peptides as therapeutics and carriers. *Organic and Biomolecular Chemistry, 14*(34): 8002-8013.

Guo, X., Guo, X., Yu, S., & Kong, F. (2018). Influences of the different chemical components of sugar beet pectin on the emulsifying performance of conjugates formed between sugar beet pectin and whey protein isolate. *Food Hydrocolloids, 82*: 1-10.

Gupta, P., & Nayak, K. K. (2015). Characteristics of protein-based biopolymer and its application. *Polymer Engineering & Science, 55*(3): 485-498.

Habeeb, A. F. S. A. (1966). Determination of free amino groups in proteins by trinitrobenzenesulfonic acid. *Analytical Biochemistry, 14*(3): 328-336.

Hamdani, A. M., Wani, I. A., Bhat, N. A., & Siddiqi, R. A. (2018). Effect of guar gum conjugation on functional, antioxidant and antimicrobial activity of egg white lysozyme. *Food Chemistry, 240*: 1201-1209.

Hartree, E. F. (1972). Determination of Protein- A Modification of the Lowry Method That Gives a Linear Photometric Response *Analytical biochemistry, 48*: 422-427.

Harukaze, A., Sugiyama, S., Iwamoto, Y., Murata, M., & Homma, S. (2000). Convenient Analysis and Quantification of Diferulic Acids in Foods. *Food Science and Technology Research, 6*(2): 122-125.

Hawe, A., Sutter, M., & Jiskoot, W. (2008). Extrinsic fluorescent dyes as tools for protein characterization. *Pharmaceutical Research, 25*(7): 1487-1499.

Heck, T., Faccio, G., Richter, M., & Thony-Meyer, L. (2013). Enzyme-catalyzed protein crosslinking. *Applied Microbiology and Biotechnology, 97*(2): 461-475.

Hermanson, G. T. (2013). The Reactions of Bioconjugation. In *Bioconjugate Techniques* (pp. 229-258).

Hiller, B., & Lorenzen, P. C. (2008). Surface hydrophobicity of physicochemically and enzymatically treated milk proteins in relation to techno-functional properties. *Journal of Agricultural and Food Chemistry, 56*(2): 461-468.

Hiller, B., & Lorenzen, P. C. (2009). Functional properties of milk proteins as affected by enzymatic oligomerisation. *Food Research International, 42*(8): 899-908.

Hiller, B., & Lorenzen, P. C. (2011). Optimization of enzymatic oligomerization reaction conditions for three milk protein products via ceteris-paribus approach. *Food Research International, 44*(9): 3118-3122.

Holck, J., Lorentzen, A., Vigsnæs, L. K., Licht, T. R., Mikkelsen, J. D., & Meyer, A. S. (2011). Feruloylated and Nonferuloylated Arabino-oligosaccharides from Sugar Beet Pectin Selectively Stimulate the Growth of Bifidobacterium spp. in Human Fecal in Vitro Fermentations. *Journal of Agricultural and Food Chemistry, 59*(12): 6511-6519.

Hollmann, F., & Arends, I. W. C. E. (2012). Enzyme Initiated Radical Polymerizations. *Polymers, 4*(1): 759-793.

Houde, M., Khodaei, N., Benkerroum, N., & Karboune, S. (2018). Barley protein concentrates: Extraction, structural and functional properties. *Food Chemistry, 254*: 367-376.

Hu, Z., Qiu, L., Sun, Y., Xiong, H., & Ogra, Y. (2019). Improvement of the solubility and emulsifying properties of rice bran protein by phosphorylation with sodium trimetaphosphate. *Food Hydrocolloids, 96*: 288-299.

Hunter, T. N., Pugh, R. J., Franks, G. V., & Jameson, G. J. (2008). The role of particles in stabilising foams and emulsions. *Advances in Colloid and Interface Science, 137*(2): 57-81.

Ibrahim, H. R., Higashiguchi, S., Koketsu, M., Juneja, L. R., Kim, M., Yamamoto, T., Sugimoto, Y., & Aoki, T. (1996). Partially Unfolded Lysozyme at Neutral pH Agglutinates and Kills Gram-Negative and Gram-Positive Bacteria through Membrane Damage Mechanism. *Journal of Agricultural and Food Chemistry, 44*(12): 3799-3806.

Isaschar-Ovdat, S., Davidovich-Pinhas, M., & Fishman, A. (2016). Modulating the gel properties of soy glycinin by crosslinking with tyrosinase. *Food Research International, 87*: 42-49.

Isaschar-Ovdat, S., & Fishman, A. (2017). Mechanistic insights into tyrosinase-mediated crosslinking of soy glycinin derived peptides. *Food Chemistry, 232*: 587-594.

Isaschar-Ovdat, S., & Fishman, A. (2018). Crosslinking of food proteins mediated by oxidative enzymes – A review. *Trends in Food Science & Technology, 72*: 134-143.

Isaschar-Ovdat, S., Rosenberg, M., Lesmes, U., & Fishman, A. (2015). Characterization of oil-in-water emulsions stabilized by tyrosinase-crosslinked soy glycinin. *Food Hydrocolloids, 43*: 493-500.

James, P., & Numat, K. (2013). Polymerization of Peptide Polymers for Biomaterial Applications. In *Polymer Science*.

Jarpa-Parra, M., Bamdad, F., Tian, Z., Zeng, H., Temelli, F., & Chen, L. (2015). Impact of pH on molecular structure and surface properties of lentil legumin-like protein and its application as foam stabilizer. *Colloids Surf B Biointerfaces, 132*: 45-53.

Jia, N., Zhang, F., Liu, Q., Wang, L., Lin, S., & Liu, D. (2019). The beneficial effects of rutin on myofibrillar protein gel properties and related changes in protein conformation. *Food Chemistry, 301*: 125206.

Jiang, Z., Yuan, X., Yao, K., Li, X., Zhang, X., Mu, Z., Jiang, L., & Hou, J. (2017). Laccase-aided modification: Effects on structure, gel properties and antioxidant activities of α-lactalbumin. *LWT - Food Science and Technology, 80*: 355-363.

Jimenez-Saiz, R., Benede, S., Miralles, B., Lopez-Exposito, I., Molina, E., & Lopez-Fandino, R. (2014). Immunological behavior of in vitro digested egg-white lysozyme. *Molecular Nutrition & Food Research, 58*(3): 614-624.

Jung, & Wicker. (2012a). Laccase mediated conjugation of sugar beet pectin and the effect on emulsion stability. *Food Hydrocolloids, 28*(1): 168-173.

Jung, J., & Wicker, L. (2012b). Laccase mediated conjugation of heat treated beta-lactoglobulin and sugar beet pectin. *Carbohydrate Polymer, 89*(4): 1244-1249.

Jung, J., & Wicker, L. (2014). β-Lactoglobulin conformation and mixed sugar beet pectin gel matrix is changed by laccase. *LWT - Food Science and Technology, 55*(1): 9-15.

Jung, S., Murphy, P. A., & Johnson, L. A. (2005). Physicochemical and Functional Properties of Soy Protein Substrates Modified by Low Levels of Protease Hydrolysis. *Journal of Food Science, 70*(2): C180-C187.

Jus, S., Stachel, I., Fairhead, M., Meyer, M., Thöny-meyer, L., & Guebitz, G. M. (2012). Enzymatic cross-linking of gelatine with laccase and tyrosinase. *Biocatalysis and Biotransformation, 30*(1): 86-95.

Jus, S., Stachel, I., Schloegl, W., Pretzler, M., Friess, W., Meyer, M., Birner-Gruenberger, R., & Guebitz, G. M. (2011). Cross-linking of collagen with laccases and tyrosinases. *Materials Science and Engineering: C, 31*(5): 1068-1077.

Juvonen, K. R., Macierzanka, A., Lille, M. E., Laaksonen, D. E., Mykkanen, H. M., Niskanen, L. K., Pihlajamaki, J., Makela, K. A., Mills, C. E., Mackie, A. R., Malcolm, P., Herzig, K. H., Poutanen, K. S., & Karhunen, L. J. (2015). Cross-linking of sodium caseinate-structured emulsion with transglutaminase alters postprandial metabolic and appetite responses in healthy young individuals. *British Journal of Nutrition, 114*(3): 418-429.

K, A., & Bandyopadhyay, P. (2012). Polysaccharide-Protein Interactions and Their Relevance in Food Colloids. In *The Complex World of Polysaccharides*.

Kato, A., Tsutsui, N., Matsudomi, N., Kobayashi, K., & Nakai, S. (2014). Effects of Partial Denaturation on Surface Properties of Ovalbumin and Lysozyme. *Agricultural and Biological Chemistry, 45*(12): 2755-2760.

Kazlauskas, R. J. (2000). Molecular modeling and biocatalysis: explanations, predictions, limitations, and opportunities. *Current Opinion in Chemical Biology, 4*(1): 81-88.
Khodaei, N., & Karboune, S. (2013). Extraction and structural characterisation of rhamnogalacturonan I-type pectic polysaccharides from potato cell wall. *Food Chemistry, 139*(1-4): 617-623.
Kieliszek, M., & Misiewicz, A. (2014). Microbial transglutaminase and its application in the food industry. A review. *Folia Microbiologica, 59*(3): 241-250.
Kim, S., & Cavaco-Paulo, A. (2011). Laccase-catalysed protein–flavonoid conjugates for flax fibre modification. *Applied Microbiology and Biotechnology, 93*(2): 585-600.
Komarnytsky, S., Cook, A., & Raskin, I. (2011). Potato protease inhibitors inhibit food intake and increase circulating cholecystokinin levels by a trypsin-dependent mechanism. *International Journal of Obesity, 35*(2): 236-243.
Kowalczewski, P. L., Olejnik, A., Bialas, W., Rybicka, I., Zielinska-Dawidziak, M., Siger, A., Kubiak, P., & Lewandowicz, G. (2019). The Nutritional Value and Biological Activity of Concentrated Protein Fraction of Potato Juice. *Nutrients, 11*(7).
Kudanga, T., Nemadziva, B., & Le Roes-Hill, M. (2017). Laccase catalysis for the synthesis of bioactive compounds. *Applied Microbiology and Biotechnology, 101*(1): 13-33.
Kuijpers, A. J., Engbers, G. H. M., Feijen, J., De Smedt, S. C., Meyvis, T. K. L., Demeester, J., Krijgsveld, J., Zaat, S. A. J., & Dankert, J. (1999). Characterization of the Network Structure of Carbodiimide Cross-Linked Gelatin Gels. *Macromolecules, 32*(10): 3325-3333.
Kunamneni, A., Plou, F. J., Ballesteros, A., & Alcalde, M. (2008). Laccases and their applications: a patent review. *Recent Patents on Biotechnology, 2*(1): 10-24.
Kurniawati, S., & Nicell, J. A. (2009). A comprehensive kinetic model of laccase-catalyzed oxidation of aqueous phenol. *Biotechnology Progress, 25*(3): 763-773.
Kwang-Soo, S., & Chang-Jin, K. (1998). Properties of laccase purified from nitrogen limited culture of white-rot fungus Coriolus hirsutus. *Biotechnology Techniques, 12*(2): 101-104.
Labat, E., Morel, M. H., & Rouau, X. (2001). Effect of laccase and manganese peroxidase on wheat gluten and pentosans during mixing. *Food Hydrocolloids, 15*(1): 47-52.
Laemmli, U. K. (1970). Cleavage of Structural Proteins during the Assembly of the Head of Bacteriophage T4. *Nature, 227*(5259): 680-685.
Lamsal, B. P., Reitmeier, C., Murphy, P. A., & Johnson, L. A. (2006). Enzymatic hydrolysis of extruded-expelled soy flour and resulting functional properties. *Journal of the American Oil Chemists' Society, 83*(8): 731-737.
Lantto, R., Puolanne, E., Kalkkinen, N., Buchert, J., & Autio, K. (2005). Enzyme-aided modification of chicken-breast myofibril proteins: effect of laccase and transglutaminase on gelation and thermal stability. *Journal of Agricultural and Food Chemistry*

, 53(23): 9231-9237.
Lee, H., Yildiz, G., dos Santos, L. C., Jiang, S., Andrade, J. E., Engeseth, N. J., & Feng, H. (2016). Soy protein nano-aggregates with improved functional properties prepared by sequential pH treatment and ultrasonication. *Food Hydrocolloids, 55*: 200-209.
Leroux, J., Langendorff, V., Schick, G., Vaishnav, V., & Mazoyer, J. (2003). Emulsion stabilizing properties of pectin. *Food Hydrocolloids, 17*(4): 455-462.
Li, C., & Xiong, Y. L. (2015). Disruption of secondary structure by oxidative stress alters the cross-linking pattern of myosin by microbial transglutaminase. *Meat science, 108*: 97-105.

Li, C., Xiong, Y. L., & Chen, J. (2012). Oxidation-induced unfolding facilitates Myosin cross-linking in myofibrillar protein by microbial transglutaminase. *Journal of Agricultural and Food Chemistry, 60*(32): 8020-8027.

Li, M., & Karboune, S. (2020). Laccase-catalyzed conjugation of potato protein with selected pectic polysaccharides: conjugation efficiency and emulsification properties. *Food Chemistry*: Under peer review.

Li, M., Liu, L., Kermasha, S., & Karboune, S. (2020). Laccase-Catalyzed Oxidative Cross-linking of Tyrosine and Potato Patatin- and Lysozyme-Derived Peptides: Molecular and Kinetic Study *Enzyme and Microbial Technology*: Under peer review.

Li, S., Huang, Y., An, F., Huang, Q., Geng, F., & Ma, M. (2019). Hydroxyl radical-induced early stage oxidation improves the foaming and emulsifying properties of ovalbumin. *Poultry Science, 98*(2): 1047-1054.

Liang, H.-N., & Tang, C.-H. (2013). Emulsifying and Interfacial Properties of Vicilins: Role of Conformational Flexibility at Quaternary and/or Tertiary Levels. *Journal of Agricultural and Food Chemistry, 61*(46): 11140-11150.

Littoz, F., & McClements, D. J. (2008). Bio-mimetic approach to improving emulsion stability: Cross-linking adsorbed beet pectin layers using laccase. *Food Hydrocolloids, 22*(7): 1203-1211.

Liu, F., Ma, C., Gao, Y., & McClements, D. J. (2017). Food-Grade Covalent Complexes and Their Application as Nutraceutical Delivery Systems: A Review. *Comprehensive Reviews in Food Science and Food Safety, 16*(1): 76-95.

Liu, F., Sun, C., Yang, W., Yuan, F., & Gao, Y. (2015). Structural characterization and functional evaluation of lactoferrin–polyphenol conjugates formed by free-radical graft copolymerization. *RSC Advances, 5*(20): 15641-15651.

Liu, J., Ru, Q., & Ding, Y. (2012). Glycation a promising method for food protein modification: Physicochemical properties and structure, a review. *Food Research International, 49*(1): 170-183.

Liu, K., Chen, S., Chen, H., Tong, P., & Gao, J. (2018). Cross-linked ovalbumin catalyzed by polyphenol oxidase: Preparation, structure and potential allergenicity. *International Journal of Biological Macromolecules, 107*(Pt B): 2057-2064.

Liu, Y., Qiu, S., Li, J., Chen, H., Tatsumi, E., Yadav, M., & Yin, L. (2015). Peroxidase-mediated conjugation of corn fiber gum and bovine serum albumin to improve emulsifying properties. *Carbohydrate Polymer, 118*: 70-78.

Liu, Y., Selig, M. J., Yadav, M. P., Yin, L., & Abbaspourrad, A. (2018). Transglutaminase-treated conjugation of sodium caseinate and corn fiber gum hydrolysate: Interfacial and dilatational properties. *Carbohydrate Polymer, 187*: 26-34.

Liu, Y., Wang, D., Wang, J., Yang, Y., Zhang, L., Li, J., & Wang, S. (2019). Functional properties and structural characteristics of phosphorylated pea protein isolate. *International Journal of Food Science & Technology*.

Liu, Y. Y., Zeng, X. A., Deng, Z., Yu, S. J., & Yamasaki, S. (2011). Effect of pulsed electric field on the secondary structure and thermal properties of soy protein isolate. *European Food Research and Technology, 233*(5): 841-850.

Loi, M., Quintieri, L., De Angelis, E., Monaci, L., Logrieco, A. F., Caputo, L., & Mulè, G. (2020). Yield improvement of the Italian fresh Giuncata cheese by laccase–induced protein crosslink. *International Dairy Journal, 100*.

Loi, M., Quintieri, L., Fanelli, F., Caputo, L., & Mule, G. (2018). Application of a recombinant laccase-chlorogenic acid system in protein crosslink and antioxidant properties of the curd. *Food Research International, 106*: 763-770.

Løkra, S., & Strætkvern, K. (2009). Industrial Proteins from Potato Juice. A Review. *Food, 3*: 88-95.

Lv, L., Tian, S., Ahmed, I., Ramesh Pavase, T., Lin, H., Xu, L., Li, Z., & Liu, F. (2019). Effect of laccase-catalyzed cross-linking on the structure and allergenicity of Paralichthys olivaceus parvalbumin mediated by propyl gallate. *Food Chemistry, 297*: 124972.

Ma, H., Forssell, P., Partanen, R., Buchert, J., & Boer, H. (2011). Improving laccase catalyzed cross-linking of whey protein isolate and their application as emulsifiers. *Journal of Agricultural and Food Chemistry, 59*(4): 1406-1414.

Ma, L., Li, A., Li, T., Li, M., Wang, X., Hussain, M. A., Qayum, A., Jiang, Z., & Hou, J. (2020). Structure and characterization of laccase-crosslinked α-lactalbumin: Impacts of high pressure homogenization pretreatment. *LWT - Food Science and Technology, 118*: 108843.

Ma, X., Chen, W., Yan, T., Wang, D., Hou, F., Miao, S., & Liu, D. (2020). Comparison of citrus pectin and apple pectin in conjugation with soy protein isolate (SPI) under controlled dry-heating conditions. *Food Chemistry, 309*: 125501.

Ma, X., Lozano-Ojalvo, D., Chen, H., Lopez-Fandiño, R., & Molina, E. (2015). Effect of high pressure-assisted crosslinking of ovalbumin and egg white by transglutaminase on their potential allergenicity. *Innovative Food Science & Emerging Technologies, 29*: 143-150.

Madzak, C., Mimmi, M. C., Caminade, E., Brault, A., Baumberger, S., Briozzo, P., Mougin, C., & Jolivalt, C. (2006). Shifting the optimal pH of activity for a laccase from the fungus Trametes versicolor by structure-based mutagenesis. *Protein Engineering, Design and Selection, 19*(2): 77-84.

Mäkinen, O. E., Sozer, N., Ercili-Cura, D., & Poutanen, K. (2017). Protein From Oat. In *Sustainable Protein Sources* (pp. 105-119).

Malencik, D. A., & Anderson, S. R. (2003). Dityrosine as a product of oxidative stress and fluorescent probe. *Amino Acids, 25*(3-4): 233-247.

Manhivi, V. E., Amonsou, E. O., & Kudanga, T. (2018). Laccase-mediated crosslinking of gluten-free amadumbe flour improves rheological properties. *Food Chemistry, 264*: 157-163.

Maravić, N., Šereš, Z., Nikolić, I., Dokić, P., Kertész, S., & Dokić, L. (2019). Emulsion stabilizing capacity of sugar beet fibers compared to sugar beet pectin and octenyl succinate modified maltodextrin in the production of O/W emulsions: individual and combined impact. *LWT - Food Science and Technology, 108*: 392-399.

Maria, K., Irina, Y., Manol, O., Yordan, G., & Veselin, K. (2012). Isolation, characterization and modification of citrus pectins. *Journal of BioScience and Biotechnology, 1*(3), 223-233.

Martins, A. C., Ribeiro, F. W., Zanatta, G., Freire, V. N., Morais, S., de Lima-Neto, P., & Correia, A. N. (2016). Modeling of laccase inhibition by formetanate pesticide using theoretical approaches. *Bioelectrochemistry, 108*: 46-53.

Matera, I., Gullotto, A., Tilli, S., Ferraroni, M., Scozzafava, A., & Briganti, F. (2008). Crystal structure of the blue multicopper oxidase from the white-rot fungus Trametes trogii complexed with p-toluate. *Inorganica Chimica Acta, 361*(14–15): 4129-4137.

Mattinen, M. L., Hellman, M., Permi, P., Autio, K., Kalkkinen, N., & Buchert, J. (2006). Effect of protein structure on laccase-catalyzed protein oligomerization. *Journal of Agricultural and Food Chemistry, 54*(23): 8883-8890.

Mattinen, M. L., Kruus, K., Buchert, J., Nielsen, J. H., Andersen, H. J., & Steffensen, C. L. (2005). Laccase-catalyzed polymerization of tyrosine-containing peptides. *FEBS 272*(14): 3640-3650.

McKerchar, H. J., Clerens, S., Dobson, R. C. J., Dyer, J. M., Maes, E., & Gerrard, J. A. (2019). Protein-protein crosslinking in food: Proteomic characterisation methods, consequences and applications. *Trends in Food Science & Technology, 86*: 217-229.

Medina-Navarro, R., Duran-Reyes, G., Diaz-Flores, M., & Vilar-Rojas, C. (2010). Protein antioxidant response to the stress and the relationship between molecular structure and antioxidant function. *PLoS One, 5*(1): e8971.

Mehra, R., Muschiol, J., Meyer, A. S., & Kepp, K. P. (2018). A structural-chemical explanation of fungal laccase activity. *Scientific Reports, 8*(1): 17285.

Meyer, S., Cartelat, A., Moya, I., & Cerovic, Z. G. (2003). UV-induced blue-green and far-red fluorescence along wheat leaves: a potential signature of leaf ageing. *Journal of Experimental Botany, 54*(383): 757-769.

Miedzianka, J., Pęksa, A., & Aniołowska, M. (2012). Properties of acetylated potato protein preparations. *Food Chemistry, 133*(4): 1283-1291.

Miedzianka, J., Peksa, A., Pokora, M., Rytel, E., Tajner-Czopek, A., & Kita, A. (2014). Improving the properties of fodder potato protein concentrate by enzymatic hydrolysis. *Food Chemistry, 159*: 512-518.

Mihajlovic, L., Radosavljevic, J., Nordlund, E., Krstic, M., Bohn, T., Smit, J., Buchert, J., & Cirkovic Velickovic, T. (2016). Peanut protein structure, polyphenol content and immune response to peanut proteins in vivo are modulated by laccase. *Food & Function, 7*(5): 2357-2366.

Minamihata, K., Goto, M., & Kamiya, N. (2011). Site-specific protein cross-linking by peroxidase-catalyzed activation of a tyrosine-containing peptide tag. *Bioconjugate Chemistry, 22*(1): 74-81.

Mine, Y., Ma, F., & Lauriau, S. (2004). Antimicrobial peptides released by enzymatic hydrolysis of hen egg white lysozyme. *Journal of Agricultural and Food Chemistry, 52*(5): 1088-1094.

Mine, Y., & Zhang, J. W. (2002). Comparative studies on antigenicity and allergenicity of native and denatured egg white proteins. *Journal of Agricultural and Food Chemistry, 50*(9): 2679-2683.

Minussi, R. C., Pastore, G. M., & Durán, N. (2002). Potential applications of laccase in the food industry. *Trends in Food Science & Technology, 13*(6): 205-216.

Mirmoghtadaie, L., Shojaee Aliabadi, S., & Hosseini, S. M. (2016). Recent approaches in physical modification of protein functionality. *Food Chemistry, 199*: 619-627.

Mokoonlall, A., Pfannstiel, J., Struch, M., Berger, R. G., & Hinrichs, J. (2016). Structure modification of stirred fermented milk gel due to laccase-catalysed protein crosslinking in a post-processing step. *Innovative Food Science & Emerging Technologies, 33*: 563-570.

Mokoonlall, A., Sykora, L., Pfannstiel, J., Nöbel, S., Weiss, J., & Hinrichs, J. (2016). A feasibility study on the application of a laccase-mediator system in stirred yoghurt at the pilot scale. *Food Hydrocolloids, 60*: 119-127.

Murray, B. S. (2002). Interfacial rheology of food emulsifiers and proteins. *Current Opinion in Colloid & Interface Science, 7*(5): 426-431.

Nicolas, J., Mura, S., Brambilla, D., Mackiewicz, N., & Couvreur, P. (2013). Design, functionalization strategies and biomedical applications of targeted biodegradable/biocompatible polymer-based nanocarriers for drug delivery. *Chemical Society Reviews, 42*(3): 1147-1235.

Nieto-Nieto, T. V., Wang, Y. X., Ozimek, L., & Chen, L. (2014). Effects of partial hydrolysis on structure and gelling properties of oat globular proteins. *Food Research International, 55*: 418-425.

Niku-Paavola, M. L., Karhunen, E., Kantelinen, A., Viikari, L., Lundell, T., & Hatakka, A. (1990). The effect of culture conditions on the production of lignin modifying enzymes by the white-rot fungus Phlebia radiata. *Journal of Biotechnology, 13*(2): 211-221.

Nwachukwu, I. D., & Aluko, R. E. (2019). Structural and functional properties of food protein-derived antioxidant peptides. *Journal of Food Biochemistry, 43*(1): e12761.

Oosterveld, A., Pol, I. E., Beldman, G., & Voragen, A. G. J. (2001). Isolation of feruloylated arabinans and rhamnogalacturonans from sugar beet pulp and their gel forming ability by oxidative cross-linking. *Carbohydrate Polymers, 44*(1): 9-17.

Osma, J. F., Toca-Herrera, J. L., & Rodríguez-Couto, S. (2010). Uses of Laccases in the Food Industry. *Enzyme Research, 2010*: 1-8.

Partanen, R., Paananen, A., Forssell, P., Linder, M. B., Lille, M., Buchert, J., & Lantto, R. (2009). Effect of transglutaminase-induced cross-linking of sodium caseinate on the properties of equilibrated interfaces and foams. *Colloids and Surfaces A: Physicochemical and Engineering Aspects, 344*(1-3): 79-85.

Patova, O. A., Golovchenko, V. V., & Ovodov, Y. S. (2014). Pectic polysaccharides: structure and properties. *Russian Chemical Bulletin, 63*(9): 1901-1924.

Perez, A. A., Sanchez, C. C., Patino, J. M., Rubiolo, A. C., & Santiago, L. G. (2010). Milk whey proteins and xanthan gum interactions in solution and at the air-water interface: a rheokinetic study. *Colloids Surf B Biointerfaces, 81*(1): 50-57.

Permana, D., Minamihata, K., Goto, M., & Kamiya, N. (2018). Laccase-catalyzed bioconjugation of tyrosine-tagged functional proteins. *Journal of Bioscience and Bioengineering, 126*(5): 559-566.

Permana, D., Minamihata, K., Sato, R., Wakabayashi, R., Goto, M., & Kamiya, N. (2020). Linear Polymerization of Protein by Sterically Controlled Enzymatic Cross-Linking with a Tyrosine-Containing Peptide Loop. *ACS Omega, 5*(10): 5160-5169.

Perna, V., Agger, J. W., Andersen, M. L., Holck, J., & Meyer, A. S. (2019). Laccase Induced Lignin Radical Formation Kinetics Evaluated by Electron Paramagnetic Resonance Spectroscopy. *ACS Sustainable Chemistry & Engineering, 7*(12): 10425-10434.

Pezennec, S., Gauthier, F., Alonso, C., Graner, F., Croguennec, T., Brulé, G., & Renault, A. (2000). The protein net electric charge determines the surface rheological properties of ovalbumin adsorbed at the air–water interface. *Food Hydrocolloids, 14*(5): 463-472.

Piber, M., & Koehler, P. (2005). Identification of dehydro-ferulic acid-tyrosine in rye and wheat: evidence for a covalent cross-link between arabinoxylans and proteins. *Journal of Agricultural and Food Chemistry, 53*(13): 5276-5284.

Piontek, K., Antorini, M., & Choinowski, T. (2002). Crystal structure of a laccase from the fungus Trametes versicolor at 1.90-A resolution containing a full complement of coppers. *Journal of Biological Chemistry, 277*(40): 37663-37669.

Polyakov, K. M., Fedorova, T. V., Stepanova, E. V., Cherkashin, E. A., Kurzeev, S. A., Strokopytov, B. V., Lamzin, V. S., & Koroleva, O. V. (2009). Structure of native laccase from Trametes hirsuta at 1.8 A resolution. *Acta Crystallographica Section D Structural Biology 65*(Pt 6): 611-617.

Pots, A. M., Gruppen, H., Hessing, M., van Boekel, M. A. J. S., & Voragen, A. G. J. (1999). Isolation and Characterization of Patatin Isoforms. *Journal of Agricultural and Food Chemistry, 47*(11): 4587-4592.

Pouvreau, L., Gruppen, H., Piersma, S. R., van den Broek, L. A. M., van Koningsveld, G. A., & Voragen, A. G. J. (2001). Relative Abundance and Inhibitory Distribution of Protease Inhibitors in Potato Juice from cv. Elkana. *Journal of Agricultural and Food Chemistry, 49*(6): 2864-2874.

Pouvreau, L., Gruppen, H., van Koningsveld, G. A., van den Broek, L. A. M., & Voragen, A. G. J. (2004). Tentative Assignment of the Potato Serine Protease Inhibitor Group as β-II Proteins Based on Their Spectroscopic Characteristics. *Journal of Agricultural and Food Chemistry, 52*(25): 7704-7710.

Qi, P. X., Chau, H. K., & Hotchkiss, A. T. (2019). Molecular characterization of interacting complexes and conjugates induced by the dry-state heating of β-lactoglobulin and sugar beet pectin. *Food Hydrocolloids, 91*: 10-18.

Qian, J.-Y., Ma, L.-J., Wang, L.-J., & Jiang, W. (2016). Effect of pulsed electric field on structural properties of protein in solid state. *LWT - Food Science and Technology, 74*: 331-337.

Ralet, M.-C., & Guéguen, J. (2001). Foaming Properties of Potato Raw Proteins and Isolated Fractions. *LWT - Food Science and Technology, 34*(4): 266-269.

Ranadheera, C. S., Liyanaarachchi, W. S., Chandrapala, J., Dissanayake, M., & Vasiljevic, T. (2016). Utilizing unique properties of caseins and the casein micelle for delivery of sensitive food ingredients and bioactives. *Trends in Food Science & Technology, 57*: 178-187.

Ravisankar, S., Abegaz, K., & Awika, J. M. (2018). Structural profile of soluble and bound phenolic compounds in teff (Eragrostis tef) reveals abundance of distinctly different flavones in white and brown varieties. *Food Chemistry, 263*: 265-274.

Renzetti, S., Courtin, C. M., Delcour, J. A., & Arendt, E. K. (2010). Oxidative and proteolytic enzyme preparations as promising improvers for oat bread formulations: Rheological, biochemical and microstructural background. *Food Chemistry, 119*(4): 1465-1473.

Ribotta, P. D., Colombo, A., & Rosell, C. M. (2012). Enzymatic modifications of pea protein and its application in protein–cassava and corn starch gels. *Food Hydrocolloids, 27*(1): 185-190.

Riva, S. (2006). Laccases: blue enzymes for green chemistry. *Trends in Biotechnology, 24*(5): 219-226.

Rivera-Hoyos, C. M., Morales-Álvarez, E. D., Poutou-Piñales, R. A., Pedroza-Rodríguez, A. M., RodrÍguez-Vázquez, R., & Delgado-Boada, J. M. (2013). Fungal laccases. *Fungal Biology Reviews, 27*(3-4): 67-82.

Rodriguez Patino, J., Minones Conde, J., Linares, H., Pedroche Jimenez, J., Carrera Sanchez, C., Pizones, V., & Rodriguez, F. (2007). Interfacial and foaming properties of enzyme-induced hydrolysis of sunflower protein isolate. *Food Hydrocolloids, 21*(5-6): 782-793.

Romero, A., Beaumal, V., David-Briand, E., Cordobes, F., Guerrero, A., & Anton, M. (2011). Interfacial and oil/water emulsions characterization of potato protein isolates. *Journal of Agricultural and Food Chemistry, 59*(17): 9466-9474.

Rouilly, A., Orliac, O., Silvestre, F., & Rigal, L. (2003). Thermal denaturation of sunflower globulins in low moisture conditions. *Thermochimica Acta, 398*(1-2): 195-201.

Ruíz-Henestrosa, V. P., Sanchez, C. C., & Rodríguez Patino, J. M. (2007). Formulation engineering can improve the interfacial and foaming properties of soy globulins. *Journal of Agricultural and Food Chemistry, 55*(15): 6339-6348.

Rytioja, J., Hilden, K., Yuzon, J., Hatakka, A., de Vries, R. P., & Makela, M. R. (2014). Plant-polysaccharide-degrading enzymes from Basidiomycetes. *Microbiology Molecular Biology Reviews, 78*(4): 614-649.

Sánchez-González, J., Ruiz-García, J., & Gálvez-Ruiz, M. J. (2003). Langmuir–Blodgett films of biopolymers: a method to obtain protein multilayers. *Journal of Colloid and Interface Science, 267*(2): 286-293.

Santiago, G., de Salas, F., Lucas, M. F., Monza, E., Acebes, S., Martinez, Á. T., Camarero, S., & Guallar, V. (2016). Computer-Aided Laccase Engineering: Toward Biological Oxidation of Arylamines. *ACS Catalysis, 6*(8): 5415-5423.

Sato, A. C. K., Perrechil, F. A., Costa, A. A. S., Santana, R. C., & Cunha, R. L. (2015). Cross-linking proteins by laccase: Effects on the droplet size and rheology of emulsions stabilized by sodium caseinate. *Food Research International, 75*: 244-251.

Schmidt, J. M., Damgaard, H., Greve-Poulsen, M., Larsen, L. B., & Hammershøj, M. (2018). Foam and emulsion properties of potato protein isolate and purified fractions. *Food Hydrocolloids, 74*: 367-378.

Schuh, S., Schwarzenbolz, U., & Henle, T. (2010). Cross-linking of hen egg white lysozyme by microbial transglutaminase under high hydrostatic pressure: localization of reactive amino acid side chains. *Journal of Agricultural and Food Chemistry, 58*(24): 12749-12752.

Selinheimo, E., Autio, K., Kruus, K., & Buchert, J. (2007). Elucidating the mechanism of laccase and tyrosinase in wheat bread making. *Journal of Agricultural and Food Chemistry, 55*(15): 6357-6365.

Selinheimo, E., Lampila, P., Mattinen, M. L., & Buchert, J. (2008). Formation of protein-oligosaccharide conjugates by laccase and tyrosinase. *Journal of Agricultural and Food Chemistry, 56*(9): 3118-3128.

Seo, S., Karboune, S., & Archelas, A. (2014). Production and characterisation of potato patatin–galactose, galactooligosaccharides, and galactan conjugates of great potential as functional ingredients. *Food Chemistry, 158*: 480-489.

Seo, S., Karboune, S., L'Hocine, L., & Yaylayan, V. (2013). Characterization of glycated lysozyme with galactose, galactooligosaccharides and galactan: Effect of glycation on structural and functional properties of conjugates. *LWT - Food Science and Technology, 53*(1): 44-53.

Seo, S., Karboune, S., Yaylayan, V., & L'Hocine, L. (2012). Glycation of lysozyme with galactose, galactooligosaccharides and potato galactan through the Maillard reaction and optimization of the production of prebiotic glycoproteins. *Process Biochemistry, 47*(2): 297-304.

Seo, S., Rebehmed, J., de Brevern, A. G., & Karboune, S. (2015). Enzymatic Synthesis of Galactosylated Serine/Threonine Derivatives by beta-Galactosidase from Escherichia coli. *International Journal of Molecular Sciences, 16*(6): 13714-13728.

Shen, L., Tian, Z., Liu, W., & Li, G. (2015). Influence on the physicochemical properties of fish collagen gels using self-assembly and simultaneous cross-linking with the N-hydroxysuccinimide adipic acid derivative. *Connect Tissue Research, 56*(3): 244-252.

Sheng, L., Tang, G., Wang, Q., Zou, J., Ma, M., & Huang, X. (2020). Molecular characteristics and foaming properties of ovalbumin-pullulan conjugates through the Maillard reaction. *Food Hydrocolloids, 100*.

Sheng, L., Ye, S., Han, K., Zhu, G., Ma, M., & Cai, Z. (2019). Consequences of phosphorylation on the structural and foaming properties of ovalbumin under wet-heating conditions. *Food Hydrocolloids, 91*: 166-173.

Si, J. Q. (2001). US Patent No: US6296883

Singh, D., Rawat, S., Waseem, M., Gupta, S., Lynn, A., Nitin, M., Ramchiary, N., & Sharma, K. K. (2016). Molecular modeling and simulation studies of recombinant laccase from Yersinia enterocolitica suggests significant role in the biotransformation of non-steroidal anti-inflammatory drugs. *Biochemical and Biophysical Research Communications, 469*(2): 306-312.

Singh, D., Sharma, K. K., Dhar, M. S., & Virdi, J. S. (2014). Molecular modeling and docking of novel laccase from multiple serotype of Yersinia enterocolitica suggests differential and multiple substrate binding. *Biochemical and Biophysical Research Communications, 449*(1): 157-162.

Smirnov, S. A., Koroleva, O. V., Gavrilova, V. P., Belova, A. B., & Klyachko, N. L. (2001). Laccases from Basidiomycetes: physicochemical characteristics and substrate specificity towards methoxyphenolic compounds. *Biochemistry (Moscow), 66*(7): 774-779.

Song, Y., Babiker, E. E., Usui, M., Saito, A., & Kato, A. (2002). Emulsifying properties and bactericidal action of chitosan–lysozyme conjugates. *Food Research International, 35*(5): 459-466.

Spicer, C. D., & Davis, B. G. (2014). Selective chemical protein modification. *Nature Communications, 5*: 4740.

Spotti, M. J., Tarhan, Ö., Schaffter, S., Corvalan, C., & Campanella, O. H. (2017). Whey protein gelation induced by enzymatic hydrolysis and heat treatment: Comparison of creep and recovery behavior. *Food Hydrocolloids, 63*: 696-704.

Srinivasan, D. (1994). Structure-Function Relationship of Food Proteins. In *Protein functionality in food systems*. New York: Marcel Dekker.

Stanic, D., Monogioudi, E., Dilek, E., Radosavljevic, J., Atanaskovic-Markovic, M., Vuckovic, O., Raija, L., Mattinen, M., Buchert, J., & Cirkovic Velickovic, T. (2010). Digestibility and allergenicity assessment of enzymatically crosslinked beta-casein. *Molecular Nutrition & Food Research, 54*(9): 1273-1284.

Steffensen, C. L., Andersen, M. L., Degn, P. E., & Nielsen, J. H. (2008). Cross-linking proteins by laccase-catalyzed oxidation: importance relative to other modifications. *Journal of Agricultural and Food Chemistry, 56*(24): 12002-12010.

Steffensen, C. L., Stensballe, A., Kidmose, U., Degn, P. E., Andersen, M. L., & Nielsen, J. H. (2009). Modifications of amino acids during ferulic acid-mediated, laccase-catalysed cross-linking of peptides. *Free Radical Research, 43*(12): 1167-1178.

Stein, P. E., Leslie, A. G. W., Finch, J. T., & Carrell, R. W. (1991). Crystal structure of uncleaved ovalbumin at 1·95 Å resolution. *Journal of Molecular Biology, 221*(3): 941-959.

Stevens, J. C., Das, L., Mobley, J. K., Asare, S. O., Lynn, B. C., Rodgers, D. W., & Shi, J. (2019). Understanding Laccase–Ionic Liquid Interactions toward Biocatalytic Lignin Conversion in Aqueous Ionic Liquids. *ACS Sustainable Chemistry & Engineering, 7*(19): 15928-15938.

Stojadinovic, M., Pieters, R., Smit, J., & Velickovic, T. C. (2014). Cross-linking of beta-lactoglobulin enhances allergic sensitization through changes in cellular uptake and processing. *Toxicological Sciences, 140*(1): 224-235.

Struch, M., Linke, D., Mokoonlall, A., Hinrichs, J., & Berger, R. G. (2015). Laccase-catalysed cross-linking of a yoghurt-like model system made from skimmed milk with added food-grade mediators. *International Dairy Journal, 49*: 89-94.

Sun-Waterhouse, D., Zhao, M., & Waterhouse, G. I. N. (2014). Protein Modification During Ingredient Preparation and Food Processing: Approaches to Improve Food Processability and Nutrition. *Food and Bioprocess Technology, 7*(7): 1853-1893.

Tadesse, M. A., D'Annibale, A., Galli, C., Gentili, P., & Sergi, F. (2008). An assessment of the relative contributions of redox and steric issues to laccase specificity towards putative substrates. *Organic and Biomolecular Chemistry, 6*(5): 868-878.

Tang, C. H., Choi, S. M., & Ma, C. Y. (2007). Study of thermal properties and heat-induced denaturation and aggregation of soy proteins by modulated differential scanning calorimetry. *International Journal of Biological Macromolecules, 40*(2): 96-104.

Tantoush, Z., Stanic, D., Stojadinovic, M., Ognjenovic, J., Mihajlovic, L., Atanaskovic-Markovic, M., & Cirkovic Velickovic, T. (2011). Digestibility and allergenicity of β-lactoglobulin following laccase-mediated cross-linking in the presence of sour cherry phenolics. *Food Chemistry, 125*(1): 84-91.

Ter Haar, R., Westphal, Y., Wierenga, P. A., Schols, H. A., & Gruppen, H. (2011). Cross-linking behavior and foaming properties of bovine alpha-lactalbumin after glycation with various saccharides. *Journal of Agricultural and Food Chemistry, 59*(23): 12460-12466.

Tong, P., Chen, S., Gao, J., Li, X., Wu, Z., Yang, A., Yuan, J., & Chen, H. (2018). Caffeic acid-assisted cross-linking catalyzed by polyphenol oxidase decreases the allergenicity of ovalbumin in a Balb/c mouse model. *Food and Chemical Toxicology, 111*: 275-283.

van Koningsveld, G. A., Gruppen, H., de Jongh, H. H., Wijngaards, G., van Boekel, M. A., Walstra, P., & Voragen, A. G. (2001). Effects of pH and heat treatments on the structure and solubility of potato proteins in different preparations. *Journal of Agricultural and Food Chemistry, 49*(10): 4889-4897.

Vismeh, R., Lu, F., Chundawat, S. P., Humpula, J. F., Azarpira, A., Balan, V., Dale, B. E., Ralph, J., & Jones, A. D. (2013). Profiling of diferulates (plant cell wall cross-linkers) using ultrahigh-performance liquid chromatography-tandem mass spectrometry. *Analyst, 138*(21): 6683-6692.

Voragen, A. G. J., Coenen, G.-J., Verhoef, R. P., & Schols, H. A. (2009). Pectin, a versatile polysaccharide present in plant cell walls. *Structural Chemistry, 20*(2): 263-275.

Waglay, A., Achouri, A., Karboune, S., Zareifard, M. R., & L'Hocine, L. (2019). Pilot plant extraction of potato proteins and their structural and functional properties. *LWT - Food Science and Technology, 113*.

Waglay, A., & Karboune, S. (2016a). Enzymatic generation of peptides from potato proteins by selected proteases and characterization of their structural properties. *Biotechnology Progress, 32*(2): 420-429.

Waglay, A., & Karboune, S. (2016b). Potato Proteins. In *Advances in Potato Chemistry and Technology* (pp. 75-104).

Waglay, A., Karboune, S., & Khodadadi, M. (2016). Investigation and optimization of a novel enzymatic approach for the isolation of proteins from potato pulp. *LWT - Food Science and Technology, 65*: 197-205.

Wang, D., Lv, P., Zhang, L., Yang, S., & Gao, Y. (2019). Structural and Functional Characterization of Laccase-Induced beta-Lactoglobulin-Ferulic Acid-Chitosan Ternary Conjugates. *Journal of Agricultural and Food Chemistry, 67*(43): 12054-12060.

Wang, G., & Wang, T. (2009). Egg yolk protein modification by controlled enzymatic hydrolysis for improved functionalities. *International Journal of Food Science & Technology, 44*(4): 763-769.

Wang, K., Sun, D., Pu, H., & Wei, Q. (2017). Principles and applications of spectroscopic techniques for evaluating food protein conformational changes: A review. *Trends in Food Science & Technology, 67*: 207-219.

Wang, L. L., & Xiong, Y. L. (2005). Inhibition of Lipid Oxidation in Cooked Beef Patties by Hydrolyzed Potato Protein Is Related to Its Reducing and Radical Scavenging Ability. *Journal of Agricultural and Food Chemistry, 53*(23): 9186-9192.

Wang, Q., Jin, Y., & Xiong, Y. L. (2018). Heating-Aided pH Shifting Modifies Hemp Seed Protein Structure, Cross-Linking, and Emulsifying Properties. *Journal of Agricultural and Food Chemistry, 66*(41): 10827-10834.

Wang, Y., Gan, J., Li, Y., Nirasawa, S., & Cheng, Y. (2019). Conformation and emulsifying properties of deamidated wheat gluten-maltodextrin/citrus pectin conjugates and their abilities to stabilize β-carotene emulsions. *Food Hydrocolloids, 87*: 129-141.

Wang, Y., Gan, J., Zhou, Y., Cheng, Y., & Nirasawa, S. (2017). Improving solubility and emulsifying property of wheat gluten by deamidation with four different acids: Effect of replacement of folded conformation by extended structure. *Food Hydrocolloids, 72*: 105-114.

Wang, Y. F., Xu, H., Feng, L., Shen, X. F., Wang, C., Huo, X. K., Tian, X. G., Ning, J., Zhang, B. J., Sun, C. P., & Deng, S. (2019). Oxidative coupling of coumarins catalyzed by laccase. *International Journal of Biological Macromolecules, 135*: 1028-1033.

Wang, Z., Li, Y., Jiang, L., Qi, B., & Zhou, L. (2014). Relationship between Secondary Structure and Surface Hydrophobicity of Soybean Protein Isolate Subjected to Heat Treatment. *Journal of Chemistry, 2014*: 1-10.

Ward, G., Hadar, Y., Bilkis, I., Konstantinovsky, L., & Dosoretz, C. G. (2001). Initial steps of ferulic acid polymerization by lignin peroxidase. *Journal of Biological Chemistry, 276*(22): 18734-18741.

Weiss, M. S., Palm, G. J., & Hilgenfeld, R. (2000). Crystallization, structure solution and refinement of hen egg-white lysozyme at pH 8.0 in the presence of MPD. *Acta Crystallographica Section D, 56*(8): 952-958.

Wouters, A. G. B., Fierens, E., Rombouts, I., Brijs, K., Blecker, C., & Delcour, J. A. (2017). Air-water interfacial properties of enzymatically hydrolyzed wheat gluten in the presence of sucrose. *Food Hydrocolloids, 73*: 284-294.

Wouters, A. G. B., Rombouts, I., Legein, M., Fierens, E., Brijs, K., Blecker, C., & Delcour, J. A. (2016). Air–water interfacial properties of enzymatic wheat gluten hydrolyzates determine their foaming behavior. *Food Hydrocolloids, 55*: 155-162.

Wu, W., Clifford, M., & Howell, N. K. (2007). The effect of instant green tea on the foaming and rheological properties of egg albumen proteins. *Journal of the Science of Food and Agriculture, 87*(10): 1810-1819.

Wu, W., Zhang, C., Kong, X., & Hua, Y. (2009). Oxidative modification of soy protein by peroxyl radicals. *Food Chemistry, 116*(1): 295-301.

Xia, Y., Bamdad, F., Gänzle, M., & Chen, L. (2012). Fractionation and characterization of antioxidant peptides derived from barley glutelin by enzymatic hydrolysis. *Food Chemistry, 134*(3): 1509-1518.

Xu, K., Zhao, Z., Guo, M., & Du, J. (2019). Conjugation between okra polysaccharide and lactoferrin and its inhibition effect on thermal aggregation of lactoferrin at neutral pH. *LWT - Food Science and Technology, 107*: 125-131.

Yang, H., Yang, S., Kong, J., Dong, A., & Yu, S. (2015). Obtaining information about protein secondary structures in aqueous solution using Fourier transform IR spectroscopy. *Nature Protocols, 10*(3): 382-396.

Yang, J., Li, W., Ng, T. B., Deng, X., Lin, J., & Ye, X. (2017). Laccases: Production, Expression Regulation, and Applications in Pharmaceutical Biodegradation. *Frontiers in Microbiology, 8*: 832.

Yang, J., Liu, G., Zeng, H., & Chen, L. (2018). Effects of high pressure homogenization on faba bean protein aggregation in relation to solubility and interfacial properties. *Food Hydrocolloids, 83*: 275-286.

Yang, T., & Lesnierowski, G. (2019). Changes in selected physicochemical properties of lysozyme modified with a new method using microwave field and oxidation. *PLoS One, 14*(2): e0213021.

Yang, W., Deng, C., Xu, L., Jin, W., Zeng, J., Li, B., & Gao, Y. (2020). Protein-neutral polysaccharide nano- and micro-biopolymer complexes fabricated by lactoferrin and oat β-glucan: Structural characteristics and molecular interaction mechanisms. *Food Research International, 132*.

Yapo, B. M., Lerouge, P., Thibault, J.-F., & Ralet, M.-C. (2007). Pectins from citrus peel cell walls contain homogalacturonans homogenous with respect to molar mass, rhamnogalacturonan I and rhamnogalacturonan II. *Carbohydrate Polymers, 69*(3): 426-435.

Ye, Q., Han, Y., Zhang, J., Zhang, W., Xia, C., & Li, J. (2019). Bio-based films with improved water resistance derived from soy protein isolate and stearic acid via bioconjugation. *Journal of Cleaner Production, 214*: 125-131.

Yoshida, H. (1883). LXIII.—Chemistry of lacquer (Urushi). Part I. Communication from the Chemical Society of Tokio. *RSC Journal of the Chemical Society 43*(0): 472-486.

You, S.-J., Udenigwe, C. C., Aluko, R. E., & Wu, J. (2010). Multifunctional peptides from egg white lysozyme. *Food Research International, 43*(3): 848-855.

Yu, X. X., Liu, C., Lu, M. H., Liu, Y. L., Yin, J. Y., & Zhang, Y. H. (2019). Impact of enzymatic hydrolysis followed by transglutaminase-induced cross-linking on decreasing antigenicity and reserving partial interfacial properties of whey protein isolate. *Food & Function, 10*(3): 1653-1660.

Yuan, X., Li, X., Zhang, X., Mu, Z., Gao, Z., Jiang, L., & Jiang, Z. (2018). Effect of ultrasound on structure and functional properties of laccase-catalyzed α-lactalbumin. *Journal of Food Engineering, 223*: 116-123.

Zaidel, D. N., Arnous, A., Holck, J., & Meyer, A. S. (2011). Kinetics of enzyme-catalyzed cross-linking of feruloylated arabinan from sugar beet. *Journal of Agricultural and Food Chemistry, 59*(21): 11598-11607.

Zaidel, D. N. A., & Meyer, A. S. (2012). Biocatalytic cross-linking of pectic polysaccharides for designed food functionality: Structures, mechanisms, and reactions. *Biocatalysis and Agricultural Biotechnology, 1*(3): 207-219.

Zayas, J. F. (1997). Introduction. In *Functionality of Proteins in Food* (pp. 1-5). Berlin, Heidelberg: Springer Berlin Heidelberg.

Zeeb, B., Gibis, M., Fischer, L., & Weiss, J. (2012). Crosslinking of interfacial layers in multilayered oil-in-water emulsions using laccase: Characterization and pH-stability. *Food Hydrocolloids, 27*(1): 126-136.

Zeeb, B., McClements, D. J., & Weiss, J. (2017). Enzyme-Based Strategies for Structuring Foods for Improved Functionality. *Annual Review of Food Science and Technology, 8*: 21-34.

Zeeb, B., Salminen, H., Fischer, L., & Weiss, J. (2013). Impact of Heat and Laccase on the pH and Freeze-Thaw Stability of Oil-in-Water Emulsions Stabilized by Adsorbed Biopolymer Nanoparticles. *Food Biophysics, 9*(2): 125-137.

Zhang, J., & Wolf, B. (2019). Physico-Chemical Properties of Sugar Beet Pectin-Sodium Caseinate Conjugates via Different Interaction Mechanisms. *Foods, 8*(6).

Zhang, Y., He, S., & Simpson, B. K. (2017). A cold active transglutaminase from Antarctic krill (Euphausia superba): Purification, characterization and application in the modification of cold-set gelatin gel. *Food Chemistry, 232*: 155-162.

Zhang, Y., He, S., & Simpson, B. K. (2018). Enzymes in food bioprocessing — novel food enzymes, applications, and related techniques. *Current Opinion in Food Science, 19*: 30-35.

Zhang, Y., Zeng, Z., Zeng, G., Liu, X., Liu, Z., Chen, M., Liu, L., Li, J., & Xie, G. (2012). Effect of Triton X-100 on the removal of aqueous phenol by laccase analyzed with a combined approach of experiments and molecular docking. *Colloids Surfaces B: Biointerfaces, 97*: 7-12.

Zheng, Y., Guo, M., Zhou, Q., & Liu, H. (2019). Effect of lignin degradation product sinapyl alcohol on laccase catalysis during lignin degradation. *Industrial Crops and Products, 139*.

Zhu, L., Yin, P., Xie, T., Liu, X., Yang, L., Wang, S., Li, J., & Liu, H. (2020). Interaction between soyasaponin and soy beta-conglycinin or glycinin: Air-water interfacial behavior and foaming property of their mixtures. *Colloids Surfaces B: Biointerfaces, 186*: 110707.